LIÈGE université
Gembloux
Agro-Bio Tech

Featuring secondary metabolites in *Bacillus-Pseudomonas* molecular interactions: roles in signaling and defense response

Sofija Andrić

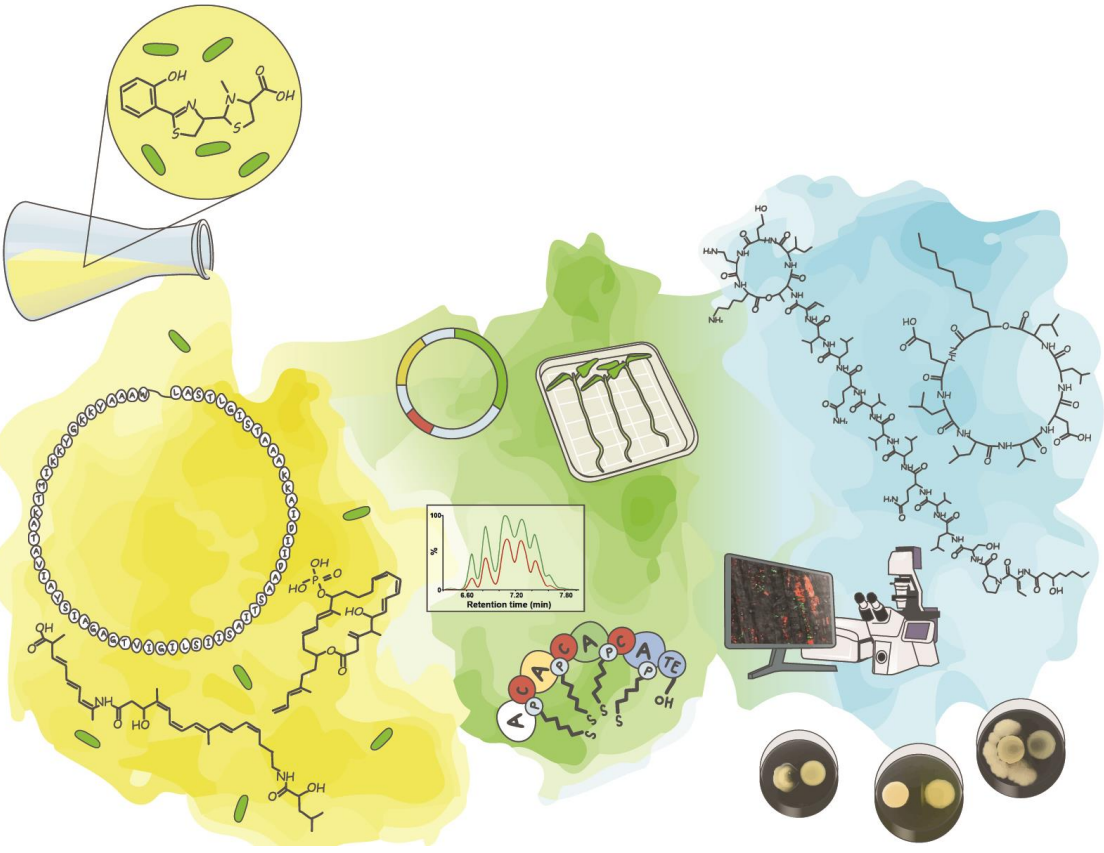

COMMUNAUTÉ FRANÇAISE DE BELGIQUE

UNIVERSITÉ DE LIÈGE – GEMBLOUX AGRO-BIO TECH

Featuring secondary metabolites in *Bacillus-Pseudomonas* molecular interactions: roles in signaling and defense response

ANDRIĆ Sofija

Dissertation originale présentée en vue de l'obtention du grade de docteur de l'Université de Liège – Gembloux Agro-Bio Tech en sciences agronomiques et ingénierie biologique

Promoteur : Dr. Marc ONGENA

Année académique :2021

Abstract

Bacillus velezensis, belonging to the *Bacillus subtilis* complex, represents an excellent model species as a plant-associated and plant beneficial bacterium. It promotes plant health and growth mainly due to the potential to secrete a wide range of bioactive secondary metabolites (BSMs). The researches on those BSMs have, so far, primarily focused on the characterization of their biological activities. However, their ecological roles and the impact of multitrophic interactions that may modulate their expression in the competitive rhizosphere niche are still limited. It is why we want to evaluate better how and to what extent this chemically diverse metabolome may contribute to the fitness and competitiveness of *B. velezensis* upon interaction with *Pseudomonas* spp., as a soil-dwelling competitor, and what is the molecular mechanisms underlying this interaction.

In this context, our data first showed that upon bacterial contact-independent *in vitro* interaction, a multifaceted macroscopic outcome was observed and characterized by *B. velezensis* growth inhibition, white-line formation in the interaction zone and enhanced motility. We further correlated these *B. velezensis* phenotypes with the production of surfactin lipopeptide which not only enhanced motility but also, by acting as a shield, prevented newly discovered antibacterial toxicity of lipopeptide sessilin, formed by *Pseudomonas*. Further, we show that *B. velezensis* can also mobilize a substantial part of its metabolome upon a perception of *Pseudomonas*. This metabolite response reflects a multimodal defensive strategy as it includes, besides surfactin, polyketides and the bacteriocin amylocyclicin, with broad antibacterial activity. Furthermore, we identified the secondary siderophore pyochelin as info-chemical, which triggers this response via a mechanism independent of iron stress, illustrating a new facet of siderophore-mediated interactions beyond the concept of competition for iron and siderophore piracy. Finally, we also demonstrated the relevance of these unsuspected roles of *B. velezensis* and *Pseudomonas* BSMs in the context of their competitive tomato root colonization.

Our work thus illustrates the multifaceted phenotypic and molecular response of *B. velezensis* in the presence of *Pseudomonas* spp. and highlights new roles for BSMs produced by the two bacteria acting as key drivers of social interactions. Moreover, discovering new ecological functions for *B. velezensis* and *Pseudomonas* spp. BSMs are crucial to rationally design compatible consortia, more efficient than single species inoculants, to promote plant health and growth by fighting economically important pathogens in sustainable agriculture.

Key words: Bioactive secondary metabolites (BSMs), *Bacillus velezensis*, interspecies interaction, *Pseudomonas sessiligenes* CMR12a, sessilin, surfactin, pyochelin, molecular cross-talk

Résumé

Bacillus velezensis appartenant au complexe *Bacillus subtilis* représente une excellente espèce modèle en tant que bactérie bénéfique associée aux plantes qui favorise la santé et la croissance des plantes, principalement en raison de sa capacité à sécréter une large gamme de métabolites secondaires bioactifs (BSMs). Jusqu'à présent, les recherches sur ces BSMs se sont principalement concentrées sur la caractérisation de leurs activités biologiques. Cependant, l'impact des interactions multitrophiques sur la modulation de leur expression dans la niche compétitive de la rhizosphère n'est pas encore assez élucidé. C'est pourquoi, nous voulons mieux évaluer comment et dans quelle mesure ce métabolome chimiquement diversifié peut contribuer à l'aptitude et la compétitivité de *B. velezensis* lors de l'interaction avec *Pseudomonas* spp., un compétiteur d'origine tellurique, ainsi que d'exploiter les mécanismes moléculaires sous-jacents à cette interaction.

Dans ce contexte, les données ont d'abord montré que lors d'une interaction *in vitro* indépendante du contact bactérien, un fort impact à multiples facettes est constaté au niveau macroscopique avec l'observation et la caractérisation d'une inhibition de la croissance de *B. velezensis*, la formation d'un précipité blanc dans la zone d'interaction et une motilité améliorée. En outre, ces phénotypes de *B. velezensis* ont été correlés avec la production d'un lipopeptide, la surfactine. En plus de l'amélioration de la motilité, il a été découvert pour la première fois que ce composé agit comme un piège chimique afin d'empêcher la toxicité de la sessiline, un lipopeptide formé par *Pseudomonas*. Egalement, il a été démontré que *B. velezensis* peut mobiliser une partie substantielle de son métabolome lors d'une perception de *Pseudomonas*. Cette réponse métabolique reflète d'une stratégie défensive multimodale car elle inclut les polykétides et la bactériocine amylocycline, à large activité antibiotique, ainsi que la surfactine. De plus, la pyocheline, un sidérophore secondaire de *Pseudomonas*, a été identifié comme molécule signal déclenchant cette réponse par un mécanisme indépendant du stress au fer. Ce résultat illustre une nouvelle facette des interactions médiées par les sidérophores, au-delà du concept de compétition pour le fer et de chélation. Enfin, la pertinence de ces rôles insoupçonnés des BSMs de *B. velezensis* et *Pseudomonas* dans le cadre de la compétition pour la colonisation des racines de tomate a été démontrée.

Notre travail illustre ainsi la réponse phénotypique et moléculaire multiforme de *B. velezensis* en présence de *Pseudomonas* et met en évidence de nouveaux rôles pour leurs BSMs qui agissent comme des moteurs clés des interactions sociales. De plus, les nouvelles fonctions écologiques des BSMs produits par *B. velezensis* et *Pseudomonas* spp. découvertes sont essentielles pour concevoir de manière rationnelle des consortiums compatibles, plus efficaces que les inocula monospécifiques. Cette efficacité accrue permettra de promouvoir la santé et la croissance des plantes en luttant contre les agents pathogènes économiquement importants dans une agriculture durable.

Mots clés : Métabolites secondaires bioactifs (MSB), *Bacillus velezensis*, interaction interspécifique, *Pseudomonas sessiligenes* CMR12a, sessiline, surfactine, pyocheline, communication moléculaire

Acknowledgments

This thesis is the culmination of four years of intensive research, brainstorming sessions, professional and personal development. However, it was not done in isolation but in synergy with many researchers whose input made this possible.

Firstly, I would like to express my profound gratitude to my promotor **Dr. Marc Ongena** for giving me a chance to pursue my research and work on a very challenging subject. Also, thank you very much for your time, patient guidance and support. Marc, your enthusiasm about research was fantastic and motivated me to keep alive my curiosity and to tow the unknown paths. Every day was a learning process leading to new ideas. I appreciated our long discussions, from which I learned a lot. Thank you for teaching me to slow down and be patient sometimes and giving me the freedom to choose my own path.

Further, I would like to express my gratitude to the reading committee members for taking the time to review my thesis and for your feedback. **Prof. Monica Höfte**, I am grateful for the privilege of working with *Pseudomonas* strains from your laboratory and your great support and contribution to the articles raised from this invaluable collaboration. **Dr. Claire Prigent-Combaret**, I am incredibly thankful for the warm reception I received in your group at University Claude Bernard, Lyon I. Besides the tricks you taught me about CLSM, you took great care of me, supported great discussions, and motivated me even when we could not observe any bacteria on the root. **Dr. Alexandre Jousset**, without your support and trust in me at the beginning of my studies, I would never be here today. The opportunity and experiences in which you involved me were crucial for my professional but also personal development. Also, your constant presence and interest in my career are precious and unforgettable. Your company during my roasting events in Serbia was inevitable for the great atmosphere and fun, thanks! **Dr. Sébastien Rigali, Prof. Philippe Jacques** and **Prof. Frank Delvigne,** tremendous gratitude for the support offered during these four years and the unforgettable, enriching discussions you offered me.

Through these years, I had great scientific support from my colleagues. Firstly, **Dr. Anthony Argüelles Arias**, thank you for being here for me from my first until my last day in Gembloux. Besides being a member of my thesis jury and revising my manuscript, I would like to express many thanks for your support with experiments, data analysis and scientific writing. **Augustin and Guillaume**, I am thrilled for the opportunity to work with super smart guys as you are and for bringing together much exciting information that resulted in two articles. Augustin, your help with article organization and writing was much appreciated. **Dr. Thibault Meyer** and **Sébastien Steels**, it is impossible to express by words how much I am grateful to have you as a colleague. Besides your precious scientific contribution to my work, I am outstandingly thankful for all your advice and support, which helped me overcome difficult periods during the last four years. **Jelena, Farah, Adri,**

Andreea, Ikram, Verginie, Francois, and **Greg** thank you for the great company and good vibes you provided until the last day of my Ph.D. I loved and will always miss a great time, hikes, mushroom picking, parties, dinners, and discussions! Jelena, posebno hvala za svu podršku koju si mi pružila. Sada je red na tebe! My **Barbie**, I am very privileged to meet you that first week at the beginning of our PhD journey. From that moment, I have you as a friend, by my side, on whom I can rely in any situation. We spent together the bad and the good times in the past years and I am grateful for having such great support. Enfin, en croisant les doigts pour ne manquer personne, sincères remerciements à tous les autres collègues de Gembloux: **Marina, Cathy, Olivia, Margue, Martine, Danielle, Romain, Aurelien, Papa, Sam, Andrew, Ghazal, Sokny, Imen, Hannah, Boris, Diem, Antoine**.

I would like to thank all my **friends from Serbia, Italy, Belgium, Luxembourg** and **Netherlands** for luring me away from my computer and helping me to refresh my mind with various activities, dancing, hikes, dinners, and trips. Thanks for emitting inexhaustible positive energy!

Last but not least, I would like to thank all my ‘’Serbian’’ and ‘’Italian’’ families. Posebno hvala mojim roditeljima **Slavici** i **Radovanu** kao i **Neveni**, najboljoj sestri na svetu! Hvala vam što ste uvek bili uz mene, ohrabrivali me u teškim trenutcima, ali bili tu i da poslavite moje uspehe. **Paola, Stefano** e **Mart**i, grazie per tutto il supporto e l'energia positiva che mi avete fornito negli anni passati.

Finally, to my boyfriend, **Riccardo**, your love, understanding and many sacrifices have been an anchor for me. Your support and motivation with the common saying ‘’dai, this is the last step’’ has been one of the most significant pushes for me to be here, where I am today. Thank you!

List of content

List of figures

Chapter 1 – General Introduction

Chapter 2 - Lipopeptide interplay mediates molecular interactions between soil bacilli and pseudomonads

Chapter 3 – Chelator sensing mediates molecular interactions between soil bacilli and pseudomonads

List of tables

Chapter 1 – General Introduction

Chapter 2 - Lipopeptide interplay mediates molecular interactions between soil bacilli and pseudomonads

Chapter 3 – Chelator sensing mediates molecular interactions between soil bacilli and pseudomonads

List of abbreviations

2H-bae: Dihydrobacillaene
A domain: Adenylation domain
ACN: Acetonitrile
ACP: Acyl carrier protein
Ala: Alanine
ANOVA: Analysis of variance
Arg: Arginine
Asn: asparagine
Asp: aspartic acid
AT domain: Acyltransferase domain
bae: Bacillaene
BCA: Biocontrol agent
BGC: Biosynthetic gene clusters
BSM: Bioactive secondary (soluble) metabolite
C domain: Condensation domain
CFS: Cell-free supernatant
CFU: colony forming unit
CLP: Cyclic lipopeptide
CLSM: Confocal laser scanning microscopy
CoA: Coenzyme A
CTRL: Control
Cys: cysteine
DAD: Diode array detector
DAPG: 2,4-diacetylphloroglucinol
DH domain: Dehydratase domain
Dha: Dehydroalanine
Dhb: Dehydrobutyrine
diff: difficidin
DIP: 2,2′-dipyridine
E domain: Epimerisation domain
EDTA: Ethylenediamine tetraacetic acid
EM: Root exudate mimicking medium
CAA: Casamino acid medium
E-PCH: Enantio-pyochelin
ER domain: Enoylreductase domain
FA: Fatty acid
GFP: Green fluorescent protein
Gln: Glutamine

Glu: Glutamic acid
Gly: Glycine
HCCA: α-cyano-4-hydroxycinnamic acid
His: Histidine
HSD: Honestly significant difference
Ile: Isoleucine
ISR: Induced systemic resistance
ITC: Isothermal titration calorimetry
KB: King's B medium
KR domain: β-ketoreductase domain
KS domain: Ketosynthase domain
Lan: Lanthionine
LB: Lysogeny broth medium
Leu: Leucine
Lys: Lysine
M domain: Methylase domain
M domain: Methylation domain
MALDI-FT-ICR MS: Mapping via matrix-assisted laser desorption/ionization-Fourier transform-ion cyclotron resonance mass spectrometry
MCT domain: Malonyl-CoA transacylase domain
MeLan: Methyl-lanthionine
MeOxz: Methoxazole
Met: Methionine
NR: Non ribosomal
NRP: Non-ribosomal peptide
NRPS: Non-ribosomal peptide synthetase
OD: optical density
oxy-diff: Oxy-difficidin
Oxz: Oxazole
PCA: Phenazine-1- carboxylic acid
PCH: Pyochelin
PCN: Phenazine-1-carboxamide
PGPR: Plant growth promoting rhizobacteria
Phe: Phenylalanine
PK: Polyketide
PKS: Polyketide synthetase
PPTase: 4'-phosphopantetheine transferases
Pro: Proline
PVD: Pyoverdine

R domain: Reduction domain
RiPP: Post-translationally modified peptides
RNA: Ribonucleic acid
RT-qPCR: Quantitative reverse transcription polymerase chain reaction
SD: Standard deviation
Ser: Serine
TE domain: Thioesterase domain
Thr: Threonine
TIC: Total ion chromatograms
EIC: Extracted ion chromatogram
Trp: Tryptophan
Tyr: Tyrosine
UPLC MS: Ultrahigh performance liquid chromatography mass spectrometry
UPLC-qTOF MS: Ultrahigh performance liquid chromatography-quadrupole time-of-flight mass spectrometry
Val: Valine
VOC: Volatile organic compound

Chapter 1

General introduction

This chapter is partially adapted from: Andrić S., Meyer T. and Ongena M. (2020). *Bacillus* responses to plant-associated fungal and bacterial communities. *Front. Microbiol.* 11:1350.

1. Research background and thesis outline

Over past years, the trend of population growth has constantly been rising and it is expected to reach 10 billion inhabitants by the end of the century. Consequently, the demands for food production also increase [1,2]. To meet this requirement and guarantee an adequate quantity of high-quality products, the producers have to fight one of the biggest global threats for food production, the phytopathogens, that cause yearly economic losses of 20-40% of the yield [3,4]. For instance, among them up to date, there are over 200 species of bacterial pathogens, including the most destructive and economically important bacterial pathogens such as *Pseudomonas* spp., *Xanthomonas* spp., *Erwinia* spp., *Ralstonia* spp., *Agrobacterium* spp., *Xylella* spp., *Pectobacterium* spp. and *Clavibacter* spp. [5].

The developments in microbiology, genetic, molecular biology, and chemistry allowed us to advance in the fight against microorganisms causing plant diseases and improve plant growth. Chemicals with an antimicrobial effect (pesticides) became the most widely used method in agriculture for this purpose [6]. Even though being highly effective in protecting plants, they have many drawbacks, such as harming people's health and the environment, causing the development of phytopathogen's resistance to pesticides and alternation of the natural microbial community [6]. Given the many drawbacks observed during the years, several measures have been taken to avoid or reduce consequences caused by chemicals. Regulations have emerged to limit the number of used products and forbid certain products whose toxic effect harms the other aspects of the environment.

In this context, from the 20th century, scientists began to focus their efforts on developing alternatives to chemical pesticides by proposing new ecologically friendly solutions [6,7]. These solutions consider utilization of biocontrol agents (BCA) either derived from or containing living (micro-)organisms, such as viruses, bacteria, fungi, insects, plants and nematodes, that can prevent or suppress plant pathogens and improve plant growth [7]. Among them, root-associated and plant growth-promoting rhizobacteria (PGPR) are seen as an important management strategy to control phytopathogens [7,8]. These PGPRs are present in a thin zone of soil surrounding plant roots, called the rhizosphere. This zone is highly influenced by the root system and its exudates, which create an exclusive and nutritionally rich environment for microbes [9]. The PGPRs include a various genus of rhizosphere bacteria such as *Bacillus*, *Pseudomonas*, *Streptomyces*, *Azospirillum*, *Acetobacter*, *Burkholderia*, *Paenibacillus*, *Herbaspirillum*, *Rhodococcus*, *Rhizobium* and *Serratia* [10,11]. These rhizosphere microorganisms can indirectly influence plant health by inducing the plant immune system, or directly, by developing various strategies to inhibit plant pathogens, including competition for space and nutrients, parasitism and/or antagonism [9,12].

Nowadays, it is expected that BCAs represent approximately 10% of the global plant protection market with a predicted yearly increasement rate of 15% to 20%

[13,14]. However, the number of PGPRs-containing products remains relatively low compared to chemical products, which can be explained by the high production cost, reduced field competence, and variable effectiveness caused mainly by various abiotic and biotic factors that can occur in nature [15,16]. Thus, bringing biocontrol products to the central position on the agriculture market requires further studies and improvements in production technology but also in a better understanding of the influence of abiotic and biotic factors on the fitness of PGPRs and the expression of plant protective functions.

2. Root-associated *Bacillus velezensis*

2.1 General characteristics and classification

Genus *Bacillus* contains some of the most important PGPRs [10]. It comprises endospore-forming, Gram-positive and rod-shaped bacteria. *Bacilli* are motile thanks to flagella and are aerobic or facultatively anaerobic [17]. They produce endospores that are highly resistant to stresses caused during industrial production or by long-term storage. Further, endospores can be successfully combined with adjuvants, additives and surfactants, giving them additional value for BCA formulation and agro-industrial applications [18].

Up to date, genus *Bacillus* counts 291 known species grouped in 19 monophyletic clades. However, according to the recent phylogenetic and molecular advances, the study proposed that 206 of known *Bacillus* species should be reclassified to novel genera. Another 28 and 19 species, should be considered subtilis clade, mainly containing soil species, and cereus clade, containing human pathogenic species [19]. Most of the members belonging to *Bacillus* genus, recognized as promising BCAs, are commonly found in the soil and are mostly isolated from plant rhizosphere, with few exceptions of isolates from the phyllosphere. These members belong to the so-called *Bacillus subtilis* complex (within the subtilis clade) [20].

In the comparative genomic era, numerous adjustments have been made in the last years to clarify the phylogeny of the *Bacillus subtilis* complex, which includes *B. velezensis*, *Bacillus amyloliquefaciens*, *Bacillus atrophaeus*, *Bacillus subtilis* subsp. *subtilis*, *Bacillus licheniformis*, *Bacillus pumilus*, and *Bacillus siamensis* with potential as BCAs [21–23], and which led to some confusion in species names but also misassignments [20,24–27]. Many isolates, such as strains S499, GA1, FZB42, QST713, or SQR9 formerly assigned to the *B. subtilis* or *Bacillus amyloliquefaciens* subsp. *plantarum* species have been re-classified as *B. velezensis*, representing the model species for plant-associated bacilli [20,24].

The plant-associated *B. velezensis* species was for the first time identified in 2005 after isolation (CR-502T and CR-14b strains) from samples collected from the soil of Vélez riverbank in Málaga (South of Spain) [28]. This species belongs to *B. amyloliquefaciens* operational group together with the other species such as *B.*

amyloliquefaciens (soil-borne), *B. siamensis* (plant-associated), and the producer of black pigment *B. nakamurai* (soil-borne) species [20,24].

2.2 BSMs produced by B. velezensis

A large part of the genome of *B. velezensis* is devoted to the production of antimicrobial compounds with up to 13% annotated as involved in the synthesis of secondary metabolites, compared to the other species of the complex, i.e., *B. subtilis* with only 4% devoted to its production [20,29]. *B. velezensis* secondary metabolite arsenal with bioactive characteristics contains soluble (BSMs) and volatile organic compounds (VOCs) with a broad spectrum of activities.

VOCs are synthesized from the mediates of the primary metabolism (mostly from oxidation of glucose and tricarboxylic acid cycle) [30,31] and include alcohols, aldehydes, ketones, hydrocarbons, acids and terpenes [32]. These low-weight (100–500 Da) metabolites usually have less than 20 carbon atoms and lipophilic moiety in their structure [31]. They are involved in plant protection due to their strong antimicrobial activity leading to direct antagonism of plant pathogens such as *Sclerotinia sclerotiorum* [33], *Botrytis cinerea* [34], *Alternaria solani* [35], *Monilinia fructicola* [36] or *Ralstonia solanacearum* [37]. VOCs mainly affect fungal spores' germination and growth [38] or bacterial motility and biofilm formation [37]. Moreover, VOCs can induce plant immunity, as observed on *Arabidopsis thaliana* seedlings. When *A. thaliana* roots were treated with VOCs, synthesized by *B. amyloliquefaciens* IN937a and GBO3 strains, the lesions caused by pathogen *Pectobacterium carotovorum* were fewer as a result of inducing plant immunity [39]. Related to this, several studies associated the induction of systemic resistance to VOCs such as acetoin, 2,3-butanediol and 3-pentanol [39–42].

Furthermore, the genome of *B. velezensis*, contains eight known biosynthetic gene clusters (*srf*, *itu*/*bmy*, *fen/pps*, *dhb*, *bac*, *mln*, *bae* and *dfn*) encoding the biosynthetic enzymes responsible for the production of non-ribosomal metabolites such as cyclic lipopeptides (CLPs), siderophore, dipeptides as well as polyketides (PKs). Moreover, several gene clusters (*pzn*, *mrs*, *aml* and *acn*) are found in certain *B. velezensis* strains to encode ribosomal peptides, bacteriocins [29,43].

2.2.1 Non-ribosomally synthesized metabolites

Non-ribosomal peptides (NRPs) and PKs are metabolites whose synthesis does not require ribosomes but enzymatic complexes termed as non-ribosomal peptide synthetases (NRPSs), polyketide synthases (PKSs), or hybrid NRPS-PKS complex. In general, these enzymatic complexes consist of several modules encoded by corresponding genes grouped in operons [25] that act as an assembly-line catalyzing different steps of metabolite synthesis [44]. The modules are divided into at least three main domains (Fig. 1-1 for NRPS and Fig. 1-2 for PKS).

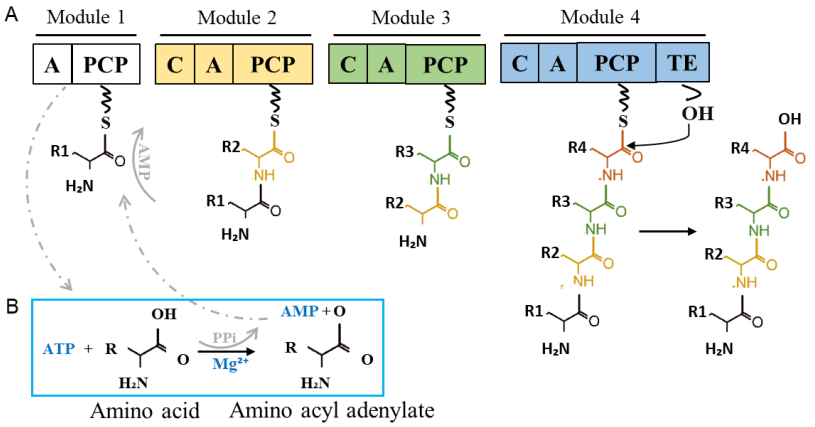

Figure 1-1. NRPS assembly-line (modified from Donadio *et al*. (2007)). A: NRPS enzymatic complex and the main domains of the modules: A: adenylation; C: condensation; PCP: peptidyl carrier protein; TE: thioesterase. B: The reaction of amino acid activation by A domain requires one molecule of adenosine triphosphate (ATP) and Mg^{2+}. The final product of the reaction is active amino acyl adenylate.

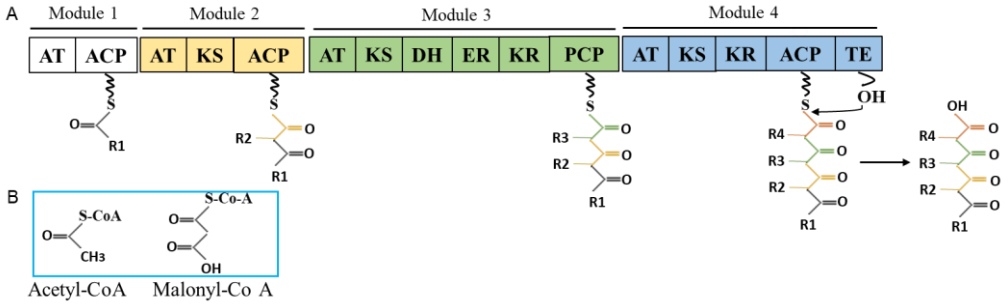

Figure 1-2. PKS assembly-line (modified from Donadio *et al.* (2007)). A: PKS enzymatic complex and the commonly found domains of the modules: AT: acyltransferase; ACP: acyl carrier protein; KS: ketosynthase; DH: dehydratase; ER: enoylreductase; KR: ketoreductase; TE: thioesterase. B: Monomers acetyl- and malonyl-CoA are used in the process of PKs synthesis.

The first domain represents the adenylation domain (A domain) in NRPS or acyltransferase domain (AT domain) in PKS. The A or AT domain specifically selects the substrate unit (monomer) such as amino or hydroxy acids and malonyl- or acetyl-coenzyme A (CoA), respectively [45,46]. In addition, A domain of NRPS activates the amino acid while this step is absent in AT domain of PKS (Fig. 1-1). Further, A and AT domains transfer the monomers to the peptidyl carrier protein (PCP domain) of NRPS or acyl carrier protein (ACP domain) of PKS, respectively

(Fig. 1-1, 1-2) where they form thioester bonds with monomers. To be able to play a carrier role, PCP/ACP domains have to be firstly transformed from the nonactive (apo-) to the activated (holo-) form (Fig. 1-3). This process requires the domain's reaction with coenzyme A and it is catalyzed by 4'-phosphopantetheine transferases (PPTase), an enzyme encoded by the *sfp* gene. Further, the condensation (C domain) in NRPS or ketosynthase domain (KS domain) in PKS catalyzes the formation of the bonds between the monomer of the upstream PCP/ACP domain and the elongating chain bound to the downstream PCP/ACP domain. (Fig. 1-1, 1-2) [25]. Finally, the last module of the assembly-line has a thioesterase domain (TE domain) that allows the detachment of the metabolite from the synthetase due to the hydrolysis of the thioester bond (Fig. 1-1, 1-2) [45,46].

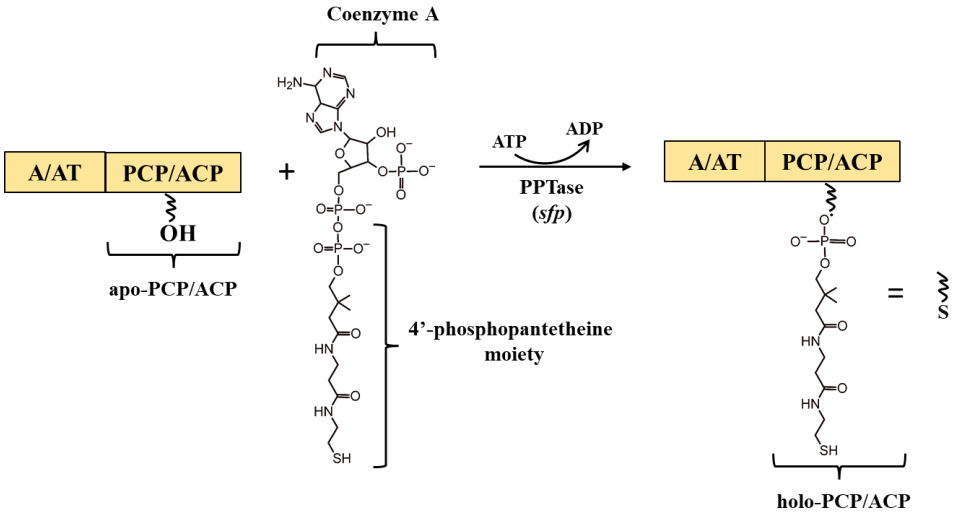

Figure 1-3. Post-translational activation of the PCP and ACP domains in NRPS and PKS. The serine residue of apo-PCP/ACP domains forms a bond with 4'-phosphopantetheine moieties of coenzyme A, in the presence of PPTase and ATP. The final product of the reaction is holo-PCP/ACP with the sulfhydryl (SH) group responsible for the thioester bond formations between monomers and carrier protein.

For some NRPs, a release is accompanied by cyclization (i.e., cyclic lipopeptides). In addition, epimerisation (E), methylation (M), reduction (R) or β-ketoreductase (KR), dehydratase (DH), malonyl-CoA transacylase (MCT), enoylreductase (ER), methylase (M) domains could be present in the synthetases [45]. These specific domains afford an immense structural diversity of products that result in a plethora of bioactivity [47].

2.2.1.1 Cyclic lipopeptides

Cyclic lipopeptides (CLPs) are NRPs composed of a cyclized peptidyl backbone linked to a hydrophobic fatty acid chain. They have a cyclic structure created by a link between two amino acids formed via an ester or amide bond [45]. The peptidic part is linked either to a β-hydroxy or a β-amino fatty acid (FA) chain added to the amino acid-activated in the first module of the NRPS. This FA chain can also be either linear (*n*-FA) or branched (*iso*-FA or *anteiso*-FA) [45].

Up to date, five families of CLPs have been reported to be produced by *Bacillus*: kurstakin, locillomycin, surfactin, fengycin and iturin. Seven amino acid CLPs, kurstakin, and nine amino acid CLPs, locillomycin are reported to be produced by *B. thuringiensis* and *B. subtilis*, respectively but not by *B. velezensis* [48,49]. However, *B. velezensis* has been found to produce surfactin, fengycin, and iturin with remarkable structural diversity [25,50].

Surfactin NRPS synthesis is encoded by four genes *srfAA-D* grouped in *srfA* operon [25,51]. The members of the surfactin family are composed of a heptapeptide ring which is bound to a β-hydroxy fatty acid moiety with 12 to 17 carbon atoms (Fig. 1-4). Besides variations in the number of carbon atoms, several changes in amino acid composition can occur at positions two, four and seven in the peptide ring, which allow the formation of surfactin variants (Fig. 1-4) [50–52]. Among these variants, commonly detected are pumilacidin and lichenysin among *B. pumilus* and *B. licheniformis* [52]. However, their production by *B. velezensis* is not confirmed so far [25].

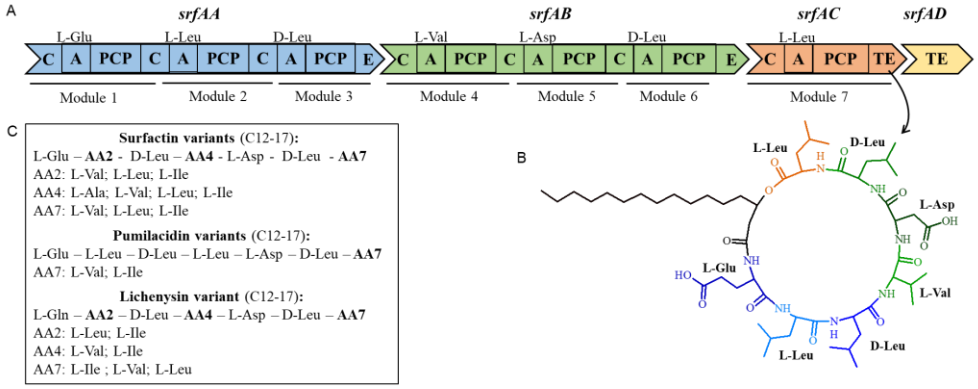

Figure 1-4. Illustration of surfactin synthesis (modified from Sieber and Marahiel (2005) and Théatre *et al*. (2021)). A: The *srfAA-D* genes of *srfA* operon (26.5 kb) encode four proteins (SrfAA-SrfAD) that form NRPS responsible for surfactin synthesis. The proteins SrfAA-C contain one to three modules encompassing A, C, PCP domains and E (epimerisation) domain that additionally catalyze the conversion of D-amino acid to its L-form. Above each A domain, the specific amino acid that the domain selects, activates and incorporates is indicated. The TE domain of SrfAC is responsible for the release and cyclization of surfactin. The SrfAD protein encodes the external thioesterase enzyme assumed to support amino acid activation in previous modules of the NRPS [45]. B: The canonical structure of surfactin C14. The amino acids involved in the structure are indicated by different colors and correspond to the amino acids presented in NRPS modules in A. Fatty acid chain is labeled in black. C: Potential surfactin structure diversity comprising the different compositions of amino acids and fatty acid chain length (C atom number).

Further, fengycin family encompasses fengycin A and B and, structurally similar, plipastatin A and B. The NRPS responsible for their synthesis is designated by *fenA-E* or *ppsA-E* genes grouped in the *fen* or *pps* operon, respectively [25] (Fig. 1-5). Fengycins and plipastatins are composed of ten amino acids, including non-proteogenic amino acid ornithine (Orn), linked to a β-hydroxy fatty acid chain with 14 to 19 atoms of carbon (Fig. 1-5). The different amino acid compositions at positions three, six and nine of the peptide can appear and form the aforementioned variants (Fig. 1-5) [50].

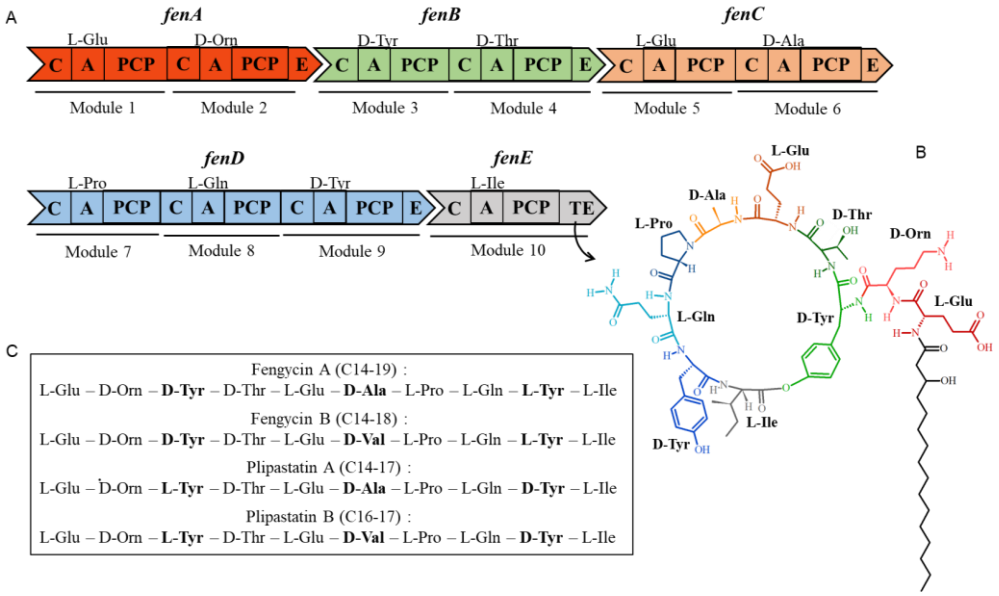

Figure 1-5. Illustration of fengycin synthesis (modified from Sieber and Marahiel (2005)). The *fenA-E* genes of *fen* operon (38.2 kb) encode five proteins (FenA-FenD) that form NRPS responsible for fengycin synthesis. FenA-E proteins contain one to three modules encompassing A, C, PCP and E domains. Above each A domain, the specific amino acid that the domain selects, activates and integrates is presented. The TE domain of FenE is responsible for the release and cyclization of fengycin. The synthesis of plipastatins follows the same rules. B: The structure of fengycin A. The amino acids involved in the structure are indicated by different colors and correspond to the amino acids presented in NRPS modules in A. Fatty acid chain is labeled in black. C: The fengycin and plipastatin structure diversity comprise the different compositions of amino acids and fatty acid chain length (C atom number).

The Iturin family includes CLPs such as iturin A, C, bacillomycin D, F, L or LC (bacillopeptin) and mycosubtilin. They are synthesized by hybrid PKS-NRPS complex as the first genes in the *itu* (synthesis of iturin), *bmy* (synthesis of bacillomycin) or *myc* (synthesis of mycosubtilin) operon are related to PKS synthesis (Fig. 1-6). Members of iturin family are composed of heptapeptide ring linked to β-amino fatty acid that can contain 13-18 carbon atoms and differ in the amino acid incorporated in the first, fourth, fifth, sixth or seventh position in the peptide ring [50,53] (Fig. 1-6).

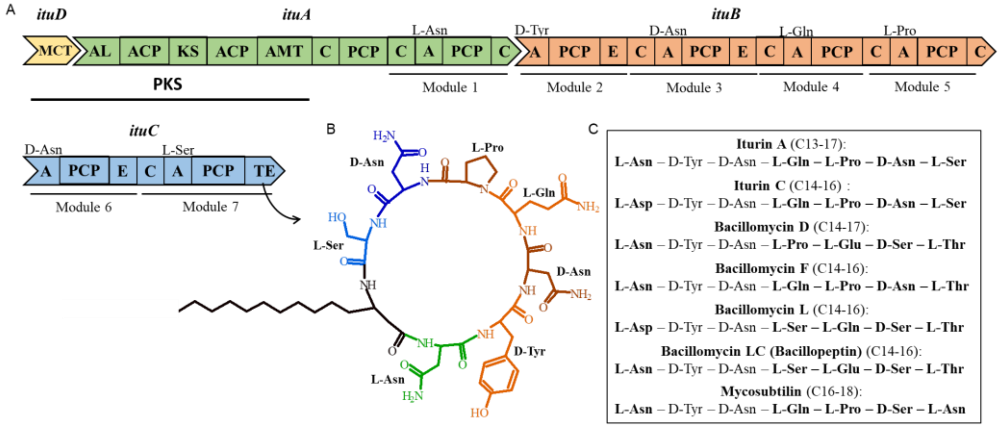

Figure 1-6. Illustration of iturin A synthesis (modified from Sieber and Marahiel 2005). The *ituA-C* and *ituD* genes of *itu* operon (38 kb) encode five proteins (ItuA-ItuD) of the PKS-NRPS hybrid complex responsible for iturin synthesis. The first protein (encoded by *ituD* in *itu* or *fenF* in *myc* and *bmy* operons) has malonyl-CoA transacylase (MCT) domain while the second protein (encoded by *ituA*) beside ACP and KS contains AL (acyl-CoA ligase) and AMT (amino transferase) domains present in PKS. Further proteins (ItuB and C) are related to the NRPS and thus the addition of amino acids into the assembly line. The synthesis of bacillomycin and mycosubtilin follow the same rules. B: The structure of iturin A. The amino acids involved in the structure are indicated by different colors and correspond to the amino acids presented in NRPS modules in A. Fatty acid chain is labeled in black. C. The iturin, bacillomycin and mycosubtilin structure diversity comprise the different compositions of amino acids and fatty acid chain length (C atom number).

2.2.1.2 Siderophore

The synthesis of siderophore bacillibactin requires three-modular NRPS complex encoded by *dhbA-F* genes, grouped in *dhb* operon. Bacillibactin is composed of 2,3-dihydroxybenzoic acid, glycine and threonine [54] (Fig. 1-7). As a final product, bacillibactin has trilactone ring and three catecholate units that allow strong affinity for iron and other metals, and thus their successful chelation [54].

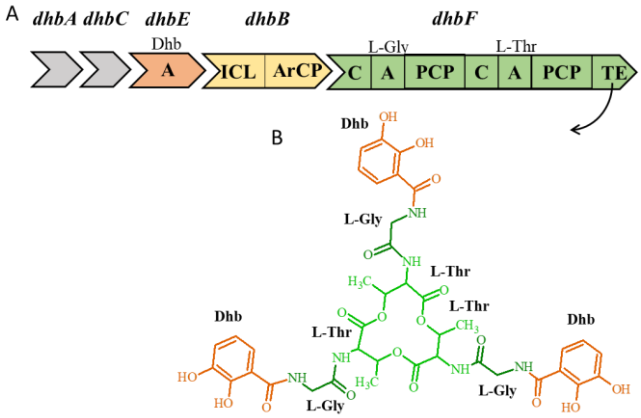

Figure 1-7. Illustration of bacillibactin synthesis (modified from May, *et al.* (2001)). The *dhbA, C, E, B, F* genes of *dhb* operon (12.8 kb) encode five corresponding proteins (DhbA-F) that form NRPS responsible for bacillibactin synthesis. The DhbC and DhbA are involved in the synthesis of the 2,3-dihydroxybenzoic acid monomer from chorismite (product of the primary metabolism) while DhbE, DhbB and DhbF are responsible for the additions of 2,3-dihydroxybenzoic acid (Dhb) to the aryl carrier protein (ArCP), glycine (Gly) and threonine (Thr) to PCP, respectively. Further, Dhb, glycine and threonine form the Dhb-Gly-Thr unit on the last PCP domain which is further transferred to the TE domain that catalysis the condensation and release of three Dhb-Gly-Thr units [54]. B: The structure of bacillibactin. The Dhb, Gly and Thr involved in the structure are indicated by different colors and correspond to the Dhb, Gly and Thr presented in NRPS modules in A.

2.2.1.3 Dipeptides

Bacilysin (syn. tetaine) and its chlorinated form, chlorotetaine, are dipeptides composed of a L-alanine and the nonproteinogenic amino acid L-anticapsin or chlorine-L-anticapsin, respectively [55,56]. They are synthesized by a specific non-thiotemplate NRPS enzymatic complex where the precursors are not amino acids but prephenate, a derivative of the aromatic amino acid pathway [57–59] (Fig. 1-8). Moreover, it has been shown that bacylisin synthesis does not depend on *sfp* [57,58].

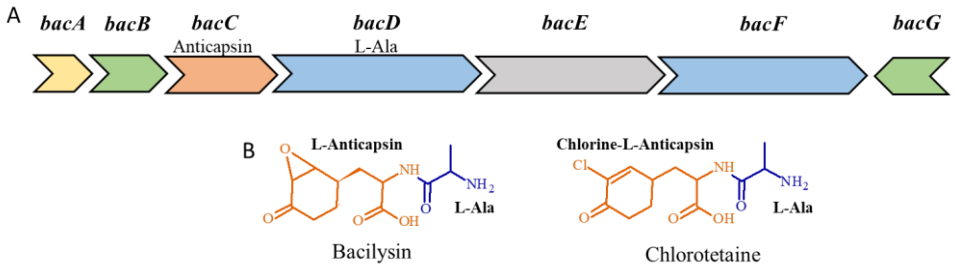

Figure 1-8. Illustration of bacylisin and chlorotetaine synthesis (modified from Parker and Walsh 2013; Wu et al, 2015). A: The *bacA-G* genes of *bac* operon (7.3 kb) encode seven proteins (BacA-G) forming non-thiotemplate NRPS responsible for bacylisin and chlorotetaine synthesis. The precursor of their synthesis, prephenate, is transformed to the anticapsin via the activity of BacABCGF [58]. The further addition of L-alanine amino acid (L-Ala) to the amino group of anticapsin is under the control of BacD. Further, *bacE* gene may be involved in self-resistance to bacilysin by permitting efflux of this antibiotic [57]. B: The structure of bacylisin and chlorotetaine. The anticapsin and L-Ala involved in the structure are indicated by different colors and correspond to the anticapsin and L-Ala presented in NRPS modules in A.

2.2.1.4 Polyketide

B. velezensis species co-produces three types of PKs difficidins, macrolactins, and bacillaenes [60,61]. Interestingly, the composition of domains in their PKS modules partially deviates from the ‘’classical’’ model proposed in Fig. 1-2 [25,60]. One of the most important differences is the absence of AT domains in PKS modules and, instead, the presence of *trans*-AT domains encoded by isolated genes. Thus, these *trans*-AT domains load ACP domains of each PKS module with acyl- or malonyl-CoA monomers, instead of their absent AT domains [60,62].

The bacillaene type of PKs includes bacillaene and dihydrobacillaene as the most commonly produced compounds of this group. They are PKs with a linear structure and are synthesized by multimodular hybrid NRPS-PKS complex, encoded by *bae* operon [63] (Fig. 1-9). This complex compasses three NRPS modules responsible for incorporation of α-hydroxy-isocaproic, glycine and alanine amino acids into assembly line, and three *trans*-AT domains that load PKS ACP domains with malonyl-CoA [64]. It has been proposed that the first product of the NRPS-PKS complex is dihydrobacillaene which can be further oxidized by cytochrome P450 and form bacillaene [63,65] (Fig. 1-9).

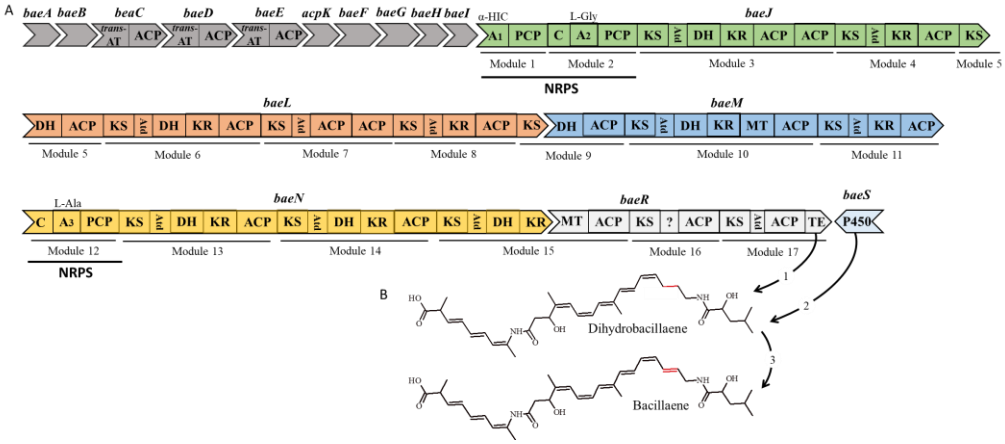

Figure 1-9. Illustration of dihydrobacillaene and bacillaene synthesis (adapted from Butcher *et al.* (2007)). A: The genes of *bae* operon (74 kb) encode synthesis of the hybrid NRPS-PKS complex responsible for the metabolite synthesis. The first genes of the *bae* operon, *baeA-I* and *acpK*, are involved in the synthesis of free-standing enzymes with three *trans*-AT domains. The core assembly-line is formed by the hybrid NRPS-PKS encoded by *baeJ-N* genes [64]. A domain of NRPS is distributed in modules 1, 2 and 12 and are responsible for the incorporation of α-hydroxy-isocaproic (α-HIC), L-glycine (L-Gly) and L-alanine (L-Ala) amino acids into the assembly line, respectively [64]. Other modules are related to the PKS and contain domains responsible for acceptation of malonyl monomers from *trans*-AT (ACP and Atd: AT docking), dehydration (DH), ketosynthesis (KS), ketoreduction (KR), transfer of methyl groups (MT) and release of the dihydrobacillaene form the assembly-line (TE) (1). The last gene of the operon *baeS* encodes the synthesis of cytochrome P450, which oxidases the C14′–C15′ bond of dihydrobacillaene (2) what results in the establishment of the double bond at this site and the formation of bacillaene (3). B: The structural difference between dihydrobacillaene and bacillaene is indicated in red.

Further, difficidin family comprises difficidin and oxydifficidin as the main structural variant produced. They are polyene metabolites made of a 22-member macrolide cycle and a phosphate group. Difficidin is synthesized by PKS which is encoded by *dfnA-N* genes grouped in *dfn* operon [61,66] (Fig. 1-10). The PKS contains one *trans*-AT domain responsible for the incorporation of the acetyl monomers to the assembly line [61] that results in the formation of difficidin that can be further hydroxylated by cytochrome P450 (encoded by *dfnM*) to form oxydifficidin [61,66] (Fig. 1-10).

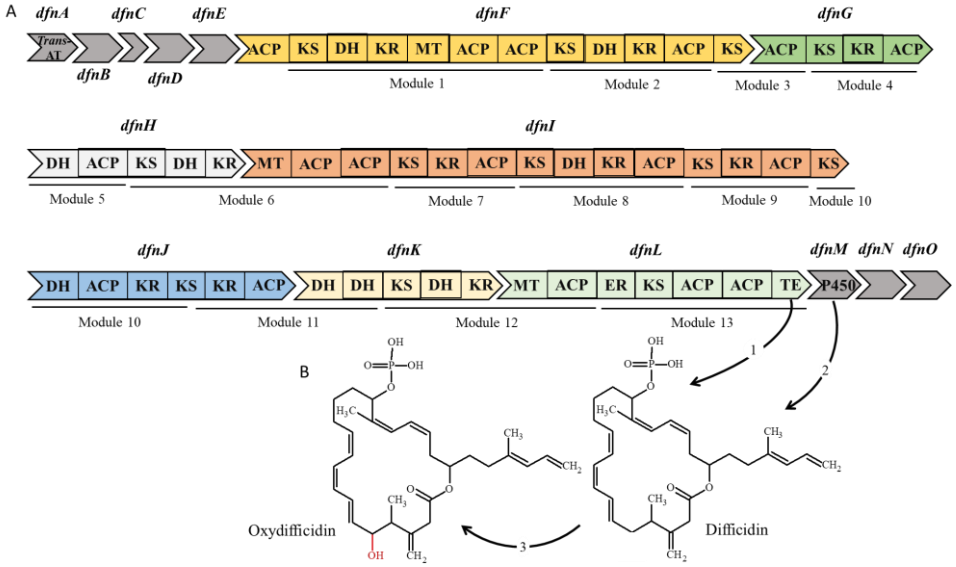

Figure 1-10. Illustration of difficidin and oxydifficidin synthesis (adapted from Chen *et al.* (2006)). A: The genes of *dfn* operon (71 kb) encode the synthesis of the PKS proteins (DfnA-O) responsible for the metabolite synthesis. The first protein, DfnA is a free-standing enzyme with one *trans*-AT domain, while DfnB protein is involved in the metabolite phosphorylation [61]. Further, genes *dfnC* and *dfnD* are assumed to be responsible for the synthesis of putative ACP and acyl-CoA synthetase, respectively. The DfnF-L comprises PKS modules with ACP, KS, DH, KR, MT and TE domains that use acyl-CoA from the *trans*-AT domain to synthesize difficidins (1). Further, among genes of the *dfn* operon, *dfnM* is found to encode cytochrome P450 monooxygenase, proposed to be involved in the incorporation of a hydroxyl group at position C5 in difficidin molecule (2), resulting in the formation of oxydifficidin (3) [61,66]. The last genes of the operon are *dfnN* and *dfnO* encode the synthesis of a protein with a function similar to a 3-hydroxy-3-methylglutaryl-CoA synthase and an enoyl-CoA hydratase, respectively [61]. B: The structural difference between difficidin and oxydifficidin is indicated in red.

Finally, macrolactins encompass several isoforms such as macrolactin A- R, 7-*O*-malonyl-macrolactin A and 7-*O*-succinyl-macrolactin A which are all 24-membered ring lactones synthesized by PKS, which is encoded by *mln* gene cluster that consists of *mlnA-H* genes [67] (Fig. 1-11). The PKS contains one *trans*-AT domain that loads malonyl-CoA on PKS modules [61,67]. Finally, macrolactin can be modified by the activity of external methyl-, acyl- and glycosyltransferases causing O-methylation, glycosylation, the addition of malonyl or succinyl residue, which lead to the synthesis of aforementioned macrolactin forms [60,67].

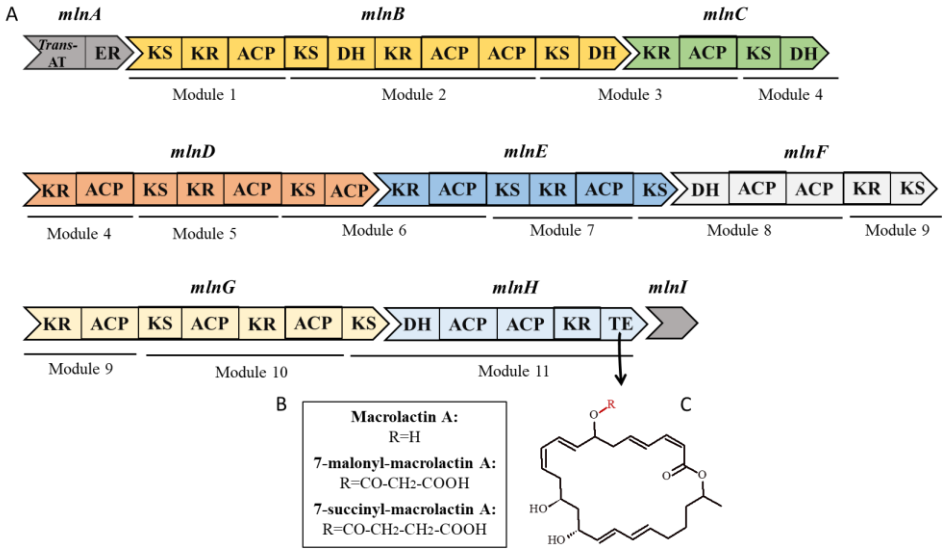

Figure 1-11. Illustration of macrolactin synthesis (adapted from Schneider *et al.* (2007)). A: The genes of *mln* operon (53.9 kb) are involved in synthesis of the MlnA-I proteins responsible for further macrolactin synthesis. The first MlnA contains one trans-AT domain, in charge for malonyl-CoA incorporation into further PKS modules, synthesized by *mlnB-H* [67]. These PKS modules contain ACP, KS, KR, DH and TE domains. The final step of macrolactin synthesis is the cyclization of the polyketide chain. B: The macrolactin structure diversity. C: The structure of the macrolactin. R group is labeled in red and corresponds to the group presented in B [67].

2.2.2 Ribosomally synthesized peptides

B. velezensis are producers of antimicrobial ribosomally synthesized and post-translationally modified peptides (RiPPs) such as lantibiotics (Lanthionine containing antibiotics), circular bacteriocins and microcins [47,68]. Their synthesis is encoded by the genes grouped in corresponding operons. In general, RiPP operon contains a group of structural genes, encoding amino acids involved in the synthesis of inactive precursor peptides, which are linked to an N-terminal leader sequence [68] (Fig. 1-12). The leader sequence may direct dehydration, efficient transport, and/or maintain the precursor inactive within the cell. The precursors are further post-translationally modified by the enzymes encoded by specific genes (Fig. 1-13) within the operon, in order to generate modified amino acids. During this process, the leader sequence of RiPP precursors is cleaved to create the mature active molecule [43,69] (as illustrated in Fig. 1-12 on the example of lantibiotic synthesis). To exert its antimicrobial activity, precursor or mature RiPP have to be translocated across the cytoplasmic membrane by specific transporters which are encoded by corresponding genes (Fig. 1-13) within the operon. Additionally, several genes (Fig. 1-13) of the operon encode a group of immunity proteins that protect the producer

against the RiPP antimicrobial effect, while several of them (Fig. 1-13) encodes regulatory proteins [68,69].

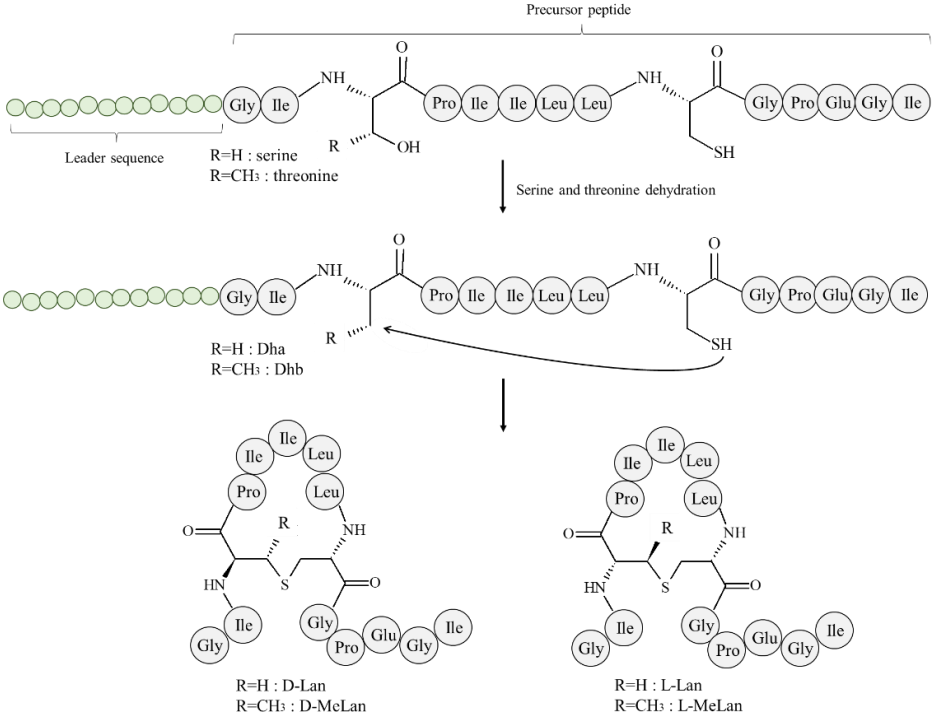

Figure 1-12. Illustration of the synthesis of lanthionine and β-methyllanthionine (adapted from [43,69]. During the formation of lanthionine and β-methyllanthionine bridges, Dha or Dhb and cysteine (Cys) are converted to Ala–S–Ala (alanine–S–alanine) or Abu–S–Ala (aminobutyrate–S–alanine), respectively.

B. velezensis produces several lantibiotics. During their synthesis, post-translational peptide modifications result in the generation of specific amino acids dehydroalanine (Dha) and dehydrobutyrine (Dhb). The Dha and Dhb can further react with a free cysteine in the peptide, forming thioether bridges called lanthionine (Lan) or methyl-lanthionine (MeLan), respectively [69] (Fig. 1-12). Lantibiotics could be divided into two subgroups: type-A and type-B [69]. Type A lantibiotics are positively charged (pH neutral) metabolites with linear secondary structures. Their precursors amino acids (encode by *lanA* gene) are modified by two distinct enzymes (LanD and LanC responsible for dehydration and cyclization, respectively) and are usually processed by one transporter (LanT). Among type A lantibiotics, ericins A and S (Fig. 1-13A), structurally similar to the subtilin (formed by *B. subtilis*), are produced by several *B. velezensis* strains (i.e., RC 218 and QST713) [29,70,71]. Type-B lantibiotics have a globular structure and are non- or slightly charged. They are modified by a single modification enzyme (LanM), responsible for both activities cited above and processed by two transporters [69]. In this

context, it has been well documented that some *B. velezensis* strains (i.e., B9601-Y2 and AMB-y1 and GB03) produce type B, mersacidin peptide containing 20 amino acids (Fig. 1-13B) [72–74]. Type-B lantibiotics also include the so-called two-component lantibiotics consisting of two synergistically acting peptides modified by a single enzyme. The type B lantibiotic, such as α-peptide amylolysin, is produced by several *B. velezensis* strains (i.e., GA1, S499) (Fig. 1-13C) [75,76]. In addition, the operon encoding synthesis of lantibiotics contains immunity proteins LanI and/or LanEFG and a two-component regulation system LanR-K that regulates the synthesis of the metabolite [69].

Furthermore, *B. velezensis* (i.e., GA1, S499) can produce circular non-lantibiotic RiPP amylocyclicin [77,78]. The mature peptide contains 64 amino acids and specific head-to-tail cyclization occurred between the N-terminal Leu and the C-terminal Trp [77] (Fig. 1-13D).

Several *B. velezensis* strains (i.e., FZB42, Rs-MS87, Sc-K143, LM2302) have been found to produce microcin-type RiPP, plantazolicin [79–81]. Plantazolicin is a linear peptide, characterized by the presence of oxazoles (Oxz, MeOxz), thiazoles and heterocyclic amino acids [82]. As a mature peptide, plantazolicin consists of the core peptide composed of 14 amino acids (Fig. 1-13E) [79,82].

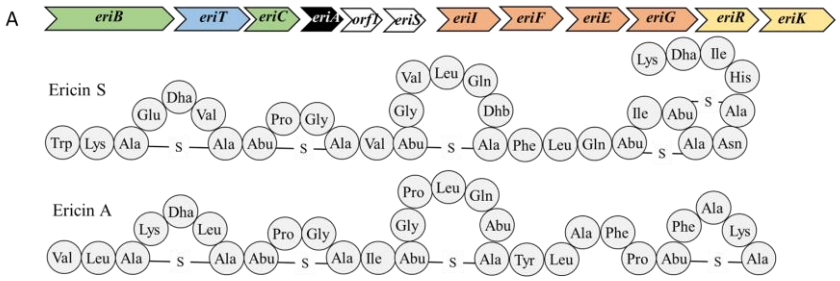
A
eriB
eriT
eriC
eriA
orf1
eriS
eriI
eriF
eriE
eriG
eriR
eriK
Ericin S
Ericin A

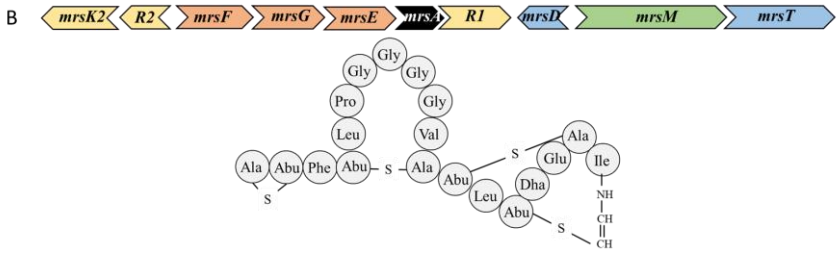
B
mrsK2
R2
mrsF
mrsG
mrsE
mrsA
R1
mrsD
mrsM
mrsT

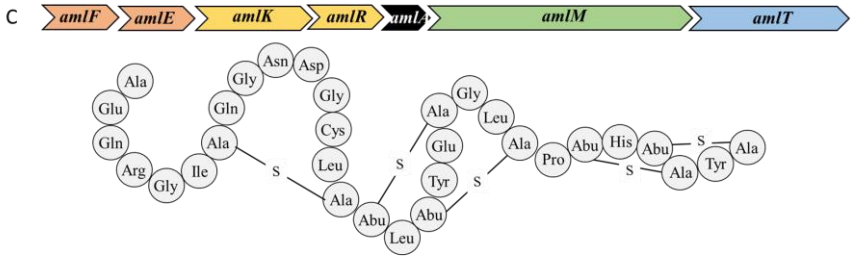
C
amlF
amlE
amlK
amlR
amlA
amlM
amlT

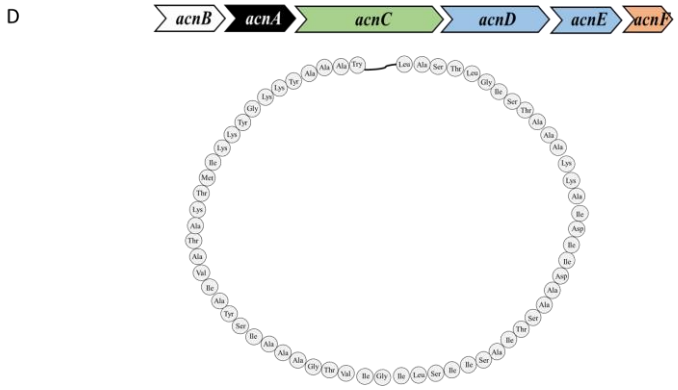
D
acnB
acnA
acnC
acnD
acnE
acnF

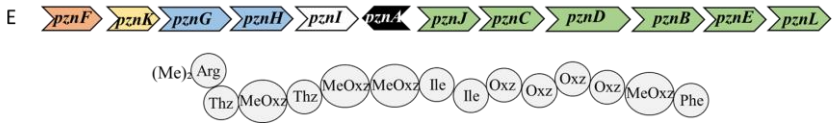
E
pznF
pznK
pznG
pznH
pznI
pznA
pznJ
pznC
pznD
pznB
pznE
pznL

Figure 1-13. Illustration of the organization of biosynthetic operon and schematic structure illustration of the RiPP produced by *B. velezensis*. Structural genes are indicated in black and genes involved in the maturation process in green. Genes involved in transporter synthesis, regulation and proteins responsible for immunity function are represented as blue, yellow and orange, respectively. Genes with unknown functions are labeled as white. A: ericins (adapted from Palazzini *et al.* (2016)), B: mersacidin (adapted from Emam and Dunlap (2020)), C: amylolysin (adapted from Arguelles Arias *et al.* (2013, 2014)), D: amylocyclicin (adapted from Scholz *et al.* (2014)) and E: plantazolicin (adapted from Banala *et al.* (2013)).

3. Natural functions of BSMs produced by *B. velezensis*

The multiple beneficial aspects of *Bacillus* rely on the ability to produce a wide range of chemically diverse BSMs. Firstly, these BSMs are involved in plant root colonization via stimulation of motility and biofilm formation, thereby largely contributing to *Bacillus'* ecological fitness. The successful root colonization further enables *Bacillus* access to the nutritional pool of root exudates and physical support for its further development. Secondly, these BSMs can be highly beneficial for the host plant, i.e., by providing plant protection from phytopathogens. Besides depriving pathogens of space and nutrients, *Bacillus* can stimulate induced systemic resistance (ISR) or directly act as an antagonistic agent due to its BSMs arsenal [20,43]. Thus, during the last decades, *Bacillus* potential use as biocontrol agents with protective activity toward economically important plant pathogens has been highlighted, thereby representing a promising alternative to chemical pesticides [12,20–22,83].

3.1 Motility, biofilm formation, and root colonization

Primary to the successful *Bacillus* root colonization, its motility towards the root surface is enhanced by the plant roots exuding organic metabolites (i.e., organic acids, phyto-siderophores, sugars, vitamins, amino acids) acting as a chemoattractant for *Bacillus* [9,84–86]. In general, *Bacillus* motility can be active swarming which depends on flagellar moves or passive, such as sliding translocation on the surface. To date, it has been well documented that surfactin family is the main BSM family involved in both types of *Bacillus* motilities [87–92], most probably due to its amphiphilic characteristics contributing to the reduction of surface tension [93] and its ability to promote flagellar synthesis [92].

Once it reaches roots, *Bacillus* attempts to attach to the root surface and form biofilm. Biofilm formation capability is broadly present within the *Bacillus* genus. It represents one of the most important characteristics for successful root colonization and protection of the cells from unfavorable surrounding factors [94–96]. Biofilm consists of a non-motile multicellular community coated with an extracellular matrix composed mainly of exopolysaccharides. The majority of these exopolysaccharides contribute to biofilm formation and its architecture. At the same time, some of them,

such as protein EpsE, are responsible for the transition of the cells from motile to the sessile state by inhibition of flagellar rotation [97]. Further, the extracellular matrix contains TasA, TapA protein fibers, which provide structural integrity of biofilm [98], and BslA protein which affords hydrophobicity to the biofilm community [99,100]. Like motility, biofilm formation in *Bacillus* is strongly impacted by surfactin production [101]. Surfactin contribution is primarily due to its ability to act as a signal which induces the phosphorylation of Spo0A [101], the master regulator of *Bacillus* sporulation and an indirect regulator of biofilm formation [102]. Moreover, a recent study showed the influence of surfactin produced by *B. subtilis* 3610 on the expression of *tapA* gene responsible for the synthesis of TapA fiber protein [103]. On the other hand, another study has been recently demonstrated that biofilm formation by *B. subtilis* 3610 did not require surfactin, the only CLP produced by the strain. This finding indicates that the role of surfactin in biofilm formation could be more complex than previously described and may also require other *Bacillus* BSMs [104]. Further, Luo *et al.* (2015) suggested that iturin-like, bacillomycin can play a key role in biofilm formation. However, the same study showed that in synergy with bacillomycin, surfactin was involved in the biofilm formation and improved rice leaves colonization of *B. subtilis* 916 [105]. In agreement, it has been shown that bacillomycin D produced by *B. velezensis* SQR9 increased the expression of genes involved in biofilm formation [106] while fengycin and iturin improved it in *B. velezensis* Y6 and F7 strains [107]. Up to date, iturin was not found to affect biofilm formation when acting alone.

3.2 Induced systemic resistance

Like other PGPRs, i.e., *Pseudomonas* and *Serratia*, *Bacillus* can indirectly contribute to plant protection by stimulating ISR in the host plant. ISR is based on activating a latent defense mechanism named priming. Priming occurs on a transcriptional level and is associated with the expression of genes, regulated mainly by the plant hormones jasmonic acid and ethylene [108–111]. Priming caused by PGPR results only in slight transcriptome changes, which are further intensified by the pathogen's attack. Thus, priming is viewed as a mechanism acting to prepare and accelerate the defense of the whole plant to more efficiently fight future phytopathogen attacks [108–111]. Up to date, numerous chemically diverse, small-size elicitors have been described [112].

Among *Bacillus* BSMs, surfactin is the most studied and recognized as the main elicitor stimulating the ISR of various host plants [113]. For instance, surfactin produced by *B. velezensis* FZB42, triggered ISR in lettuce plants and contributed to the plant protection against *Rhizoctonia solani* [114]. Furthermore, surfactin activation of ISR has been well documented in other dicotyledons to fight against *B. cinerea* in bean, tomato and *A. thaliana* [115,116], *Podosphaera fusca* in melon [117], rhizomania disease vector *Polymyxa betae* in sugar beet [118], *Colletotrichum gloeosporioides* in strawberry [119], and *Plasmopara viticola* in grapevine [120]. The effective pathogen suppression due to surfactin activation of ISR was reported

to the lesser extent also in monocotyledons and is directed against *Zymoseptoria tritici* in wheat [121] and *Magnaporthe oryzae* in ryegrass [122]. Interestingly, it has been discovered that surfactin's potential for ISR induction may depend on its chemical structure. For instance, surfactin variants with long fatty acid chains (C14-C15) have been found to cause ISR more efficiently than the short-chain variants (C12-13) [123].

Stimulation of host plant ISR has been, to a lesser extent, reported for the members of fengycin and iturin families. It has been recently shown that iturin and fengycin produced by *B. velezensis* GA1, in synergy, induced ISR in rice plants and protected them from *Pyricularia oryzae* [124]. For instance, fengycin induced ISR in several pathosystems and protected tomato against *B. cinerea* and *Sclerotinia sclerotiorum* [115,120] or grapevine against *P. viticola* [125]. On the other hand, iturin variants activated ISR against *C. gloeosporioides* in strawberry [119], *Phytophthora capsica* in chili pepper [126], *Z. tritici* in wheat [121] and *Verticillium dahliae* in cotton [127]. Moreover, iturin was the most efficient *Bacillu*s CLP causing plant defense stimulation in grapevine [128]. However, several studies showed that iturin, produced by *B. velezensis* S499 and *B. subtilis* UMAF6639 failed to induce ISR in tobacco [129] and melon [117]. Thus, it can be assumed that CLPs show certain specificity for each pathosystem.

Finally, the molecular mechanisms of ISR induction by *Bacillus* elicitors are still poorly understood. As demonstrated for surfactin, it might act by insertion into the cell membrane where it interacts with the membrane lipids, causing the membrane's disruption, rather than being precepted via a membrane receptor [123,130].

3.3 Antagonism

B. velezensis BSMs have great potential in plant protection as they can directly affect the growth of numerous plant pathogens and pests. These metabolites are known to be active against (micro)-organisms such as viruses (i.e., macrolactin A against herpes simplex viruses [67]), nematodes (i.e., plantazolicin A against *Meloidogyne incognita* [131]) and insects (*B. thuringiensis*). However, most of them are well recognized for their antifungal and antibacterial activities.

3.3.1 Antifungal activity

The major compounds with antifungal activities produced by *B. velezensis* are CLPs, especially iturin and fengycin families. The mode of action of these metabolites is based on their amphiphilic characteristics and related to fungal plasma membranes distortion. It is assumed that CLPs are forming pores in the fungal membrane and disrupting transmembrane ion fluxes leading to the fungal cell lysis, which can cause fungal cell death [132–134]. In this context, it has been evidenced that bacillomycin D and fengycin produced by *B. velezensis* FZB42 and C06 could cause hyphae and conidia damage of *Fusarium graminearum* [135,136] and *Monilinia fructicola* [137], respectively. Similarly, iturin and fengycin produced by

B. velezensis GA1 inhibited mycelial growth and spore formation of *P. oryzae* [124]. Moreover, fengycin produced by *B. subtilis* and *B. velezensis* successfully affected *Rhizopus stolonifera* [138], *M. grisea* [139], *F. oxysporum* [140] or *R. solani* [141] but could also inhibit the synthesis of destructive mycotoxin produced by *F. graminearum* [136]. Further, iturin produced by *B. velezensis* HN-a and AK-0 [142] or bacillomycin D from *B. subtilis* fmbJ [143] act against *C. gloeosporioides* and *Aspergillus flavus* [144], respectively. The variations in the structure of iturin could influence its activity. In this context, it has been shown that bacillomycin D, produced by *B. velezensis* 83, with a shorter fatty acid chain (C14), was less active than the one with a longer fatty acid chain (C15-17) against *C. gloeosporioides* [145]. The same study further indicated that bacillomycin D had different antifungal activities against the same pathogen depending on the physiological stage of the fungi, affecting rather a mycelium than spores [145]. Finally, the antifungal activity of surfactin in biologically relevant concentrations has not been reported so far. However, it has been noted that antifungal activity could be performed in synergy with mycosubtilin, produced by *B. subtilis* Bs2504 and BBG131 strains, against *F. oxysporum* f. sp. *iridacearum* [146].

In addition, the siderophore bacillibactin can show antimicrobial activity. Bacillibactin's mode of action is mainly related to its ability to chelate iron and make it unavailable for plant fungal pathogens [147]. However, it has been shown that bacillibactin, produced by *B. velezensis* SQR9, antagonized *F. oxysporum*, *F. solani* and *P. parasitica* in synergy with CLPs (bacillomycin D, fengycin, and surfactin) [148]. However, up to the knowledge, there is no evidence of individual bacillibactin antimicrobial activity. Among other non-ribosomally synthetized metabolites, it has been shown that PK macrolactin, produced by *B. velezensis* NJN-6, could inhibit the growth of *F. oxysporum* [149] while dipeptide bacylisin, produced by *B. amyloliquefaciens* 17A-B3 and *B. subtilis* 30B-B6, was active against oomycete *P. infestans* [147].

3.3.2 Antibacterial activity

The antibacterial activity of *B. velezensis* is mainly related to the PKs and RiPPs. They exhibit antibacterial activities by inhibiting protein and bacterial cell wall synthesis or forming pores in the cell membrane, leading to cell death [43,150].

For example, it has been shown that difficidin, produced by *B. velezensis* FZB42, inhibited *E. amylovora* [151], *Xanthomonas oryzae* [152] and *R. solanacearum* while its structural variant, oxydifficidin, showed three times stronger activity against the latter pathogen, demonstrating structure-dependent activity [153]. Furthermore, macrolactin produced by *B. velezensis* CLA178 has also been reported to be active against *A. tumefaciens* [154]. Finally, bacillaene has been found to suppress *E. amylovora* [151] and protect *Bacillus* spp. cells against the degrading-enzymatic activity caused by competitors (*Streptomyces* sp. Mg1 and *Myxococcus xanthus*) [155–157]. Furthermore, bacteriocin amylocyclicin, produced by *B.*

velezensis FZB42, appeared to exhibit activity against *C. michiganensis*, while strains Bac IH7 and Bac14B inhibited the growth of *A. tumefaciens*, *Pseudomonas* spp. and *P. carotovora* [77,158,159]. On the other hand, the antibacterial activity of amylolysin, ericins, plantazolicin A and mersacidin is directed mainly against Gram-positive bacteria [70,76,79,150].

Additionally, several data indicated the involvement of dipeptide bacilysin, produced by *B. velezensis* FZB42, in inhibition of peptidoglycan synthesis in pathogenic bacteria such as *E. amylovora* and *X. oryzae* [151,152]. The antibacterial activity of fengycin and iturin have been sporadically noted against *R. solanacearum* [140,160], *Pectobacterium carotovorum*, *X. campestris* [161,162] and *X. axonopodis* pv. *vesicatoria* [163].

4. Factors influencing *B. velezensis* metabolite and phenotypic traits

As rhizosphere-dwelling bacteria, plant-associated *B. velezensis* are influenced by various abiotic environmental factors, such as temperature, pH, moisture, light, and nutrient composition [164]. Moreover, in this competitive niche, *Bacillus* species are also surrounded by biotic factors such as host plants and a myriad of other (micro)organisms [10,165–167] that can impact BSMs production and phenotypic traits dictating their ecological fitness. However, gaining a precise knowledge of the exact impact of each factor is difficult due to their constant and complex interactions in the natural environment [164].

4.1 Abiotic factors

4.1.1 Oxygen

Oxygen represents one of the most important elements constantly consumed by plants and microorganisms and it is further involved in cellular respiration and various biochemical and physiological processes [168]. The physiochemical changes of the soil (i.e., water content, soil structure) can also influence the level of oxygen what often leads to its depletion [169]. However, how oxygen reduction can affect *Bacillus* BSMs production is scarce. In this context, several studies showed that the lack of oxygen could decrease expression of the genes related to iturin and fengycin production in *B. velezensis* S499 but also in *B. subtilis* ATCC6633 and *B. megaterium* MTCC8280 cells [170–172]. On the other hand, the oxygen starvation did not decrease surfactin production by *B. velezensis* S499 and *B. subtilis* BGS3 in the rhizosphere [171,173]. Moreover, the enhanced production of surfactin in bioreactor conditions was reported in *B. subtilis* ATCC21332 and BS-37 strains [174].

4.1.2 Temperature

Temperature stress is one of the main factors influencing *Bacillus*'s primary and secondary metabolism. As the natural temperature of the soil is lower than the one

usually obtained in the laboratory conditions, it is important to understand better the impact of lower temperatures similar to the natural environment. In this context, it has been well documented that low temperature led to an increasement in CLPs production by several *B. velezensis* [175–177]. A recent study demonstrated that the temperature corresponding to the one in the soil, of 16°C, appeared optimal for the surfactin production by *B. velezensis* 1B-23 [177]. Similarly, the exposition to the temperature of 15°C resulted in increasement of surfactin production by *B. velezensis* S499 in tomato and bean which improved motility and colonization, in contrast to the temperatures more than 35°C [175]. This enhancement can be related to the effect of the low temperature on the down-regulation of genes encoding RapF and RapH repressors of surfactin gene expression and its production [178,179]. Moreover, low temperature may balance the decreased growth of *B. velezensis* S499 on tomato and bean roots, sustaining its potential to trigger ISR under low-temperature conditions [175]. However, the effect of the temperature appears to be strain-dependent as the obtained increased surfactin production by *B. velezensis* S499 and FZB42 could not be found in *B. velezensis* QST713 [175]. Moreover, it has also been demonstrated that lower temperature can increase surfactin production in *B. velezensis* FJAT-2349 [176], oppositely to *B. velezensis* FJAT-46737 where a higher temperature caused a higher production of surfactin [140].

The influence of temperature on the production of other *Bacillus* CLPs was sporadically investigated. It has been shown that iturin synthesis by *B. velezensis* S499 or *B. subtilis* RB14 and ATCC6633 strains could be significantly improved by decreasing the temperature from 37 to 25°C [180–182].

4.1.3 pH

The production of BSMs by *B. velezensis* under the effect of pH is scarce. Few researches were done on *B. subtilis* where it has been shown that its surfactin production is decreased at pH5 [174]. In this context, it has been documented that lipopeptide biosynthesis is ideal in slightly-acidified to neutral pH conditions. This pH value is commonly found in the rhizosphere due to the content of plant root exudates and microbial activities [183,184].

4.2 Biotic factors

4.2.1 Interaction with host plant

Plant roots exudates represent the principal supply of carbon sources to plant-associated bacteria and are essential for bacterial rhizosphere establishment [9,86]. Furthermore, several studies showed that root exudates are species-specific and serve as an important signal molecule between the plant roots and rhizosphere organisms, influencing bacterial development and metabolite production [185–187].

In this context, it has been shown that the exudates of maize such as organic acids (citric, malic, and oxalic acids), amino acids (glycine, proline and phenylalanine) and sugars (glucose, fructose, sucrose) acted as a very strong chemoattractant to *B.*

velezensis FZB42 and strain S3-1, what improves their motility and biofilm formation [188,189].

Further studies provided more insights into *B. velezensis* BSMs production changes upon a perception of plant exudates. It has been shown that compared to sugars, the organic and amino acids from tomato root exudates significantly improved the production of surfactin, by *B. velezensis* S499 [171]. Additionally, the same study indicated that organic and amino acids improved the synthesis of surfactin C15, compared to sugars, showing how carbon sources can modulate the presence of different homologs of a metabolite. In agreement, Hoff *et al.* (2021) illustrated that tobacco root exudates promoted *srfAA* gene expression in *B. velezensis* GA1 and enhanced the production of surfactin homologs with a long fatty acid chain and variants containing valine [190]. Furthermore, this study demonstrated the positive effect of cell wall polymer homogalacturonan on surfactin production [190]. Besides homogalacturonan, xylan was also found to act as a trigger of surfactin biosynthesis [116,191,192]. These studies also showed *Bacillus* improved motility, biofilm formation, early root colonization and plant-host ISR [116,190–193]. Similarly, it has been demonstrated that maize and cucumber root exudates improved the expression of genes related to the synthesis of fengycin, surfactin and PKs in *B. velezensis* FZB42 and SQR9 [188,194,195].

On the other hand, these plant signals can act as a ‘’call for help’’ molecules in the presence of phytopathogens. Related to this, several studies showed how root exudation could be changed in the presence of plant pathogens. For example, the presence of cucumber pathogen *F. oxysporum* f. sp. *cucumerinum* increased the attractiveness of this plant to *B. velezensis* SQR9 by changing the proportion of chemoattractant compounds such as citric and fumaric acid [196,197]. A similar observation of improved *B. velezensis* 32a motility and colonization has been noted upon infection of tomato roots by *Agrobacterium tumefaciens* [198]. On the other hand, *A. thaliana* foliar infection by *P. syringae* also induced root secretion of L-malic acid, attracting *B. subtilis* FB17 and stimulating its biofilm formation [199]. So far, up to ten metabolites of root exudate compounds, such as amino acids, organic acids or sugars, have been characterized to positively influence *B. subtilis* NCIB 3610 and *B. velezensis* SQR9 root colonization [186,200–202].

4.2.2 Interaction with fungi

Many studies have illustrated the impact of phytopathogenic fungi on BSMs production by plant-associated *B. velezensis*. Some *B. amyloliquefaciens*, *B. velezensis*, and *B. subtilis* strains respond to the presence of antagonistic fungi by stimulating the production of the antifungal CLPs fengycin and/or iturin (Table 1-1). The production of specific CLPs varies in a species-dependent manner, but it is also highly dependent on the interacting fungal species. For example, much higher production of iturin and fengycin by *B. subtilis* 98S was observed in confrontation with *Pythium aphanidermatum* and *F. oxysporum* but not with *B. cinerea* [203]. Further, upon interaction with fungi, some *B. velezensis* strains (SQR9, FZB42, and

S499) overproduced either iturin or fencycin [114,148,204]. For instance, Li *et al.* (2014) showed that *B. velezensis* SQR9, confronted with *Sclerotinia sclerotiorum*, overproduces bacillomycin D (iturin family), but not fengycin. An overproduction of bacillomycin and reduced production of fengycin was also reported by Chowdhury *et al.* (2015) upon *B. velezensis* FZB42 interaction with *R. solani* in the rhizosphere of lettuce plants. Differentially, Kulimushi *et al.* (2017) showed that strains S499 and FZB42 improved the production of fengycin but not iturin upon interaction with *Rhizomucor variabilis*. Most of these studies also indicated that fengycin and iturin are the main BSMs responsible for antifungal activities (Table 1-1). Thus, *Bacillus* cells could specifically sense the presence of fungal competitors and accordingly overproduce appropriate antifungal BSMs to outcompete the interacting fungi. Moreover, besides modulating the production of fengycin and iturin, some strains of *B. velezensis* (SQR9, FZB42, and QST713) and *B. subtilis* (B9-5) may overproduce surfactin when sensing phytopathogenic fungi [114,148,205,206]. In support of this hypothesis, surfactin production of *B. velezensis* FZB42 was highly induced in the presence of fungal pathogen *R. solani* in the lettuce rhizosphere where it was found as the main produced compound [114]. A similar response was recorded when *B. velezensis* SQR9 was confronted with *S. sclerotiorum* and *Phytophthora parasitica* [148] or when *B. subtilis* B9-5 interacted in liquid medium with *Rhizopus stolonifer* [205]. In contrast to fengycin and iturin, surfactin is not strong direct antifungal metabolites in biologically relevant concentrations [207]. Thus, it stays unclear why *Bacillus* responded by surfactin overproduction to the presence of antagonistic fungi. A possible explanation could be rooted in its global role in rhizosphere colonization, thereby contributing to competition for nutrients and space with the interacting fungi [50,208].

Even though the siderophore bacillibactin is produced by all members of the *B. subtilis* complex, its possible overproduction upon microbial interactions has been poorly investigated. Interestingly, Li et al. (2014) showed that *B. velezensis* SQR9 overproduces bacillibactin when grown in the presence of a range of fungi, including *V. dahliae*, *S. sclerotiorum*, *F. oxysporum*, *R. solani*, *F. solani*, and *P. parasitica*. This may be interpreted as a response of the bacterium to some iron limitation in medium caused by fungal chelators.

Also, in *B. subtilis*, the expression of many BSMs biosynthesis genes is transcriptionally fine-tuned by compound-specific regulation and global regulators, governing the transition to crucial developmental processes like motility, biofilm formation and sporulation [209–211]. Fungal triggers may affect both types of regulatory systems involved in BSMs production. For instance, upon sensing *F. verticillioides*, the global stress-related regulator SigB is activated in *B. subtilis* NCIB3610 which in return enhances surfactin production [212]. In interaction with *F. culmorum* under biofilm-conducive conditions, *B. subtilis* Bs12 down-regulates the expression of the *sinR* gene known as a repressor of biofilm formation, which also negatively regulates surfactin production [213–215].

These observations strongly suggest that specific soluble signals emitted by fungal pathogens, could be perceived by bacilli which in turn modulate BSMs synthesis. Bartolini et al. (2019) observed that cells of the *Bacillus* colony, physically close to the fungal culture, responded to their signals by over-expressing genes coding transcription factors involved in CLPs synthesis regulation. In contrast, colony cells positioned on the opposite side of the fungi did not react to the fungus [212]. This phenomenon indicates that the specific fungal metabolite diffuses on a short distance and influences closely located *Bacillus* cells. Currently, no fungal compounds have been identified as triggers of BSM stimulation in *Bacillus*. Nonetheless, few commonly produced metabolites by *Fusarium* species were suggested to modify *Bacillus* behavior. It was shown that two cyclic depsipeptides (enniatins B1 and enniatins A1) and a pyrone (lateropyrone) had an antagonistic effect on *B. subtilis* growth [216]. Fusaric acid also modified the antibacterial activity of *B. mojavensis* but it was not related to a decrease in the production of specific BSMs [217–219]. These metabolites could also play a triggering role at sub-inhibitory concentration and could have an inducible effect on the range of *Bacillus* responses, as has been shown for other signal metabolites [220,221].

Differentially, the impact of plant-growth-promoting fungi and arbuscular mycorrhizal fungi on BSMs production by *Bacillus*, in general, is limited. In this context, the recent study showed the synergistic effect of *B. velezensis* Bs006 and *Trichoderma virens* Gl006, in a consortium, against cape gooseberry wilt caused by *F. oxysporum* f. sp. *physalis.* Additionally, it has been shown that *B. velezensis* Bs006 improved antifungal activity of *T. virens* Gl006. However, no impact of *T. virens* Gl006 on *B. velezensis* Bs006 has been demonstrated [222]. However, overproduction of BSMs has also been reported upon the interaction of *B. subtilis* 22 with *T. atroviride* SG3403 or *B. amyloliquefaciens* 1841 and *T. asperellum* GDFS1009 [223,224].

Table 1-1. Change in expression and bioactivity of BSMs produced by members of *B. subtilis* group, upon interaction with fungal species.

''0'' indicates no changes, ''+'' enhanced and ''-'' decreased BSMs production by *Bacillus* upon interaction with fungi. ''Yes'' indicates fungitoxic activity, ''No'' no antifungal activity, ''ND'' indicates that BSM with antifungal activity is not detected.

BSMs	Change in expression	Involvement in antifungal activity	*Bacillus* species (strains)	Fungal species	Ref.
Fengycin	0	Yes	*B. subtilis* (98S)	*B. cinerea*	[203]
	+	Yes	*B. subtilis* (98S)	*F. oxysporum*	[203]
	+	No	*B. subtilis* (98S)	*P. aphanidermatum*	[203]
	+	Yes	*B.velezensis* (S499)	*R. variabilis*	[204]
	+	Yes	*B. velezensis* (FZB42)	*R. variabilis*	[204]
	0	Yes	*B. velezensis* (QST713)	*R. variabilis*	[204]
	+	Yes	*B. velezensis* (SQR9)	*Verticillium dahliae*	[148]
	+	Yes	*B. velezensis* (SQR9)	*F. oxysporum*	[148]
	+	Yes	*B. velezensis* (SQR9)	*Phytophthora parasitica* var. *nicotianae*	[148]
	-	mediating the plant defense expression	*B. velezensis* (FZB42)	*R. solani*	[114]
	+	ND	*B. subtilis* (B9-5)	*R. stolonifer*	[205]
	+	ND	*B. subtilis* (B9-5)	*Fusarium sambucinum*	[205]
	+	ND	*B. subtilis* (B9-5)	*V. dahliae*	[205]
	+	ND	*B. velezensis* (QST713)	*Trichoderma aggressivum* f. *europaeum*	[206]

Iturin	0	Yes	*B. subtilis* (98S)	*B. cinerea*	[203]
	+	Yes	*B. subtilis* (98S)	*F. oxysporum*	[203]
	+	No	*B. subtilis* (98S)	*P. aphanidermatum*	[203]
	+	No	*B. velezensis* (SQR9)	*V. dahliae*	[148]
	+	No	*B. velezensis* (SQR9)	*S. sclerotiorum*	[148]
	+	Yes	*B. velezensis* (SQR9)	*F. oxysporum*	[148]
	+	Yes	*B. velezensis* (SQR9)	*P. parasitica*	[148]
	+	mediating the plant defense expression	*B. velezensis* (FZB42)	*R. solani*	[114]
Surfactin	+	Yes	*B. velezensis* (SQR9)	*S. sclerotiorum*	[148]
	+	Yes	*B. velezensis* (SQR9)	*R. solani*	[148]
	+	Yes	*B. velezensis* (SQR9)	*Fusarium solani*	[148]
	+	Yes	*B. velezensis* (SQR9)	*P. parasitica*	[148]
	+	mediating the plant defense expression	*B. velezensis* (FZB42)	*R. solani*	[114]
	+	ND	*B. subtilis* (B9-5)	*R. solani*	[205]
	+	ND	*B. subtilis* (B9-5)	*F. sambucinum*	[205]
	+	ND	*B. subtilis* (B9-5)	*V. dahliae*	[205]
	+	ND	*B. velezensis* (QST713)	*T. aggressivum f. europaeum*	[206]

Bacillibactin	+	Yes	*B. velezensis* (SQR9)	*V. dahliae*	[148]
	+	No	*B. velezensis* (SQR9)	*S. sclerotiorum*	[148]
	+	No	*B. velezensis* (SQR9)	*F. oxysporum*	[148]
	+	Yes	*B. velezensis* (SQR9)	*R. solani*	[148]
	+	Yes	*B. velezensis* (SQR9)	*F. solani*	[148]
	+	Yes	*B. velezensis* (SQR9)	*P. parasitica*	[148]

4.2.3 Interaction with bacteria

Up to date, data concerning *B. velezensis* response to other bacterial species are scarce and there is little direct evidence for enhanced expression of BSMs upon these interbacteria interactions. The only convincing examples of such stimulation of BSMs were reported upon *Bacillus* interaction with plant pathogens, such as *R. solanacearum* [225] and *P. fuscovaginae* [226]. These two studies showed improved expression of surfactin, bacilysin and iturin biosynthesis genes when *Bacillus* and pathogens were grown together in dual-cultures (Table 1-2). Nevertheless, no clear indication about the enhanced production of the aforementioned BSMs based on their quantification nor improved antibacterial activities of *Bacillus* was presented as a result of this interaction. On the other hand, the recent study indicated reduced production of CLPs but an improved synthesis of bacillibactin by *B. velezensis* FZB42 upon interaction with *X. campestris* pv. *campestris*, when compared to the monoculture [162] (Table 1-2).

However, some *Bacillus* BSMs may act as molecular determinants driving outcomes of interactions between *B. subtilis* and bacterial competitors as illustrated for the bacillaene polyketide displaying an essential protective role for survival in competition with *Streptomyces* and *Myxococcus* soil isolates [155,156,227]. In agreement, it has been recently shown that *B. velezensis* FZB42 utilizes bacillaene to protect itself from *P. chlororaphis* PCL1606 and thus co-exist with this interacting PGPR [228].

Interestingly, at the phenotypical level, the development of soil bacilli is differentially altered upon sensing other bacteria from the same natural environment (Table 1-2). Some of these phenotypical changes can be associated with or modulated production of specific BSMs. First, exogenous antibiotics or signals may stimulate biofilm formation which depends, to some extent, on surfactin production

[210,229] and which may be viewed as a defensive response against exogenous toxic compounds and/or infiltration by competitors [95,230,231]. For instance, *B. subtilis* increased its relative subpopulation of biofilm matrix-producing cells or increased wrinkle formation in response to small molecules secreted by other bacterial species [210,229,232,233]. On the other hand, it has been recently shown that *B. velezensis* SQR9 can successfully establish biofilm and synergistic interaction with another plant-associated bacteria, *P. stutzeri* XL272. During the interaction, it has been observed that the presence of *P. stutzeri* XL272 downregulated six pathways related to amino acids synthesis in *B. velezensis* SQR9. This specific response of *B. velezensis* SQR9 has been further correlated with possible reduction of the metabolic costs related to these pathways and the cross-feeding phenomenon between bacteria, as the main amino acids could be compensated by the ounces produced by *P. stutzeri* XL272 [234]. Similarly, the biofilm formation of *B. subtilis* and *B. amyloliquefaciens* was improved in the presence of *Agrobacterium*, *Variovorax*, *Brevundimonas* and *Methylobacterium* by an unknown mechanism [235]. However, no change in surfactin production associated with the stimulation of biofilm was reported in these studies.

Besides biofilm formation, other mechanisms drive bacteria to initiate protective responses upon the detection of competitors (Table 1-2). The flagellum-independent sliding motility is considered as an adaptive mechanism that allows bacterial cells to physically relocate in the context of a competitive interaction [236–238]. Upon sensing *S. venezuelae* or *Streptomyces* sp. Mg1, the *B. subtilis* ability to slide was increased [221,239]. It depends partly on the production of surfactin [240,241], but a potential boost in lipopeptide synthesis upon the perception of the *Streptomyces* challenger was not demonstrated. Chloramphenicol and derivatives or linearmycins produced by *S. venezuelae* or *Streptomyces* sp. Mg1, respectively, were identified as molecular triggers acting at subinhibitory concentrations for inducing *Bacillus* motility [221,239].

Some bacteria promote sporulation in *B. subtilis* which represents another example of alteration of the physiological development of this species (Table 1-2). In the context of distant interactions, exogenous siderophores accelerate the differentiation of *Bacillus* cells into spores. It was notably shown for enterobactin from *E. coli* and for ferrioxamine E produced by *Streptomycetes* [242]. In iron-limited environments, *B. subtilis* cells would thus respond by taking up those “piratable” siderophores and start sporulating. This is not a general response to xenosiderophores since, for instance, pyochelin from *Pseudomona*s does not affect *Bacillus* sporulation [231]. Nevertheless, the ability of siderophore to alter cellular differentiation in *B. subtilis* suggests that those molecules are likely to mediate complex microbial interactions in iron-depleted conditions, as often met in a soil environment. However, induction of *B. subtilis* sporulation by other bacteria may also occur in a cell-to-cell contact or predator-prey situation. Upon interaction with *P. chlororaphis*, its type VI secretion system triggered sporulation, independently from its established role as cargo for delivering toxic effectors into the target *Bacillus* cells [231]. Differentially, soil

predatory bacteria, *Myxococcus xanthus* induced spore-filled megastructures formation in *B. subtilis* which served as a protection towards the predator [157].

That said, interspecies interactions may also result in inhibition rather than in stimulation of key developmental processes determining the fate of *Bacillus* multicellular communities. As an example, 2,4-diacetylphloroglucinol (DAPG) and linearmycins, broad-spectrum antibiotics synthesized by fluorescent *Pseudomonas* or *Streptomyces*, respectively, alter colony morphology and inhibits biofilm formation resulting in cell lysis and sporulation in *B. subtilis* populations grown adjacent to *P. protegens* or *Streptomyces* sp. Mg1 colonies [239,243] (Table 1-2). These antibiotics thus seem to act as interspecific signaling molecules that inhibit *Bacillus* differentiation but also activate the development of antibiotic resistance mechanisms to promote the competitive fitness of bacteria [243].

Table 1-2. The response of *B. subtilis* group members to the interaction with bacterial species.

‘’0‘’ indicates no changes, ‘’+’’ enhanced and ‘’-’’ decreased BSMs BGCs expression or phenotype in *Bacillus* upon interaction with bacteria and ‘’ND’’ indicates not detected bacterial trigger or its mode of action.

***Bacillus* response**	**Change**	**Bacterial trigger**	**Mode of action**	***Bacillus* species (strains)**	**Bacterial species (strains)**	**Ref.**
BSMs BGCs expression						
iturin, surfactin, bacilysin	+	ND	ND	*B. amyloliquefaciens* (Am1)	*R. solanacearum*	[225]
fengycin	-	ND	ND	*B. amyloliquefaciens* (Am1)	*R. solanacearum*	[225]
iturin, surfactin, fengycin, bacilysin	+	ND	ND	*B. amyloliquefaciens* (D29)	*R. solanacearum*	[225]
iturin, surfactin, bacilysin	+	ND	ND	*B. amyloliquefaciens* (Bk7)	*P. fuscovaginae*	[226]
bacillibactin	0	ND	ND	*B. velezensis* (FZB42)	*X. campestris* pv. *campestris*	[162]
surfactin, fengycin,	-	ND	ND	*B. velezensis* (FZB42)	*X. campestris* pv. *campestris*	[162]

bacillomycin						
all BSMs BGC	-	ND	ND	*B. velezensis* (SQR9)	*P. stutzeri* (XL272)	[234]
Growth						
	-	DAPG	ND	*B. subtilis*	*P. protegens* (Pf-5)	[243]
	-	linearmycins	ABC transpo-rter YfiLMN	*B. subtilis*	*Streptomyces* sp. (Mg1)	[239]
Motility						
	+	linearmycins	ND	*B. subtilis*	*Streptomyces* sp. (Mg1)	[239]
	+	Chloramphen icol and derivatives	ND	*B. subtilis*	*S. venezuelae*	[221]
Biofilm						
	+	surfactin, Skf and Sdp cannibalism toxins	activation of KinC	*B. subtilis* (NCIB3610)	*B. subtilis* (NCIB3610)	[210]
	+	surfactin, cannibalism toxins	activation of KinD	*B. subtilis*	*Bacillus* spp.	[232]
	+	hypoxanthine	ND	*B. subtilis* (168)	*Lysinibacillus fusiformis* (M5)	[229]
	+	exopolysacch -aride	amyloid-like protein TasA	*B. subtilis*	*P. agglomerans*	[233]
	+	ND	ND	*B. velezensis* (SQR9)	*P. stutzeri* (XL272)	[234]
	-	DAPG	ND	*B. subtilis*	*P. protegens* (Pf-5)	[243]
	+	ND	ND	*B. subtilis, B. amyloliquefaciens*	*Agrobacterium, Variovorax,Brev-undimonas* and *Methylobacterium*	[235]

Sporulation						
	+	T6SS	via KinA and KinB	*B. subtilis* 3610	*P.chlororaphis* (PCL1606)	[231]
	+	predation	ND	*B. subtilis* NCIB3610	*M. xanthus*	[157]
	+	enterobactin and ferrioxamine E	activation of ybbA,	*B. subtilis* NCBI3610	*E. coli* (JW0578), *Streptomyces*	[242]
	-	DAPG	ND	*B. subtilis*	*P. protegens* (Pf-5)	[243]

5. Objectives and research strategy

Thanks to advanced genomics, analytics and imaging technologies, substantial progress has been made in deciphering the molecular basis of microbial interactions. However, the steadily growing insights gained from the last decades also illustrate how complex and diverse chemical dialogue and warfare can be, involving various BSMs underpinning interactions between isolates from competitive niches like the rhizosphere [166,167]. However, our knowledge of BSMs modulations and their direct ecological relevance under the interactions is still limited.

In the context of plant-associated bacilli, which represent one of the most important members of the rhizosphere community, some of these BSMs appeared to be boosted as an outcome of interactions with plant pathogenic fungi (see Chapter 1). This is of ecological value since *Bacillus* employed boosted BSMs to directly antagonize the interacting fungal pathogens, bringing benefit to plant protection and its better persistence upon such interaction [12,244,245]. By contrast to the interaction with fungi, direct evidence for an impact of inter-bacteria interactions on the expression of the secondary metabolome in *Bacillus* is still poorly understood. Nevertheless, interaction-mediated variations in phenotypic traits such as colony morphology, motility [221,239], biofilm formation [95,96,210,230,232,233,235], or sporulation [157,242] illustrate how soil bacilli can protect themselves from antimicrobials emitted by bacterial competitors. Thus, we assume that such bacterial impact on key developmental processes of *Bacillus* is coupled with significant modulation in the production of *Bacillus* specific BSMs, which are driving these phenotypes.

In that context, this thesis's **general objective** is to understand better the molecular interactions between rhizosphere bacilli and bacterial competitors from the same niche. We wanted to focus on *B. velezensis* as a model for plant-associated species.

We used *Pseudomonas* as a challenger in order to characterize the effects of *Pseudomonas* on *B. velezensis* phenotype and secondary metabolite production.

This work thus includes three specific objectives:

- understanding the roles of BSMs, produced by interacting bacteria, that they can play in such interspecies interaction,
- deciphering to what extent the production of *B. velezensis* BSMs can be modulated upon this interaction,
- exploring how this interaction affects *B. velezensis* ecological competitiveness and phenotypic traits crucial for rhizosphere establishment and persistence in that niche.

The main criteria to choose *Pseudomonas* spp. to confront to *B. velezensis* were that 1) these bacteria are prominent among the rhizosphere microbial community, 2) they have been amply described as plant beneficial bacteria with biocontrol capacities, 3) they are genomically well-characterized and 4) they produce a wide array of secondary metabolites (e.g., phenazine, phloroglucinol, pyoluteorin, pyrrolnitrin, CLPs). Finally, the high diversity of metabolites allows investigating the interplay between BSMs from both species, as possibly the main drivers of interbacterial interaction.

To reflect the real situation in the natural environment, where microbes are not necessarily in direct physical contact with neighboring cells, we performed most experiments in contact-independent settings, *in vitro* bipartite system adequate to uncovering cell-cell communication cues. Moreover, most of the research was conducted using nutritional conditions reflecting the content in major carbon sources released by roots of Solanaceae plants in the rhizosphere. In addition, to evaluate the relevance of the results in a more natural context, the experimental procedure was also included *in planta* conditions, with both bacteria interacting upon tomato root co-colonization.

Chapter 2

Lipopeptide interplay mediates molecular interactions between soil bacilli and pseudomonads

This chapter is adapted from: Andrić S., Meyer T., Rigolet A., Prigent-Combaret C., Höfte M., Balleux G., Steels S., Hoff G., De Mot R., McCann A., De Pauw E., Argüelles Arias A. and Ongena M. (2021). Lipopeptide interplay mediates molecular interactions between soil bacilli and pseudomonads. *Microbiology Spectrum*, 8:e0203821

1. Introduction

Bacilli, belonging to the *Bacillus subtilis* complex, are ubiquitous members of the rhizosphere microbiome, which contains a subset of the bulk soil microbes that evolve to dwell in this compartment surrounding roots, nutrient-enriched due to continued exudation [10,166,246]. Among these species, *Bacillus velezensis* is emerging as a model for plant-associated bacilli, displaying strong potential as a biocontrol agent reducing diseases caused by phytopathogens [247]. *B. velezensis* is distinguished from other species of the *B. subtilis* group by its richness in biosynthetic gene clusters (BGCs, representing up to 13% of the whole genome) responsible for the synthesis of bioactive secondary metabolites (BSMs) [25,248]. This chemically diverse secondary metabolome includes volatiles, terpenes, ribosomally synthesized lantibiotics and bacteriocins (RiPPs), non-ribosomally (NR) synthesized metabolites such as polyketides (PKs), dipeptides, siderophores and cyclic lipopeptides (CLPs) [208,249]. Due to their amphiphilic and antimicrobial properties, CLPs of the surfactin, iturin and fengycin families are clearly involved in the biocontrol activity of the producing strains via direct inhibition of phytopathogenic microbes and/or via stimulation of the plant immune system leading to induced systemic resistance (ISR) against aggressors [12,109,165,207,250]. Moreover, these multifunctional compounds may also act as drivers of some developmental traits in multicellular communities like biofilm formation and motility, thereby contributing more globally to bacterial competitiveness in the rhizosphere niche.

However, our knowledge about the production and biological activities of *Bacillus* CLPs or BSMs in general mainly relies on data obtained from monocultures of the producing strains which is far from natural conditions. Soil is indeed one of the richest ecosystems in terms of microbial diversity and abundance [251] but the scarcity of resources makes it also one of the most privileged environments for competitive interspecies interactions [166,167]. As the rhizosphere is more densely populated [167] than the bulk soil, it is assumed that microbial warfare in this habitat is even more intense. In that context, both rivalries for nutrients and interference competition are considered key factors driving microbial interactions and community assembly [252]. The production and role of *Bacillus* BSMs may thus undergo anticipated changes upon interaction with other species from the same niche but this interplay remains poorly understood [253]. Some previous works have illustrated how soil bacilli may adapt their behavior and protect themselves upon sensing bacterial competitors, notably by improving biofilm formation [95,96,210,220,232,233,235,254], enhancing motility [221,255] or inducing sporulation [157,242]. Most of these reports mainly focus on the adaptation of such developmental traits but there is little information about *Bacillus* response at the molecular level upon interspecies interactions [253].

It is why, through this work, we wanted to investigate further the possible roles of BSMs in the molecular interactions of *B. velezensis* with other bacterial species. We selected fluorescent pseudomonads as challengers because these bacteria are also

prominent among the rhizosphere microbial community [10,166,246,256]. Numerous species have been amply described for their biocontrol capacities, are genomically well-characterized and produce a wide array of secondary metabolites [257–259]. This includes various antibiotics (e.g., phenazine, phloroglucinols, pyoluteorin, pyrrolnitrin) but also CLPs formed by many species belonging to the *P. fluorescens* group. There is a huge structural diversity among *Pseudomonas* CLPs, reported to date, that are classified into 14 groups according to the length of the oligopeptide and the size of the macrolactone ring [260,261]. However, by contrast to *B. velezensis*, most plant-associated and beneficial *Pseudomonas* isolates only produce one type of CLP [262]. Studies on interactions between *Bacillus* and specific *Pseudomonas* isolates that have been reported recently revealed sophisticated competition strategies between these two genera [228,231,234,243,263].

Here, to highlight the possible role of BSMs as small-size diffusible compounds, we first used contact-independent settings to investigate pairwise interaction between *B. velezensis* and ten *Pseudomonas* isolates. The two bacteria initiated multifaceted interactions illustrated by *Bacillus* growth inhibition, enhanced motility and white-line formation near the *Bacillus* colony, as main outcomes. We could correlate these phenotypes with BSMs production and identify specific lipopeptides as the main compounds involved in the interference interaction and motile response. We also illustrated the relevance of these unsuspected roles of CLPs in the context of competitive tomato root colonization.

2. Material and methods

2.1 Bacterial strains and growth conditions

Strains and plasmids used in this study are listed in Table 2-1. *B. velezensis* strains were grown at 30°C on a half-diluted recomposed exudate (EM) [171] solid medium or in liquid EM with shaking (160 rpm). EM was prepared by combining 3 solutions (pH=7) after autoclaving, as follows: 1/4 of sugar solution (4 g L^{-1} glucose, 6.8 g L^{-1} fructose, 0.8 g L^{-1} maltose, and 1.2 g L^{-1} ribose), 1/2 of organic acid solution (8 g L^{-1} citrate, 8 g L^{-1} oxalate, 6 g L^{-1} succinate, 2 g L^{-1} malate, and 2 g L^{-1} fumarate), and 1/2 of all media [0.685 g L^{-1} KH_2PO_4, 21 g L^{-1} morpholinepropanesulfonic acid (MOPS), 0.5 g L^{-1} $MgSO_4$ x $7H_2O$, 0.5 g L^{-1} KCl, 1 g L^{-1} yeast extract, 1 g L^{-1} casamino acids, 2 g L^{-1} $(NH_4)_2SO_4$, and 100 ml of each trace solution of $Fe_2(SO_4)_3$ (12 g L^{-1}), $MnSO_4$ (4 g L^{-1}), $CuSO_4$ (16 g L^{-1}), and Na_2MoO_4 (40 g L^{-1})]. Mutants of *B. velezensis* GA1 were selected on an appropriate antibiotic (chloramphenicol at 5 µg mL^{-1}) in Lysogeny broth (LB) (10 g L^{-1} NaCl, 5 g L^{-1} yeast extract and 10 g L^{-1} tryptone). *Pseudomonas* spp. strains were grown on LB and casamino acid (CAA) solid and liquid medium (10 g L^{-1} casamino acid, 0.3 g L^{-1} K_2HPO_4, 0.5 g L^{-1} $MgSO_4$ and pH=7) with shaking (160 rpm), at 30°C. When necessary, *Pseudomonas* spp. mutant strains were selected on appropriate antibiotics (gentamycin 20 µg mL^{-1}, kanamycin 25 µg mL^{-1} or tetracyclin 10 µg mL^{-1}) on LB.

Table 2-1. Strains and plasmids used in this study.

	Relevant genotype, description (Genome bank number when sequenced)	References or sources
Bacillus velezensis		
GA1	Wild type (CP046386)	[264]
GA1 Δ*amyE*::cat P_{veg}-*gfpmut3* (called GA1 GFP)	GA1 disrupted of *amyE* gene; Cm^R and harbouring a constitutive transcriptional fusion (P_{veg}-*gfpmut3*).	This study
GA1 Δ*srfAA*::*cat*	GA1 deleted of *srfAA* gene; Cm^R; unable to produce surfactin	This study
S499	Wild type (NZ_CP014700)	[78]
FZB42	Wild type (NC_009725)	[265]
QST713	Wild type (NZ_CP025079)	[29]
Pseudomonas sessilinigenes		
CMR12a	Wild type (NZ_CP027706)	[266,267]
Δ*sesA*	CMR12a disrupted of *sesA* gene; Gm^R; unable to produce sessilin	[268]
Δ*ofaBC*	CMR12a deleted of *ofaB* and *ofaC* genes; Gm^R; unable to produce orfamide	[269]
Δ*phz*	CMR12a deleted of phenazine biosynthesis operon; unable to produce phenazine	[268]
Δ*sesA-ofaBC*	CMR12a disrupted of *sesA* gene and deleted *ofaB* and *ofaC* genes; Gm^R; unable to produce sessilin and orfamide	[269]
Δ*sesA-phz*	CMR12a disrupted of *sesA* gene and deleted phenazine biosynthesis operons; Gm^R; unable to produce sessilin and phenazine	[268]
Δ*ofaAC-phz*	CMR12a deleted of *ofaB* and *ofaC* genes and phenazine biosynthesis operons; unable to produce orfamide and phenazine	[269]
Δ*sesA-ofaBC-phz*	CMR12a disrupted of *sesA* gene and deleted *ofaB* and *ofaC* genes and phenazine biosynthesis operons; Gm^R; unable to produce sessilin, orfamide and phenazine	[269]
ΔpchA	CMR12a deleted of *pchA* gene; unable to produce enantio-pyochelin	This study
ΔpvdI	CMR12a deleted of *pvdI* gene; unable to produce pyoverdine	This study
ΔpvdI-pchA	CMR12a deleted of *pvdI* and *pchA* genes; unable to produce pyoverdine and enantio-pyochelin	This study
Pseudomonas protegens		
Pf-5	Wild type; orfamide producer (NC_004129)	[270]
CHA0	*mCherry* tagged derivative of CHA0; orfamide producer (NC_021237)	[271]
Pseudomonas chlororaphis		
JV497	*mCherry* tagged derivative of JV497; non-CLPs producer (NZ_VWPC00000000)	[258]
JV395B	*mCherry* tagged derivative of JV395B; non-CLPs producer (NZ_VWPB00000000)	[258]
Pseudomonas wayambapalatensis		
RW10S2	Wild type; WLIP producer	[272]
Pseudomonas mosselii		
BW11M1	Wild type; xantholysins producer	[273]
Pseudomonas putida		
WCU_64	Wild type; putisolvins producer	[274]
Pseudomonas lactis		

SS101	Wild type; massetolides producer (NZ_CM001513)	[262]
Pseudomonas kilonensis		
F113	Wild type; viscosines producer (NC_016830)	[275]
Pseudomonas tolaasii		
CH36	Wild type; tolaasin and pseudodesmin producer	[272]
CH36Δ*tolA*	CH36 disrupted of *tolA* gene; Gm^R; unable to produce tolaasin	[272]
E. coli		
DH5α*λpir*	*supE44, ΔlacU169 (ΦlacZΔM15), recA1, endA1, hsdR17, thi-1, gyrA96, relA1, λpir*	[276]
DH5α p497	Helper strain harboring p497 plasmid	C. Keel laboratory
Plasmids		
pGEM-T	pGEM-T Easy derivative harboring the recombinant region *amyE*::*cat* P_{veg}-*gfpmut3* ; Cm^R	[277]
pOT1eM	pOT1e derivative harboring *Ptac-m-cherry* inserted in Clal-Sall site ; Gm^R	[278]
pME6010-*eforRed*	pME6010 derivative harboring *PJ23101-eforRed* inserted in Xhol site; TetR	(T. Meyer, unpublished data)
pEMG	pSEVA212S; oriR6K, *lacZα* with two flanking I-*Sce*I sites; Km^r, Ap^r	[279]
pEMG-*pchA*	Suicide plasmid used for the deletion of *pchA*	This study
pEMG-*pvdI*	Suicide plasmid used for the deletion of *pvdI*	This study
pSW-2	oriRK2, *xylS*, P_m::*I-sceI*; Gm^R	[279]

2.2 Construction of deletion mutant of B. velezensis *GA1*

GA1 mutant unable to produce surfactin was constructed by marker replacement. Briefly, 1 kb of the upstream region of the *srfAA* gene, an antibiotic marker (chloramphenicol cassette) and downstream region of the *srfAA* gene was PCR amplified with specific primers (Table 2-2). The three DNA fragments were linked by overlap PCR to obtain a DNA fragment containing the antibiotic marker flanked by the two homologous recombination regions. This latter fragment was introduced into *B. velezensis* GA1 by natural competence induced by nitrogen limitation [280]. Homologous recombination event was selected by chloramphenicol resistance on LB medium. The *srfAA* gene deletion was confirmed by PCR analysis with the corresponding UpF (TCAGCAAAACTGCGTGGTAG) and DwR (AAGAAATGATCATAAATACC) specific primers and by the loss of the surfactin production.

Table 2-2. Primers used in this study.

Primer Name		Primer sequence (5'->3')	Targeted genes
Deletion mutant			
***B. velezensis* GA1**			
	UpsrfAAF	TCAGCAAAACTGCGTGGTAG	*srfAA*
	UpsrfAAR	CCAATTTTCGAATTCTTTTACCGCGATAAAAAGTTATTTC CATATGTGTGC	
	DwsrfAAF	CAGCTCCAGATCCTCTACGCCGGACACGCTTTATATCGTG CCGAA	
	DwsrfAAR	AAGAAATGATCATAAATACC	
***P. sessilinigenes* CMR12a**			
	UppvdIF	GGCATTCTTGACCGGTCGTC	*pvdI*
	UppvdIR	GTGTTGTCCATTACACAGCCTCCATTGCATTCATCGGGAG TCATCC	
	DwpvdIF	ATGGAGGCTGTGTAATGGACAACA	
	DwpvdIR	TGTAGCGGTGTAGCAGAG	
	pvdICheckF	CCTGCTGCTGGAAGGATTGA	
	pvdICheckR	GGATCGAGCTGCCAAAGGAA	
	UppchAF	GACCAACTGCCGGCGGAT	*pchA*
	UppchAR	CCTTCAGCGATCGGCCGGTGCATCACATCTTGCGCTCCTT GCTCC	
	DwpchAF	TGATGCACCGGCCGATC	
	DwpchAR	GTGGTGAAGCTTTCCATGCC	
	pchACheckF	TCATCCACTGGAACATCGCC	
	pchACheckR	GCGGACTGATTTCCTCGGTA	
Antibiotic marker			
	CatF	CGCGGTAAAAGAATTCGAAAA	Chloramphenicol marker
	CatR	GTCCGGCGTAGAGGATCTG	
	PhleoF	GTCATAGCTGTTTCCTGCCAAAAGGGGGTTTCATTTT	Phleomycin marker
	PhleoR	ACTGGCCGTCGTTTTACTCCAATAAATGCGACACCAA	
	KanF	GTCATAGCTGTTTCCTGCTTAGCTCCTGAAAATCTCGG	Kanamycin marker
	KanR	ACTGGCCGTCGTTTTACCTGATAATTACTAATACTAGGAG AAG	
	nptIIF	GAGGATCGTTTCGCATGATT	Kanamycin marker for *Pseudomonas*
	nptIIR	CGCTCAGAAGAACTCGTCAA	
	psw-F	GGACGCTTCGCTGAAAACTA	pSW-II insertion
	psw-R	AACGTCGTGACTGGGAAAAC	

Transformation of the GA1 strain was performed following the protocol previously described [280] with some modifications. One fresh GA1 colony was inoculated into LB liquid medium at 37°C (160 rpm) until reaching an OD_{600nm} of 1.0. Afterward, cells were washed one time with peptone water and one time with a modified Spizizen minimal salt liquid medium (MMG) (19 g L^{-1} K_2HPO_4

anhydrous; 6 g L^{-1} KH_2PO_4; 1 g L^{-1} Na_3 citrate anhydrous; 0.2 g L^{-1} $MgSO_4$ $7H_2O$; 2 g L^{-1} Na_2SO_4; 50 µM $FeCl_3$ (sterilized by filtration at 0.22 µm); 2 µM $MnSO_4$; 8 g L^{-1} glucose; 2 g L^{-1} L-glutamic acid; pH 7.0), 1 µg of DNA recombinant fragment was added to the GA1 cells suspension adjusted to an OD_{600nm} of 0.01 into MMG liquid medium. One day after incubation at 37°C with shaking at 165 rpm, bacteria were spread on LB plates supplemented with the chloramphenicol (5 µg mL^{-1}) antibiotic to select positive colonies.

To follow *B. velezensis* GA1 colonization of roots, we designed an integrative vector region containing *gfp* gene under the control of the *Veg* promoter (constitutive expression) which was further inserted into the GA1 chromosome by a double cross-over event at the *amyE* loci following the already described protocol [277]. The tagged cells were selected on solid LB containing 5 mg mL^{-1} of chloramphenicol at 30°C.

2.3 Construction of deletion mutants of P. sessilinigenes *CMR12a*

Enantio-pyochelin and pyoverdine mutants of CMR12a were constructed using the I-SceI system and the pEMG suicide vector [279,281]. Briefly, the upstream and downstream regions flanking the *pchA* (*C4K39_5481*) or the *pvdI* (*C4K39_6027*) genes were PCR amplified (primers listed in Table 2-2), linked via overlap PCR and inserted into the pEMG vector. The resulting plasmid (Table 2-1) was integrated by conjugation into the CMR12a chromosome via homologous recombination. Kanamycin (25 µg mL^{-1}) resistant cells were selected on King B agar plates and transformed by electroporation with the pSW-2 plasmid (harboring I-SceI system). Gentamycin (20 µg mL^{-1}) resistant colonies on agar plates were transferred to King B medium with and without kanamycin to verify the loss of the antibiotic (kanamycin) resistance. *Pseudomonas* mutants were identified by PCR with the corresponding UpF (GGCATTCTTGACCGGTCGTC *for pvdI* and GACCAACTGCCGGCGGAT for *pchA*) and DwR (GGATCGAGCTGCCAAAGGAA for *pvdI* and GCGGACTGATTTCCTCGGTA for *pchA*) specific primers and via the loss of enantio-pyochelin and/or pyoverdine production.

2.4 Construction of eforRed-tagged P. sessilinigenes *CMR12a Δ*sesA *mutant*

To monitor *P. sessilinigenes* CMR12a *ΔsesA* mutant colonization of roots, we introduced, by electroporation, into *P. sessilinigenes* CMR12a Δ*sesA* the pME6010-*eforRed* plasmid (Table 2-1). The *eforRed* gene was controlled by the PJ23101 promoter leading to its constitutive expression. Tetracycline (10µg/ml) resistant colonies containing the pME6010-*eforRed* plasmid were selected on agar KB plates, after 24 h incubation at 28 °C. The presence of plasmid into the *P. sessilinigenes*

CMR12a *ΔsesA* was visualized by the production of red-colored colonies due to the presence of eforRed proteins.

2.5 Pseudomonas *spp. metabolite production on solid medium*

To analyze metabolites produced by *Pseudomonas* spp. upon confrontation with GA1 on solid medium, produced metabolites from the area of agar (0.7 cm x 2.5 cm) near the colony was cut and transferred to Eppendorf tubes. The mass of the agar plug was recorded and 75% of acetonitrile (ACN) was added in proportion to the mass of the agar plug (50-50 (m/v)). The metabolites were extracted under continuous rotation shaking at room temperature (22°C) for 30 min. The samples were centrifuged for 2 min at 10000 rpm and the supernatant was filtrated on 0.22 µm before UPLC-MS analysis. Data are collected from two biological repetitions.

The procedure for sample preparation and analysis of BSMs production *in planta* are presented in the section ‘’Bacterial root colonization’’ below.

2.6 Confrontation, white-line formation and motility test

For confrontation assays on agar plates, *B. velezensis* and *Pseudomonas* spp. strains were grown overnight in EM and CAA liquid mediums, respectively. After bacterial washing in peptone water and adjustment of OD_{600nm} to 0.1, 5 µL of bacterial suspension was applied at a 1 mm distance onto CAA medium to observe white-line formation and inhibition. For the motility assay, bacterial suspension was applied at 1 mm, 5 mm and 7.5 mm distance onto an EM agar plate. Plates were incubated at 30°C and images were taken after 24 h. Photographs were captured using CoolPix camera (NiiKKOR 60x WIDE OPTICAL ZOOM EDVR 4.3-258 mm 1:33-6.5). Three technical repetitions within each of three biological repetitions were performed for all tested strains.

2.7 Pseudomonas *spp. cell-free supernatant extraction and metabolite production in liquid medium*

To analyze BSMs produced by *Pseudomonas* spp. and to test the effect of *Pseudomonas* spp. on *Bacillus* in a liquid medium, *Pseudomonas* spp. cell-free supernatants were first prepared. *Pseudomonas* spp. strains were grown overnight on LB solid medium, at 30°C. After washing in peptone water, the cell suspension was adjusted to OD_{600nm} 0.05 by resuspension in 100 mL of CAA or EM. Cultures were shaken at 120 rpm at 30°C for 48 h and then centrifuged at 5000 rpm at room temperature (22°C) for 20 min. The supernatant was filter-sterilized (0.22 µm pore size filters) and stored at -20°C until further utilization and UPLC-qTOF MS analysis.

2.8 B. velezensis *and* Pseudomonas *spp. interaction in liquid medium*

To study the effect of *Pseudomonas* spp. on the growth of *B. velezensis* strains, the continuous growth kinetics of *B. velezensis* was followed. Firstly, *B. velezensis* strains were grown overnight on LB solid medium, at 30°C. After washing in peptone water and adjusting cell OD_{600nm} to 0.1, the bacterial suspension has been transferred to microtiter 96-well plates in addition of 4% (v/v) *Pseudomona*s spp. supernatant with the final volume of 200 µL per well. Control remained un-supplemented. The growth kinetics of *B. velezensis* (OD_{600nm}) strains was followed every 30 min during 24 h with a Spectramax® (Molecular Devices, Wokingham, UK), continuously shaken, at 30°C.

To observe the effect of CMR12a on surfactin production by GA1 in a liquid medium, GA1 cells from preculture were washed and resuspended in 2 mL of EM liquid medium to a final OD_{600nm} of 0.1 and placed into a 24-well plate. The bacterial culture was supplemented with 4% (v/v) of CMR12a cell-free supernatant while the control remained un-supplemented. GA1 liquid cultures were shaken in an incubator at 300 rpm at 30 °C for 24 h. Afterward, the *Bacillus* supernatants were sampled at 24 h, centrifugated at 5000 rpm at room temperature (approx. 22°C) for 10 min to extract supernatants and the cells were collected. Further, cell-free supernatants were filtered (0.22 µm) and used for analytical analysis of surfactin production.

2.9 Analysis of BSMs produced by Pseudomonas *spp. and* B. velezensis *GA1*

The cell-free supernatants of *Pseudomonas* spp. and GA1, prepared as previously described, were analyzed by UPLC-MS and UPLC-qTOF MS. *Pseudomonas* spp. metabolites were identified using Agilent 1290 Infinity II coupled with DAD detector and Mass detector (Jet Stream ESI-Q-TOF 6530) in positive mode with the parameter set up as follows: capillary voltage: 3.5 kV; nebulizer pressure: 35 psi; drying gas: 8 L min^{-1}; drying gas temperature: 300°C; flow rate of sheath gas: 11 L min^{-1}; sheath gas temperature: 350°C; fragmentor voltage: 175 V; skimmer voltage: 65 V; octopole RF: 750 V. Accurate mass spectra were recorded in the range of m/z=100-1700. A C18-Acquity UPLC BEH column (2.1 × 50 mm × 1.7 µm; Waters, milford, MA, USA) was used at a flow rate of 0.6 mL min^{-1} and a temperature of 40°C. The injection volume was 5 µL and the diode array detector (DAD) scanned a wavelength spectrum between 190 and 600 nm. A gradient acidified water (0.1% formic acid) (solvent A) and acidified acetonitrile (0.1% formic acid) (solvent B) was used as mobile phase with a constant flow rate at 0.6 mL min^{-1} starting at 10% B and raising to 100% B in 20 min. Solvent B was kept at 100% for 4 min before going back to the initial ratio. MassHunter Workstation v10.0 and ChemStation software were used for data collection and analysis. Surfactin quantification was performed by using UPLC–MS with UPLC (Acquity H-class, Waters) coupled to a single quadrupole mass spectrometer (SQD mass analyzer,

Waters) using a C18 column (Acquity UPLC BEH C18 2.1 mm × 50 mm, 1.7 µm). Elution was performed at 40°C with a constant flow rate of 0.6 mL min^{-1} using a gradient of acetonitrile (solvent B) and water (solvent A) both acidified with 0.1% formic acid as follows: 2 min at 15% B followed by a gradient from 15% to 95% during 5 min and maintained at 95% up to 9.5 min before going back to initial conditions at 10 min during 2 min before next injection. Compounds were detected in both electrospray positive and negative ion mode by setting SQD parameters as follows: cone voltage: 60 V; source temperature 130°C; desolvation temperature 400°C, and nitrogen flow: 1000 L h^{-1} with a mass range from m/z 300 to 2048. MassLynx software v4.1 software was used for data collection and analysis. 3D chromatograms were generated using the open-source software MzMine 2 [282].

2.10 MALDI-FT-ICR MS imaging

Mass spectrometry images were obtained as recently described [283] using a FT-ICR mass spectrometer (SolariX XR 9.4T, (Bruker Daltonics, Bremen, Germany)) mass calibrated from 200 m/z to 2,300 m/z to reach a mass accuracy of 0.5 ppm. Region of interest from agar microbial colonies was directly collected from the Petri dish and transferred onto an ITO Glass slide (Bruker, Bremen, Germany), previously covered with double-sided conductive carbon tape. The samples were dried under vacuum and covered with an α-cyano-4-hydroxycinnamic acid (HCCA) matrix solution at 5 mg/mL (70 : 30 acetonitrile : water v/v). In total, 60 layers of HCCA matrix were sprayed using the SunCollect instrument (SunChrom, Friedrichsdorf, Germany). FlexImaging 5.0 (Bruker Daltonics, Bremen, Germany) software was used for MALDI-FT-ICR MS imaging acquisition, with a pixel step size for the surface raster set to 100 µm.

2.11 Bacterial root colonization

Root colonization patterns of the bacteria were performed on tomato plants under gnotobiotic conditions. Tomato seeds were primarily sterilized in 70% ethanol (v/v) by gently shaking for 2 min. Further, ethanol was removed and seeds were added to the 50 mL sterilization solution (4.5 mL of bleach-containing 9.5% of active chlorine, 0.01 g of Tween 80 and 45.5 mL of sterile water) and thus gently shaken for 10 min. Seeds were thereafter washed 10 times with water to eliminate sterilization solution residues. Further, sterilized seeds were placed on square Petri dishes (5 seeds per plate) containing Hoagland solid medium (14 g L^{-1} agar, 5 mL stock 1 [EDTA 5,20 mg L^{-1}; $FeSO_4x7H_2O$ 3,90 mg L^{-1}; H_3BO_3 1,40 mg L^{-1}; $MgSO_4x7H_2O$ 513 mg L^{-1}; $MnCl_2x4H_2O$ 0,90 mg L^{-1}, $ZnSO_4x7H_2O$ 0,10 mg L^{-1}; $CuSO_4x5H_2O$ 0,05 mg L^{-1}; 1 mL in 50 mL stock 1, $NaMoO_4x2H_2O$ 0,02 mg L^{-1} 1 mL in 50 mL stock 1], 5 mL stock 2 [KH_2PO_4 170 mg L^{-1}; 5 mL stock 3: KNO_3 316 mg L^{-1}, $Ca(NO_3)_2x4H_2O$ mg L^{-1}], pH=6,5) and were placed in the dark to germinate for three days. Further, 15 germinated seeds were inoculated with 2 µL of a $6.5x10^8$ CFU mL^{-1} suspension (i.e. $1.3x10^6$ CFU/plant) of GA1, $1.1x10^6$ CFU/mL suspension (i.e. $2.2x10^3$ CFU/plant) of JV497, $2.2x10^5$ CFU/mL suspension (i.e.

$4.5x10^2$ CFU/plant) of CMR12a or $1.1x10^5$ CFU/mL suspension (i.e. $2.2x10^2$ CFU/plant) of CMR12a Δ*sesA*. These inocula were prepared from overnight cultures, previously washed three times in peptone water. The appropriate strains (control) or a mix of GA1 and *Pseudomonas* cells (co-inoculation) were applied onto germinated seeds while the same volume of sterile water solution was added for uninoculated controls. The plants were grown at 22°C under a 16 h day / 8 h night cycle and 75% humidity for six days in the growth chamber.

For observing the effect of surfactin on GA1 root colonization upon (co-)inoculation of the tomato roots, slight changes in bacterial inoculation were implemented. For this purpose, 10 tomato seeds were inoculated with 2 µL of $1.2x10^8$ CFU mL^{-1} suspension of GA1 (i.e. $2.4x10^5$ CFU/plant), $1.1x10^8$ CFU/mL suspension of GA1 Δ*srfAA* (i.e. $2.3x10^5$ CFU/plant), $2.2x10^5$ CFU/mL suspension (i.e. $4.4x10^2$ CFU/plant) of CMR12a and $1.1x10^5$ CFU/mL suspension (i.e. $2.2x10^2$ CFU/plant) of CMR12a Δ*sesA* (control) or with a mix of *Bacillus* and *Pseudomonas* spp. cells (co-inoculation). Plants were further grown at 22°C under a 16/8 h night/day cycle with constant light for three or six days. After the incubation period, to determine bacterial colonization levels, bacteria from roots of six plants per condition were detached from roots and proceeded as explained below.

For the analysis of BSMs production *in planta*, a rectangular piece of agar (1 cm width x 2.5 cm length x 0.7 cm height) surrounding the colonized root starting from the inoculation point was sampled. BSMs were extracted for 15 min, with 1.5 mL of acetonitrile (85% (v/v)). After centrifugation for 5 min at 4000 rpm, the supernatant was recovered for UPLC-MS analysis as previously described.

2.12 Bacterial CFU counting

To quantify bacterial colonization of tomato roots, three and six days after (co-)inoculation, bacteria from roots of six plants, divided into 3 samples (each containing two plants per condition) were detached from roots by vortexing for 5 min in 15 mL falcon tubes containing 6 mL of peptone water solution supplemented with 0.1% (v/v) of Tween 80 and 8 glassy beads. Further, serial dilutions were prepared and 200 µL of each were plated onto LB medium using plating beads. Plates were incubated for 24 h at different temperatures to favor the growth of one of the interacting bacteria. *Pseudomonas* spp. was incubated at 28°C and GA1 at 42°C. The colonies were counted by using Scan® 1200 – INTERSCIENCE (version 8.0.4.0). Further, colonization results were log-transformed and statistically analyzed. At least three independent assays were performed with 3 technical repetitions (three samples each containing two plants) each for *in planta* assays.

2.13 Confocal laser-scanning microscopy analysis of bacterial root colonization

For confocal laser scanning microscopy (CLSM), samples of 1–2 cm length were cut from the apical root, hair root and mature root zones (i.e., root zone between 1

cm below the seed) and mounted in Aqua-Poly/Mount (Poly-sciences, Eppelheim, Germany). For analysis of green and red fluorescence emitted by bacteria, a microscope Confocal Zeiss LSM 800 (Carl Zeiss, Le Pecq, France) equipped with argon–krypton and He-Ne lasers was used by setting excitation at 548 nm and emission between 570 and 646 nm for mCherry, excitation at 548 nm and emission between 596 and 646 nm for eforRed and excitation at 488 nm and emission between 504 and 555 nm for GFPmut3. Images were processed with the LSM software, Zen 3.3 blue edition (Carl Zeiss). Five root systems were analyzed per treatment, and 3 images per root system were taken. Representative photos for each condition are presented in the figures.

2.14 Statistical analysis

Statistical analyses were performed using GraphPad PRISM 8 software with Student paired T-test or Mann-Whitney test. For multiple comparisons, one-way ANOVA and Tukey's honest significant distance (HSD) tests were performed, and the groups with different letters differed significantly from each other at α=0.05. The RStudio 1.1.423 statistical software environment (R language version 4.03) was used for this purpose [284].

3. Results

3.1 Diverse bioactive secondary metabolites of plant-associated Pseudomonas *are involved in interaction with* Bacillus

We first evaluated the interaction outcomes upon confrontation of *B. velezensis* strain GA1 with several plant-associated *Pseudomonas* strains belonging to different species. We used the recently sequenced (Genbank: CP046386) *B. velezensis* strain GA1 as a BSM-rich and genetically amenable isolate, representative of the species. Genome mining with AntiSMASH 6.0 [285] confirmed the presence of all BGCs necessary for the biosynthesis of known BSMs typically formed by this bacterium (Fig. 2-1A). Based on the accurate mass determined via ultrahigh performance liquid chromatography-quadrupole time-of-flight mass spectrometry (UPLC-qTOF MS) (Fig. 2-1B and C), most of the predicted NR secondary metabolites were identified in cell-free crude supernatants obtained from the culture in a so-called exudate-mimicking (EM) medium. This medium has been mostly used in this study to grow *Bacillus* as it reflects the specific content in major carbon sources typically released by roots of *Solanaceae* plants, such as tomato and tobacco [171]. Most compounds were also produced, but in lower amounts, upon growth in the casamino acid medium (CAA), commonly used for secondary metabolite production by *Pseudomonas* (Fig. 2-1B).

A

BSM predicted	Category	Biosynthetic gene cluster(s)
Surfactins	NRPs/CLPs	*srfaABCD*
Fengycins	NRPs/CLPs	*fenABCDE*
Iturins	NRPs/CLPs	*ituDABC*
Macrolactins	NRPs/PKs	*mlnABCDEFGHI*
Bacillaene	NRPs/PKs	*baeBCDEGHIJLMNRS*
Dihydrobacillaene	NRPs/PKs	*baeBCDEGHIJLMNRS*
Difficidin	NRPs/PKs	*dfnABDEFGHIJKLMNO*
Oxydifficidin	NRPs/PKs	*dfnABDEFGHIJKLMNO*
Bacillibactin	NRPs/ Siderophore	*dhbACEBF*
Bacilysin	Dipeptide	*bacABC*
Amylocyclicin	RiPP	*acnBACDEF*
Amylolysin	RiPP	*amlFEKRAMT*

C

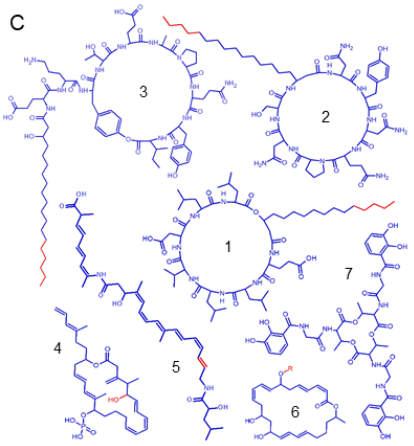

B

BSM	Main described activities	Raw formula of variants	Detected m/z $[M+H]^+$ (mass error (ppm))	EM	CAA
Surfactins[1]	Induced systemic resistance Motility	**C12** : $C_{50}H_{87}N_7O_{13}$ **C13** : $C_{51}H_{89}N_7O_{13}$ **C14** : $C_{52}H_{91}N_7O_{13}$ **C15** : $C_{53}H_{93}N_7O_{13}$ **C16** : $C_{54}H_{95}N_7O_{13}$	994.6420 (1,5) 1008.6582 (0,9) 1022.6743 (0,5) 1036.6904 (4,8) 1050.7061 (1,7)	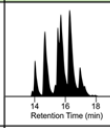	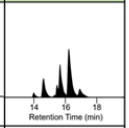
Iturins[2]	Antifungal	**C13** : $C_{47}H_{72}N_{12}O_{14}$ **C14** : $C_{48}H_{74}N_{12}O_{14}$ **C15** : $C_{49}H_{76}N_{12}O_{14}$ **C16** : $C_{50}H_{78}N_{12}O_{14}$ **C17** : $C_{51}H_{80}N_{12}O_{14}$	1043.5510 (1,0) 1057.5653 (2,2) 1071.5809 (2,3) 1085.5967 (2,1)	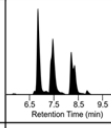	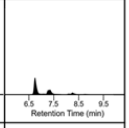
Fengycins[3]	Antifungal	**C15** : $C_{71}H_{108}N_{12}O_{20}$ **C16** : $C_{72}H_{110}N_{12}O_{20}$ **C17** : $C_{73}H_{112}N_{12}O_{20}$ **C18** : $C_{74}H_{114}N_{12}O_{20}$ **C19** : $C_{75}H_{116}N_{12}O_{20}$	1449.7806 (4,8) 1463.8004 (1,9) 1477.8171 (2,5) 1491.8305 (2,7) 1505.8440 (4,1)	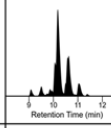	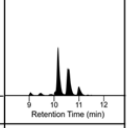
Difficidins[4]	Antibacterial	**Difficidin** : $C_{31}H_{45}O_6P$ **Oxy-** : $C_{31}H_{45}O_7P$	567.2828 (3,2) 583.2795 (7,8)	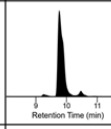	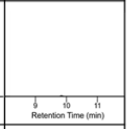
Bacillaenes[5]	Antibacterial	**Bacillaene** : $C_{34}H_{48}N_2O_6$ **Dihydro** : $C_{34}H_{50}N_2O_6$	581.3585 (2,3) 583.3726 (2,7)	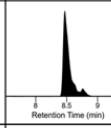	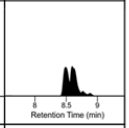
Macrolactins[6]	Antibacterial	**A** : $C_{24}H_{34}O_5$ (R=H) **7-O-malonyl-A** : $C_{27}H_{36}O_8$ (R=CO-CH_2-COOH) **7-O-succinyl-A** :$C_{28}H_{36}O_8$ (R=CO-CH_2-CH_2-COOH) **D** : $C_{34}H_{48}O_{13}$ (R=6-O-syccinyl-β-gluc)	435.2298 (6,7) 511.2292 (2,0) 525.2459 (0,0) 687.2991 (0,6)	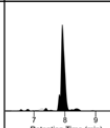	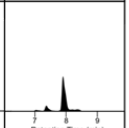
Bacillibactins[7]	Siderophore	$C_{39}H_{42}N_6O_{18}$	883.2620 (0,1)	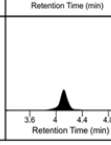	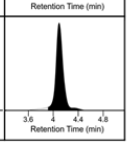

Figure 2-1. Diversity of predicted and detectable bioactive secondary metabolites (BSMs) produced by *B. velezensis* strain GA1. A: Prediction of *B. velezensis* GA1 secondary metabolites. Biosynthetic gene clusters (genome annotation, Genbank: CP046386) were predicted by antiSMASH 6.0 [285]. B: GA1 BSMs and their corresponding main described activities and raw formula. Detected m/z ($[M+H]^+$) of each variant and mass error (in ppm, compared to theoretical mass) are calculated based on UPLC-MS analyses of supernatants coming from exudate mimicking (EM) and casamino acid (CAA) medium culture. Relative abundance of each BSMs is shown for both media. The numbers (superscript) next to the molecule name indicate the corresponding BSMs structure depicted in C: Structural changes leading to variants are indicated in red.

The same approach combining genome mining (when available) and UPLC-qTOF MS was used to determine the BSMs produced by each of the ten *Pseudomonas* strains grown as planktonic cells in liquid CAA (Fig. 2-2). All isolates produced the siderophore pyoverdine, typical of fluorescent *Pseudomonas* species, but some strains also synthesized a secondary siderophore such as (enantio-)pyochelin or achromobactin with a lower affinity for iron [286]. The ten *Pseudomonas* strains also differed in their potential to form broad-spectrum antibiotics such as phenazine derivatives (phenazine-1-carboxamide [PCN] and phenazine-1-carboxylic acid [PCA]), 2,4-diacetylphloroglucinol (DAPG) and/or pyoluteorin [258,262,287]. CLPs represent the most structurally diverse group of metabolites in the selected isolates (see Fig. 2-3 for the CLPs structures). Most strains produced a single CLP belonging either to the viscosin (massetolide) (*Pseudomonas lactis* SS101), orfamide (*Pseudomonas protegens* Pf-5 and CHA0), putisolvin (*Pseudomonas putida* WCU_64) and xantholysin (*Pseudomonas mosselii* BW11M1) groups. *P. sessilinigenes* CMR12a and *Pseudomonas tolaasii* CH36 were the only strains co-producing two structurally distinct CLPs (sessilin and orfamide or tolaasin and pseudodesmin, respectively) while no CLP were predicted and detected in the extracts from *P. chlororaphis* JV497 and JV395B or *Pseudomonas kilonensis* F113 (Fig. 2-2).

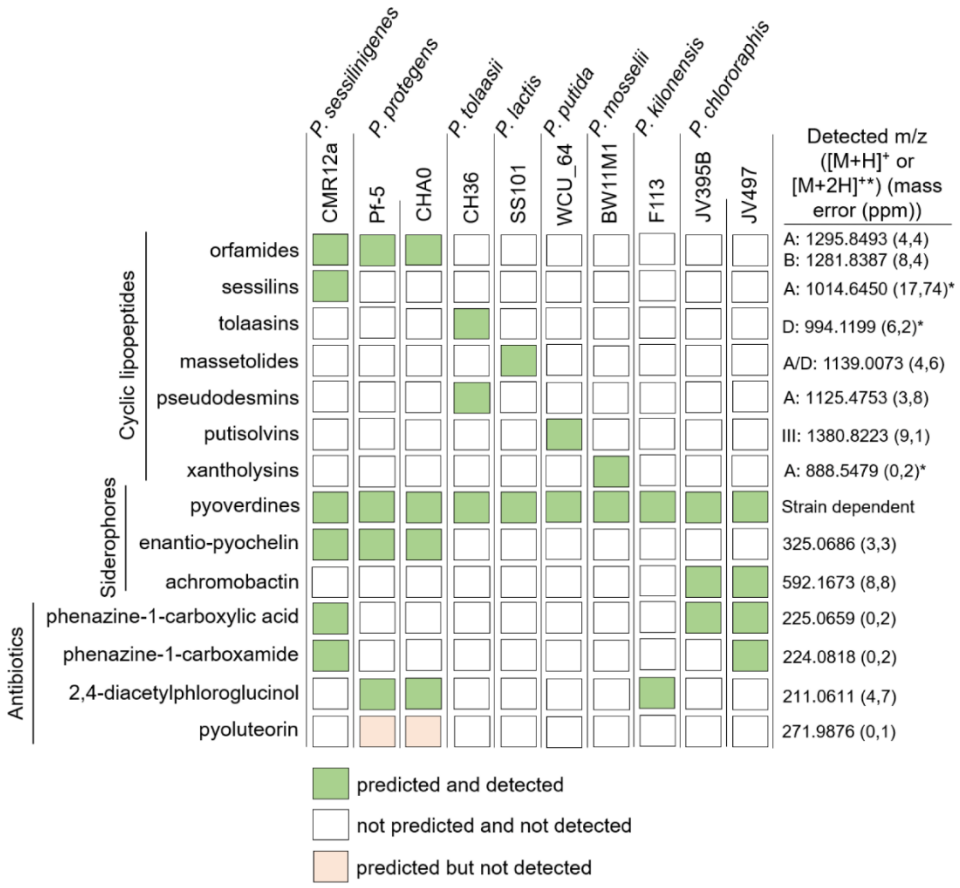

Figure 2-2. Predicted and detected bioactive secondary metabolites (BSMs) produced by the *Pseudomonas* strains used in this study. Metabolites with biosynthetic gene clusters (BGCs) predicted by antiSMASH [285] and detected ($[M+H]^+$ or $[M+2H]^+$, the latter is indicated with an asterisk) by UPLC-qTOF MS in crude cell-free supernatant after growth in CAA medium are represented by green squares, while undetected BSMs are represented by light red squares. Detected m/z and mass errors in parts per million (based on one measurement from one strain [orfamide, CMR12a; achromobactin, JV497; phenazine, CMR12a; 2,4-diacetylphloroglucinol, Pf-5]) corresponding to the main variant(s) (indicated with the letters) detected are presented. The data are representative of the two independent repetitions.

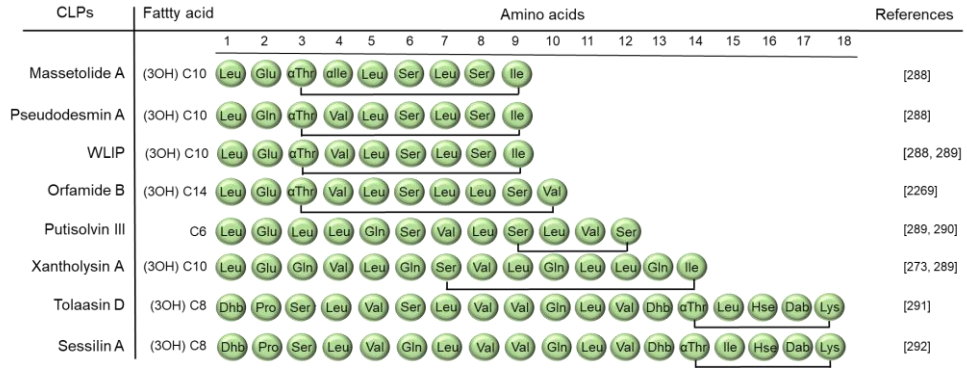

Figure 2-3. Simplified structural representation of the cyclic lipopeptides (CLPs) produced by *Pseudomonas* strains used in this study. The fatty acid chain length is presented and the amino acid composition are depicted indicating where cyclization occurs. For each CLP, only the main form detected is represented, for more details about minor variants see the also corresponding associated references [269,273,288–292].

Upon dual confrontation on solid CAA medium, strains JV395B, F113, Pf-5, CH36 and CMR12a displayed some inhibitory activity toward the growth of a GA1 colony due to the production of soluble metabolites diffusing in the interaction zone (Fig. 2-4A). This inhibitory activity was also illustrated in liquid cultures when growth reduction of GA1 planktonic cells was observed upon supplementation of the medium with *Pseudomonas* cell-free supernatant (CFS), previously prepared from the culture in CAA medium (Fig. 2-4B). However, the relative inhibitory activity of the different *Pseudomonas* isolates varied according to the experimental conditions on plates or in liquid cultures. For instance, the addition of CFS from strains CHA0, WCU_64, JV497 and SS101 strongly reduced GA1 cell growth in liquid culture while the corresponding isolates displayed only low inhibition of *Bacillus* colony on solid medium (Fig. 2-4A, B). This may be explained by the fact that for some isolates the antibiotic production rate is very different for cells forming biofilm-like microcolonies on plates compared to planktonic cells in liquid cultures, as already reported [258].

However, the *Pseudomonas* inhibitory effect was strongly reduced or disappeared between the bacteria confronted at a longer distance where, interestingly, the formation of a white-line was observed between the bacterial colonies in the case of CMR12a and CH36, but not for other strains (Fig. 2-4C). Additional confrontation assays performed on EM medium showed enhanced motility of GA1 as another phenotype observed in response to *Pseudomonas*, which was the most marked upon confrontation with CMR12a and JV497 (Fig. 2-4D).

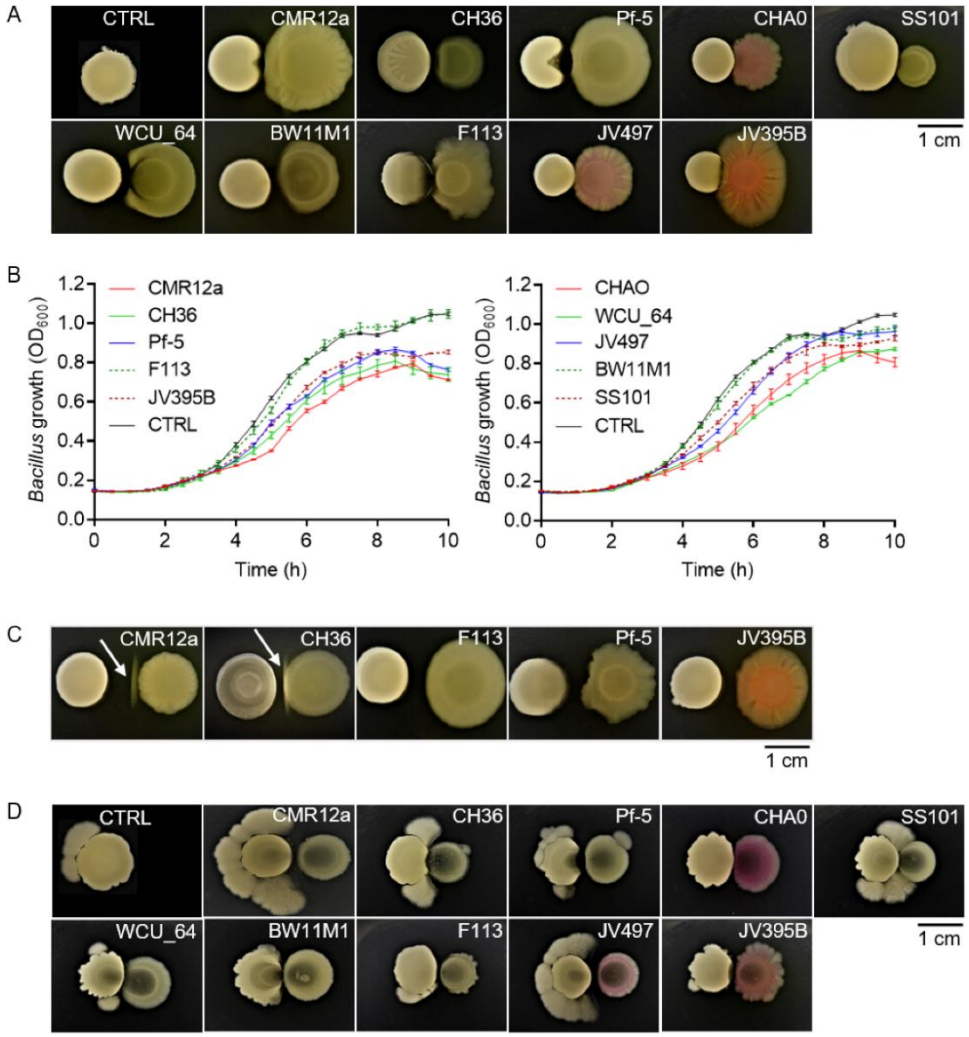

Figure 2-4. Phenotype and growth of *B. velezensis* GA1 following confrontation with different *Pseudomonas* strains. A: *B. velezensis* GA1 (left colony) phenotypic response on solid CAA medium following short distance (1 mm) confrontation with different *Pseudomonas* strains (right colony). The control (CTRL) colony shows GA1 cultured alone. B: GA1 growth curve in EM liquid medium supplemented with 4% (vol/vol) of different *Pseudomonas* cell-free supernatants. The control (CTRL) corresponds to un-supplemented GA1 culture (data represent means ± standard deviations [SD]; n=9). C: White-line formation (indicated by arrow) between colonies of GA1 (left colony) and some *Pseudomonas* strains (right colony) on jellified CAA medium following longer distance (5 mm) confrontation. D: GA1 (left colony) motile response on EM medium following confrontation with different *Pseudomonas* strains (right colony). The control (CTRL) colony shows GA1 cultured alone. Pictures in panels A, C, and D are representative of the response observed in three independent repetitions with three technical replicates (n=9).

3.2 The interplay between CLPs drives antagonistic interactions and white-line formation

Based on these data, we selected CMR12a as a challenger for further investigation of the molecular basis of the interactions. The CMR12a was chosen because the three responses of GA1, inhibition, white-line formation and enhanced motility, were observed upon confrontation with this strain. Firstly, we hypothesized that the inhibitory effect of CMR12a could be due to the production of CLPs and/or phenazine as main compounds with potential antimicrobial activity (Fig. 2-2). We, therefore, tested the effect of CFS from various CMR12a mutants impaired in the synthesis of these metabolites. As already described, the production level of the non-impaired metabolites in each of those mutant was not affected [268]. CFS of the mutant unable to produce sessilin (Δ*sesA*) displayed a significantly reduced ability to inhibit GA1 growth compared to CFS of CMR12a wild type (Fig. 2-5A). Moreover, a similarly reduced ability to inhibit GA1 has been observed in double or triple mutants affected both in sessilin and orfamide synthesis or in CLPs and phenazine production, whereas the growth of GA1 was weakly reduced by a double mutant affected in phenazine and orfamide synthesis (Fig. 2-5A). Even if some minor effects of the other compounds could not be ruled out, it indicated that sessilin is the main CMR12a metabolites responsible for toxic activity toward GA1 cells. Nevertheless, we observed that the sessilin-mediated inhibitory effect was markedly reduced by delaying CMR12a CFS supplementation until 6 h of GA1 culture, instead of adding it at the beginning of the incubation (Fig. 2-5B). This suggested that some early secreted GA1 compounds may counteract the toxic effect of sessilin. We hypothesized that surfactin can play this role as it is the first detectable BSM to accumulate in significant amounts in the medium early in the growth phase [190]. We tested a surfactin-deficient mutant and observed that its growth was more strongly affected compared to GA1 wild type upon CMR12a CFS supplementation. Chemical complementation with purified surfactin restored growth of the Δ*srfAA* mutant to a large extent, providing further evidence for a protective role of this lipopeptide toward sessilin toxicity (Fig. 2-5B).

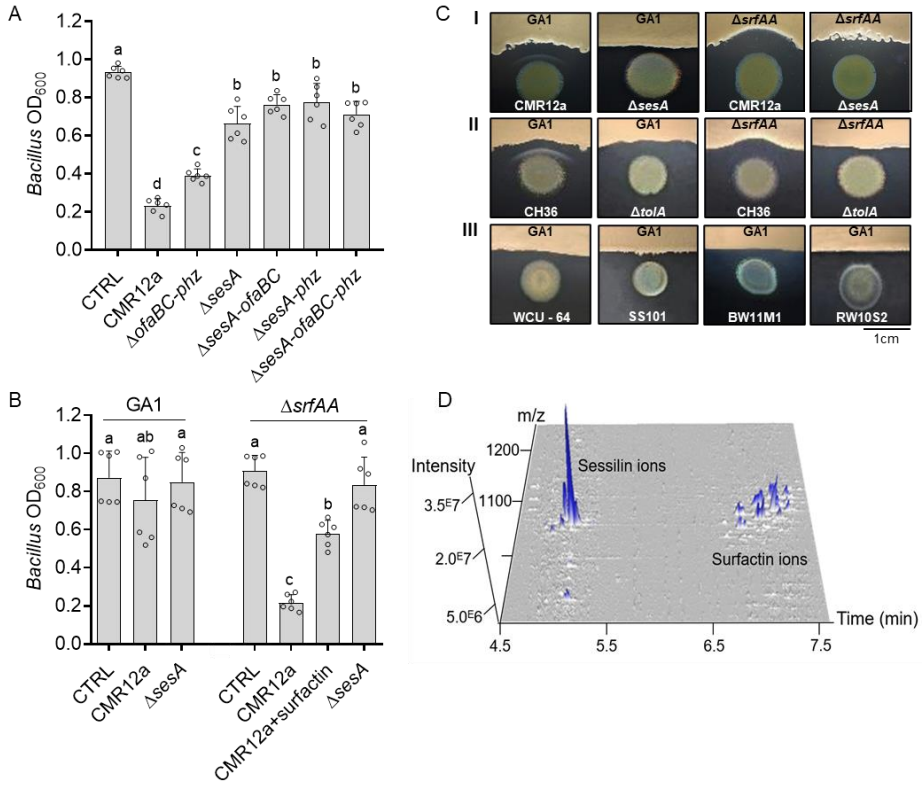

Figure 2-5. Surfactin attenuates sessilin-mediated toxicity via white-line formation. A: GA1 biomass level measured after 10 h of growth in EM liquid medium supplemented or not (CTRL) with 4% (vol/vol) of cell-free supernatants from CAA cultures of CMR12a wild type or its mutants repressed in the synthesis of orfamide and phenazine (Δ*ofaBC-phz*), sessilin (Δ*sesA*), sessilin and orfamide (Δ*sesA-ofaBC*), sessilin and phenazine (Δ*sesA-phz*), or all compounds (Δ*sesA-ofaBC-phz*) (for metabolome, see Table 2-S1 in the supplemental material). Data show means ± SD calculated from two independent experiments each with three culture replicates (n=6) and different letters indicating statistically significant differences between the treatments (ANOVA and Tukey's HSD tests, α=0.05). B: Growth inhibition of GA1 wild type and its Δ*srfAA* mutant repressed in surfactin synthesis after 10 h of culture and following delayed supplementation (added 6 h after incubation start) with cell-free supernatants from CMR12a wild type (alone or together with 10 µM pure surfactin as chemical complementation) and with cell-free supernatants from the sessilin mutant (Δ*sesA*). Un-supplemented cultures of GA1 were used as a control (CTRL). Experiments were replicated, and data were statistically processed as described in panel A (n=6). C: White-line formation and/or *Bacillus* inhibition observed following confrontation of GA1 wild type or the surfactin mutant Δ*srfAA* with (I) CMR12a or its Δ*sesA* derivative, (II) *P. tolaasii* CH36 or its tolaasin-defective mutant Δ*tolA*, and (III) other *Pseudomonas* CLP producers (for metabolome, see Table 2-S1). Pictures are representative of three independent repeats. D: 3D representation of UPLC-MS analysis of metabolites present in the white-line zone between GA1 and CMR12a showing the specific accumulation of sessilin and surfactin molecular ions.

Such sessilin-dependent inhibition also occurred when bacteria were confronted on solid CAA medium favoring *Pseudomonas* BSMs production. In these conditions, the formation of a white precipitate in the interaction zone was observed with CMR12a wild type but not when GA1 was confronted with the Δ*sesA* mutant (Fig. 2-5C-I). UPLC-MS analysis of ethanol extracts from this white-line area confirmed the presence of sessilin ions but also revealed an accumulation of surfactin from GA1 in this zone (Fig. 2-5D). The involvement of surfactin in precipitate formation was confirmed by the absence of this white-line upon testing the Δ*srfAA* mutant in confrontation with CMR12a (Fig. 2-5C-I). Interestingly, the loss of surfactin production and white-line formation was associated with a higher sensitivity of the GA1 colony to the sessilin toxin secreted by CMR12a. Altogether, these data indicate that surfactin acts as a protective agent, preventing GA1 colony from sessilin toxicity via co-aggregation into insoluble complexes.

Similar CLP-dependent antagonistic interaction and white-line formation were observed upon co-cultivation of GA1 with *P. tolaasii* strain CH36 producing tolaasin (Fig. 2-5C-II), a CLP structurally similar to sessilin (only differing by two amino acid residues, Fig. 2-3). However, this chemical interaction leading to co-precipitation is quite specific regarding the type of CLPs involved, as it was not visible upon confrontation of GA1 with other *Pseudomonas* strains forming CLPs belonging to different structural groups that were not toxic for GA1 (Fig. 2-5C-III, see Fig. 2-3 and 2-6 for structures).

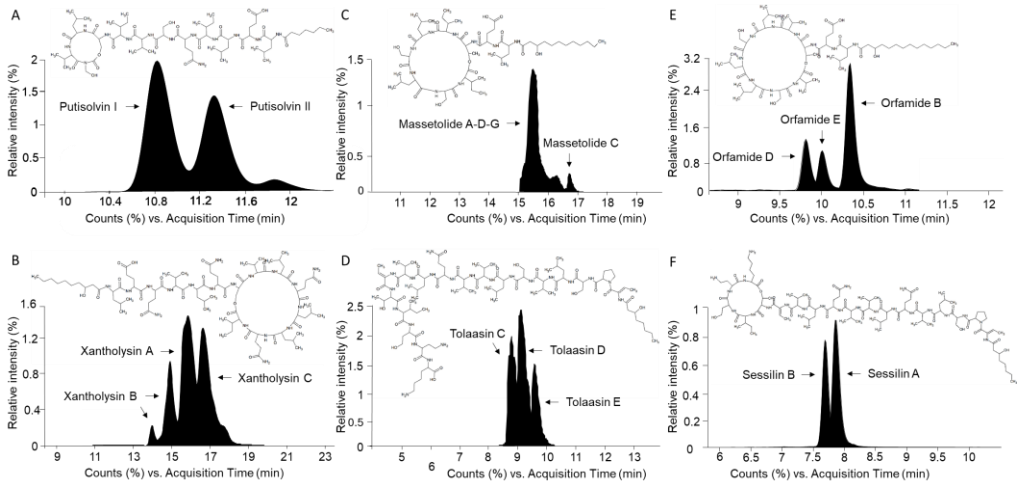

Figure 2-6. Main cyclic lipopeptides produced by *P. sessilinigenes* CMR12a, *P. putida* WCU-64, *P. lactis* SS101, *P. mosselii* BW11M1 and *P. tolaasii* CH36. A: Extracted ion chromatogram of putisolvin I and II produced by *P. putida* WCU-64. The structural formula of putisolvin I is presented. B: Extracted ion chromatogram of xantholysin A, B and C produced by *P. mosselii* BW11M1. The structural formula of xantholysin A is presented. C: Extracted ion chromatogram of massetolide A-D-G, C produced by *P. lactis* SS101. The structural formula of massetolide C is indicated. D: Extracted ion chromatogram of tolaasin C, D and E produced by *P. tolaasii* CH36. The structural formula of tolassin C is presented. E: Extracted ion chromatogram of orfamide B, D and E produced by *P. sessilinigenes* CMR12a. The structural formula of orfamide B is presented. F: Extracted ion chromatogram of sessilin A and B produced by *P. sessilinigenes* CMR12a. The structural formula of sessilin A is presented.

White-line formation and sessilin/tolaasin-dependent toxicity were also observed when other surfactin-producing *B. velezensis* strains (FZB42, S499 and QST713) were confronted to CMR12a and CH36 on solid and in liquid medium (Fig. 2-7A and B, respectively).

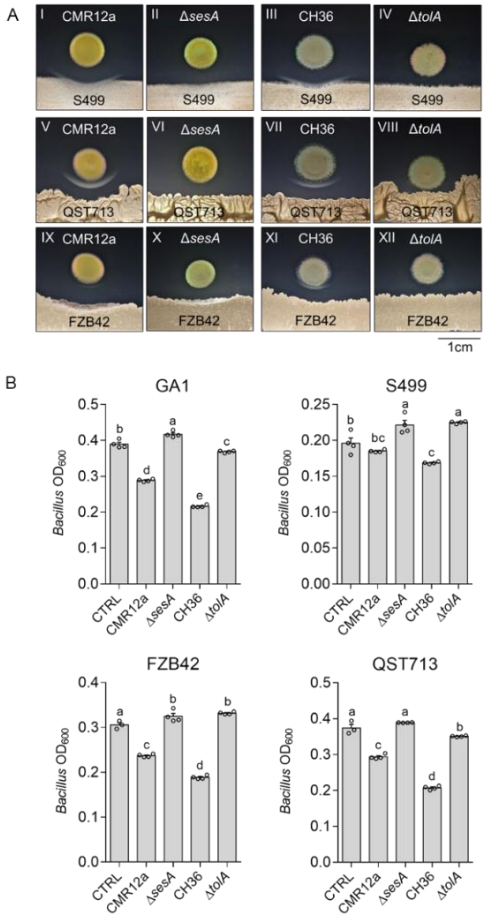

Figure 2-7. The interplay between surfactin and sessilin/tolaasin is conserved within *B. velezensis.* A: The white-line formation is dependent on the co-presence of surfactin and sessilin/tolaasin producers while during the interaction between *B. velezensis* wild type strains (S499, QST713, FZB42) and *P. sessilinigenes* CMR12a (CMR12a) or *P. tolaasii* CH36 (CH36) mutants impaired in the production of sessilin (Δ*sesA*) or tolaasin (Δ*tolA*), respectively, no white-line is observed. Sessilin/tolaasin production induces slight growth inhibition of all tested *B. velezensis* strains (panels I, III, V, VII, IX, XI). No inhibition is observed in confrontation assays with *Pseudomonas* mutants unable to produce sessilin or tolaasin (panels II, IV, VI, VIII, X, XII). The figure shows one representative repetition of three biological replicates with three technical repetitions (n=9). B: Optical density (at 600nm) of different *B. velezensis* (GA1, S499, FZB42 and QST713) after 10 h culture supplemented with 4% (v/v) CMR12a or CH36 supernatants and their mutants unable to produce sessilin or tolaasin, respectively. Un-supplemented culture is represented as control (CTRL). Graphs show means ± SD calculated from four replicate cultures (n=4). Letters a to d indicate statistically significant differences according to Tukey's HSD test (α=0.05).

The chemical basis and stoichiometry of such molecular interaction between surfactin and sessilin leading to white-line formation remain to be determined. However, it probably follows similar rules as observed for the association between sessilin/tolaasin and other *Pseudomonas* CLPs such as white-line-inducing principle (WLIP) or orfamide [261] or between CLPs and other unknown metabolites [293,294].

3.3 Pseudomonas *triggers enhanced surfactin-mediated motility of* Bacillus

We next wanted to understand better the observed impact of CMR12a on the motile phenotype of GA1 upon co-cultivation on solid EM medium (Fig. 2-4D). This phenotype occurring on medium containing high agar concentrations (1.5% (m/v)) macroscopically resembles the sliding-type of motility [241] (Fig. 2-8A). This migration pattern is flagellum independent but depends on multiple factors, including the synthesis of surfactin, which reduces friction at the cell-substrate interface [89,91,241]. We, therefore, suspected such improved motility to correlate with increased production of this lipopeptide. This hypothesis was supported by the almost full loss of migration of the Δ*srfAA* mutant in these interaction conditions (Fig. 2-8B). We also observed a distance-dependent effect of CMR12a on GA1 motility (Fig. 2-8C). The spatial mapping via matrix-assisted laser desorption/ionization-Fourier transform-ion cyclotron resonance mass spectrometry (MALDI-FT-ICR MS) imaging confirmed a higher accumulation of surfactin ions in the interaction zone and around the GA1 colony when growing at a short or intermediate distance from the *Pseudomonas* challenger, compared to the largest distance where the motile phenotype was much less visible (Fig. 2-8C). Stimulation of surfactin synthesis by GA1 colonies as a response to *Pseudomonas* perception was supported by the significantly enhanced surfactin production by planktonic GA1 cells upon supplementation with CMR12a but also JV497 CFS (Fig. 2-8D and E). These data indicate that GA1 cells in the microcolony perceive a soluble signal diffusing from the *Pseudomonas* colony over a limited distance.

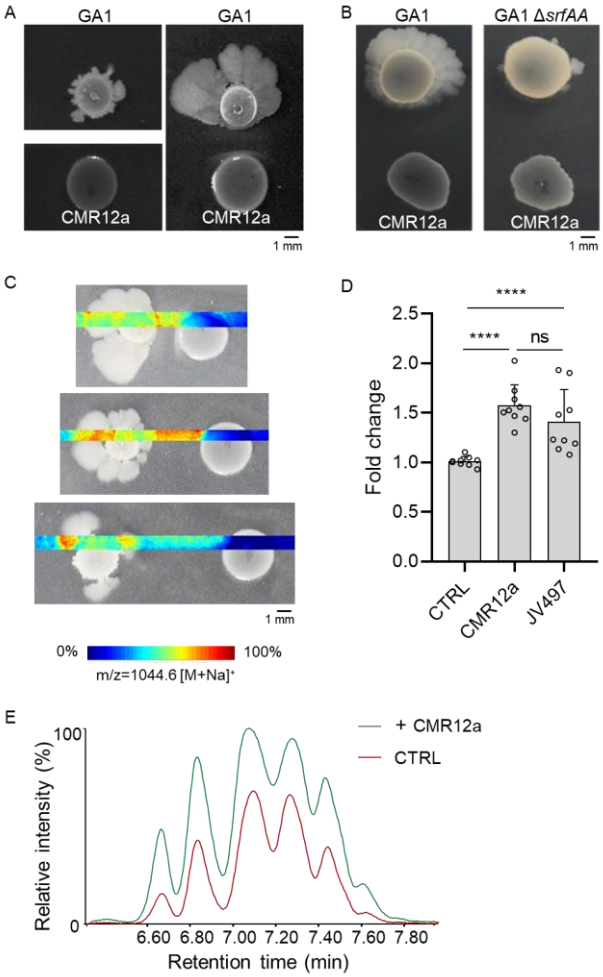

Figure 2-8. Distance- and surfactin-dependent enhanced motility of *B. velezensis* GA1 mediated by interaction with *Pseudomonas*. A: GA1 motility phenotype on EM jellified medium when cultured alone (left) or in confrontation with CMR12a (1 mm) (right). B: Motility pattern of GA1 or the Δ*srfAA* surfactin-deficient mutant in confrontation with CMR12a (5 mm). C: MALDI FT-ICR mass spectrometry imaging (MSI) heat maps showing spatial localization and relative abundance of ions corresponding to the C14 surfactin homolog (most abundant) when GA1 is confronted with CMR12a at increasing distances. D: Comparison of surfactin production (expressed in fold change) in GA1 culture supplemented with 4% (vol/vol) of CMR12a or JV497 supernatants. The un-supplemented culture was fixed at 1 (CTRL). Bars show means ± SD (n=9). Statistical comparisons between treatments were assessed with the Mann-Whitney test; ns, not significant; ****, $P < 0.0001$. E: UPLC-MS extracted ion chromatogram (EIC) illustrating the relative abundance of surfactin produced in GA1 EM medium when cultured alone (CTRL in red) or supplemented with 4% (vol/vol) CMR12a (1CMR12a in green). The different peaks correspond to the structural variants differing in fatty acid chain length.

To examine if the compounds diffusing in the interaction zone may act as a trigger of GA1 enhanced motility, we analyzed the content of produced metabolites in the interaction zone between the confronted bacteria. The UPLC-MS analysis of ethanol extracts from the confrontation area detected the presence of CLPs (sessilin and orfamide) and phenazine antibiotics (PCN and PCA) (Fig. 2-9A, B).

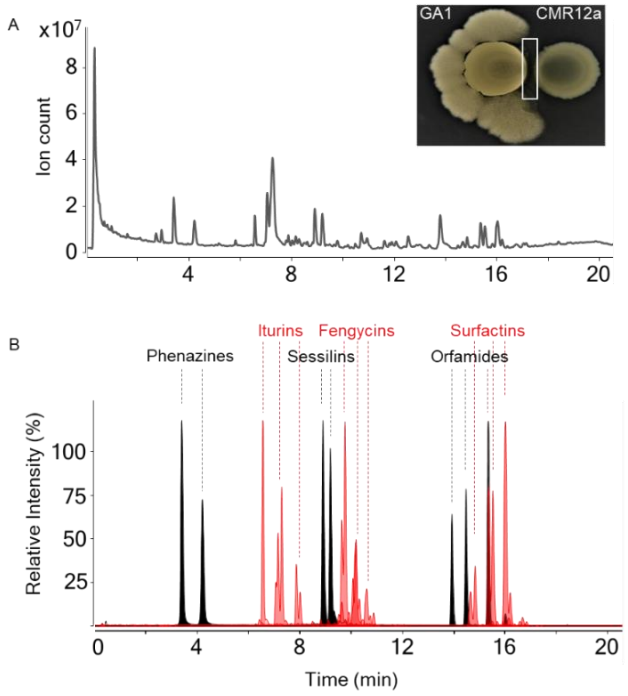

Figure 2-9. *P. sessilinigenes* CMR12a and *B. velezensis* GA1 BSMs production upon confrontation on solid EM medium. A: Total ion chromatogram (TIC) and B: Extracted ion chromatograms (EICs) overlaid for each BSMs produced by CMR12a (black) and GA1 (red) in the confrontation zone (labelled as a white rectangle on the upper-right confrontation figure) on solid EM medium after 24h. The intensity was fixed to 100% for the main variant of each family. The figure shows one representative repetition of two biological replicates with three technical repetitions (n=6).

In an attempt to identify the CMR12a compound responsible for triggering GA1 motility, we analyzed the effects of CMR12a mutants specifically suppressed in the production of CLPs, phenazine and siderophores in confrontation assay. However, none of the mutants lost the ability to enhance GA1 motility, indicating the involvement of another CMR12a metabolite as an inducer of the GA1 response (Fig. 2-10).

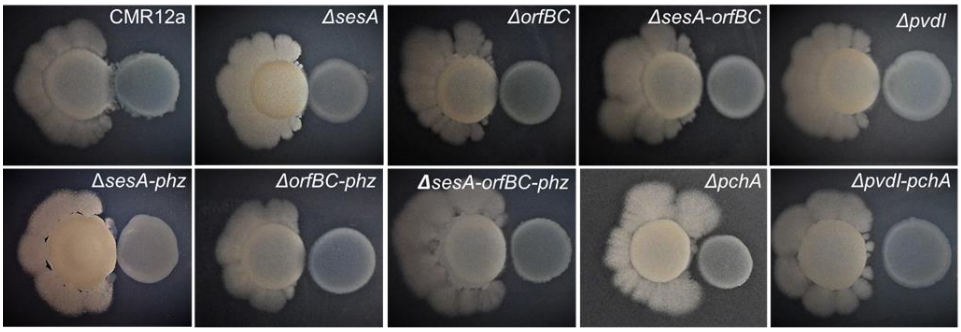

Figure 2-10. Effect of *P. sessilinigenes* CMR12a mutants on *B. velezensis* GA1 motility. GA1 (left colony) enhanced motility upon confrontation with CMR12a wild type (CMR12a) or mutants repressed in the synthesis of sessilin (Δ*sesA*), orfamide (Δ*ofaBC*), orfamide and phenazine (Δ*ofaBC-phz*), sessilin and orfamide (*ΔsesA-ofaBC*), sessilin and phenazine (Δ*sesA-phz*), their triple mutant (Δ*sesA-ofaBC-phz*), pyoverdine (Δ*pvdI*), enantio-pyochelin (Δ*pchA*) or their double mutant (Δ*pvdI-pchA*) (see Table 2-S1 for metabolome of each mutant). The figure shows one representative repetition of three biological replicates with three technical repetitions (n=9).

3.4 BSMs-mediated interactions drive competitive root colonization

To appreciate the relevance of our *in vitro* observations in a more natural context, we further evaluated whether such BSMs interplay may also occur upon root co-colonization and to what extent it may impact *Bacillus* rhizosphere fitness. To that end, we compared the dynamics of GA1 populations on tomato roots when inoculated alone or upon co-inoculation with CMR12a and its sessilin-repressed Δ*sesA* mutant or with the JV497 strain, which also triggered GA1 motility but was not inhibitory for GA1 growth upon confrontation on solid medium (Fig. 2-4A and D). Thus, JV497 which does not produce CLPs and Δ*sesA* represented the appropriate controls for the evaluation of CLP involvement in CMR12a effect on GA1 in *in planta* conditions.

Population assessment via plate counting first revealed that upon single inoculation, the three *Pseudomona*s strains colonized roots more rapidly and extensively than GA1 (Fig. 2-11A). While *Pseudomonas* populations were not affected upon co-inoculation with GA1 (Fig. 2-11B, C and D), GA1 colonization ability was significantly reduced in the presence of CMR12a but not in presence of JV497 after 3 days (Fig. 2-12A). The effect of these two wild type *Pseudomonas* strains on the GA1 population was not significantly changed between the third and sixth day after co-inoculation (Fig. 2-12A). On the other hand, GA1 colonization rate in presence of the Δ*sesA*, was much less impacted (3 dpi) compared to co-

inoculation with CMR12a wild type, even if some negative effect of Δ*sesA* mutant on GA1 colonization was observed six days post-inoculation (Fig. 2-12A).

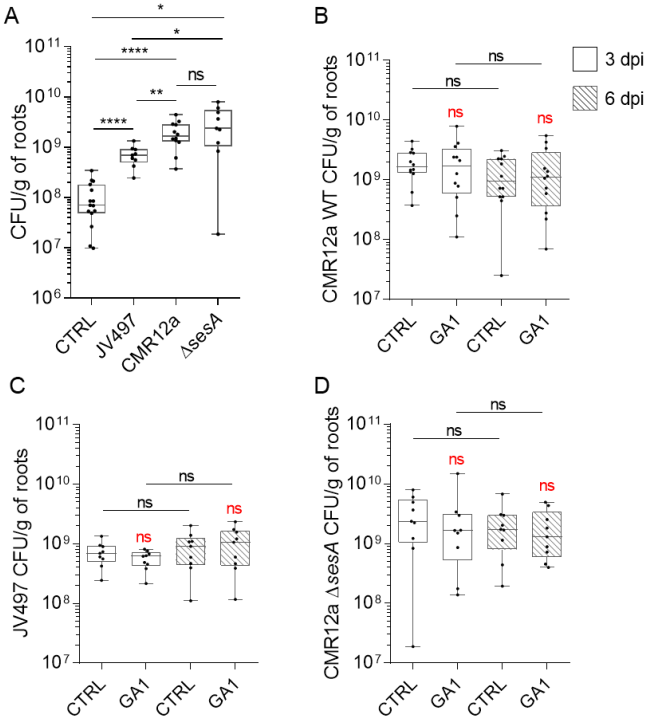

Figure 2-11. *B. velezensis* GA1 and *Pseudomonas* spp. tomato root colonization. A: GA1, JV497, CMR12a and Δ*sesA* population, expressed as colony forming units per gram of tomato roots (CFU/g of roots) recovered three days after single inoculation. Comparison between single (CTRL) and co-colonization (GA1) of tomato roots (CFU/g of roots) by CMR12a (B), JV497 (C), and CMR12a mutant Δ*sesA* (D) between three (3 dpi, empty bars) and six (6 dpi, hatched bars) days after (co-)inoculation. Box plots were generated based on data from at least three independent assays each involving 6 plants per treatment (n=18). The whiskers extend to the minimum and maximum values, and the midline indicates the median. Statistical comparisons between treatments were realized with Mann–Whitney-test,''ns'' no significant difference and "****", $P<0.0001$. The statistical differences between mono- and co-inoculated conditions are indicated as red-coloured labels while the statistical differences of the same condition between 3 and 6 dpi are indicated as black-coloured labels.

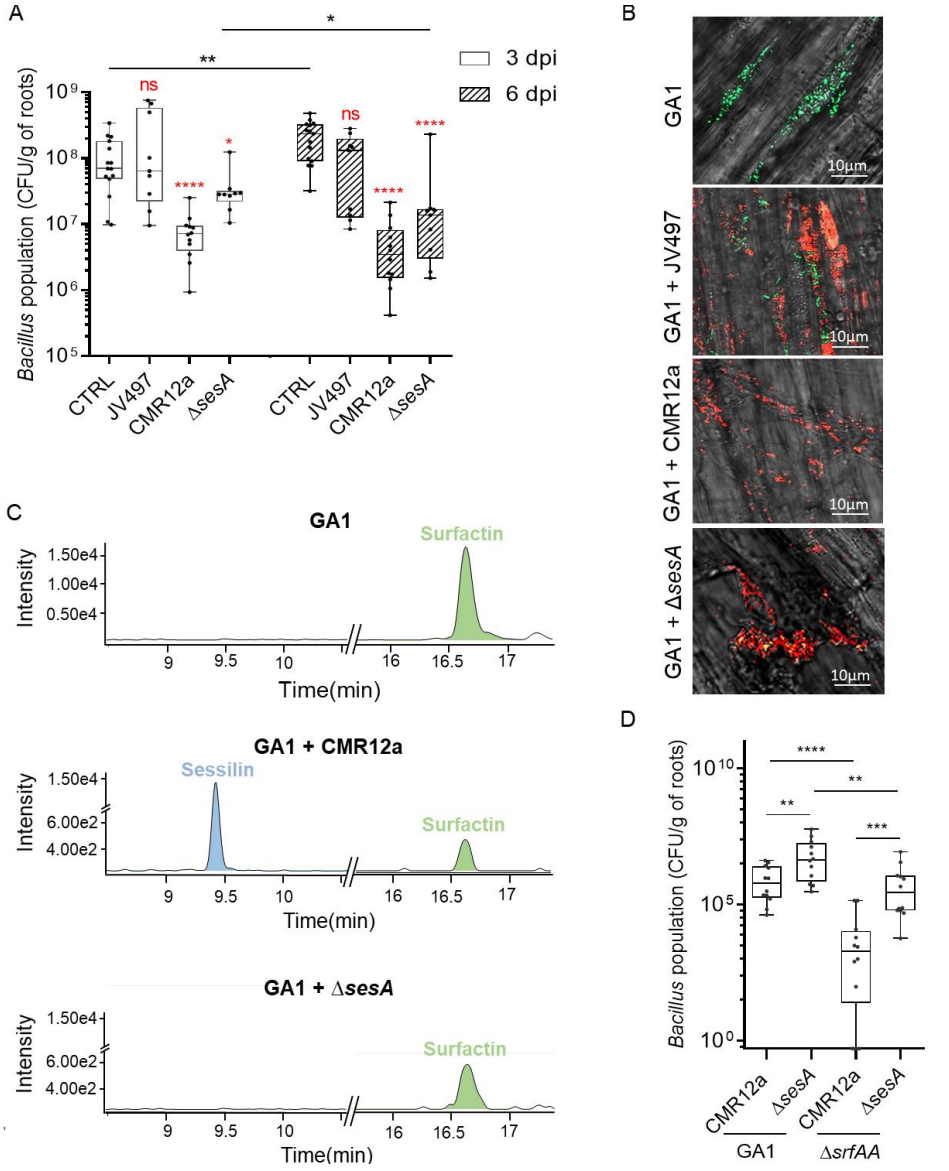

Figure 2-12. Competitive root colonization assays support the roles of BSMs in *Bacillus-Pseudomonas* interaction *in planta*. A: GA1 population (CFU per gram of tomato root) recovered at 3 days (empty bars) and 6 days (hatched bars) after co-inoculation (dpi) with JV497, CMR12a, and its sessilin-repressed mutant compared to GA1 inoculated alone. Box plots were generated based on data from a minimum of three biologically independent assays each involving 6 plants per treatment (n=18). The whiskers extend to the minimum and maximum values, and the midline indicates the median. Statistical differences between data at the same dpi are compared to the control (CTRL) and are labeled in red, while differences between treatments at different dpi are indicated with horizontal lines and a black asterisk

when significant. Statistical analyses were performed using a Mann-Whitney test; ns, no significant difference; *, $P < 0.05$; ****, $P < 0.0001$. B: Confocal laser scanning microscopy images of tomato root colonization by GA1 (elongation root zone) at 6 dpi after mono-inoculation (CTRL) or co-inoculation with JV497, CMR12a, or CMR12a Δ*sesA*. GA1 tagged with GFPmut3 is depicted in green, while mCherry- or eforRed-labeled cells in red correspond to CMR12a and JV497 wild types or CMR12a Δ*sesA*, respectively. C: UPLC-MS EIC illustrating relative production in planta of sessilin (blue peak) and surfactin (green peak) after 6 dpi of GA1 alone (GA1) or coinoculated with wild type *Pseudomonas* (GA1 + CMR12a) or its sessilin-impaired mutant (GA1 + Δ*sesA*). D: Cell populations recovered at 3 dpi for GA1 wild type (GA1) or the surfactin-impaired mutant (Δ*srfAA*) co-inoculated with CMR12a wild type (CMR12a) or its sessilin-impaired mutant (Δ*sesA*). Box plots were generated based on data from four biologically independent assays each involving at least 4 plants per treatment (n=16). The whiskers extend to the minimum and maximum values, and the midline indicates the median. Statistical differences between the treatments were calculated using a Mann-Whitney test; **, $P < 0.01$; ***, $P < 0.001$; ****, $P < 0.0001$.

Root colonization patterns upon single and dual inoculation were further investigated by confocal laser scanning microscopy (CLSM) using green fluorescent protein (*GFPmut3)*-tagged GA1, *mCherry*-tagged CMR12a or JV497 and *eforRed*-tagged CMR12a Δ*sesA*. When inoculated separately, GA1 was able to colonize the elongation and upper root zones and form biofilm-like multicellular communities, but no colonization of the apical meristem was observed (Fig. 2-13). However, *Pseudomonas* strains efficiently colonized the three root zones (Fig. 2-13). Focusing on the elongation zone, CLSM analysis of co-inoculated roots (6 dpi) revealed that GA1 and JV497 or Δ*sesA* cells or microcolonies were co-localized in the same area. In contrast, GA1 was clearly excluded from CMR12a-colonized zones as no GA1 cells could be detected nearby CMR12a colonies (Fig. 2-12B).

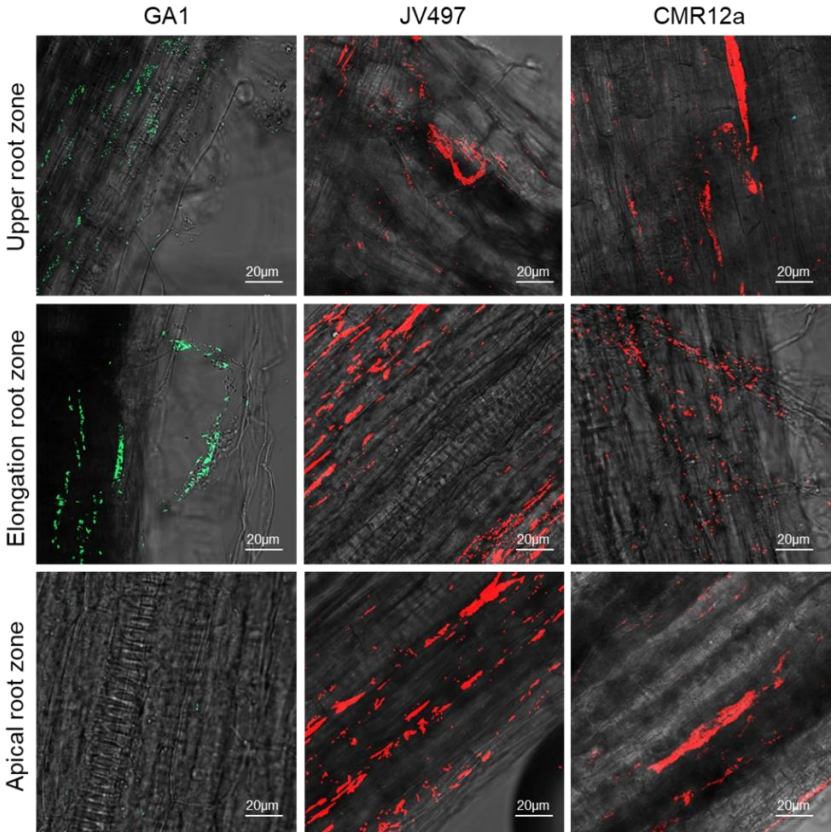

Figure 2-13. Confocal laser microscopy images of colonization and distribution of *B. velezensis* GA1, *P. chlororaphis* JV497 or *P. sessilinigenes* CMR12a along tomato roots. GA1, JV497, CMR12a root colonization and distribution on apical, elongation and upper root zones of tomato, 6 dpi. Cells expressing *GFPmut3* are green and correspond to GA1 cells while *mCherry*-labeled cells are red and correspond to *Pseudomonas* spp. cells. The grey backgrounds correspond to root views observed with transmitted light. Images are representative of the analysis of 9 images per condition.

Based on *in vitro* data, we hypothesized that the toxic activity of sessilin from CMR12a impacted GA1 development on roots. This is supported by the fact that this CLP was readily formed *in planta* as revealed by UPLC-MS analysis of methanolic extracts prepared from co-bacterized roots and the surrounding medium (Fig. 2-12C). These results also confirmed the importance of interference competition due to sessilin in the early phase of colonization but also indicated that another compound or factor might be involved in *in planta* competitive interaction, excluding competition for space, as *Pseudomonas* spp. populations were constant during the time (Fig. 2-11B, C and D).

Besides sessilin, UPLC-MS analysis also revealed the presence of surfactin produced by GA1 during mono or dual colonization of tomato roots (Fig. 2-12C). To evaluate the importance of surfactin in GA1 colonization, a GA1 mutant unable to produce surfactin (Δ*srfAA*) was co-inoculated with CMR12a wild type or the mutant unable to produce sessilin. The results showed that colonization by the Δ*srfAA* mutant was more impacted compared to GA1 wild type when co-inoculated with CMR12a while a significant gain in root establishment was recovered upon co-colonization with the Δ*sesA* mutant (Fig. 2-12D). The sessilin-surfactin interplay thus also occurs *in planta.*

4. Discussion

Our knowledge of the diversity of bacterial BSMs, especially from species dwelling in very competitive environmental niches such as soil, has been enriched in the last decade. This further boosted the discovery of BSMs with strong antimicrobial activity for their applications in medicine and agroindustry [25,251,164]. Nonetheless, most of these compounds have obviously other biological functions contributing to the persistence of the producing bacteria in natural settings [25,165,166]. However, our vision of BSM ecological relevance is still limited and to what extent these crucial metabolites may impact bacterial interspecies interactions is still poorly known. The current data on the molecular interaction between soil bacilli and pseudomonads is rather limited, except the fact that the pseudomonads Type VI secretion system and antibiotic 2,4-diacetylphloroglucinol may impact key developmental traits in *B. subtilis* such as biofilm formation and/or sporulation rate [231,243]. Through the present work, we point out unsuspected roles for lipopeptides, especially surfactin and sessilin, as the main BSMs driving some facets of this interaction between *B. velezensis* and *Pseudomonas* spp.

We discovered here for the first time to our knowledge, that by contrast with short ones, long *Pseudomonas* CLPs such as sessilin and tolaasin retained some toxicity against *B. velezensis* as observed *in vitro*. According to data available so far, sessilin/tolaasin-type CLPs are formed by a limited number of species such as *P. tolaasii*, *P. costantinii* and *P. sessilinigenes* isolates as illustrated by CMR12a. This isolate has recently been taxonomically positioned as *P. sessilinigenes* [267] having certain similarities with strains belonging to the *P. protegens* subgroup including many soil *Pseudomonas* biocontrol strains [295–298]. Considering the ever-growing number of new CLP producers discovered in recent years and the diversity/modularity of *Pseudomonas* NR secondary metabolites, we suspect that the potential to form CLPs from the tolaasin family could be more widespread among environmental *Pseudomonas* [274] . In addition, other long CLPs such as nunapeptin or corpeptin are also formed by plant-beneficial species like *P. corrugata* and *P. fluorescens* [299–301]. They deserve to be tested for antibacterial activity against *Bacillus* and other rhizosphere bacteria in order to further support and extend the

relevance of these compounds in interference competition that pseudomonads may engage in with other soil microbes. Here we evidence that these CLPs also confer a significant competitive advantage to *Pseudomonas* for rhizosphere colonization of tomato plantlets in the presence of *Bacillus*. If this toxic activity extends to other bacteria, such sessilin-favored fitness may also apply under natural conditions.

On the other hand, this work also highlights a new role for the *Bacillus* lipopeptide surfactin in counteracting the toxicity of *Pseudomonas* CLPs. Our data show that surfactin acts as a protective agent which inactivates sessilin and tolaasin via co-aggregation into insoluble supra-molecular complexes observed as a white-line on a solid medium. This aggregation occurs quite specifically since this white-line was not visible in confrontation with other *Pseudomonas* strains forming non-toxic CLPs from different structural groups. From an ecological viewpoint, the role of sessilin in white-line formation for *Pseudomonas* species still remains unclear even if it has been proposed that sessilin production hampers the release of orfamide in the medium which in turn reduces the swarming motility of *Pseudomonas* [269]. Here, we provide the first example that CLPs co-precipitation can be directly involved in the interference competition between two different genera. *In planta*, this new function of surfactin contributes to *Bacillus* competitiveness for root surface. This new role as a shield to prevent sessilin-mediated toxicity has to be added to other previously reported implications of surfactin in *B. subtilis* interspecies interactions, such as interfering with the growth of closely related species in synergy with cannibalism toxins [302], inhibiting the development of *Streptomyces* aerial hyphae [303–306], participating in the expansion and motility of the interacting species but also acting as a chemoattractant to *Paenibacillus dendritiformis* [307].

B. velezensis also recruits its surfactin lipopeptide to improve multicellular mobility upon sensing *Pseudomonas*. Improved motility of *B. subtilis* has been already described upon sensing antibiotics chloramphenicol and linearmycins produced by the competitors such as *Streptomyces venezuelae* and *Streptomyces* sp. Mg1, respectively [221,239]. However, no relationship was so far established with the enhanced production of BSMs which is potentially involved in the enhanced motility of *B. subtilis*. The competitive fitness advantage, conferred by sliding mobility activation, would provide an opportunity to outcompete other microorganisms for rhizosphere colonization and/or could be an escape mechanism to antimicrobials enabling the cells to relocate rapidly upon sensing competitors. As observed in this study, CMR12a mutants impaired in CLPs, phenazine and siderophores production did not lose the ability to enhance GA1 motility, indicating a possible involvement of other BSMs. Thus, the diffusible metabolite(s) from *Pseudomonas* that stimulates surfactin-dependent motility in nearby *Bacillus* colonies still remains to be identified. According to the principle of hormesis, antibiotics may be stimulatory metabolites at subinhibitory concentrations [165,308] as reported for chloramphenicol produced by *S. venezuelae*, which was demonstrated to induce a mobile response in *B. subtilis* [221]. Further in-depth investigations should be conducted in order to evaluate whether phenazine

antibiotics, pyoverdine/pyochelin siderophores or the other molecule may act as *Pseudomonas* signals stimulating surfactin production and thus the motility in *Bacillus* cells.

In general, soil bacteria retain the potential to form and secrete a wide array of BSMs but our understanding of the true ecological roles of these compounds formed under natural conditions at inhibitory or subinhibitory concentrations has just began to be deciphered. Beyond the notion of specialized metabolites, this work points out unsuspected functions for some of these bacterial, small molecules in the context of interactions between clades that are important members of the plant-associated microbiome. We postulate that the *Bacillus* metabolite response reported here largely contributes to mount a multi-faceted defensive strategy in order to gain fitness and persistence in its natural competitive niche. One of our challenges is to expand and integrate this knowledge in order to anticipate the antagonistic or mutualistic nature of the interaction in order to rationally design compatible consortia instead of single species inoculants that are more efficient to promote plant growth and health towards economically important pathogens in sustainable agriculture.

Chapter 3

Chelator sensing mediates molecular interactions between soil bacilli and pseudomonads

This chapter is adapted from: Andrić S., Rigolet A., Argüelles Arias A., Steels S., Hoff G., Balleux G., Ongena L., Höfte M., Meyer T. and Ongena M. (2021). Chelator sensing mediates molecular interactions between soil bacilli and pseudomonads. *ISME J*, in prep.

1. Introduction

Due to continuous root exudation, the nutrient-enriched rhizosphere compartment of the soil is viewed as one of the richest habitats in terms of microbial abundance and diversity [251]. It, therefore, represents a privileged environment for interspecies interactions within the so-called rhizobiome [166,167]. Rhizobacteria developed a tight network of interactive patterns consisting of cooperative traits, but also competitive and antagonistic action modes. This interspecies competition is considered a key factor driving community assembly. It involves signal interference or toxins deployed by contact-dependent delivery systems [309,310] but is also mediated through the emission of volatiles [309,311] and various small-size soluble metabolites (referred here as bioactive secondary metabolites or BSMs) easily diffusing into areas close to the producing microorganism [252,309].

Some *Bacillus* species belonging to the *B. subtilis* group are ubiquitous habitants of the rhizobiome [10,166,246]. It includes *B. velezensis*, considered a model for plant-associated bacilli, providing benefits to its host in terms of growth and health [312]. Multiple isolates have been described and are valorised for their strong potential as biocontrol agents reducing diseases caused by phytopathogens [247]. *B. velezensis* differentiates from other members of the *B. subtilis* group by devoting up to 13% of its genome to the biosynthetic gene clusters (BGCs), responsible for the synthesis of BSMs [25,248] . This secondary metabolome is chemically diverse and includes volatile compounds, terpenes, non-ribosomal (NR) dipeptides, cyclic lipopeptides (CLPs) and polyketides (PKs), but also ribosomally-synthesized and post translationally-modified lantibiotics and bacteriocins (RiPPs) [208,249]. Mostly guided by practical concerns, the research on *Bacillus* BSMs has so far mainly focused on the characterization of their biological activities in the context of biocontrol, describing their involvement in direct inhibition of phytopathogens and their activity as elicitors of plant systemic resistance toward the attackers [12,109]. Nevertheless, from an ecological viewpoint, these BSMs retain other functions contributing to the persistence of the producing bacteria in natural settings. However, for *B. velezensis*, as for other species, our knowledge about such ecological relevance is still limited. Multiple functions of BSMs as drivers of developmental traits, or as compounds playing key antagonistic and/or signaling roles in multitrophic interactions remain to be discovered [165,207,250].

The molecular basis of interference interactions and their phenotypic outcomes between diverse soil bacterial species have been thoroughly investigated in the last decades [253,313]. In general, it is assumed that interspecies interactions and competitor sensing are among the main biotic factors affecting the bacterial production of BSMs in crowded environmental niche [167,309] Some recent reports have demonstrated how soil bacilli can modulate their behavior when facing bacterial competitors but almost exclusively describe the effect on

developmental traits such as social motility, biofilm formation and sporulation (reviewed in [253]). Modulation of BSM production by *Bacillus* in response to the perception of fungi and plants has been occasionally reported [148,190,191,203–205,253] but how and to what extent the formation of these crucial metabolites can be impacted upon interbacterial interactions is still largely unknown.

In this work, we primarily wanted to evaluate the potential of *B. velezensis* in modulating its secondary metabolome upon a perception of bacterial competitors sharing the same niche. We studied pairwise interaction with *Pseudomonas* in a simplified bipartite system adequate to uncovering cell-cell communication cues. We performed most experiments in contact-independent settings, which somehow reflects the real situation in the soil where microbes are not necessarily in direct physical contact with neighboring cells [167,314]. The *Pseudomonas* species used here belongs to the *P. fluorescens* lineage and was selected as plant beneficial, but a highly competitive challenger commonly encountered in rhizobiomes [10]. Importantly, it also retains the potential to form a wide array of specialized secondary metabolites [10] allowing to investigate of the interplay between BSMs from both species, as the main drivers of chemical relationships occurring at distance [165,167].

By combining molecular and analytical methods with mutational approaches, we observed that *B. velezensis* mobilizes a substantial part of its secondary metabolome by chemically sensing the *Pseudomonas* competitor. As it includes some polyketides and the bacteriocin amylocyclicin, such metabolite response correlates with an enhanced global antibacterial potential. Production of the surfactin is also stimulated upon interaction which may contribute to rhizosphere fitness since it favors biofilm formation and motility [241]. Furthermore, we identified the *Pseudomonas* secondary siderophore (enantio-)pyochelin (E-PCH) as a signal specifically perceived by *Bacillus* and therefore point out a new role for this siderophore in interspecies chemical signaling. *Bacillus*'s potential benefits of such a chelator sensing phenomenon in microbial interactions are also discussed.

2. Material and methods

2.1 Bacterial strains and growth conditions

Strains and plasmids used in this study are listed in Table 3-1. All bacteria were overnight cultured in Lysogeny broth (LB) (10 g L^{-1} NaCl, 5 g L^{-1} yeast extract and 10 g L^{-1} tryptone) medium, at 30 °C. After being washed three times in peptone water, bacteria were used for the experimental setup. *B. velezensis* strains were grown at 30 °C on, half diluted, recomposed exudate medium (EM) [171]. EM was made by mixing 3 solutions (pH=7) after autoclaving, as follows: 1/4 of sugar solution (4 g L^{-1} glucose, 6.8 g L^{-1} fructose, 0.8 g L^{-1} maltose, and 1.2 g L^{-1} ribose), 1/2 of organic acid solution (8 g L^{-1} citrate, 8 g L^{-1} oxalate, 6 g L^{-1}

succinate, 2 g L^{-1} malate, and 2 g L^{-1} fumarate), and 1/2 of all media [0.685 g L^{-1} KH_2PO_4, 21 g L^{-1} morpholinepropanesulfonic acid (MOPS), 0.5 g L^{-1} $MgSO_4$ x $7H_2O$, 0.5 g L^{-1} KCl, 1 g L^{-1} yeast extract, 1 g L^{-1} Casamino Acids, 2 g L^{-1} $(NH_4)_2SO_4$, and 100 ml of each trace solution of $Fe_2(SO_4)_3$ (12 g L^{-1}), $MnSO_4$ (4 g L^{-1}), $CuSO_4$ (16 g L^{-1}), and Na_2MoO_4 (40 g L^{-1}]). *Pseudomonas* strains were cultured in EM and casamino acid (CAA) liquid medium (10 g L^{-1} casamino acid, 0.3 g L^{-1} K_2HPO_4, 0.5 g L^{-1} $MgSO_4$ and pH=7), at 30 °C. The phytopathogenic bacterial strains were grown in LB liquid medium, at 30 °C.

Table 3-1. Strains and plasmids used in this study.

	Relevant genotype and description	**References or sources**
B. velezensis		
GA1	Wild type	[264]
GA1 Δ*sfp* ::cat	GA1 deleted of *sfp* gene; unable to produce lipopeptides, polyketides and bacillibactin	This study
GA1 Δ*srfAA* ::cat	GA1 deleted of *srfAA* gene; unable to produce surfactin	This study
GA1 Δ*ituA* ::cat	GA1 deleted of *ituA* gene; unable to produce iturin	This study
GA1 Δ*fenA* ::cat	GA1 deleted of *fenA* gene; unable to produce fengycin	This study
GA1 Δ*dhbC* ::cat	GA1 deleted of *dhbC* gene; unable to produce bacillibactin	This study
GA1 Δ*baeJ* ::cat	GA1 deleted of *baeJ* gene; unable to produce bacillaene and dihydrobacillaene	This study
GA1 Δ*baeS* ::cat	GA1 deleted of *baeS* gene; unable to produce bacillaene	This study
GA1 Δ*dfnA* ::cat	GA1 deleted of *dfnA* gene; unable to produce difficidin and oxydifficidin	This study
GA1 Δ*dfnM* ::cat	GA1 deleted of *dfnM* gene; unable to produce oxydifficidin	This study
GA1 Δ*baeJ* ::cat Δ*dfnA* ::phleo	GA1 deleted of *baeJ* and *dfnM* genes; unable to produce bacillaenes and difficidins	This study
GA1 Δ*mlnA* ::cat	GA1 deleted of *mlnA* gene; unable to produce macrolactins	This study
GA1 Δ*acnA* ::cat	GA1 deleted of *acnA* gene; unable to produce amylocyclicin	This study
GA1 Δ*acnA*::cat Δ*sfp*::phleo	GA1 deleted of *sfp* and *acnA* genes; unable to produce lipopeptides, polyketides, bacillibactin and amylocyclicin	This study
GA1 Δ*amlA* ::cat	GA1 deleted of *amlA* gene; unable to produce amylolysin	This study
GA1 Δ*bacA* ::cat	GA1 deleted of *bacA* gene; unable to produce bacilysin	This study
GA1 Δ*fur* ::cat	GA1 deleted of *fur* gene; devoted of FurR function	This study
GA1 Δ*per* ::cat	GA1 deleted of *per* gene; devoted of PerR function	This study
S499	Wild type	[78]
FZB42	Wild type	[265]
QST713	Wild type	[29]
P. sessiligenes		
CMR12a	Wild type	[266,267]
Δ*sesA*	CMR12a disrupted of *sesA* gene; Gm^R; unable to produce sessilin	[268]
Δ*ofaBC*	CMR12a deleted of *ofaB* and *ofaC* genes; Gm^R; unable to produce orfamide	[269]
Δ*phz*	CMR12a deleted of phenazine biosynthesis operon; unable to produce phenazine	[268]
Δ*sesA-ofaBC*	CMR12a disrupted of *sesA* gene and deleted *ofaB* and *ofaC* genes; Gm^R; unable to produce sessilin and orfamide	[269]
Δ*sesA-phz*	CMR12a disrupted of *sesA* gene and deleted phenazine biosynthesis operons; Gm^R; unable to produce sessilin and phenazine	[268]
Δ*ofaAC-phz*	CMR12a deleted of *ofaB* and *ofaC* genes and phenazine biosynthesis	[269]

	operons; unable to produce orfamide and phenazine	
Δ*sesA-ofaBC-phz*	CMR12a disrupted of *sesA* gene and deleted *ofaB* and *ofaC* genes and phenazine biosynthesis operons; Gm^R; unable to produce sessilin, orfamide and phenazine	[269]
Δ*pchA*	CMR12a deleted of *pchA* gene; unable to produce enantio-pyochelin	This study
Δ*pvdI*	CMR12a deleted of *pvdI* gene; unable to produce pyoverdine	This study
Δ*pvdI-pchA*	CMR12a deleted of *pvdI* and *pchA* genes; unable to produce pyoverdine and enantio-pyochelin	This study
P. protegens		
Pf-5	Wild type; enantio-pyochelin producer	[270]
P. aeruginosa		
PA01	Wild type; pyochelin producer	[315]
E. coli		
DH5αpir	supE44, ΔlacU169 (ΦlacZΔM15), recA1, endA1, hsdR17, thi-1, gyrA96, relA1, λpir	[276]
DH5α p497	Helper strain harboring P497 plasmid	C. Keel laboratory
Plasmids		
pEMG	pSEVA212S; oriR6K, *lacZα* with two flanking I-SceI sites; Km^r, Ap^r	[279]
pEMG-*pchA*	Suicide plasmid used for the deletion of *pchA*	This study
pEMG-*pvdI*	Suicide plasmid used for the deletion of *pvdI*	This study
pSW-2	oriRK2, *xylS*, P_m*::I-sceI*; Gm^R	[279]
Phytopathogenic strains		
Xanthomonas campestris pv. *campestris*		DSMZ[1] N°3586
Clavibacter michiganensis subsp. *michiganensis*		DSMZ[1] N°20741
Pectobacterium carotovorum		De Mot laboratory
Pseudomonas fuscovaginae		De Mot laboratory
Pseudomonas cichorii		De Mot laboratory
Agrobacterium tumefaciens		De Mot laboratory
Rhodoccocus fascians		De Mot laboratory

2.2 Construction of deletion mutants of B. velezensis *GA1*

All deletion mutants were created by marker replacement, following the protocol described in Hoff *et al.* (2021). Briefly, 1 kb of the upstream region of the targeted gene, antibiotic marker (chloramphenicol or phleomycin cassette) and downstream region of the targeted gene were PCR amplified with appropriate primers (Table 3-2). To obtain the DNA fragment containing three aforementioned components, the overlap PCR has been used. The modified cells were further selected according to chloramphenicol resistance (phleomycin resistance for double mutants) on LB medium. All gene deletions were verified by PCR with the specific UpF and DwR primers (Table 3-2) and by the loss of the corresponding BSMs production.

Table 3-2. Primers used in this study.

Deletion mutant	Primer Name	Primer sequence (5'->3')	Targeted genes
***B. velezensis* GA1**			
	UpsrfAAF	TCAGCAAAACTGCGTGGTAG	*srfAA*
	UpsrfAAR	CCAATTTTCGAATTCTTTTACCGCGATAAAAAGTTATTTCCATATGTGTGC	
	DwsrfAAF	CAGCTCCAGATCCTCTACGCCGGACACGCTTTATATCGTGCCGAA	
	DwsrfAAR	AAGAAATGATCATAAATACC	
	UpFenAF	AGCAAAAACCGGGTCACTAA	*fenA*
	UpFenAR	CCAATTTTCGAATTCTTTTACCGCGTTCGTCTGACATGACAAGCA	
	DwFenAF	CAGCTCCAGATCCTCTACGCCGGACAAAGGACTTTAATTTCATAAAAAGGTG	
	DwFenAR	CCTTTTTGAGAAGAGAAGAAAAAG	
	UpItuAF	ATGCAGGAAATAGGGGTGAA	*ituA*
	UpItuAR	CCAATTTTCGAATTCTTTTACCGCGGGTATACATAGGTCCCCTCCTG	
	DwItuAF	CAGCTCCAGATCCTCTACGCCGGACCAATTGAACTTTTAGGGAAAAGCA	
	DwItuAR	GCGACTAACGTATCGGGTTG	
	UpDfnAF	GACTTTTGAATAATCTACAGTGTCTCC	*dfnA*
	UpDfnAR	TTTTCGAATTCTTTTACCGCGAAACGCGTTTGCGATTCAG	
	UpDfnAphleoR	CAGGAAACAGCTATGACAAACGCGTTTGCGATTCAG	
	DwDfnAphleoF	GTAAAACGACGGCCAGTACAGGCTGAGTATGACCAGACA	
	DwDfAF	CAGCTCCAGATCCTCTACGCCGGACACAGGCTGAGTATGACCAGACA	
	DwDfnAR	TCCGGAATATGATCTTGTGAAG	
	UpDfnMF	GGGCAGTGGAGCTGTACC	*dfnM*
	UpDfnMR	CCAATTTTCGAATTCTTTTACCGCGGGTCATTTTCATTCCTCCAAGA	
	DwDfnMF	CAGCTCCAGATCCTCTACGCCGGACCTTGTTGAGTTTTGAACGAAAAA	
	DwDfnMR	AGCCGTTATCAATCGTGCTG	
	UpBaeJF	GTATGCGTCCCAGACTCAGC	*baeJ*
	UpBaeJR	CCAATTTTCGAATTCTTTTACCGCGTTTCATAGAGCTGCCTCCAT	
	DwBaeJF	CAGCTCCAGATCCTCTACGCCGGACGGGATACCTATGAAGTGGAGGTT	
	DwBaeJR	TCATAGTAGCCGACTTGAGAATCA	
	UpBaeSF	GTACAGCAAGGTGCCATGAG	*baeS*
	UpBaeSR	CCAATTTTCGAATTCTTTTACCGCGTTTTTGAAAAGACATAACCAACAG	
	DwBaeSF	CAGCTCCAGATCCTCTACGCCGGACTTTTAATATCGCCCCCTGTTT	
	DwBaeSR	GAGGCGTTGAAGCATACCAG	
	UpsfpF	TCGTCACCCATGAAATCAAA	*sfp*
	UpsfpR	CCAATTTTCGAATTCTTTTACCGCGCATGTCCAGATCCTCCGTCT	
	DwsfpF	CAGCTCCAGATCCTCTACGCCGGACGACGGGATTGAGATGAAAA	
	DwsfpR	CATTGAGACGTACCCGCTTT	
	UpdhbCF	GCGTTTCTGCCTGAATCC	*dhbC*

	UpdhbCR	CCAATTTTCGAATTCTTTTACCGCGCATGTTTGTCCCTCCTTTTCGT	
	DwdhbCF	CAGCTCCAGATCCTCTACGCCGGACGGCTTTACCAAGATGA	
	DwdhbCR	GCAGCACTTGAAGGCTTGAT	
	UpmlnAF	CGGAAAAACCGTTTCAAAAA	
	UpmlnAR	CAGGAAACAGCTATGACTTTTAAAATTGTCATTTACTCTAAGCA	*mlnA*
	DwmlnAF	GTAAAACGACGGCCAGTCTAAGGCGCAGATTGGATA	
	DwmlnAR	TGTACCTGTGCCATGTGCTT	
	UpbacAF	GATGGGTCTGATCGTGTCAA	
	UpbacAR	CCAATTTTCGAATTCTTTTACCGCGCATGAGCACCAACCAATCTG	*bacA*
	DwbacAF	CAGCTCCAGATCCTCTACGCCGGACAACTGAACAAGATTTGCAGG	
	DwbacAR	GAATCGGGGCGACAATTT	
	UpacnAF	TCCTTGTCACTGGGTGATGA	
	UpacnAR	TTTCGAATTCTTTTACCGCGGTTCATCATAACATCTCCCTACTCTG	*acnA*
	DwacnAF	CCAGATCCTCTACGCCGGACGCAGCTGCTTGGTAAAATCG	
	DwacnAR	CGCAAAATCAGCGTTTGTC	
	UpamlAF	GGGCTGACAGGGATAAAAGA	
	UpamlAR	TTTCGAATTCTTTTACCGCGCTCATTCATTAATATTCCTCCCTTTG	*amlA*
	DwamlAF	CCAGATCCTCTACGCCGGACTGGTGTTAAAACAACCCGAAA	
	DwamlAR	TCATGATCTCTAATTTTCTCATTCAAA	
	UpfurF	TCTCAGAAGAAACGGGATGC	
	UpfurR	CAGGAAACAGCTATGACCATGTCTTTCCCTCCTACGC	*fur*
	DwfurF	GTAAAACGACGGCCAGTTAAAAGCCTATGAACCTTTTCTGC	
	DwfurR	ATCCCTGACGGCTGATCT	
	UpperRF	GTACAGCACGCCGTTTTCC	
	UpperRR	CAGGAAACAGCTATGACCATCCGTCATGCACCTCTC	*per*
	DwperRF	GTAAAACGACGGCCAGTAAAGAAAACCACTAAACGAAGCTG	
	DwperRR	CGCTTTTCCTTCTACAAATCTTC	
***P. sessiligenes* CMR12a**			
	UppvdIF	GGCATTCTTGACCGGTCGTC	
	UppvdIR	GTGTTGTCCATTACACAGCCTCCATTGCATTCATCGGGAGTCATCC	
	DwpvdIF	ATGGAGGCTGTGTAATGGACAACA	*pvdI*
	DwpvdIR	TGTAGCGGTGTAGCAGAG	
	pvdICheckF	CCTGCTGCTGGAAGGATTGA	
	pvdICheckR	GGATCGAGCTGCCAAAGGAA	
	UppchAF	GACCAACTGCCGGCGGAT	
	UppchAR	CCTTCAGCGATCGGCCGGTGCATCACATCTTGCGCTCCTTGCTCC	
	DwpchAF	TGATGCACCGGCCGATC	*pchA*
	DwpchAR	GTGGTGAAGCTTTCCATGCC	
	pchACheckF	TCATCCACTGGAACATCGCC	
	pchACheckR	GCGGACTGATTTCCTCGGTA	
Antibiotic marker			
	CatF	CGCGGTAAAAGAATTCGAAAA	Chloramphenicol marker
	CatR	GTCCGGCGTAGAGGATCTG	

	PhleoF	GTCATAGCTGTTTCCTGCCAAAAGGGGGTTTCATTTT	Phleomycin marker
	PhleoR	ACTGGCCGTCGTTTTACTCCAATAAATGCGACACCAA	
	nptIIF	GAGGATCGTTTCGCATGATT	Kanamycin marker for *Pseudomonas*
	nptIIR	CGCTCAGAAGAACTCGTCAA	
	psw-F	GGACGCTTCGCTGAAAACTA	pSW-II insertion
	psw-R	AACGTCGTGACTGGGAAAAC	
RT-qPCR			
***B. velezensis* GA1**			
	AcnA_F_qPCR	CCAAGCAGCTGCGTATTTTT	*acnA*
	AcnA_R_qPCR	CTTCGACTCTGGGCATCTCT	
	QgyrA_F	GAGACGCACTGAAATCGTGA	*gyrA*
	QgyrA_R	GCCGGGAGACGTTTAACATA	
	BaeJQ_F_qPCR	CCGATGACGATTCCTGAAGT	*baeJ*
	BaeJQ_R_qPCR	GCCCTTTCACAATCGAAAGA	
	DfnA_F_qPCR	GGCGTTTTTGCCTCTTCGTT	*dfnA*
	DfnA_R_qPCR	ATCAGACGGCGTATCGTGTC	
	SrfAA_F_qPCR	ATTGTTTACGGTGGCTCTGG	*srfAA*
	SrfAA_R_qPCR	CGCTGCGATAGTCAAAATCA	

2.3 Construction of deletion mutants of P. sessiligenes *CMR12a*

PVD and E-PCH mutants of CMR12a were created by the I-SceI system and the pEMG suicid vector [279,281]. Briefly, the upstream and downstream regions flanking the *pvdI* (*C4K39_6027*) or the *pchA* (*C4K39_5481*) genes were amplified by PCR, connected via overlap PCR and introduced to the pEMG vector, while using kanamycin as an antibiotic marker. The primers used for this purpose are presented in Table 3-2. The resulting plasmid (Table 3-1) was integrated into the CMR12a chromosome by conjugation via homologous recombination. Further, the kanamycin (25 µg/mL) resistant cells were selected on solid, King B plates and transformed by electroporation with the pSW-2 plasmid (harboring I-SceI system and gentamycin). Gentamycin (20 µg/mL) resistant colonies on the plates were transmitted to King B medium with and without kanamycin to verify the loss of kanamycin resistance. Finally, CMR12a mutants were confirmed by PCR with the appropriate UpF and DwR primers (Table 3-2) and via the loss of E-PCH and PVD production.

2.4 RNA isolation and RT-qPCR

RNA extraction and DNAse treatment were carried out using the NucleoSpin RNA Kit (Macherey Nagel, Germany), following the Gram-positive manufacturer's protocol. RNA quality and quantity were performed with Thermo scientific NanoDrop 2000 UV-vis Spectrophotometer. Primer 3 program available online was used for primer design and primers were synthesized by Eurogentec.

The primers used for this purpose are listed in Table 3-2. The primer efficiency was evaluated and primer pairs showing an efficiency between 90 and 110% in the qPCR analysis were selected. Reverse transcriptase and RT-qPCR reactions were conducted using the Luna® Universal One-Step RT-qPCR Kit (New England Biolabs, Ipswich, MA, United States). The reaction was performed with 50 ng of total RNA in a total volume of 20 µL: 10 µL of luna universal reaction mix, 0.8 µL of each primer (10 µM), 5 µL of cDNA (50ng), 1 µL of RT Enzyme MIX, 2.4 µL of Nuclease-free water. The thermal cycling program applied on the ABI StepOne was: 55 °C for 10 min, 95 °C for 1 min, 40 cycles of 95 °C for 10 s and 60 °C for 1 min, followed by a melting curve analysis performed using the default program of the ABI StepOne qPCR machine (Applied Biosystems). The real-time PCR amplification was run on the ABI step-one qPCR instrument (Applied Biosystems) with software version 2.3. The relative gene expression analysis was conducted by using the $2^{\Delta Ct}$ method with the *gyrA* gene as a housekeeping gene to normalize mRNA levels between different samples. The target genes in this study were *srfAA, dfnA, baeJ* and *acnA.*

2.5 Pseudomonas *cell-free supernatant*

Pseudomonas cell suspension was adjusted to OD_{600nm} 0.05, in 100 mL of CAA and, when appropriate, supplemented with 20 µg/L of $FeCl_3x6H_2O$ (iron supplementation). Cultures were orbitally shaken at 120 rpm at 30 °C for 48 h. Finally, the cultures were centrifuged at 5000 rpm at room temperature (approx. 22 °C) for 20 min. The supernatants were further filter-sterilized (0.22 µm pore size filters) and stored at -20 °C until further use.

2.6 Dual interactions

B. velezensis cells were diluted in 2 mL of liquid EM medium to a final OD_{600nm} of 0.1, in which 2% (v/v) of CMR12a cell-free supernatant (CFS) was added while the control remained un-supplemented. *B. velezensis* liquid cultures were then orbitally shaken in an incubator at 300 rpm, at 30 °C for 24 h (if not indicated differentially). Finally, 2 mL of the *Bacillus* culture supernatants were sampled, centrifugated at 5000 rpm at room temperature (approx. 22 °C) for 10 min to extract supernatants and collect the cells. Further, the supernatants were filter-sterilized (0.22 µm) and used for analytical analysis of BSMs and antibacterial assays. The remaining cells after supernatant collection were stored at -80 °C to avoid RNA degradation, until performing RT-qPCR analysis.

2.7 Antimicrobial activity assays

Antibacterial activity of the GA1 wild type or GA1 mutants' supernatants was tested against *Xanthomonas campestris* and *Clavibacter michiganensis.* The activity of GA1 supernatants was quantified in microtiter plates (96-well) filled with 250 µL of LB liquid medium, inoculated at OD_{600nm}=0.1 with *X. campestris* or *C. michiganensis* and supplemented with 2% or 6% (v/v) of the supernatants, respectively. The activity of GA1 supernatants was estimated by measuring the

pathogen OD_{600nm} every 30 min for 24 h with a Spectramax® (Molecular Devices, Wokingham, UK), continuously shaken at 150 rpm, at 30 °C. Two independent assays each, involving three technical repetitions were performed.

For estimating the activity of GA1 supernatants on a solid medium, 5 µL of the supernatant was applied to a sterile paper disk (5 mm diameter). After drying, disks were placed on solid LB square plates previously inoculated with a confluent layer of *X. campestris*, *C. michiganensis*, *Pectobacterium carotovorum*, *Pseudomonas fuscovaginae*, *Pseudomonas cichorii*, *Agrobacterium tumefaciens*, or *Rhodococcus fascians*. The same volume of LB liquid medium was used as a negative control. Plates were incubated at 25 °C for 48 h. Three repetitions were done and the inhibition zones was measured from the edge of the paper discs to the edge of the inhibition zone.

2.8 Secondary metabolite analysis

For targeted and untargeted analysis of BSMs, GA1 and CMR12a were cultured in EM and/or CAA, as described above, and on tomato plantlets roots (see the section ‘’*in planta* competition’’ below).

Untargeted analyses of metabolites produced by GA1 (presented on Fig. 3-4A, 3-1, 3-6 and 3-18) and CMR12a were performed using UPLC MS (Agilent 1290 Infinity II) coupled Jet Stream ESI-Q-TOF 6530 mass spectrometers used in positive and negative (for difficidins) mode. The parameters for untargeted analyses of metabolites identification by UPLC-qTOF MS were set up as follows: parameters: capillary voltage: 3.5 kV; nebulizer pressure: 35 psi; drying gas: 8 L/min; drying gas temperature: 300 °C; flow rate of sheath gas: 11 L/min; sheath gas temperature: 350 °C; fragmentor voltage: 175 V; skimmer voltage: 65 V; octopole RF: 750 V. Accurate mass spectra for *Pseudomonas* BSMs were recorded in the range of m/z=40-2500. Accurate mass spectra for *Bacillus* BSMs were recorded in the range of m/z =100–1700. A C18 Acquity UPLC BEH column (2.1 × 50 mm × 1.7 µm; Waters, milford, MA, USA) was used at a flow rate of 0.3 ml/min (for *Pseudomonas* BSMs) or 0.6 ml/min (for *Bacillus* BSMs) and a temperature of 40 °C. The injection volume was 20 µL (for *Pseudomonas* BSMs) or 10 µL (for *Bacillus* BSMs) and the diode array detector (DAD) scanned a wavelength spectrum between 190 and 600 nm. For *Pseudomonas* BSMs, a gradient of 0.1% formic acid water (solvent A) and acetonitrile acidified with 0.1% formic acid (solvent B) was used as a mobile phase with a constant flow rate at 0.45 mL/min starting at 10% B and raising to 100% B in 20 min. Solvent B was kept at 100% for 2 min before going back to the initial ratio. For *Bacillus* BSMs, a gradient of 0.1% formic acid (solvent A) and acetonitrile acidified with 0.1% formic acid (solvent B) was used as a mobile phase with constant flow rate at 0.6 mL/min starting at 10% B and raising up to 100% B in 20 min. Solvent B was kept at 100% for 4 min before going back to initial ratio and kept as such for 4 min before next injection. MassHunter Workstation v10.0 and ChemStation software were used for data collection and analysis.

Targeted analysis of metabolites produced by GA1 (presented on Fig. 3-4B, 3-13, 3-7 and 3-19) were made by UPLC–MS with UPLC (Acquity H-class, Waters) coupled to a single quadrupole mass spectrometer (SQD mass analyzer, Waters), using a C18 column (Acquity UPLC BEH C18 2.1 mm × 50 mm, 1.7 µm), in negative (difficidins) and positive mode. Elution for targeted GA1 BSMs analysis by UPLC MS were performed at 40 °C with a constant flow rate of 0.6 mL/min using a gradient of Acetonitrile (solvent B) and water (solvent A) both acidified with 0.1% formic acid as follows: 2 min at 15% B followed by a gradient from 15% to 95% during 5 min and maintained at 95% up to 9.5 min before going back to initial conditions at 10 min during 2 min before next injection. Compounds were detected in both electrospray positive and negative ion mode by setting SQD parameters as follows: cone voltage: 60V; source temperature 130 °C; desolvation temperature 400 °C, and nitrogen flow: 1000 L/h with a mass range from m/z 300 to 2048. MassLynx software v4.1 software was used for data collection and analysis.

2.9 MZmine analysis

Mzmine 2 parameters used in this study were set up as follows: MS 1 noise level was set at $1x10^4$. Further, the ADAP chromatogram builder was used (min group size in scans=5, Group intensity threshold=$2x10^4$ and minimum highest intensity=$3x10^4$, m/z tolerance=20 ppm). The chromatogram deconvolution was made by Local minimum search (chromatographic threshold=5%, Search min Rt range=0.15 min, Min relative height=10%, Min absolute height=$3x10^4$, min ration of peak top/edge=1.5, peak duration range=0.1-1 min, m/z center calculation is the median, m/z range for MS2 pairing=0.02 Da, Rt range for MS2 scan pairing=0.2 min) while isotope peak grouper was setup as follow: m/z tolerance=20 ppm, retention time tolerance=0.2 min, maximum charge=2. Further, the join aligner was using the following parameters: m/z tolerance=20 ppm, weight for m/z=75, retention time tolerance=0.2 min, weight for Rt=25. Finally, the data was adapted with a feature list filter (minimum peaks in a row=3, minimum peaks in an isotope pattern=2, Retention time range from 1.5 to 20 min).

2.10 Bioguided fractionation

CMR12a CFS were concentrated with a C18 cartridge ‘Chromafix, small’ (Macherey-Nagel, Düren, Germany). The column was conditioned with 10 mL of MeOH followed by 10 mL of milliQ water. Then, 20 mL of supernatant flowed through the column. The metabolites were eluted with 1 mL of a solution of increasing acetonitrile/water ratio from 5:95 to 100:0 (v/v). The triggering effect of these fractions on GA1 PKs production was tested as previously described in the section ‘’Dual interactions’’.

2.11 Purification of PVD, E-PCH and PCH

Pyoverdine (PVD) and enantio-pyochelin (E-PCH) or pyochelin (PCH), produced by CMR12a or *Pseudomonas aeruginosa* PA01, respectively, were purified in two steps. Firstly, *Pseudomonas* CFS were concentrated with a C18 cartridge (as indicated in section Bioguided fractionation) and eluted with 2 times 2 mL of a solution of water and ACN (15 and 30% of ACN (v/v)). Secondly, the fractions were injected on HPLC for purification performed on an Eclipse + C18 column (L=150 mm, D=3.0 mm, Particle's diameter 5 µm) (Agilent, Waldbronn, Germany).

The volume injected was 100 µL. The UV-Vis absorbance was measured with a VWD Agilent technologies 1100 series (G1314A) detector (Agilent, Waldbronn, Germany). The lamp used was a Deuterium lamp G1314 Var Wavelength Det. (Agilent, Waldbronn, Germany). Two wavelengths were selected: 320 nm, used for the detection of E-PCH and PCH, and 380 nm, used to detect PVD. The fractions containing the siderophores were collected directly at the detector output. Further, the purity of the samples was verified by two detectors, a diode array detector (DAD) 190 to 601 nm (steps: 1 nm) and a q-TOF (tandem mass spectrometry, quadrupole and Time of flight detector combined) (Agilent, Waldbronn, Germany). Electrospray ionization was performed in positive mode (ESI+) (Dual AJS ESI) (Vcap=3500 V, Nozzle Voltage=1000 V), with a mass range from m/z 200 to 1500.

Finally, the concentration of siderophores was estimated using Beer-Lambert law formula, $A=\varepsilon lc$ (A: absorbance; ε: molar attenuation coefficient or absorptivity of the attenuating species; l: optical path length and c: concentration of molecule). l value for E-PCH and PVD is 1 cm while ε is 4000 L mol^{-1} cm^{-1} or 16000 L mol^{-1} cm^{-1}, respectively and as established previously [316]. The absorbance was measured with VWR, V-1200 Spectrophotometer, at 320 nm (pH=8) for E-PCH or PCH and 380 nm (pH=5) for PVD [316]. Further, the absorbance value was used for calculating the final concentration.

The fragmentation pattern of CMR12a PVD was obtained by UPLC-qTOF MS/MS analysis of m/z=1288.5913 ion in positive mode with fragmentation energy at 75 V and compared to the one described in *P. protegens* Pf-5 [317].

2.12 Confrontation assay

To evaluate the inhibition of *Pseudomonas* strains by GA1, the confrontation assays on LB medium were done. The 5 µL of bacterial suspension of OD_{600nm}=0.1 was spotted at 1 mm distance onto LB plate, which was further incubated at 30 °C for 24 h. Photographs were taken by CoolPix camera (NiiKKOR 60x WIDE OPTICAL ZOOM EDVR 4.3-258 mm 1:33-6.5). Three independent assays each, involving three technical repetitions were performed.

2.13 In planta *competition*

For *in planta* studies, tomato seeds (*Solanum lycopersicum* var. Moneymaker) were sterilized following the protocol described by Hoff *et al.* (2021). Further, seeds were placed on square Petri dishes (5 seeds/plate) containing Hoagland solid medium [190] and placed in the dark for three days. Afterward, 10 seeds were inoculated with 2 µL of the culture (OD_{600}=0.1) of the appropriate strains (mono-inoculation) or with a mix of GA1 and CMR12a cells (95:5 ration) (co-inoculation) and grown at 22 °C under a 16/8 h night/day cycle with constant light for three days. After the incubation period, to determine bacterial colonization levels, bacteria were separated from roots by vertexing for 5 min in peptone water solution supplemented with 0.1% (v/v) of Tween 80. Serial dilutions were prepared and 200 µl of each were plated onto solid LB medium using plating glassy beads. After 24 h of incubation at 30 °C for CMR12a and at 42 °C for GA1, colonies were counted. Finally, the colonization results were log-transformed and further statistically analyzed.

For GA1 and CMR12a BSMs production analysis in *in planta* conditions plants were inoculated and incubated as indicated above, for 7 days. An agar part (1 x 2.5 cm) near the tomato roots was cut and the extraction of BSMs was done with 1.5 mL of acetonitrile (85% (v/v)) for 15 min at room temperature (approx. 22 °C). Further, the samples were centrifuged for 5 min at 4000 rpm and the supernatant was collected for UPLC-MS analysis as described above. Four independent assays each, involving at least four plants per treatment, were performed.

2.14 Statistical analysis

For statistical analyses, software GraphPad PRISM 8 with Mann-Whitney or Student paired T-test was performed. Further, the RStudio 1.1.423 statistical software environment (R language version 4.03) [284] was used for multiple comparisons where one-way ANOVA and Tukey's Honest Significant Distance (HSD) tests were performed. The groups that differed significantly from each other, at α=0.05, were labeled with different letters.

3. Results

3.1 B. velezensis *modulates its secondary metabolome upon sensing* Pseudomonas *metabolites*

In this work, we used the rhizosphere *B. velezensis* strain GA1 as genetically amenable natural isolate, representative of the species regarding BSM richness. Upon growth in the so-called exudate-mimicking (EM) medium, reflecting the content in major carbon sources released by roots of *Solanaceae* plants [279], strain GA1 indeed efficiently produces the whole range of NR BSMs typically formed by GA1 (Fig. 3-1).

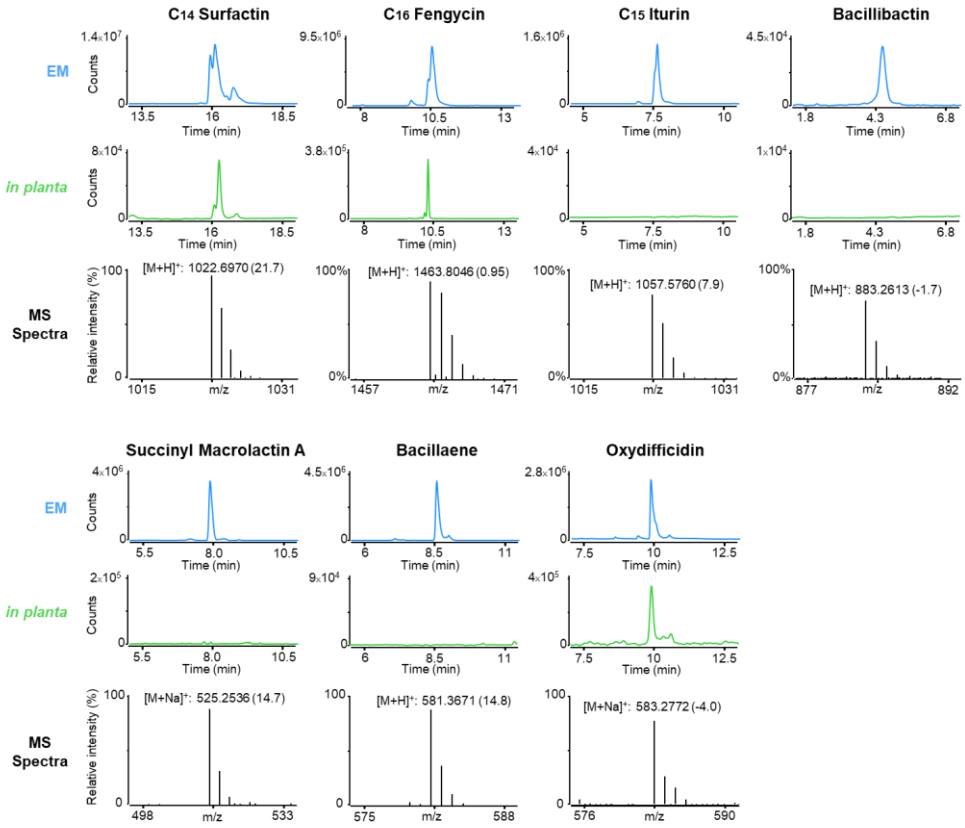

Figure 3-1. The relative amount of BSMs produced by *B. velezensis* GA1 in different conditions. Extracted ion chromatograms (EICs) of the different BSMs detected in 24 h liquid culture (EM: exudates mimicking medium) or recovered from agar surrounding colonized tomato plantlets at 7 dpi (*in planta*). Structural variant and MS spectra with ion species and mass error (in ppm) are mentioned for each BSM.

In addition to these NR metabolites, genes encoding RiPPs such as amylocyclicin and amylolysin are also present in the GA1 genome [318], but these compounds could not be reliably detected in culture broths based on the accurate mass determined via UPLC-qTOF MS. We selected as the main interaction partner the plant-associated *P. sessiligenes* CMR12a based on its biocontrol potential and its production of multiple secondary metabolites. It includes antimicrobial phenazine, the siderophores pyoverdine (genomic and structural comparison with the described *P. protegens* PF-5 pyoverdine in Fig. 3-2A and B) and enantio-pyochelin as well as two structurally distinct CLPs, sessilin and orfamide [266,269,319–321].

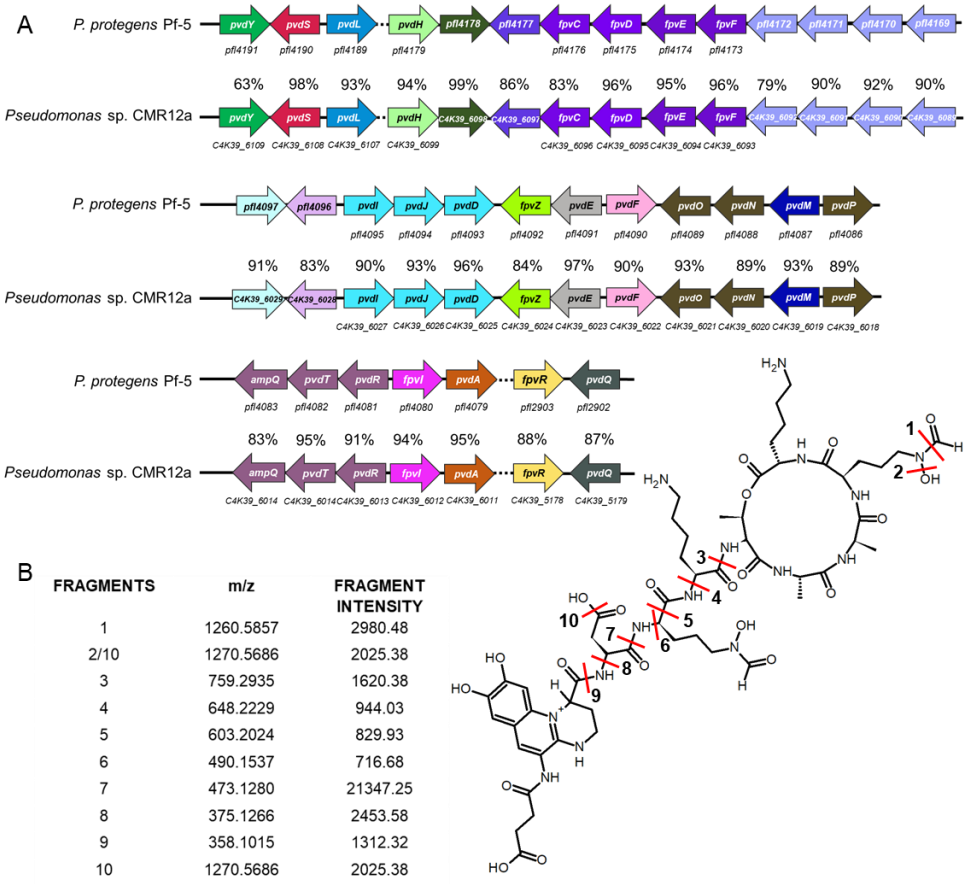

FRAGMENTS	m/z	FRAGMENT INTENSITY
1	1260.5857	2980.48
2/10	1270.5686	2025.38
3	759.2935	1620.38
4	648.2229	944.03
5	603.2024	829.93
6	490.1537	716.68
7	473.1280	21347.25
8	375.1266	2453.58
9	358.1015	1312.32
10	1270.5686	2025.38

Figure 3-2. *P. sessiligenes* CMR12a produces a PVD structurally similar to the one of *P. protegens* Pf-5. A: *P. sessiligenes* CMR12a genes were compared to the previously described *P. protegens* Pf-5 PVD biosynthetic cluster [317]. The corresponding locus tags are indicated for each gene. The nucleotide identity was calculated by blast in the MAGE platform (https://mage.genoscope.cns.fr). B: The assigned fragments of *P. sessiligenes* CMR12a PVD confirm the structural similarity with the PVD from *P. protegens* Pf-5 [317].

All these compounds were identified in culture broth upon growth in casamino acids medium (CAA) commonly used for *Pseudomonas* cultivation in iron-limited conditions (Fig. 3-3).

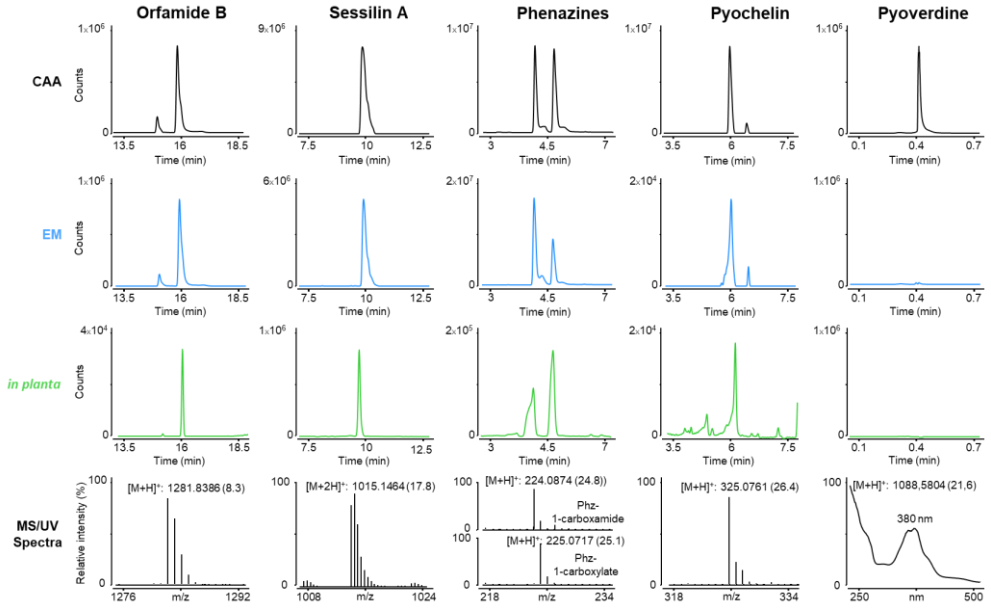

Figure 3-3. The relative amount of BSMs produced by *P. sessiligenes* CMR12a in different conditions. Extracted ion chromatograms (EICs) of the different BSMs detected in 24 h liquid culture (CAA : casamino acids medium, EM: exudates mimicking medium) or recovered from agar surrounding colonized tomato plantlets at 7 dpi (*in planta*). Structural variants and MS/UV spectra with wavelength for pyoverdine and ion species with mass error (in ppm) are mentioned for each BSM.

We wanted to evaluate the potential of GA1 to modulate its BSM production in interaction with CMR12a under conditions avoiding possible interferences due to diffusion constraints in a semi-solid matrix or due to the formation of impermeable biofilm structures. Assays were thus performed by growing GA1 in agitated liquid EM medium supplemented or not with CFS (2% (v/v)) containing metabolites produced by CMR12a in CAA medium. We first employed an untargeted UPLC-MS approach to compare metabolites secreted by GA1 in the two conditions in samples collected at three different time points corresponding to the beginning and the end of the exponential phase or to the stationary phase. Data processing with MZmine 2 [282] allowed us to detect features and the corresponding BSMs differentially produced upon interaction. It revealed a growth phase-dependent accumulation of BSMs corresponding to three different NR classes (Fig. 3-4A, Fig. 3-5 for GA1 growth kinetic).

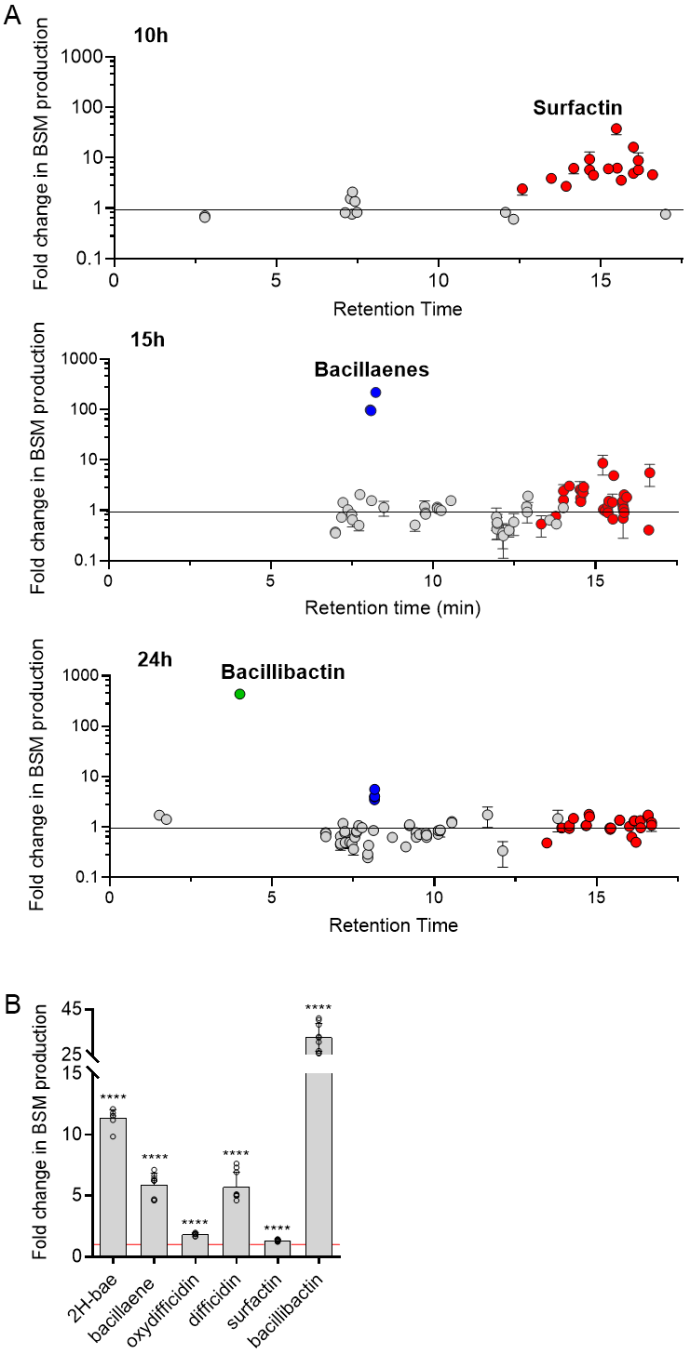
A
10h
Surfactin
Fold change in BSM production
Retention Time
15h
Bacillaenes
Retention time (min)
24h
Bacillibactin
B
2H-bae
bacillaene
oxydifficidin
difficidin
surfactin
bacillibactin

Figure 3-4. Effect of *P. sessiligenes* CMR12a supernatant on *B. velezensis* GA1 metabolite production. A: Impact of CMR12a CFS supplementation on the metabolome of GA1 at early exponential phase (10 h), late exponential phase (15 h) and stationary phase (24 h). Each dot represents a feature detected. The dots colored in red, blue and green represent the features (variants or adducts) of surfactin, bacillaene and bacillibactin respectively while grey dots represent the rest of GA1 BSMs. Overproduction data are expressed as peak area fold change OD_{600}, compared to control culture (un-supplemented GA1 culture). Error bars represent standard deviation (n=3). B: Fold increase in GA1 BSM production upon addition of CMR12a CFS (2% (v/v)) compared to un-supplemented cultures (fold change=1, red line), at stationary phase (20 h). Data are calculated as indicated in A. Mean values were calculated from data obtained in three repeats from three independent experiments (n=9). Statistical significance was calculated using Mann–Whitney test where ‘’****’’ represents a significant difference at $P<0.0001$.

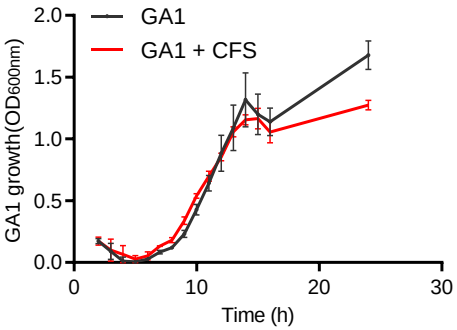

Figure 3-5. Effect of *P. sessiligenes* CMR12a metabolites on *B. velezensis* GA1 growth. *B. velezensis* GA1 (GA1) growth upon supplementation of culture medium with 2% (v/v) *P. sessiligenes* CMR12a cell-free supernatant (GA1 + CFS). Data show the means ± SD from three replicates.

The surfactin production is strongly increased at early growth, bacillaene or its dehydrated variant dihydrobacillaene (2H-bae) is stimulated at the transition from exponential to stationary phase and synthesis of the siderophore bacillibactin is further delayed (Fig. 3-4A). The amplitude and timing of the boosting effect thus varied according to the molecule, most probably due to specific and fine-tuned transcriptional regulations. The production of the other NR BSMs fengycin, iturin, macrolactin and bacilysin is not impacted by the addition of CMR12a CFS (Fig. 3-6).

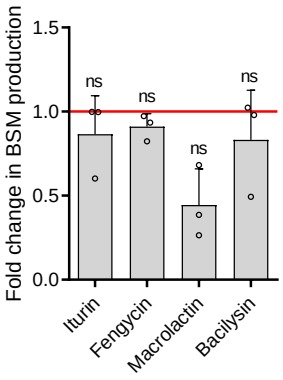

Figure 3-6. Effect of *P. sessiligenes* CMR12a supernatant on *B. velezensis* GA1 metabolite production. GA1 production of iturin, fengycin, macrolactin and bacilysin upon interaction with CMR12a CFS (2% (v/v)) during 15 h, compared to un-supplemented cultures (fold change=1, red line). Production data are expressed as peak area fold change per OD600 and compared to control culture (un-supplemented GA1 culture). Error bars represent standard deviation (n=3). Mean values were calculated from data obtained in three repeats (n=3). Statistical significance was calculated using Mann–Whitney test where ‘’ns’’ represents a non-significant difference.

Based on these data, we set out to inspect the whole range of BSMs after 20 h of growth using an optimized UPLC-MS method for targeting NR compounds. It confirmed the differential accumulation previously observed but also revealed a significantly enhanced production of difficidin or its oxidized form (only detected in ESI negative mode) upon the addition of CMR12a CFS (Fig 3-4B). Such metabolite response upon sensing CMR12a is not specific to GA1 and was also observed in other *B. velezensis* strains with established biocontrol potential such as S499, FZB42 and QST713 [17,29,78] (Fig. 3-7).

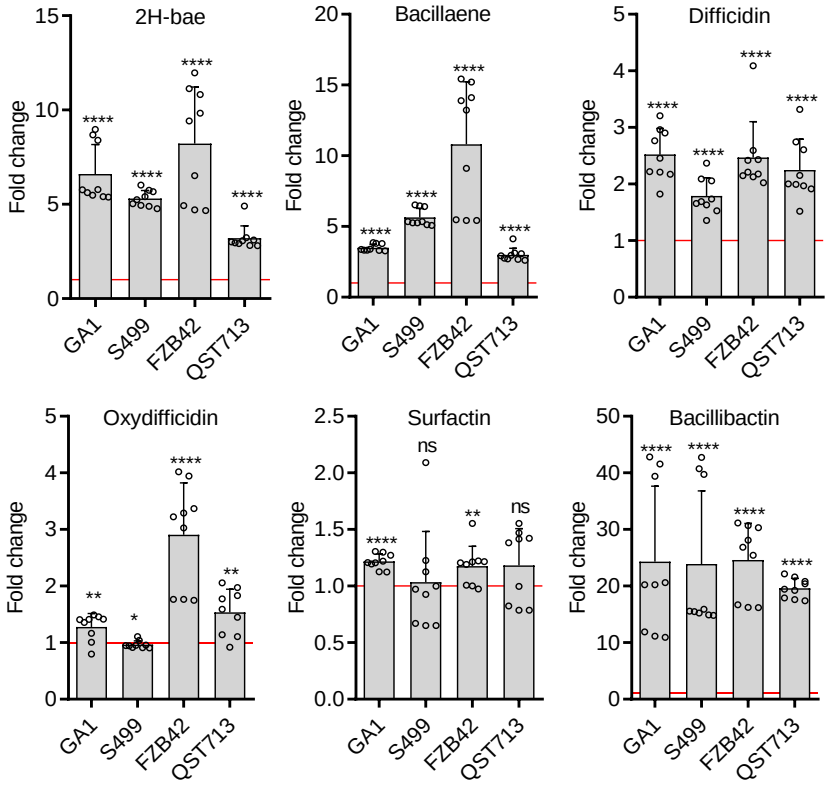

Figure 3-7. Effect of *P. sessiligenes* CMR12a metabolites on BSMs production by *B. velezensis* strains GA1, S499, FZB42 and QST713. Data indicate fold increase in BSMs production upon addition of CMR12a CFS (2% v/v) compared to un-supplemented cultures (fold change=1, red line). Data were calculated based on relative quantification of the compounds by UPLC-MS (peak area) per OD_{600}, in both conditions. Data show means ± SD were calculated from three cultures (repeats) in three independent experiments (n=9). Statistical significance was calculated using Mann–Whitney test where "ns" means no significant difference; "*", $P<0.1$; ''**'', $P<0.01$; ''****'', $P<0.0001$.

These *in vitro* data thus illustrate how *B. velezensis* modulates its secondary metabolome in response to some *Pseudomonas* compounds as secreted by planktonic cells grown in CAA medium. Based on the fact that most GA1 and CMR12a metabolites are produced in the EM medium and substantial amounts are also formed when the bacterium colonizes tomato roots (Fig. 3-1 and 3-3), we, therefore, wanted to evaluate the relevance of GA1 BSMs stimulation in a more natural context (*in planta*) with both bacteria interacting upon root co-colonization. GA1 and CMR12a both efficiently colonized roots of tomato

plantlets when inoculated individually (Fig. 3-8A). However, upon competitive root invasion, CMR12a overgrows GA1 which forms reduced populations compared to mono-inoculated plantlets (Fig. 3-8A). Due to the low populations of GA1, we could not reliably detect all GA1 BSMs in these root vicinity medium extracts from co-inoculated plants. However, a significantly enhanced expression of gene clusters responsible for the synthesis of surfactin, (2H-)bacillaene, (oxy-)difficidin and amylocyclicin was observed in GA1 cells co-inoculated with CMR12a compared to single inoculation (Fig. 3-8B). It indicates that the metabolite response observed in GA1 in *in vitro* cultures in EM medium also occurs in a more realistic context of competitive colonization where the bacteria forms biofilm and feed exclusively on root exudates.

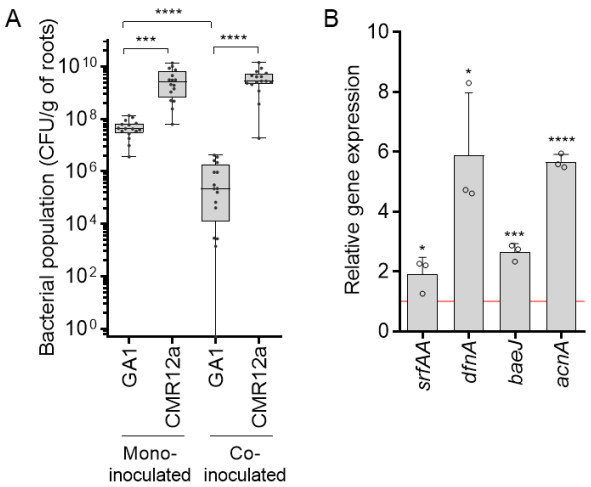

Figure 3-8. Competitive colonization assays support the roles of BSMs in *Bacillus-Pseudomonas* interaction *in planta*. A: GA1 and CMR12a cell populations as recovered from roots at 3 days post-inoculation (dpi) of tomato plantlets when mono- or co-inoculated. Box plots were created from data from four independent assays each involving at least 4 plants per treatment (n=16). The whiskers encompass to the minimum and maximum values, and the midline shows the median. Statistical differences between the treatments were analysed using Mann–Whitney test and ‘’****’’ and ‘’***’’ represent significant differences at $P<0.0001$ and $P<0.001$, respectively. B: *In planta* (3 dpi on tomato roots) GA1 relative expression of the *sfraA*, *dfnA*, *baeJ* and *acnA* genes responsible for the synthesis of respectively surfactin, (oxy)difficidin, (2H-)bacillaene and amylocyclicin, respectively. Graphs show the means ± SD calculated from three biological replicates (n=3) each involving six plants. Fold change=1 as red line corresponds to gene expressions in GA1 inoculated alone on roots used as control conditions. Statistical comparison between data in co-colonization setting and control conditions was performed based on T-test (*, $P<0.05$; ***, $P<0.001$; ****, $P<0.0001$).

3.2 BSM stimulation leads to enhanced antibacterial potential

PKs are among the BSMs best described for their inhibitory activity toward a wide range of bacteria [322,323]. We, therefore, speculated that an enhanced antibacterial activity would be a direct outcome of this GA1 metabolite response to CMR12a products. It is indeed what was observed when we tested the extracts, resulting from the interaction, for growth inhibition of *X. campestris* and *C. michiganensis*, used respectively, as representative of Gram-negative and Gram-positive plant pathogenic bacteria of agronomical importance [5] (Fig. 3-9A).

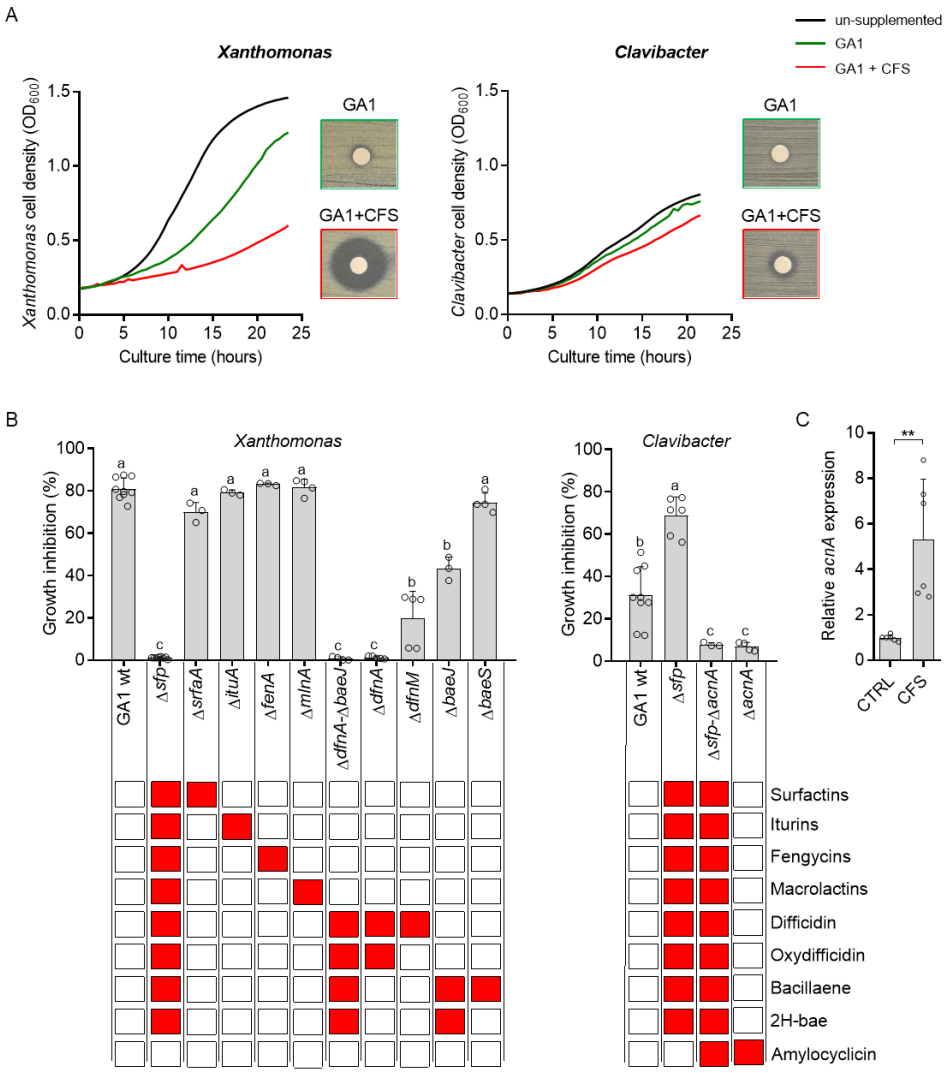

Figure 3-9. *B. velezensis* GA1 anti-bacterial activities are enhanced in response to *P. sessiligenes* CMR12a secreted metabolites and rely on the production of different BSMs according to the target species. A: The enhanced anti-*Xanthomonas campestris* and anti-*Clavibacter michiganensis* activities of GA1 extracts (cell-free culture supernatants) after 20 h growth in CMR12a CFS-supplemented medium (GA1+CFS) compared to un-supplemented control (GA1). It was assessed both on plates by the increase in inhibition zone around paper disc soaked with GA1 extracts and in liquid cultures of the pathogens by reduction of growth upon addition of GA1 extracts. Data are from one representative repetition. B: Antibacterial activities of extracts collected from GA1 wild type (GA1 wt) and mutants impaired in production of specific BSMs, after 20 h growth in EM medium. Metabolites not produced by the different mutants are illustrated with red boxes in the table below. All values represent means with error bars indicating SD calculated on data from three cultures (repeats) in two independent experiments (n=6) and 0% represents a total loss of the strain activity while 100% represents total retention of strain activity (total inhibition of the pathogen). Letters a to d indicate statistically significant differences according to one-way analysis of variance (ANOVA) and Tukey's HSD test (Honestly significantly different, α=0.05). C: Differential expression of the *acnA* gene encoding the amylocyclicin precursor, upon supplementation with CMR12a CFS compared to GA1 un-supplemented culture, after 8 h culture. Data show means ± SD recalculated from three repetitions from two biological replicates (n=6) where "**" indicates statistical significance according to Mann–Whitney test, $P<0.01$.

To determine the specific involvement of each BSM in bacterial inhibition, we generated and tested a range of GA1 knock-out mutants, including the Δ*sfp* derivative specifically repressed in 4'-phosphopantetheinyl transferase, which is essential for the proper functioning of the PK and NR peptide biosynthesis machinery. Full loss of anti-*Xanthomonas* activity in Δ*sfp* extracts indicated a key role for NR BSMs (Fig. 3-9B) and ruled out the possible involvement of other, *sfp*-independent compounds known for their antibacterial activity, as further confirmed for bacilysin or RiPPs (Fig. 3-10A).

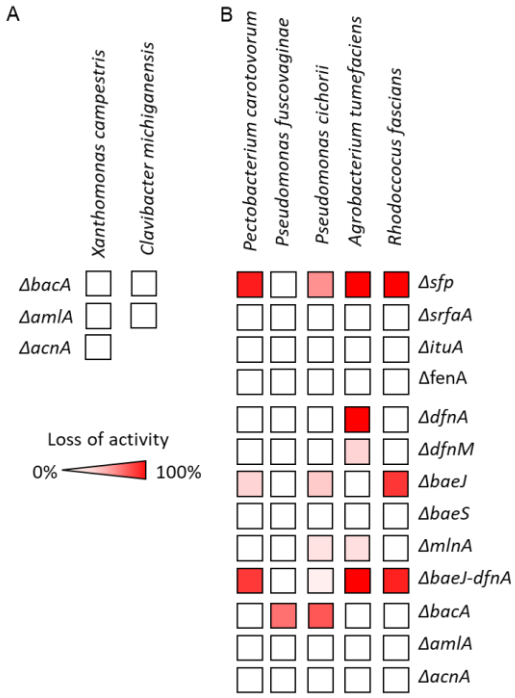

Figure 3-10. The anti-bacterial activities of *B. velezensis* GA1 rely on the production of different BSMs according to the target species. A: The heatmap indicates retention of anti-*Xanthomonas* activity of GA1 mutants unable to produce bacilysin (*ΔbacA*), amylolysin (Δ*amlA*) and amylocyclicin (*ΔacnA*) or bacilysin and amylolysin against *Clavibacter*. B: The heatmap shows the loss of anti-bacterial activity of GA1 mutants compared to the wild type strain when tested against five plant pathogenic species. The mutants are impaired in the production of NRPs and PKs (Δ*sfp*), surfactin (Δ*srfAA*), iturin (Δ*ituA*), fengycin (Δ*fenA*), difficidins (Δ*dfnA*), bacillaenes (Δ*baeJ*), difficidins and bacillaenes (Δ*baeJ-dfnA*), macrolactins (Δ*mlnA*), bacilysin (Δ*bacA*), amylolysin (Δ*amlA*) and amylocyclicin (Δ*acnA*). The intensity of activity loss is represented by the color scale where the darkest red indicates loss of 100 % and white reflects no difference compared to the wild type. None of the mutants displayed gain in activity compared to the wild-type strain. Heatmap shows the mean of three biological replicates (n=3).

Loss of function of mutants specifically repressed in the synthesis of individual compounds pointed out the key role of (oxy)difficidin and, to a lower extent, 2H-bae in *X. campestris* inhibition (Fig. 3-9B). Acting alone or in synergy, these two PKs are also responsible for GA1 inhibitory activity toward other important bacterial phytopathogens such as *P. carotovorum*, *A. tumefaciens* and *R. fasciens* but are not involved in the inhibition of plant pathogenic *Pseudomonas* species for which bacilysin may be the active metabolite (Fig. 3-10B). However, GA1 does

not display significant toxicity against non-pathogenic soil *Pseudomonas* isolate tested here (Fig. 3-11).

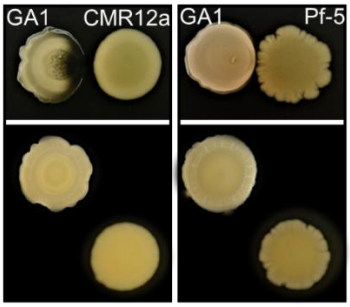

Figure 3-11. *B. velezensis* GA1 do not inhibit *P. sessiligenes* CMR12a and *P. protegens* Pf-5. Growth of CMR12a and Pf-5 during the confrontation with GA1 at a short distance (1mm) (upper panel), compared with the growth of the strains alone (panel down). Data are from one representative of three independent replicates.

In contrast to *X. campestris*, enhanced antibiotic activity against *C. michiganensis* is not mediated by NR products as shown by the fully conserved activity in the Δ*sfp* mutant (Fig. 3-9B). Therefore, we suspected from genomic data and literature [77] that RiPPs such as amylocyclicin could be involved in inhibition. This hypothesis was supported by the drastic loss in pathogen inhibition potential observed for the Δ*acnA* mutant knocked-out for the corresponding biosynthesis gene (Fig. 3-9B). Moreover, another RiPP amylolysin and NR bacilysin mutants did not lose their activity (Fig. 3-10A), pointing out amylocyclicin as a main metabolite antagonizing *Clavibacter*. Unfortunately, we were not able to provide evidence for higher accumulation of the mature peptide in the medium. However, RT-qPCR data revealed a highly induced expression of *acnA* gene in GA1 cells upon supplementation with CMR12a CFS (Fig. 3-9C). Based on genome mining, S499 is another strain of the *B. velezensis* species that also retains the potential to produce amylocyclicin [78] and enhanced expression of the *acnA* gene in presence of CMR12a products also occurred in this isolate (Fig. 3-12).

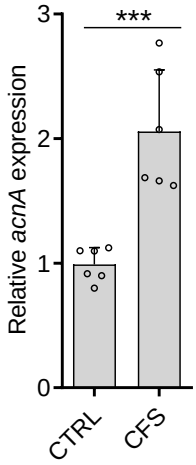

Figure 3-12. Stimulation of amylocyclicin gene expression in *B. velezensis* strain S499 in response to *P. sessiligenes* CMR12a metabolites. Relative expression of the *acnA* gene measured after 8 h (exponential phase) of incubation in presence of CMR12a cell-free supernatant (CFS) (added at 2% v/v) compared to un-supplemented cultures (CTRL). Data show means ± SD calculated from three cultures in two independent experiments (n=6). The statistical difference, in *acnA* expression, between the two conditions was calculated by using the T-test, "***", $P<0.001$.

3.3 Pyochelin acts as Pseudomonas *signal sensed by* Bacillus

Next, we wanted to investigate the molecular basis of this interaction and identify the compound(s) secreted by CMR12a that is(are) sensed by *Bacillus* cells and trigger its BSMs production. For that purpose, we used 2H-bae as the main indicator of the *Bacillus* response because it represents the most highly and consistently boosted PK.

We first performed bioactivity-guided fractionation of the CMR12a CFS on C18 SPE cartridges. It revealed that only extracts containing PVD and/or E-PCH displayed consistent PK-triggering activity (Fig. 3-13A).

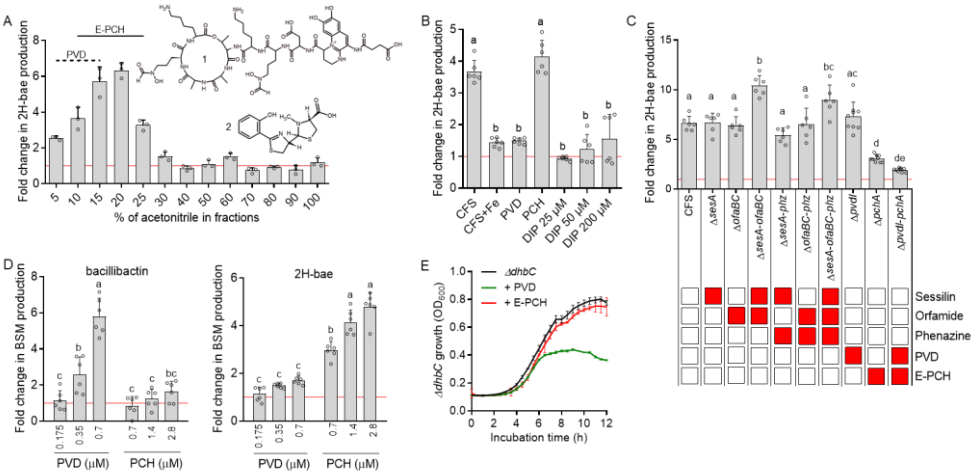

Figure 3-13. E-PCH as main *P. sessiligenes* CMR12a trigger of BSMs boost in *B. velezensis* GA1. A: The CMR12a CFS was processed through the solid-phase extraction on C18 cartridges and compounds were stepwise eluted according to their hydrophobicity with increasing acetonitrile-water ratio, expressed in ACN % (v/v). All fractions were analysed by UPLC-MS and those containing substantial amounts of PVD (1: PVD structure) and/or E-PCH (2: E-PCH structure) are labelled as dashed and solid lines, respectively. Fold changes were calculated based on relative quantification of the compounds by UPLC-MS (peak area) per OD_{600} in treated cultures compared to un-supplemented controls (fold change=1, red line). Data are from one representative experiment showing means ± SD calculated from three technical replicates. B: Differential production of 2H-bae after addition of 0.35 µM pure PVD, 1.4 µM pure E-PCH, 2% (v/v) CMR12a CFS (CFS), CMR12a CFS from iron supplemented culture (CFS+Fe) and different concentration of the iron-chelating agent 2,2'-dipyridyl (DIP). Fold changes were calculated as indicated in a C: Effect of GA1 culture supplementation with CFS (2% (v/v)) from CMR12a wild type and various mutants on 2H-bae production. Metabolites specifically repressed in the CMR12a mutants are illustrated by red boxes. Fold changes were calculated as indicated in A. D: Dose-dependent effect of pure PVD and E-PCH on bacillibactin and 2H-bae production. GA1 cultures were supplemented with the indicated concentrations of HPLC-purified CMR12a siderophores. Fold changes were calculated as indicated in A. Data represented on B, C and D are means ± SD calculated from three replicate cultures in two (n=6) independent experiments and different letters indicate statistically significant differences (ANOVA and Tukey's HSD test, α=0.05). E: Impact of the addition of pure PVD and E-PCH on the growth of GA1 Δ*dhbC* mutant repressed in bacillibactin synthesis. CMR12a siderophores were added at a final concentration similar to the one obtained by adding CMR12a CFS at 2% (v/v) (0.35 µM of PVD and 1.4 µM of E-PCH). Data show means ± SD are from three replicates. For detailed statistical analysis, see Figure 3-15.

This possible involvement of siderophores was supported by the drastic reduction in CFS activity prepared from CMR12a culture in CAA medium supplemented with Fe^{3+} where their production is repressed (Fig. 3-13B Fig. 3-14).

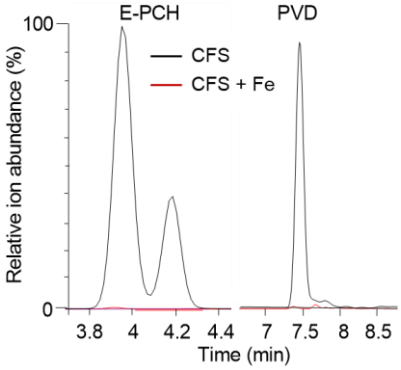

Figure 3-14. The addition of iron into the culture medium represses siderophore production by *P. sessiligenes* CMR12a. UPLC-qTOF MS extracted ions chromatograms illustrating the relative abundance of ions corresponding to PVD (m/z 1289.5928) and E-PCH (m/z 325.0665) and as produced upon growth in CAA medium (black line) or the medium supplemented with 20 µg/L of $FeCl_3x6H_2O$ (red line). The major peak at RT 3.95 min represents the main PVD form described in Fig. 3-S2, while the minor peak at RT 4.2 min corresponds to a structural variant with similar peptide moiety but most probably a different side-chain in the chromophore (not identified).

We next compared the triggering potential of CFS obtained from cultures of CMR12a knock-out mutants specifically lacking the different identified metabolites but not being disrupted in the production of other metabolites [268]. As expected, only extracts from mutants impaired in the production of E-PCH were significantly affected in PK-inducing potential (Fig. 3-13C). To confirm this differential effect of the two siderophores, we then tested independently the HPLC-purified compounds at a concentration similar to the one measured in CFS CAA extracts. Data showed a much higher PK-triggering activity for E-PCH compared to the main PVD isoform produced by CMR12a (Fig. 3-13B).

In additional dose-dependent assays, we observed that supplementation with PVD caused iron limitation in the medium, which is sensed by GA1. This is illustrated by the marked increase in production of the siderophore bacillibactin in GA1 wild type (Fig. 3-13D) and by the reduced growth of the Δ*dhbC* mutant, repressed in bacillibactin synthesis, upon PVD addition (Fig. 3-13E, Fig. 3-15 for statistical analysis).

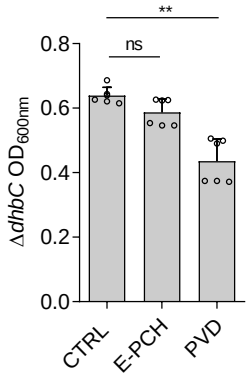

Figure 3-15. Effect of PVD and E-PCH on the growth of the bacillibactin-suppressed mutant of *B. velezensis* GA1. Pure compounds were added to the GA1 culture at a concentration corresponding to the one resulting from the addition of CFS CAA at 2% (v/v). OD600 was measured at the mid-exponential phase. Data represent means ± SD calculated from three replicate cultures in two independent experiments (n=6), T-test with 'ns'=no significant difference; "**", statistically different at $P<0.01$.

Our genome inspection revealed that the *B. velezensis* has acquired multiple transporters allowing the uptake of exogenous siderophores (Table 3-3) similar to those identified in *B. subtilis* [242,324].

Table 3-3: Conservation of genes encoding substrate-binding proteins involved in iron transport in *B. subtilis* and *B. velezensis.* The percentage of genes nucleotide identity was obtained by blast comparison performed on the MAGE platform (https://mage.genoscope.cns.fr).

	***B. velezensis* GA1**		***B. velezensis* QST713**		***B. velezensis* S499**		***B. velezensis* FZB42**	
Transporters in *B. subtilis* 168	**Gene name**	**% of identity**	**Gene name**	**% of identity**	**Gene name**	**% of identity**	**Gene name**	**% of identity**
feuA	*GL331_06035*	83	*BVQ_00990*	83	AS588_13145	83	RBAM_002120	83
fhuD	*GL331_01180*	81	*BVQ_17365*	82	AS588_15255	82	RBAM_030440	82
yxeB (frxB)	*GL331_04235*	72	*BVQ_20555*	73	AS588_18310	72	RBAM_036560	72
fpiA (*pbtQ/yclQ)*	*GL331_06955*	74	*BVQ_01985*	73	AS588_12230	74	RBAM_004080	73
yfmC (fecC)	*GL331_10185*	36	*BVQ_05570*	36	AS588_10320	36	RBAM_010510	37
yfiY(sxzY)	*GL331_04235 (yxeB)*	33	*BVQ_20555 (yxeB)*	32	AS588_18310 (*yxeB*)	33	RBAM_036560 (*yxeB*)	32

However, our data indicate that PVD (in its ferric form) cannot be taken up by GA1. As a strong chelator, PVD scavenges most of the available iron in the external medium and causes iron-stress in GA1 cells what leads to the production boost of GA1 siderophore bacillibactin in a process mediated by the transcriptional repressor Fur [325]. The addition of PVD also leads to a slight but not significant stimulation of 2H-bae synthesis (Fig. 3-13B and D). This is probably due to some stress caused by iron limitation since a similar effect is observed by supplementing GA1 culture with the 2,2'-dipyridyl (DIP) chemical chelator [325] (Fig. 3-13B). Additionally, DIP does not affect the growth of GA1 (Fig. 3-16), probably due to bacillibactin production by *Bacillus* which has higher affinity for iron than DIP [325].

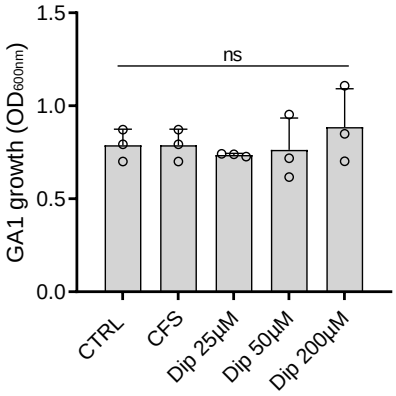

Figure 3-16. Effect of iron chelator DIP on the growth of the *B. velezensis* GA1. The OD_{600} of GA1 culture un-supplemented (CTRL) or supplemented with CMR12a Δ*sesA-ofaBC* CFS (CFS), 25 µM, 50 µM or 200 µM of DIP was measured at the mid-exponential phase. Data represent means ± SD calculated from three replicate cultures (n=3), T-test was done with 'ns'=no significant difference.

However, we could not identify any ferric uptake regulator, Fur binding site (Fur-box), in the promoter region of the *bae* operon (Table 3-4).

Table 3-4. The putative Fur box in the genome of *B. velezensis* GA1. The putative position of Fur box (palindrome sequence: TGANAATNATTNTCA) in GA1 genome was obtained by nucleotide blast performed on the NCBI platform (https://blast.ncbi.nlm.nih.gov).

Found sequence	Sequence score (14)	Upstream gene (bp)	Downstream gene (bp)
tgataatgattatca	14	Bacillibactin trilactone hydrolase (20)	2,3-dihydro-2,3-dihydroxybenzoate dehydrogenase (99)
tgataatgattttca	13	2,3-dihydro-2,3-dihydroxybenzoate dehydrogenase (43)	
tgataatgattatca	14	iron ferrichrome abc transporter (35)	iron hydroxamate abc transporter (170)
tgaaaatgattctca	12	DNA methyladenine glycosylase (148)	Iron ABC transporter (48)
tgataatcattatca	14	hypothetical prot (94)	iron hydroxamate ABC transporter (19)
tgagaatcattatca	13	Fur regulated basic protein (RNA chaperone for fsrA (regulatory ncRNA) (25)	cation facilitator family transporter (173)
tgaaaatgattctca	12	heme degrading oxygenase (45)	
tgataataattttca	13		DoxX family protein (linked to oxidative stress) (11)
tgataatcattttca	13		nitroreductase (23)
tgataattattatca	14		heavy metal translocating ATPase (162)

tgataatcattatca	14		DUF1797 family prot (domain unknown function) (360)
tgaaaatcattatca	14		flavodoxin (53)
tgaaaatcattatca	14		flavodoxin (15)
tgagaatcattttca	12	fbpC fur regulated basic protein (18)	
tgagaatgattttca	12	fbpC fur regulated basic protein (53)	

By contrast to PVD, the addition of E-PCH with a much lower affinity for iron strongly stimulates 2H-bae production, as well as amylocyclicin and surfactin (Fig. 3-17A, B), but does not activate bacillibactin synthesis (Fig. 3-13D) and does not affect Δ*dhbC* growth at the concentrations used (Fig. 3-13E, Fig. 3-15 for statistical analysis). This absence of E-PCH effect on Δ*dhbC* growth can be the result of the degradation of E-PCH as in some conditions it is unstable and its degradation products, aeruginaldehyde (a by-product of pyochelin degradation) could accumulate in the medium [326]. However, no traces of aeruginaldehyde and other products of E-PCH were detected by LC-MS in our study. Thus, this highly suggest that E-PCH, as the final product of *pch* operon, was the active metabolite.

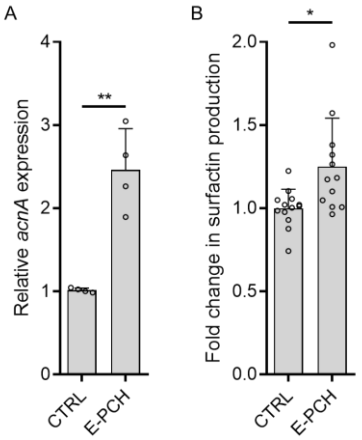

Figure 3-17. Stimulation of amylocyclicin gene expression and surfactin production in *B. velezensis* GA1 by E-PCH. A: Fold change in relative *acnA* gene expression. B: Fold increase in surfactin production. The *acnA* expression and surfactin production are measured after 8 h and 20 h, respectively, upon supplementation of GA1 culture with pure E-PCH at a final concentration of 1.4 µM. The graph shows mean ± SD calculated from two (for panel A) and four (for panel B) different assays involving two or three technical replicates for each treatment, respectively (n=4 and n=12, respectively). Statistical comparisons between treatments were realized with Mann–Whitney-test. "*", P<0.05; "**", P<0.005.

The triggering activity of this secondary siderophore is therefore not related to iron-stress as further exemplified by the fact that it is conserved in the Δ*fur* mutant (Fig. 3-18A), which growth was not impacted as well (Fig. 3-18B). On the other hand, E-PCH was described to retain some antibiotic activity by acting on the intracellular level and causing oxidative stress and damage as reported in *Escherichia coli* [327,328]. However, it does not display any toxicity toward GA1 and Δ*dhbC* nor markedly impacts the growth of the *Δper* mutant repressed in the major regulator involved in *Bacillus* oxidative stress response (Fig. 3-18B) [329]. Moreover, a consistent boost in 2H-bae is also conserved in this *Δper* mutant (Fig. 3-18A), further indicating that E-PCH does not induce oxidative stress by acting intracellularly, thereby supporting its perception as exogenous info-chemical by *Bacillus* cells. Such signaling activity is not impacted by the stereochemistry of the molecule since we observed a similar increase in PK production (6.05 ± 1.8-fold-increase, n=4) by testing the other natural isomer pyochelin (PCH) purified from *P. aeruginosa* PA01 [330].

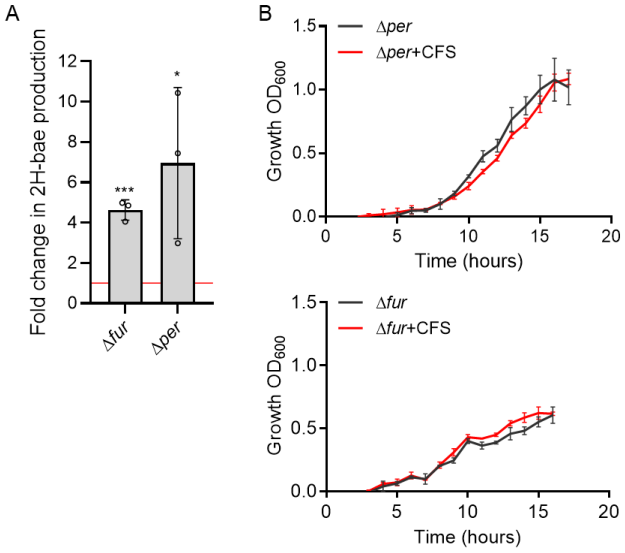

Figure 3-18. E-PCH triggering activity mechanism is not related to iron- and oxidative-stress cause in *B. velezensis* GA1. A: 2H-bae production by GA1 mutants disrupted in ferric uptake (Δ*fur*) and oxidative-stress regulator (Δ*per*) upon 2% (v/v) CMR12a CFS supplementation in comparation with the corresponding, un-supplemented control (fold change=1, labeled as a red line). Data show means ± SD were calculated from three cultures (repeats) (n=3). Statistical significance was calculated using Mann–Whitney test where "*", $P<0.1$ and "***", $P<0.001$. B: The growth of Δ*fur* and *Δper* upon supplementation of culture medium with 2% (v/v) of CMR12a CFS (Δ*fur*+CFS or Δ*per*+CFS) in comparation with un-supplemented control (Δ*fur* or Δ*per*). Data show means ± SD are from three replicates.

Some strains of the *P. protegens* species such as Pf-5 have also been described as E-PCH producers [331]. We also observed a boost in PK production similar to CMR12a upon adding CFS prepared from Pf-5 (Fig. 3-19). Interestingly, our results also demonstrate that the boost effect of *Bacillus* BSMs is not limited only on E-PCH producers, as achromobactin producer, *P. chlororaphis* JV497, also improved 2H-bae production in GA1 (Fig. 3-19).

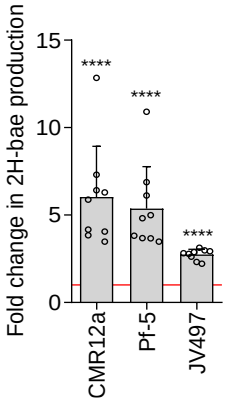

Figure 3-19. Stimulation of 2H-bae production by E-PCH and achromobactin producers. The 2H-bae production by GA1 upon culture supplementation with 2% (v/v) of CMR12a, Pf-5 and JV497 CFS. Fold change equal to 1 is represented as a red line and corresponds to the production of 2H-bae in GA1 un-supplemented culture. The graph shows the means ± SD of three biological replicates with three technical repetitions (n=9). Statistical significance was calculated using Mann–Whitney test where ''ns'', not a significant difference and "****", $P<0.0001$.

4. Discussion

Much progress has been made during the past years to understand the complex and diverse molecular basis of microbial interaction. However, much effort is still required to uncover these microbial molecular conversations comprehensively. This is important since these molecules are driving the ecological fate of individual species in the middle of competitors and presumably shaping the rhizobiome community structure as a whole [332–334]. In that context, some microbial products such as quorum sensing molecules, volatiles and antibiotics at sub-inhibitory concentrations have been described as signaling molecules [335,336]. However, here we report a new communication system featuring the *Pseudomonas* siderophore pyochelin as info-chemical sensed by *Bacillus* to selectively boost the production of some components of its BSM arsenal. This work points out a new role in interspecies interactions for pyochelin-type secondary metabolites beyond their prime function as a secondary siderophore, i.e., as additional chelator with lower affinity but with specific regulation allowing to adapt more flexibly their metal acquisition system to external conditions [337].

In the pairwise system used here, E-PCH signaling superimposes the possible effect of iron limitation in the external medium, which may also result in enhanced production of antibacterial metabolites by *Bacillus*, as occasionally reported [221,305]. That said, due to the limitation in bioavailable iron, almost all known rhizobacterial species have adapted to produce their iron-scavenging molecules to

compete for this essential element [338–340]. Siderophore production is thus widely conserved among soil-borne bacteria [252]. It means that upon recognition of exogenous siderophores, any isolate may somehow identify surrounding competitors. However, some of these siderophores are structurally very variable and almost strain-specific (such as pyoverdines from fluorescent pseudomonads), while some others are much more widely distributed across species and even genera (enterobactin-like, citrate) [339]. In both cases, their recognition would not provide accurate information about the producer because they are too specific or too general respectively.

Interactions with pseudomonads and other bacterial competitors have been reported to impact phenotypic traits but not antibiotic production [253]. To our knowledge, we provide the first evidence that, upon sensing exogenous metabolites, *B. velezensis* can mobilize a substantial part of its secondary metabolome. It includes antimicrobial active bacillaene and difficidin-type polyketides and the bacteriocin amylocyclicin. The involvement of bacillaene in antagonistic interactions with other soil habitats has been further illustrated due to its bacteriostatic activity that protects *Bacillus* from predation by *M. xanthus* [157] or inhibits *Serratia plymuthica* [341]. The bacteriostatic effect of bacillaene also confers protection to *B. amyloliquefaciens* toward *P.chlororaphis* by impeding colony expansion of this competitor [228] and plays an essential protective role for survival in competition with *Streptomyces* soil isolates [155,227].

In this work we additionally discovered that surfactin production is also stimulated by pyochelin. Surfactin can affect closely related species together with cannibalism toxins [302] or disrupt the formation of *Streptomyces* aerial hyphae [303–306] but these effects have not been directly correlated with antibiotic activity and toxicity at biologically relevant concentrations toward soil-dwelling microbes has been only occasionally reported [221,342]. Still, surfactin is important for rhizosphere fitness of the producing strains since it favors key developmental processes such as motility and biofilm formation [91,94,241]. Enhanced multicellular motility in *B. subtilis* as a response to the perception of exogenous compounds has been demonstrated and can also be observed as an escape mechanism used after detecting harmful challengers [221,237,238]. Biofilm formation on the root surface is a natural trait of *Bacillus* but boosting this surfactin-dependent process in response to external signals may also represent a way to protect the community against toxins and/or infiltration by competitors via the shield effect of the hydrophobic hull [95,231,254].

Our understanding of the actual ecological roles of bacterial BSMs formed under natural conditions (at biologically relevant concentrations) has just begun to be elucidated in recent years. Pyochelin is exploited for the acquisition of poorly available metal by the producer but we show that it can also be used as a signal by other species, thereby pointing out an unsuspected function in the context of interactions between clades that are important members of the plant-associated

microbiome. Finally, one of our future objectives is also to enlarge and combine these findings to wisely compose appropriate consortia which will more efficiently, than single species inoculants, protect plants and promote their growth in sustainable agriculture.

Chapter 4

General discussion and future perspectives

1. New insights into the chemical ecology of plant-associated bacteria

1.1 The interplay of CLPs drives soil bacilli and pseudomonads interaction

Previous studies on surfactin and sessilin CLPs have been mainly focused on their biocontrol activities such as antifungal, insecticidal activity, ISR elicitation potential, and their effects on developmental traits such as biofilm formation and motility [50,261]. However, data reporting their involvement in interactions with other PGPR bacteria are limited.

This thesis demonstrates new, and so far, unsuspected functions of sessilin/tolaasin and surfactin as drivers of antagonistic interaction between *Bacillus* and *Pseudomonas* (Chapter 2). We show that the toxicity of sessilin/tolaasin towards *B. velezensis* is an important benefit for *P. sessilinigenes* CMR12a/*P. tolaasii* CH36 to better colonize the rhizosphere during their competition. On the other hand, *B. velezensis* responds to this *Pseudomonas* attack by employing its own CLP family, surfactin, in order to protect itself. Firstly, surfactin, acting as a shield, prevent sessilin-mediated toxicity towards *B. velezensis* by forming a white precipitate. Secondly, *B. velezensis* improves its motility, due to surfactin overproduction, upon the interaction. This phenotypic response of *B. velezensis* can thus represent its escape mechanism after detecting harmful competitors such as *Pseudomonas*. Moreover, it could also be seen as the mechanism of faster root colonization during the competition for space and nutrients.

These newly identified roles of CLPs produced by *Pseudomonas* and *Bacillus* go beyond their already well-reported multi-functionalities. Consequently, one would wonder how many more undiscovered roles of other metabolites, produced by *Bacillus* and *Pseudomonas* but also other bacteria, could be found. Moreover, based on the findings of this thesis, several other questions and ideas for further research are raised.

1.1.1 Does *Pseudomonas* wisely direct its sessilin/tolaasin variants production to better compete?

The antagonistic activities of *Pseudomonas* CLPs against Gram-positive bacteria have been sporadically observed, as reviewed by Geudens and Martins (2018). However, the antibacterial activity of sessilin toward other soil-borne bacteria, and more precisely, its anti-*Bacillus* activity, is so far unobserved. Up to the knowledge, the sole work describing tolaasin (variants I, II, A-E) toxicity towards *Bacillus megaterium* indicated that its activity is structure-dependent [291]. Added at the same concentrations of pure metabolites to *B. megaterium* culture, the linear tolaasin C was inactive while the cyclic tolaasin D was the most active variant. Interestingly,

Bassarello *et al.* (2004) also pointed out that the difference in only one amino acid in the peptide ring can change the activity of the metabolite. For instance, tolaasin I is less active than tolaasin D and has Ile instead of Leu at position 15 in the peptide cycle. Interestingly, our results show that tolaasin D is also the major variant produced by *P. tolaasii* CH36 and is responsible for inhibiting *B. velezensis* (Fig. 2-6D).

Following the same logic, we could also expect some differences in activities of the three sessilin variants A, B and C, produced by *P. sessilinigenes* CMR12a. We could imagine that sessilin B may not be active as it represents the linear variant of sessilin A [269], which is the most produced according to our results (Fig.2-6F). However, cyclic variants A and C that have Hse and Gly, respectively, in their structure at position 16 of peptide ring, could also have different activities towards *B. velezensis*.

Finally, before extending this research to the other sessilin/tolaasin producers or other long CLPs as discussed in Chapter 1, further experiments could be conducted to better understand the ecological role of sessilin and tolaasin during *Pseudomonas* competition with *B. velezensis*, but also with other competitors. Therefore, it would be interesting to confirm pure tolaasin D activity against *B. velezensis* and correlate it with its highest production by *Pseudomonas*. Furthermore, the investigation of pure sessilin variants' anti-*Bacillus* activity may show that the most produced, sessilin A, is also the most active variant. Indeed, the response to this hypothesis could be beneficial for better understanding the ecological role of sessilin/tolaasin and confirming how *Pseudomonas* is producing the variant of a metabolite that is more effective to fight bacterial competitors such as *Bacillus*.

1.1.2 What is the sessilin-like CLPs mode of action?

CLPs are recognized as membrane-active molecules, acting via permeabilization of cellular membranes by pore formation which occurs mainly due to CLPs amphiphilic nature [50,261]. This consequently causes the disbalance in pH gradient through the membrane by augmenting the influx of H^+ and Ca^{2+} ions as well as the efflux of K^+ ions, which can lead to cellular content leakage and final cell death [343,344]. To date, it is documented that sessilin and tolaasin can induce cellular leakage, but almost exclusively in the framework of antifungal activity [268,345–347]. Nevertheless, the exact effect of these CLPs on the bacterial membrane has not yet been explored.

In this context, a recent study precisely explained the permeabilization mechanism of synthetic membranes, simulating Gram-positive bacterial cell membrane, by pseudodesmin A (viscosin group) [348]. It has been shown that the strong activity of pseudodesmin A largely depended on the FA chain length. The variants with ‘’intermediate’’ FA chains with C8-10 atoms were the most efficient in membrane permeabilization and acted by combining two mechanisms of pore formation (partitioning and local membrane damaging) [348]. The variants with ‘’short’’ (C4-

6) or the ‘’long’’ (C12-14) FA chains were significantly less effective and employed only one mechanism for pore formation [348]. Inspired by these observations, it could be assumed that sessilin-like CLPs, with the ‘’intermediate’’ FA chain (C8), have a similar mode of action as the aforementioned pseudodesmin A.

Most of the works focusing on *Pseudomonas* spp. CLPs mode of action on cell membranes are considering members of viscosin group and, to our knowledge, no study on sessilin-like CLPs has been undertaken. Thus, the results of this thesis, showing new roles of sessilin-like CLPs in antibacterial activity, suggest these CLPs as candidates for study in the field of biophysics. These biophysic experiments involving model membranes already gave valuable contributions for better understanding bioactivities of several CLPs such as surfactin and fengycin [349–352].

1.1.3 Could the antibacterial activity of sessilin be extended to important plant pathogens?

In general, research considering biocontrol activity of *Pseudomonas* CLPs is mostly focused on fungal phytopathogens (43% of overall studies) while the once considering their activity towards Gram-positive or Gram-negative bacteria are more limited (each 23% of overall studies) (Geudens and Martins, 2018). More precisely, the studies of the activity of tolaasin group members against phytopathogenic bacteria are scarce. In this instance, the work of Lo Cantore and collaborators (2006) showed a strong activity of tolaasin I against several Gram-positive isolates, including *C. michiganensis* and *R. fascians.* In addition, compared to anti-Gram-positive, a lower activity of tolaasin I was reported against Gram-negative pathogens from *Xanthomonas*, *Pseudomonas* and *Erwinia* genera [353], probably due to the presence of the outer membrane, which could impede access of tolaasin I to the plasma membrane [354].

Interestingly, to knowledge, the antibacterial activity of sessilin against plant pathogenic bacteria is unknown. That said, further research in this field could broaden our understanding of their antimicrobial spectrum and possibly place these CLPs and their producers as important BCAs to fight economically important phytopathogenic bacteria.

1.1.4 The chemical basis of the white-line phenomenon

Despite the macroscopic visualization as a white-line, the chemical basis of such a phenomenon is still unclear. Previous studies that observed the white-line described it as a complex and CLP structure-dependent phenomenon as it has been observed during the interaction between one short (WLIP, orfamide) and one long CLP (tolaasin, sessilin [269,272,320]. However, no more information on the chemical characteristics of the white-line was provided.

In this thesis, the structure of the white-line was not studied. However, due to existing information on CLPs properties, we can assume the reason for

sessilin/tolaasin and surfactin aggregation. Probably, it can rely on CLPs electrostatic interactions/ionic bonding (surfactin is negatively charged while sessilin is a positively charged metabolite) combined or not with hydrophobic interactions involving non-polar moieties [50,269]. Thus, further research should be conducted to reveal more details about the chemical characteristics of the white-line precipitate. To gather more data, Isothermal Titration Calorimetry (ITC) experiments can be performed to define this type of chemical interaction and measure its intensity according to the concentrations of used CLPs and pH conditions. Moreover, the tests on structural variants of surfactin with various peptides (one or no negative charge) and FA chains would be of interest to more precisely evaluate the importance of these traits for the interaction with sessilin.

1.1.5 *Pseudomonas* (pyochelin) impact on *B. velezensis* phenotypic adaptations

As previously mentioned, *P. sessilinigenes* CMR12a and *P. chlororaphis* JV497 produce diffusible metabolite(s) on EM medium that stimulates *B. velezensis* surfactin production and, consequently, its motility. Even if some other *P. sessilinigenes* CMR12a compound(s) enhances *B. velezensis* motility on EM medium (Chapter 2), the involvement of PCH cannot be discarded. Namely, this secondary siderophore enhances surfactin production by *Bacillus*, as observed by using *P. sessilinigenes* CMR12a CAA extracts and pure PCH (Chapter 3, Fig. 3-17B). In this context, an additional objective would be to determine the direct importance of PCH for *B. velezensis* motility by using enriched PCH extracts. More attention should also be paid on *P. chlororaphis* JV497 as an additional *Bacillus* motility inducer, without anti-*Bacillus* activity and with a different arsenal of secondary metabolites than *P. sessilinigenes* CMR12a. By mutant construction and possible purification of *P. chlororaphis* JV497 metabolites, additional molecules involved in such interaction could be discovered.

Nevertheless, considering surfactin involvement in other phenotypic traits of *Bacillus*, such as biofilm formation and sporulation [50], their possible modulation upon interspecies interaction should be studied. Related to this, *Bacillus* biofilm development could be compared with and without the addition of PCH, using crystal-violet staining of pellicle [355]. In parallel, the expression of key genes involved in biofilm formation (*bslA*, *tasA* and *epsA*) could be evaluated by RT-qPCR, upon PCH sensing. The impact of PCH on sporulation, could be investigated by flow cytometry and by RT-qPCR, following the expression of *spo0A*.

Finally, the effect of PCH on the phenotypic traits of *Bacillus* could be investigated under more realistic conditions. These phenotypic traits contribute to *Bacillus* fitness on roots. Therefore, it could be interesting to compare *Bacillus* colonization of, i.e. tomato or *A. thaliana*, plantlets grown in a hydroponic system supplemented or not with PCH. The impact of PCH on the formation of biofilm by

Bacillus on root tissues could also be monitored in a non-destructive way by time-lapse fluorescence microscopy.

1.2 Bacillus *specific metabolite response upon sensing* Pseudomonas *pyochelin*

Some studies involving dual-culture interaction of *Bacillus* with plant pathogenic *Pseudomonas* have reported enhanced expression of surfactin, bacilysin, or iturin BGCs but no correlation has been established with higher production and accumulation of these metabolites in the medium [225,226].

In this work, besides the boost of surfactin, we report for the first time an improved production of bacillaenes, difficidins and amylocyclicin by *B. velezensis*, upon interaction with *P. sessilinigenes* CMR12a. These metabolites have been well described for their antibiotic activities against Gram-negative and Gram-positive bacteria [77,322] and are boosted upon sensing PCH. Several works illustrate a widespread potential for the synthesis of PCH or structurally close enantio- forms among *Pseudomonas*, *Streptomyces* and possibly some other soil-dwelling species [286,356–360]. Therefore, *Bacillus* may have evolved some sensing systems targeting siderophores that are conserved enough to be detected as relevant info-chemical but, in a delicate balance, also restricted to specific microbial phylogenetic groups able to produce PCH [74]. With this mechanism, soil bacilli would rely on this specific exogenous siderophore as an eavesdropping strategy to accurately identify competitors and respond in an appropriate way like remodeling its BSM secretome.

From the practical point of view for agriculture, such response of *Bacillus* can be highly beneficial in more effective suppression of phytopathogenic bacteria. Therefore, broadening the view of chelators acting as a signal and better understanding the mechanisms of perception of this signal could further help to direct *Bacillus* metabolome for the more efficient antimicrobial activity.

1.2.1 Broadening the chelator-sensing concept

This novel concept of chelator sensing represents a new facet of siderophore-mediated interactions. It is going beyond the competition for iron, which is extensively studied as the mechanism of biocontrol where plant-beneficial bacteria indirectly inhibit pathogenic microbes. Therefore, many soil pseudomonads produce other secondary siderophores than PCH, being salicyl-capped siderophores with a similar structural scaffold or structurally unrelated compounds such as pseudomonine [361,362]. These compounds should also be tested for their activity as triggers of PKs synthesis in *Bacillus* to evaluate whether the chelator sensing concept can be broadened to a larger panel of exogenous metal scavengers or not.

Indeed, the results obtained in this thesis show that *P. chlororaphis* JV497, producer of achromobactin, significantly improved PK production by *B. velezensis*

(Fig. 3-19). This allowed us to hypothesize that the chelator sensing concept can be enlarged to the other groups of secondary siderophores. In this context, further research is planned to be conducted by testing strains belonging to three bacterial genera present in the rhizosphere (*Pseudomonas*, *Streptomyces*, *Burkholderia*) and known to produce other secondary siderophores (pseudomonine, achromobactin, rhizobactin, vibrioferrin, coelichelin, cepaciachelin, malleobactin).

1.2.2 How is pyochelin perceived by *Bacillus* cells?

Bacillus perceives PCH in a way independent of iron stress and piracy, indicating that the effect of PCH for *Bacillus* goes beyond its iron-scavenging function. However, the mechanism of PCH action is not yet clear. *B. subtilis* can uptake xenosiderophores which in turn induce sporulation [242]. However, our data (Chapter 3), supported by a recently published study showing that this compound is not an inducer of sporulation [231], suggests that PCH is not internalized. The involvement of a putative receptor at the *Bacillus* cell surface should be further investigated together with the possible downstream impact on multiple pleiotropic transcriptional regulators, fine-tuning the synthesis of these non-ribosomal BSMs.

To confirm that PCH is recognized as an external signal and not imported into *Bacillus* cells further experiments should be undertaken. Firstly, the intracellular and extracellular PCH amounts can be quantified via highly sensitive LC-MS methods after PCH addition to the *Bacillus* culture. Secondly, the growth of *Bacillus* Δ*dhbC* mutant (unable to produce bacillibactin) could be followed upon the addition of ferri-PCH. If the mutant cannot restore the growth, it would mean that *Bacillus* cannot internalize the ferri-siderophore and use it as its iron source. Further, there is evidence that PCH may cause some intracellular oxidative stress in other bacteria such as *E. coli* [327]. The ROS accumulation could be quantified by using DCFA-DA, a fluorescent reporter of ROS, and by measuring its fluorescence intensity. Additionally, ROS evaluation could be made by targeting oxidative stress and iron homeostasis marker genes such as *perR, mrgA, pfeT, katA, ahpC, hemA* and *OhrR* to evaluate the modulation of their expression via RT-qPCR upon supplementation of *Bacillus* culture with PCH. Finally, showing the ROS absence or that none of these stress genes are induced would confirm that PCH does not enter *Bacillus* cells.

Possibly proving PCH internalization by *Bacillus*, one would wonder if there are receptors on *Bacillus* membrane able to perceive PCH and further activate a signaling cascade which would finally cause PKs overproduction. In order to decipher the downstream signaling cascade, the utilization of *Bacillus bae*-gfp reporter strain, challenged by PCH, could provide more information. The *bae*-gfp reporter strain could allow us to define the best timing in terms of transcriptomic boost and define the best conditions to observe the chelator-sensing phenomenon. Based on this information and using a comparative RNAseq experiment, we would be able to highlight upregulated genes coding for receptors and/or transcription

factors involved in the perception and transduction of the signal that triggers the production of bacillaene.

2. The benefits for sustainable agriculture by improving *B. velezensis* biocontrol efficiency

From the practical point of view, the knowledge obtained during this study can be important for rational PGPR application in sustainable agriculture. The members of *B. subtilis* complex, in general, represent one of the most important BCAs [312]. Among them, *B. velezensis* appears to be one of the best candidates for developing new BCAs, due to its metabolite and phenotypic characteristics. Several products with different strains of *B. velezensis* are already available on the market [312]. However, other bacteria from soil and rhizosphere can largely modulate their efficiency. According to our study, sessilin/tolaasin producers can decrease the development of *B. velezensis* in the rhizosphere and consequently affect the efficiency of *B. velezensis* based BCAs. That said, before applying *B. velezensis* based BCA, the screening of soil microbiota is recommended. This screening would yield information about microbial content and diversity and it would also help to predict the BSMs that those microorganisms could produce in the surrounding environment. Therefore, according to this research, one should be careful when applying *B. velezensis* BCA in rhizosphere rich in *Pseudomonas* species such as *P. sessilinigenes*, i.e. red coocoyama rhizosphere [266].

Furthermore, it is already known that besides being based only on *Bacillus*, some BCAs could include additional microorganisms. For example, biofungicides such as Solanova and EcoSeedTURF contain, besides *Bacillus* spp., also *Pseudomonas* spp.. Furthermore, the application of *P. fluorescens* Pf1 and *B. subtilis* TRC reduced more successfully banana wilt caused by *F. oxysporum* f. sp. *cubense*, when compared to the mono-bacterial formulation [22]. Similarly, co-inoculation of *B. thuringiensis* and *P. aeruginosa* enhanced *Brassica campestris* plants' resistance against *X. campestris* pv. *campestris*, the causative agent of black rot of crucifers [363]. Thus, the discovery of secondary siderophores as boosters of *Bacillus* antimicrobial activity would contribute to better construction of bacterial consortium, in order to more efficiently suppress plant pathogens. In this context, the presence of pyochelin-like producer but sessilin/tolaasin non-producer would improve *Bacillus* plant protection via direct antagonism of phytopathogens, improved motility, root colonization and ISR.

Further research would be necessary to understand better the molecular communication between *Bacillus* and other organisms to evaluate which factors inhibit or enhance *Bacillus* as BCA.

Chapter 5

References

1. Reference

1. Lindsey, A.P.J., Murugan, S., and Renitta, R.E. (2020) Microbial disease management in agriculture: Current status and future prospects. *Biocatal. Agric. Biotechnol.*, **23**, 101468.

2. Desa, U. N. "World population prospects 2019: Highlights." New York, NY: United Nations Department for Economic and Social Affairs (2019).

3. Savary, S., Ficke, A., Aubertot, J.N., and Hollier, C. (2012) Crop losses due to diseases and their implications for global food production losses and food security. *Food Secur.*, **4** (4), 519–537.

4. Savary, S., Willocquet, L., Pethybridge, S.J., Esker, P., McRoberts, N., and Nelson, A. (2019) The global burden of pathogens and pests on major food crops. *Nat. Ecol. Evol.*, **3** (3), 430–439.

5. Mansfield, J., Genin, S., Magori, S., Citovsky, V., Sriariyanum, M., Ronald, P., Dow, M., Verdier, V., Beer, S. V., Machado, M.A., Toth, I., Salmond, G., and Foster, G.D. (2012) Top 10 plant pathogenic bacteria in molecular plant pathology. *Mol. Plant Pathol.*, **13** (6), 614–629.

6. Tudi, M., Ruan, H.D., Wang, L., Lyu, J., Sadler, R., Connell, D., Chu, C., and Phung, D.T. (2021) Agriculture development, pesticide application and its impact on the environment. *Int. J. Environ. Res. Public Health*, **18** (3), 1–24.

7. Raymaekers, K., Ponet, L., Holtappels, D., Berckmans, B., and Cammue, B.P.A. (2020) Screening for novel biocontrol agents applicable in plant disease management – A review. *Biol. Control*, **144**, 104240.

8. Compant, S., Samad, A., Faist, H., and Sessitsch, A. (2019) A review on the plant microbiome: Ecology, functions, and emerging trends in microbial application. *J. Adv. Res.*, **19**, 29–37.

9. Santoyo, G., Urtis-Flores, C.A., Loeza-Lara, P.D., Orozco-Mosqueda, M.D.C., and Glick, B.R. (2021) Rhizosphere colonization determinants by plant growth-promoting rhizobacteria (PGPR). *Biology (Basel).*, **10** (6), 1–18.

10. Mendes, R., Garbeva, P., and Raaijmakers, J.M. (2013) The rhizosphere microbiome: Significance of plant beneficial, plant pathogenic, and human pathogenic microorganisms. *FEMS Microbiol. Rev.*, **37** (5), 634–663.

11. Backer, R., Rokem, J.S., Ilangumaran, G., Lamont, J., Praslickova, D., Ricci, E., Subramanian, S., and Smith, D.L. (2018) Plant growth-promoting rhizobacteria: Context, mechanisms of action, and roadmap to commercialization of biostimulants for sustainable agriculture. *Front. Plant Sci.*, **9**, 1473.

12. Köhl, J., Kolnaar, R., and Ravensberg, W.J. (2019) Mode of action of microbial biological control agents against plant diseases: Relevance beyond efficacy. *Front. Plant Sci.*, **10**, 845.

13. Nishimoto, R. (2019) Global trends in the crop protection industry. *J. Pestic. Sci.*, **44** (3), 141–147.

14. Zaki, O., Weekers, F., Thonart, P., Tesch, E., Kuenemann, P., and Jacques, P. (2020) Limiting factors of mycopesticide development. *Biol. Control*, **144**, 104220.

15. Parnell, J.J., Berka, R., Young, H.A., Sturino, J.M., Kang, Y., Barnhart, D.M., and DiLeo, M.V. (2016) From the lab to the farm: An industrial perspective of plant beneficial microorganisms. *Front. Plant Sci.*, **7**, 1110.

16. Syed Ab Rahman, S.F., Singh, E., Pieterse, C.M.J., and Schenk, P.M. (2018) Emerging microbial biocontrol strategies for plant pathogens. *Plant Sci.*, **267**, 102–111.

17. Fan, B., Wang, C., Song, X., Ding, X., Wu, L., Wu, H., Gao, X., and Borriss, R. (2018) *Bacillus velezensis* FZB42 in 2018: The gram-positive model strain for plant growth promotion and biocontrol. *Front. Microbiol.*, **9**, 3389.

18. Stojanović, S.S., Karabegović, I., Beškoski, V., Nikolić, N., and Lazić, M. (2019) *Bacillus* based microbial formulations: Optimization of the production process. *Hem. Ind.*, **73** (3), 169–182.

19. Gupta, R.S., Patel, S., Saini, N., and Chen, S. (2020) Robust demarcation of 17 distinct *Bacillus* species clades, proposed as novel *Bacillaceae* genera, by phylogenomics and comparative genomic analyses: Description of *Robertmurraya kyonggiensis* sp. nov. and proposal for an emended genus *Bacillus* limiting it only to the members of the Subtilis and Cereus clades of species. *Int. J. Syst. Evol. Microbiol.*, **70** (11), 5753–5798.

20. Fan, B., Blom, J., Klenk, H.P., and Borriss, R. (2017) *Bacillus amyloliquefaciens*, *Bacillus velezensis*, and *Bacillus siamensis* form an "Operational group *B. amyloliquefaciens*" within the *B. subtilis* species complex. *Front. Microbiol.*, **8**, 22.

21. Gómez Expósito, R., de Bruijn, I., Postma, J., and Raaijmakers, J.M. (2017) Current insights into the role of rhizosphere bacteria in disease suppressive soils. *Front. Microbiol.*, **8**, 2529.

22. Fira, D., Dimkić, I., Berić, T., Lozo, J., and Stanković, S. (2018) Biological control of plant pathogens by *Bacillus* species. *J. Biotechnol.*, **285**, 44–55.

23. Maksimov, I.V., Singh, B.P., Cherepanova, E.A., Burkhanova, G.F., and Khairullin, R.M. (2020) Prospects and applications of lipopeptide-producing bacteria for plant protection. *Appl. Biochem. Microbiol.*, **56** (1), 15–28.

24. Dunlap, C.A., Kim, S.J., Kwon, S.W., and Rooney, A.P. (2016) *Bacillus velezensis* is not a later heterotypic synonym of *Bacillus amyloliquefaciens*; *Bacillus methylotrophicus*, *Bacillus amyloliquefaciens* subsp. *plantarum* and *Bacillus oryzicola* are later heterotypic synonyms. *Int. J. Syst. Evol. Microbiol.*, **66** (3), 1212–1217.

25. Harwood, C.R., Mouillon, J.M.M., Pohl, S., and Arnau, J. (2018) Secondary metabolite production and the safety of industrially important members of the *Bacillus subtilis* group. *FEMS Microbiol. Rev.*, **42** (6), 721–738.

26. Du, Y., Ma, J., Yin, Z., Liu, K., Yao, G., Xu, W., Fan, L., Du, B., Ding, Y., and Wang, C. (2019) Comparative genomic analysis of *Bacillus paralicheniformis* MDJK30 with its closely related species reveals an evolutionary relationship between *B. paralicheniformis* and *B. licheniformis*. *BMC Genomics*, **20** (1), 283.

27. Torres Manno, M.A., Pizarro, M.D., Prunello, M., Magni, C., Daurelio, L.D., and Espariz, M. (2019) GeM-Pro: A tool for genome functional mining and microbial profiling. *Appl. Microbiol. Biotechnol.*, **103** (7), 3123–3134.

28. Ruiz-García, C., Béjar, V., Martínez-Checa, F., Llamas, I., and Quesada, E. (2005) *Bacillus velezensis* sp. nov., a surfactant-producing bacterium isolated from the river Vélez in Málaga, southern Spain. *Int. J. Syst. Evol. Microbiol.*, **55** (1), 191–195.

29. Pandin, C., Le Coq, D., Deschamps, J., Védie, R., Rousseau, T., Aymerich, S., and Briandet, R. (2018) Complete genome sequence of *Bacillus velezensis* QST713: A biocontrol agent that protects *Agaricus bisporus* crops against the green mould disease. *J. Biotechnol.*, **278**, 10–19.

30. Korpi, A., Järnberg, J., and Pasanen, A.L. (2009) Microbial volatile organic compounds. *Crit. Rev. Toxicol.*, **39** (2), 139–193.

31. Schmidt, R., Cordovez, V., De Boer, W., Raaijmakers, J., and Garbeva, P. (2015) Volatile affairs in microbial interactions. *ISME J.*, **9** (11), 2329–2335.

32. Kai, M. (2020) Diversity and distribution of volatile secondary metabolites throughout *Bacillus subtilis* isolates. *Front. Microbiol.*, **11**, 559.

33. Lim, S.M., Yoon, M.Y., Choi, G.J., Choi, Y.H., Jang, K.S., Shin, T.S., Park, H.W., Yu, N.H., Kim, Y.H., and Kim, J.C. (2017) Diffusible and volatile antifungal compounds produced by an antagonistic *Bacillus velezensis* G341 against various phytopathogenic fungi. *Plant Pathol. J.*, **33** (5), 488–498.

34. Jiang, C.H., Liao, M.J., Wang, H.K., Zheng, M.Z., Xu, J.J., and Guo, J.H. (2018) *Bacillus velezensis*, a potential and efficient biocontrol agent in control of pepper gray mold caused by *Botrytis cinerea*. *Biol. Control*, **126**, 147–157.

35. Zhang, D., Yu, S., Yang, Y., Zhang, J., Zhao, D., Pan, Y., Fan, S., Yang, Z., and Zhu, J. (2020) Antifungal effects of volatiles produced by *Bacillus subtilis* against *Alternaria solani* in potato. *Front. Microbiol.*, **11**, 1–12.

36. Liu, C., Yin, X., Wang, Q., Peng, Y., Ma, Y., and Liu, P. (2018) Antagonistic activities of volatiles produced by two *Bacillus strains* against *Monilinia fructicola* in peach fruit. *J. Organ. Behav.*, **98** (15), 5756–5763.

37. Raza, W., Ling, N., Yang, L., Huang, Q., and Shen, Q. (2016) Response of tomato wilt pathogen *Ralstonia solanacearum* to the volatile organic compounds produced by a biocontrol strain *Bacillus amyloliquefaciens* SQR-9. *Sci. Rep.*, **6** (1), 1–13.

38. Yuan, J., Raza, W., Shen, Q., and Huang, Q. (2012) Antifungal activity of *Bacillus amyloliquefaciens* NJN-6 volatile compounds against *Fusarium oxysporum* f. sp. *cubense*. *Appl. Environ. Microbiol.*, **78** (16), 5942–5944.

39. Ryu, C.M., Farag, M.A., Hu, C.H., Reddy, M.S., Kloepper, J.W., and Paré, P.W. (2004) Bacterial volatiles induce systemic resistance in *Arabidopsis*. *Plant Physiol.*, **134** (3), 1017–1026.

40. Rudrappa, T., Biedrzycki, M.L., Kunjeti, S.G., Donofrio, N.M., Czymmek, K.J., Paré, P.W., and Bais, H.P. (2010) The rhizobacterial elicitor acetoin induces systemic resistance in *Arabidopsis thaliana*. *Commun. Integr. Biol.*, **3** (2), 130–138.

41. Choi, H.K., Song, G.C., Yi, H.S., and Ryu, C.M. (2014) Field evaluation of the bacterial volatile derivative 3-pentanol in priming for induced resistance in pepper. *J. Chem. Ecol.*, **40** (8), 882–892.

42. Peng, G., Zhao, X., Li, Y., Wang, R., Huang, Y., and Qi, G. (2019) Engineering *Bacillus velezensis* with high production of acetoin primes strong induced systemic resistance in *Arabidopsis thaliana*. *Microbiol. Res.*, **227**, 126297.

43. Caulier, S., Nannan, C., Gillis, A., Licciardi, F., Bragard, C., and Mahillon, J. (2019) Overview of the antimicrobial compounds produced by members of the *Bacillus subtilis* group. *Front. Microbiol.*, **10**, 302.

44. Bozhüyük, K.A., Micklefield, J., and Wilkinson, B. (2019) Engineering enzymatic assembly lines to produce new antibiotics. *Curr. Opin. Microbiol.*, **51**, 88–96.

45. Sieber, S.A., and Marahiel, M.A. (2005) Molecular mechanisms underlying nonribosomal peptide synthesis: Approaches to new antibiotics. *Chem. Rev.*, **105** (2), 715–738.

46. Donadio, S., Monciardini, P., and Sosio, M. (2007) Polyketide synthases and nonribosomal peptide synthetases: The emerging view from bacterial

genomics. *Nat. Prod. Rep.*, **24** (5), 1073–1079.

47. Argüelles Arias, A., Craig, M., and Fickers, P. (2011) Gram-positive antibiotic biosynthetic clusters: A review. *Sci. against Microb. Pathog. Commun. Curr. Res. Technol. Adv.*, **2**, 977–986.

48. Hathout, Y., Ho, Y.P., Ryzhov, V., Demirev, P., and Fenselau, C. (2000) Kurstakins: A new class of lipopeptides isolated from *Bacillus thuringiensis*. *J. Nat. Prod.*, **63** (11), 1492–1496.

49. Olishevska, S., Nickzad, A., and Déziel, E. (2019) *Bacillus* and *Paenibacillus* secreted polyketides and peptides involved in controlling human and plant pathogens. *Appl. Microbiol. Biotechnol.*, **103** (3), 1189–1215.

50. Ongena, M., and Jacques, P. (2008) *Bacillus* lipopeptides: Versatile weapons for plant disease biocontrol. *Trends Microbiol.*, **16** (3), 115–125.

51. Théatre, A., Cano-Prieto, C., Bartolini, M., Laurin, Y., Deleu, M., Niehren, J., Fida, T., Gerbinet, S., Alanjary, M., Medema, M.H., Léonard, A., Lins, L., Arabolaza, A., Gramajo, H., Gross, H., and Jacques, P. (2021) The surfactin-like lipopeptides From *Bacillus* spp.: Natural biodiversity and synthetic biology for a broader application range. *Front. Bioeng. Biotechnol.*, **9**,623701.

52. Peypoux F., Bonmatin, W.J. (1999) Recent trends in the biochemistry of surfactin. *Appl Microbiol Biotechnol.*, **51** (5), 553–563.

53. Cochrane, S.A., and Vederas, J.C. (2016) Lipopeptides from *Bacillus* and *Paenibacillus* spp.: A gold mine of antibiotic candidates. *Med. Res. Rev.*, **36** (1), 4–31.

54. May, J.J., Wendrich, T.M., and Marahiel, M.A. (2001) The *dhb* operon of *Bacillus subtilis* encodes the biosynthetic template for the catecholic siderophore 2,3-dihydroxybenzoate-glycine-threonine trimeric ester bacillibactin. *J. Biol. Chem.*, **276** (10), 7209–7217.

55. Rogers, H., Newton, G., and Abraham, E. (1965) Production and purification of bacilysin. *Biochem. J.*, **97** (2), 573–578.

56. Walker, J.E., and Abraham, E.P. (1970) The structure of bacilysin and other products of *Bacillus subtilis*. *Biochem. J.*, **118** (4), 563–570.

57. Steinborn, G., Hajirezaei, M.R., and Hofemeister, J. (2005) *bac* genes for recombinant bacilysin and anticapsin production in *Bacillus* host strains. *Arch. Microbiol.*, **183** (2), 71–79.

58. Parker, J.B., and Walsh, C.T. (2012) Stereochemical outcome at four stereogenic centers during conversion of prephenate to tetrahydrotyrosine by BacABGF in the bacilysin pathway. *Biochemistry*, **51** (28), 5622–5632.

59. Ozcengiz, G., Alaeddinoglu, N.G., and Demain, A.L. (1990) Regulation of biosynthesis of bacilysin by *Bacillus subtilis*. *J. Ind. Microbiol.*, **6** (2), 91–100.

60. Aleti, G., Sessitsch, A., and Brader, G. (2015) Genome mining: Prediction of lipopeptides and polyketides from *Bacillus* and related Firmicutes. *Comput. Struct. Biotechnol. J.*, **13**, 192–203.

61. Chen, X.H., Vater, J., Piel, J., Franke, P., Scholz, R., Schneider, K., Koumoutsi, A., Hitzeroth, G., Grammel, N., Strittmatter, A.W., Gottschalk, G., Süssmuth, R.D., and Borriss, R. (2006) Structural and functional characterization of three polyketide synthase gene clusters in *Bacillus amyloliquefaciens* FZB 42. *J. Bacteriol.*, **188** (11), 4024–4036.

62. Cheng, Y.Q., Tang, G.L., and Shen, B. (2003) Type I polyketide synthase requiring a discrete acyltransferase for polyketide biosynthesis. *Proc. Natl. Acad. Sci.*, **100** (6), 3149–3154.

63. Moldenhauer, J., Chen, X.H., Borriss, R., and Piel, J. (2007) Biosynthesis of the antibiotic bacillaene, the product of a giant polyketide synthase complex of the *trans*-AT family. *Angew. Chemie - Int. Ed.*, **46** (43), 8195–8197.

64. Butcher, R.A., Schroeder, F.C., Fischbach, M.A., Straight, P.D., Kolter, R., Walsh, C.T., and Clardy, J. (2007) The identification of bacillaene, the product of the PksX megacomplex in *Bacillus subtilis*. *Proc. Natl. Acad. Sci. U.S.A.*, **104** (5), 1506–1509.

65. Calderone, C.T., Bumpus, S.B., Kelleher, N.L., Walsh, C.T., and Magarvey, N.A. (2008) A ketoreductase domain in the PksJ protein of the bacillaene assembly line carries out both *α*- and *β*-ketone reduction during chain growth. *Proc. Natl. Acad. Sci.*, **105** (35), 12809–12814.

66. Wilson, K.E., Flor, J.E., Schwartz, R.E., Joshua, H., Smith, J.L., Pelak, B.A., Liesch, J.M., and Hensens, O.D. (1987) Difficidin and oxydifficidin: Novel broad spectrum antibacterial antibiotics produced by *Bacillus subtilis*. II. Isolation and physico-chemical characterization. **40** (12), 1682–1691.

67. Schneider, K., Chen, X.H., Vater, J., Franke, P., Nicholson, G., Borriss, R., and Süssmuth, R.D. (2007) Macrolactin is the polyketide biosynthesis product of the *pks2* cluster of *Bacillus amyloliquefaciens* FZB42. *J. Nat. Prod.*, **70** (9), 1417–1423.

68. Abriouel, H., Franz, C.M.A.P., Omar, N. Ben, and Gálvez, A. (2011) Diversity and applications of *Bacillus* bacteriocins. *FEMS Microbiol. Rev.*, **35** (1), 201–232.

69. McAuliffe, O., Ross, R.P., and Hill, C. (2001) Lantibiotics: Structure, biosynthesis and mode of action. *FEMS Microbiol. Rev.*, **25** (3), 285–308.

70. Stein, T., Borchert, S., Conrad, B., Feesche, J., Hofemeister, B., Hofemeister, J., and Entian, K.D. (2002) Two different lantibiotic-like peptides originate from the ericin gene cluster of *Bacillus subtilis* A1/3. *J. Bacteriol.*, **184** (6), 1703–1711.

71. Palazzini, J.M., Dunlap, C.A., Bowman, M.J., and Chulze, S.N. (2016) *Bacillus velezensis* RC 218 as a biocontrol agent to reduce *Fusarium* head blight and deoxynivalenol accumulation: Genome sequencing and secondary metabolite cluster profiles. *Microbiol. Res.*, **192**, 30–36.

72. Bierbaum, G. (1995) Cloning, sequencing and production of the lantibiotic mersacidin. *FEMS Microbiol. Lett.*, **127**, 121–126.

73. He, P., Hao, K., Blom, J., Rückert, C., Vater, J., Mao, Z., Wu, Y., Hou, M., He, P., He, Y., and Borriss, R. (2012) Genome sequence of the plant growth promoting strain *Bacillus amyloliquefaciens* subsp. *plantarum* B9601-Y2 and expression of mersacidin and other secondary metabolites. *J. Biotechnol.*, **164** (2), 281–291.

74. Emam, A.M., and Dunlap, C.A. (2020) Genomic and phenotypic characterization of *Bacillus velezensis* AMB-y1; a potential probiotic to control pathogens in aquaculture. *Antonie van Leeuwenhoek, Int. J. Gen. Mol. Microbiol.*, **113** (12), 2041–2052.

75. Argüelles Arias, A., Joris, B., and Fickers, P. (2014) Dual mode of action of amylolysin: A type-B lantibiotic produced by *Bacillus amyloliquefaciens* GA1. *Protein Pept. Lett.*, **21** (4), 336–340.

76. Argüelles Arias, A., Ongena, M., Devreese, B., Terrak, M., Joris, B., and Fickers, P. (2013) Characterization of amylolysin, a novel lantibiotic from *Bacillus amyloliquefaciens* GA1. *PLoS One*, **8** (12), 1–10.

77. Scholz, R., Vater, J., Budiharjo, A., Wang, Z., He, Y., Dietel, K., Schwecke, T., Herfort, S., Lasch, P., and Borriss, R. (2014) Amylocyclicin, a novel circular bacteriocin produced by *Bacillus amyloliquefaciens* FZB42. *J. Bacteriol.*, **196** (10), 1842–1852.

78. Molinatto, G., Puopolo, G., Sonego, P., Moretto, M., Engelen, K., Viti, C., Ongena, M., and Pertot, I. (2016) Complete genome sequence of *Bacillus amyloliquefaciens* subsp. *plantarum* S499, a rhizobacterium that triggers plant defences and inhibits fungal phytopathogens. *J. Biotechnol.*, **238**, 56–59.

79. Scholz, R., Molohon, K.J., Nachtigall, J., Vater, J., Markley, A.L., Süssmuth, R.D., Mitchell, D.A., and Borriss, R. (2011) Plantazolicin, a novel microcin B17/streptolysin S-like natural product from *Bacillus amyloliquefaciens* FZB42. *J. Bacteriol.*, **193** (1), 215–224.

80. Mülner, P., Schwarz, E., Dietel, K., Junge, H., Herfort, S., Weydmann, M.,

Lasch, P., Cernava, T., Berg, G., and Vater, J. (2020) Profiling for bioactive peptides and volatiles of plant growth promoting strains of the *Bacillus subtilis* complex of industrial relevance. *Front. Microbiol.*, **11**, 1432.

81. Chen, L., Heng, J., Qin, S., and Bian, K. (2018) A comprehensive understanding of the biocontrol potential of *Bacillus velezensis* LM2303 against *Fusarium* head blight. *PLoS One*, **13** (6), 1–22.

82. Banala, S., Ensle, P., and Süssmuth, R.D. (2013) Total synthesis of the ribosomally synthesized linear azole-containing peptide plantazolicin a from *Bacillus amyloliquefaciens*. *Angew. Chemie Int. Ed.*, **52** (36), 9518–9523.

83. Finkel, O.M., Castrillo, G., Herrera Paredes, S., Salas González, I., and Dangl, J.L. (2017) Understanding and exploiting plant beneficial microbes. *Curr. Opin. Plant Biol.*, **38**, 155–163.

84. Yssel, A., Reva, O., and Tastan Bishop, O. (2011) Comparative structural bioinformatics analysis of *Bacillus amyloliquefaciens* chemotaxis proteins within *Bacillus subtilis* group. *Appl. Microbiol. Biotechnol.*, **92** (5), 997–1008.

85. Sourjik V, and W.N. (2012) Responding to chemical gradients: Bacterial chemotaxis. *Curr Opin Cell Biol.*, **24** (2), 262–268.

86. Vacheron, J., Desbrosses, G., Bouffaud, M.L., Touraine, B., Moënne-Loccoz, Y., Muller, D., Legendre, L., Wisniewski-Dyé, F., and Prigent-Combaret, C. (2013) Plant growth-promoting rhizobacteria and root system functioning. *Front. Plant Sci.*, **4** (SEP), 1–19.

87. Kearns, D.B., Chu, F., Rudner, R., and Losick, R. (2004) Genes governing swarming in *Bacillus subtilis* and evidence for a phase variation mechanism controlling surface motility. *Mol. Microbiol.*, **52** (2), 357–369.

88. Kearns, D.B., and Losick, R. (2004) Swarming motility in undomesticated *Bacillus subtilis*. *Mol. Microbiol.*, **49** (3), 581–590.

89. Kinsinger, R.F., Shirk, M.C., and Fall, R. (2003) Rapid surface motility in *Bacillus subtilis* is dependent on extracellular surfactin and potassium ion. *J. Bacteriol.*, **185** (18), 5627–5631.

90. Julkowska, D., Obuchowski, M., Holland, I.B., and Séror, S.J. (2005) Comparative analysis of the development of swarming communities of *Bacillus subtilis* 168 and a natural wild type: Critical effects of surfactin and the composition of the medium. *J. Bacteriol.*, **187** (1), 65–76.

91. Angelini, T.E., Roper, M., Kolter, R., Weitz, D.A., and Brenner, M.P. (2009) *Bacillus subtilis* spreads by surfing on waves of surfactant. *Proc. Natl. Acad. Sci. U. S. A.*, **106** (43), 18109–18113.

92. Ghelardi, E., Salvetti, S., Ceragioli, M., Gueye, S. A., Celandroni, F., and

Senesi, S. (2012) Contribution of surfactin and SwrA to flagellin expression, swimming, and surface motility in *Bacillus subtilis*. *Appl. Environ. Microbiol.*, **78** (18), 6540–6544.

93. Aleti, G., Lehner, S., Bacher, M., Compant, S., Nikolic, B., Plesko, M., Schuhmacher, R., Sessitsch, A., and Brader, G. (2016) Surfactin variants mediate species-specific biofilm formation and root colonization in *Bacillus*. *Environ. Microbiol.*, **18** (8), 2634–2645.

94. Vlamakis, H., Chai, Y., Beauregard, P., Losick, R., and Kolter, R. (2013) Sticking together: Building a biofilm the *Bacillus subtilis* way. *Nat. Rev. Microbiol.*, **11** (3), 157–168.

95. Flemming, H.C., Wingender, J., Szewzyk, U., Steinberg, P., Rice, S.A., and Kjelleberg, S. (2016) Biofilms: An emergent form of bacterial life. *Nat. Rev. Microbiol.*, **14** (9), 563–575.

96. Arnaouteli, S., Bamford, N.C., Stanley-Wall, N.R., and Kovács, Á.T. (2021) *Bacillus subtilis* biofilm formation and social interactions. *Nat. Rev. Microbiol.*, **19** (9), 600–614.

97. Blair, K.M., Turner, L., Winkelman, J.T., Berg, H.C., and Kearns, D.B. (2008) A molecular clutch disables flagella in the *Bacillus subtilis* biofilm. *Science.*, **320** (5883), 1636–1638.

98. Romero, D., Aguilar, C., Losick, R., and Kolter, R. (2010) Amyloid fibers provide structural integrity to *Bacillus subtilis* biofilms. *Proc. Natl. Acad. Sci. U.S.A.*, **107** (5), 2230–2234.

99. Hobleya, L., Ostrowskia, A., Raoa, V.F., Bromleyb, M.K., Portera, M., Prescottd, A.R., MacPheeb, C.E., van Aaltena, D.M.F., and Stanley-Walla, N.R. (2015) BslA is a self-assembling bacterial hydrophobin that coats the *Bacillus subtilis* biofilm. *PNAS*, **112** (38), E5375.

100. Kobayashi, K., and Iwano, M. (2012) BslA (YuaB) forms a hydrophobic layer on the surface of *Bacillus subtilis* biofilms. *Mol. Microbiol.*, **85** (1), 51–66.

101. López, D., Fischbach, M.A., Chu, F., Losick, R., and Kolter, R. (2009) Structurally diverse natural products that cause potassium leakage trigger multicellularity in *Bacillus subtilis*. *Proc. Natl. Acad. Sci. U.S.A.*, **106** (1), 280–285.

102. Molle, V., Fujita, M., Jensen, S.T., Eichenberger, P., González-Pastor, J.E., Liu, J.S., and Losick, R. (2003) The Spo0A regulon of *Bacillus subtilis*. *Mol. Microbiol.*, **50** (5), 1683–1701.

103. Schoenborn, A.A., Yannarell, S.M., Wallace, E.D., Clapper, H., Weinstein, I.C., and Shank, E.A. (2021) Defining the expression, production, and

signaling roles of specialized metabolites during *Bacillus subtilis* differentiation. *J. Bacteriol.*, **203**, 337–358.

104. Thérien, M., Kiesewalter, H.T., Auria, E., Charron-Lamoureux, V., Wibowo, M., Maróti, G., Kovács, Á.T., and Beauregard, P.B. (2020) Surfactin production is not essential for pellicle and root-associated biofilm development of *Bacillus subtilis*. *Biofilm*, **2**, 100021.

105. Luo, Z.C., Zhou, H., Zou, J., Wang, X., Zhang, R., Xiang, Y., Chen, Z. (2015) Bacillomycin L and surfactin contribute synergistically to the phenotypic features of *Bacillus subtilis* 916 and the biocontrol of rice sheath blight induced by *Rhizoctonia solani*. *Appl Microbiol Biotechnol*, **99** (4), 1897–1910.

106. Xu, Z., Zhang, R., Wang, D., Qiu, M., Feng, H., Zhang, N., and Shen, Q. (2014) Enhanced control of cucumber wilt disease by *Bacillus amyloliquefaciens* SQR9 by altering the regulation of its DegU phosphorylation. *Appl. Environ. Microbiol.*, **80** (9), 2941–2950.

107. Cao, Y., Pi, H., Chandrangsu, P., Li, Y., Wang, Y., Zhou, H., Xiong, H., Helmann, J.D., and Cai, Y. (2018) Antagonism of two plant-growth promoting *Bacillus velezensis* isolates against *Ralstonia solanacearum* and *Fusarium oxysporum*. *Sci. Rep.*, **8**, 4360.

108. Van Wees, S.C.M., De Swart, E.A.M., Van Pelt, J.A., Van Loon, L.C., and Pieterse, C.M.J. (2000) Enhancement of induced disease resistance by simultaneous activation of salicylate- and jasmonate-dependent defense pathways in *Arabidopsis thaliana*. *Proc. Natl. Acad. Sci. U.S.A.*, **97** (15), 8711–8716.

109. Pieterse, C.M.J., Zamioudis, C., Berendsen, R.L., Weller, D.M., Van Wees, S.C.M., and Bakker, P.A.H.M. (2014) Induced systemic resistance by beneficial microbes. *Annu. Rev. Phytopathol.*, **52** (1), 347–375.

110. Verhagen, B.W.M., Glazebrook, J., Zhu, T., Chang, H.S., Van Loon, L.C., and Pieterse, C.M.J. (2004) The transcriptome of rhizobacteria-induced systemic resistance in *Arabidopsis*. *Mol. Plant-Microbe Interact.*, **17** (8), 895–908.

111. Conrath, U., Thulke O., Katz, V., Schwindling, S., and K.A. (2001) Priming as a mechanism in induced systemic resistance of plants. *Eur. J. Plant Pathol.*, **107**, 113–119.

112. Pršić, J., and Ongena, M. (2020) Elicitors of plant immunity triggered by beneficial bacteria. *Front. Plant Sci.*, **11**, 1675.

113. Cawoy, H., Mariutto, M., Henry, G., Fisher, C., Vasilyeva, N., Thonart, P., Dommes, J., and Ongena, M. (2014) Plant defense stimulation by natural isolates of *Bacillus* depends on efficient surfactin production. *Mol. Plant-*

Microbe Interact., **27** (2), 87–100.

114. Chowdhury, S.P., Uhl, J., Grosch, R., Alquéres, S., Pittroff, S., Dietel, K., Schmitt-Kopplin, P., Borriss, R., and Hartmann, A. (2015) Cyclic lipopeptides of *Bacillus amyloliquefaciens* subsp. *plantarum* colonizing the lettuce rhizosphere enhance plant defense responses toward the bottom rot pathogen *Rhizoctonia solani*. *Mol. Plant-Microbe Interact.*, **28** (9), 984–995.

115. Ongena, M., Jourdan, E., Adam, A., Paquot, M., Brans, A., Joris, B., Arpigny, J.L., and Thonart, P. (2007) Surfactin and fengycin lipopeptides of *Bacillus subtilis* as elicitors of induced systemic resistance in plants. *Environ. Microbiol.*, **9** (4), 1084–1090.

116. Debois, D., Fernandez, O., Franzil, L., Jourdan, E., de Brogniez, A., Willems, L., Clément, C., Dorey, S., De Pauw, E., and Ongena, M. (2015) Plant polysaccharides initiate underground crosstalk with bacilli by inducing synthesis of the immunogenic lipopeptide surfactin. *Environ. Microbiol. Rep.*, **7** (3), 570–582.

117. García-Gutiérrez, L., Zeriouh, H., Romero, D., Cubero, J., de Vicente, A., and Pérez-García, A. (2013) The antagonistic strain *Bacillus subtilis* UMAF6639 also confers protection to melon plants against cucurbit powdery mildew by activation of jasmonate- and salicylic acid-dependent defence responses. *Microb. Biotechnol.*, **6** (3), 264–274.

118. Desoignies, N., Schramme, F., Ongena, M., and Legrève, A. (2013) Systemic resistance induced by *Bacillus* lipopeptides in *Beta vulgaris* reduces infection by the rhizomania disease vector *Polymyxa betae*. *Mol. Plant Pathol.*, **14** (4), 416–421.

119. Yamamoto, S., Shiraishi, S., and Suzuki, S. (2015) Are cyclic lipopeptides produced by *Bacillus amyloliquefaciens* S13-3 responsible for the plant defence response in strawberry against *Colletotrichum gloeosporioides*? *Lett. Appl. Microbiol.*, **60** (4), 379–386.

120. Li, Y., Héloir, M.C., Zhang, X., Geissler, M., Trouvelot, S., Jacquens, L., Henkel, M., Su, X., Fang, X., Wang, Q., and Adrian, M. (2019) Surfactin and fengycin contribute to the protection of a *Bacillus subtilis* strain against grape downy mildew by both direct effect and defence stimulation. *Mol. Plant Pathol.*, **20** (8), 1037–1050.

121. Le Mire, G., Siah, A., Brisset, M.N., Gaucher, M., Deleu, M., and Jijakli, M.H. (2018) Surfactin protects wheat against *Zymoseptoria tritici* and activates both salicylic acid- and jasmonic acid-dependent defense responses. *Agric.*, **8** (1), 11.

122. Rahman, A., Uddin, W., and Wenner, N.G. (2015) Induced systemic resistance responses in perennial ryegrass against *Magnaporthe oryzae*

elicited by semi-purified surfactin lipopeptides and live cells of *Bacillus amyloliquefaciens*. *Mol. Plant Pathol.*, **16** (6), 546–558.

123. Henry, G., Deleu, M., Jourdan, E., Thonart, P., and Ongena, M. (2011) The bacterial lipopeptide surfactin targets the lipid fraction of the plant plasma membrane to trigger immune-related defence responses. *Cell. Microbiol.*, **13** (11), 1824–1837.

124. Lam, V.B., Meyer, T., Argüelles Arias, A., Ongena, M., Oni, F.E., and Höfte, M. (2021) *Bacillus* cyclic lipopeptides iturin and fengycin control rice blast caused by *Pyricularia oryzae* in potting and acid sulfate soils by direct antagonism and induced systemic resistance. *Microorganisms*, **9** (7), 1441.

125. Farzand, A., Moosa, A., Zubair, M., Khan, A.R., Massawe, V.C., Tahir, H.A.S., Sheikh, T.M.M., Ayaz, M., and Gao, X. (2019) Suppression of *Sclerotinia sclerotiorum* by the induction of systemic resistance and regulation of antioxidant pathways in tomato using fengycin produced by *Bacillus amyloliquefaciens* FZB42. *Biomolecules*, **9** (10), 1–17.

126. Park, K., Park, Y.S., Ahamed, J., Dutta, S., Ryu, H., Lee, S.H., Balaraju, K., Manir, M., and Moon, S.S. (2016) Elicitation of induced systemic resistance of chili pepper by iturin a analogs derived from *Bacillus vallismortis* EXTN-1. *Can. J. Plant Sci.*, **96** (4), 564–570.

127. Han, Q., Wu, F., Wang, X., Qi, H., Shi, L., Ren, A., Liu, Q., Zhao, M., and Tang, C. (2015) The bacterial lipopeptide iturins induce *Verticillium dahliae* cell death by affecting fungal signalling pathways and mediate plant defence responses involved in pathogen-associated molecular pattern-triggered immunity. *Environ. Microbiol.*, **17** (4), 1166–1188.

128. Farace, G., Fernandez, O., Jacquens, L., Coutte, F., Krier, F., Jacques, P., Clément, C., Barka, E.A., Jacquard, C., and Dorey, S. (2015) Cyclic lipopeptides from *Bacillus subtilis* activate distinct patterns of defence responses in grapevine. *Mol. Plant Pathol.*, **16** (2), 177–187.

129. Jourdan, E., Henry, G., Duby, F., Dommes, J., Barthélemy, J.P., Thonart, P., and Ongena, M. (2009) Insights into the defense-related events occurring in plant cells following perception of surfactin-type lipopeptide from *Bacillus subtilis*. *Mol. Plant-Microbe Interact.*, **22** (4), 456–468.

130. Deleu, M., Lorent, J., Lins, L., Brasseur, R., Braun, N., El Kirat, K., Nylander, T., Dufrêne, Y.F., and Mingeot-Leclercq, M.P. (2013) Effects of surfactin on membrane models displaying lipid phase separation. *Biochim. Biophys. Acta - Biomembr.*, **1828** (2), 801–815.

131. Liu, Z., Budiharjo, A., Wang, P., Shi, H., Fang, J., Borriss, R., Zhang, K., and Huang, X. (2013) The highly modified microcin peptide plantazolicin is associated with nematicidal activity of *Bacillus amyloliquefaciens* FZB42.

Appl. Microbiol. Biotechnol., **97** (23), 10081–10090.

132. Deleu, M., Paquot, M., and Nylander, T. (2008) Effect of fengycin, a lipopeptide produced by *Bacillus subtilis*, on model biomembranes. *Biophys. J.*, **94** (7), 2667–2679.

133. Wise, C., Falardeau, J., Hagberg, I., and Avis, T.J. (2014) Cellular lipid composition affects sensitivity of plant pathogens to fengycin, an antifungal compound produced by *Bacillus subtilis* strain CU12. *Phytopathology*, **104** (10), 1036–1041.

134. Zakharova, A.A., Efimova, S.S., Malev, V. V., and Ostroumova, O.S. (2019) Fengycin induces ion channels in lipid bilayers mimicking target fungal cell membranes. *Sci. Rep.*, **9** (1), 16034.

135. Gu, Q., Yang, A.Y., Yuan Q., Shi, G., Wu, L., Lou, L., Huo, R., Wu, H., Borriss, R., and Xuewen, G. (2017) Bacillomycin D produced by *Bacillus amyloliquefaciens* is involved in the antagonistic interaction with the plant-pathogenic fungus *Fusarium graminearum*. **83** (19), e01075-17.

136. Hanif, A., Zhang, F., Li, P., Li, C., Xu, Y., Zubair, M., Zhang, M., Jia, D., Zhao, X., Liang, J., Majid, T., Yan, J., Farzand, A., Wu, H., Gu, Q., and Gao, X. (2019) Fengycin produced by *Bacillus amyloliquefaciens* FZB42 inhibits *Fusarium graminearum* growth and mycotoxins biosynthesis. *Toxins (Basel).*, **11** (5), 295–306.

137. Liu, J., Zhou, T., He, D., Li, X.Z., Wu, H., Liu, W., and Gao, X. (2011) Functions of lipopeptides bacillomycin D and fengycin in antagonism of *Bacillus amyloliquefaciens* C06 towards *Monilinia fructicola*. *J. Mol. Microbiol. Biotechnol.*, **20** (1), 43–52.

138. Tao, Y., Xiao-Mei, B., Feng-Xia, L., Hai-Zhen, Z., and Zhao-Xin, L. (2011) Antifungal activity and mechanism of fengycin in the presence and absence of commercial surfactin against *Rhizopus stolonifer*. *J. Microbiol.*, **49** (1), 146–150.

139. Zhang, L., and Sun, C. (2018) Fengycins, cyclic lipopeptides from marine *Bacillus subtilis* strains, kill the plant-pathogenic fungus *Magnaporthe grisea* by inducing reactive oxygen species production and chromatin condensation. *Appl. Environ. Microbiol.*, **84** (18), e00445-18.

140. Chen, M., Wang, J., Liu, B., Zhu, Y., Xiao, R., Yang, W., Ge, C., and Chen, Z. (2020) Biocontrol of tomato bacterial wilt by the new strain *Bacillus velezensis* FJAT-46737 and its lipopeptides. *BMC Microbiol.*, **20** (1), 1–13.

141. Guo, Q., Dong, W., Li, S., Lu, X., Wang, P., Zhang, X., Wang, Y., and Ma, P. (2014) Fengycin produced by *Bacillus subtilis* NCD-2 plays a major role in biocontrol of cotton seedling damping-off disease. *Microbiol. Res.*, **169** (7–8), 533–540.

142. Kim, Y.S., Lee, Y., Cheon, W., Park, J., Kwon, H.T., Balaraju, K., Kim, J., Yoon, Y.J., and Jeon, Y. (2021) Characterization of *Bacillus velezensis* AK-0 as a biocontrol agent against apple bitter rot caused by *Colletotrichum gloeosporioides*. *Sci. Rep.*, **11** (1), 1–14.

143. Jin, P., Wang, H., Tan, Z., Xuan, Z., Dahar, G.Y., Li, Q.X., Miao, W., and Liu, W. (2020) Antifungal mechanism of bacillomycin D from *Bacillus velezensis* HN-2 against *Colletotrichum gloeosporioides* Penz. *Pestic. Biochem. Physiol.*, **163**, 102–107.

144. Gong, Q., Zhang, C., Lu, F., Zhao, H., Bie, X., and Lu, Z. (2014) Identification of bacillomycin D from *Bacillus subtilis* fmbJ and its inhibition effects against *Aspergillus flavus*. *Food Control*, **36** (1), 8–14.

145. Luna-Bulbarela, A., Tinoco-Valencia, R., Corzo, G., Kazuma, K., Konno, K., Galindo, E., and Serrano-Carreón, L. (2018) Effects of bacillomycin D homologues produced by *Bacillus amyloliquefaciens* 83 on growth and viability of *Colletotrichum gloeosporioides* at different physiological stages. *Biol. Control*, **127**, 145–154.

146. Mihalache, G., Balaes, T., Gostin, I., Stefan, M., Coutte, F., and Krier, F. (2018) Lipopeptides produced by *Bacillus subtilis* as new biocontrol products against fusariosis in ornamental plants. *Environ. Sci. Pollut. Res.*, **25** (30), 29784–29793.

147. Caulier, S., Gillis, A., Colau, G., Licciardi, F., Liépin, M., Desoignies, N., Modrie, P., Legrève, A., Mahillon, J., and Bragard, C. (2018) Versatile antagonistic activities of soil-borne *Bacillus* spp. and *Pseudomonas* spp. against *Phytophthora infestans* and other potato pathogens. *Front. Microbiol.*, **9**, 143.

148. Li, B., Li, Q., Xu, Z., Zhang, N., Shen, Q., and Zhang, R. (2014) Responses of beneficial *Bacillus amyloliquefaciens* SQR9 to different soilborne fungal pathogens through the alteration of antifungal compounds production. *Front. Microbiol.*, **5**, 636.

149. Yuan, J., Li, B., Zhang, N., Waseem, R., Shen, Q., and Huang, Q. (2012) Production of bacillomycin- and macrolactin-type antibiotics by *Bacillus amyloliquefaciens* NJN-6 for suppressing soilborne plant pathogens. *J. Agric. Food Chem.*, **60** (12), 2976–2981.

150. Chatterjee, C., Paul, M., Xie, L., and van der Donk, W.A. (2005) Biosynthesis and mode of action of lantibiotics. *Chem. Rev.*, **105** (2), 633–683.

151. Chen, X.H., Scholz, R., Borriss, M., Junge, H., Mögel, G., Kunz, S., and Borriss, R. (2009) Difficidin and bacilysin produced by plant-associated *Bacillus amyloliquefaciens* are efficient in controlling fire blight disease. *J.*

Biotechnol., **140** (1–2), 38–44.

152. Wu, L., Wu, H., Chen, L., Yu, X., Borriss, R., and Gao, X. (2015) Difficidin and bacilysin from *Bacillus amyloliquefaciens* FZB42 have antibacterial activity against *Xanthomonas oryzae* rice pathogens. *Sci. Rep.*, **5** (1), 12975.

153. Im, S.M., Yu, N.H., Joen, H.W., Kim, S.O., Park, H.W., Park, A.R., and Kim, J.C. (2020) Biological control of tomato bacterial wilt by oxydifficidin and difficidin-producing *Bacillus methylotrophicus* DR-08. *Pestic. Biochem. Physiol.*, **163**, 130–137.

154. Chen, L., Wang, X., and Liu, Y. (2021) Contribution of macrolactin in *Bacillus velezensis* CLA178 to the antagonistic activities against *Agrobacterium tumefaciens* C58. *Arch. Microbiol.*, **203** (4), 1743–1752.

155. Barger, S.R., Hoefler, B.C., Cubillos-Ruiz, A., Russell, W.K., Russell, D.H., and Straight, P.D. (2012) Imaging secondary metabolism of *Streptomyces* sp. Mg1 during cellular lysis and colony degradation of competing *Bacillus subtilis*. *Antonie van Leeuwenhoek, Int. J. Gen. Mol. Microbiol.*, **102** (3), 435–445.

156. Müller, S., Strack, S.N., Hoefler, B.C., Straight, P.D., Kearns, D.B., and Kirby, J.R. (2014) Bacillaene and sporulation protect *Bacillus subtilis* from predation by *Myxococcus xanthus*. *Appl. Environ. Microbiol.*, **80** (18), 5603–5610.

157. Müller, S., Strack, S.N., Ryan, S.E., Kearns, D.B., and Kirby, J.R. (2015) Predation by *Myxococcus xanthus* induces *Bacillus subtilis* to form spore-filled megastructures. *Appl. Environ. Microbiol.*, **81** (1), 203–210.

158. Hammami, I., Rhouma, A., Jaouadi, B., Rebai, A., and Nesme, X. (2009) Optimization and biochemical characterization of a bacteriocin from a newly isolated *Bacillus subtilis* strain 14B for biocontrol of *Agrobacterium* spp. strains. *Lett. Appl. Microbiol.*, **48** (2), 253–260.

159. Hammami, I., Jaouadi, B., Bacha, A. Ben, Rebai, A., Bejar, S., Nesme, X., and Rhouma, A. (2012) *Bacillus subtilis* bacteriocin Bac 14B with a broad inhibitory spectrum: Purification, amino acid sequence analysis, and physicochemical characterization. *Biotechnol. Bioprocess Eng.*, **17** (1), 41–49.

160. Villegas-Escobar, V., González-Jaramillo, L.M., Ramírez, M., Moncada, R.N., Sierra-Zapata, L., Orduz, S., and Romero-Tabarez, M. (2018) Lipopeptides from *Bacillus* sp. EA-CB0959: Active metabolites responsible for *in vitro* and *in vivo* control of *Ralstonia solanacearum*. *Biol. Control*, **125**, 20–28.

161. Zeriouh, H., Romero, D., García-Gutiérrez, L., Cazorla, F.M., De Vicente, A., and Pérez-García, A. (2011) The iturin-like lipopeptides are essential

components in the biological control arsenal of *Bacillus subtilis* against bacterial diseases of cucurbits. *Mol. Plant-Microbe Interact.*, **24** (12), 1540–1552.

162. Mácha, H., Marešová, H., Juříková, T., Švecová, M., Benada, O., Škríba, A., Baránek, M., Novotný, Č., and Palyzová, A. (2021) Killing effect of *Bacillus velezensis* FZB42 on a *Xanthomonas campestris* pv. *campestris* (Xcc) strain newly isolated from cabbage *Brassica oleracea* convar. *capitata* (L.): A metabolomic study. *Microorganisms*, **9** (7), 1410.

163. Medeot, D.B., Fernandez, M., Morales, G.M., and Jofré, E. (2020) Fengycins from *Bacillus amyloliquefaciens* MEP218 exhibit antibacterial activity by producing alterations on the cell surface of the pathogens *Xanthomonas axonopodis* pv. *vesicatoria* and *Pseudomonas aeruginosa* PA01. *Front. Microbiol.*, **10**, 3107.

164. Santoyo, G., Hernández-Pacheco, C., Hernández-Salmerón, J., and Hernández-León, R. (2017) The role of abiotic factors modulating the plant-microbe-soil interactions: Toward sustainable agriculture. A review. *Spanish J. Agric. Res.*, **15** (1), 1–15.

165. Traxler, M.F., and Kolter, R. (2015) Natural products in soil microbe interactions and evolution. *Nat. Prod. Rep.*, **32** (7), 956–970.

166. Fierer, N. (2017) Embracing the unknown: disentangling the complexities of the soil microbiome. *Nat. Rev. Microbiol.*, **15** (10), 579–590.

167. Schmidt, R., Ulanova, D., Wick, L.Y., Bode, H.B., and Garbeva, P. (2019) Microbe-driven chemical ecology: Past, present and future. *ISME J.*, **13** (11), 2656–2663.

168. Abdul Rahman, N.S.N., Abdul Hamid, N.W., and Nadarajah, K. (2021) Effects of abiotic stress on soil microbiome. *Int. J. Mol. Sci.*, **22** (16), 9036.

169. Brune, A., Frenzel, P., and Cypionka, H. (2000) Life at the oxic-anoxic interface: Microbial activities and adaptations. *FEMS Microbiol. Rev.*, **24** (5), 691–710.

170. Guez, J.S., Müller, C.H., Danze, P.M., Büchs, J., and Jacques, P. (2008) Respiration activity monitoring system (RAMOS), an efficient tool to study the influence of the oxygen transfer rate on the synthesis of lipopeptide by *Bacillus subtilis* ATCC6633. *J. Biotechnol.*, **134** (1–2), 121–126.

171. Nihorimbere, V., Cawoy, H., Seyer, A., Brunelle, A., Thonart, P., and Ongena, M. (2012) Impact of rhizosphere factors on cyclic lipopeptide signature from the plant beneficial strain *Bacillus amyloliquefaciens* S499. *FEMS Microbiol. Ecol.*, **79** (1), 176–191.

172. Rangarajan, V., Dhanarajan, G., and Sen, R. (2015) Bioprocess design for

selective enhancement of fengycin production by a marine isolate *Bacillus megaterium*. *Biochem. Eng. J.*, **99**, 147–155.

173. Nihorimbere, V., Fickers, P., Thonart, P., and Ongena, M. (2009) Ecological fitness of *Bacillus subtilis* BGS3 regarding production of the surfactin lipopeptide in the rhizosphere. *Environ. Microbiol. Rep.*, **1** (2), 124–130.

174. Yi, G., Liu, Q., Lin, J., Wang, W., Huang, H., and Li, S. (2017) Repeated batch fermentation for surfactin production with immobilized *Bacillus subtilis* BS-37: Two-stage pH control and foam fractionation. *J. Chem. Technol. Biotechnol.*, **92** (3), 530–535.

175. Pertot, I., Puopolo, G., Hosni, T., Pedrotti, L., Jourdan, E., and Ongena, M. (2013) Limited impact of abiotic stress on surfactin production *in planta* and on disease resistance induced by *Bacillus amyloliquefaciens* S499 in tomato and bean. *FEMS Microbiol. Ecol.*, **86** (3), 505–519.

176. Chen, M.C., Wang, J.P., Zhu, Y.J., Liu, B., Yang, W.J., and Ruan, C.Q. (2019) Antibacterial activity against *Ralstonia solanacearum* of the lipopeptides secreted from the *Bacillus amyloliquefaciens* strain FJAT-2349. *J. Appl. Microbiol.*, **126** (5), 1519–1529.

177. Li, M.S.M., Piccoli, D.A., McDowell, T., MacDonald, J., Renaud, J., and Yuan, Z.C. (2021) Evaluating the biocontrol potential of canadian strain *Bacillus velezensis* 1B-23 via its surfactin production at various pHs and temperatures. *BMC Biotechnol.*, **21** (1), 1–12.

178. Budde, I., Steil, L., Scharf, C., Völker, U., and Bremer, E. (2006) Adaptation of *Bacillus subtilis* to growth at low temperature: A combined transcriptomic and proteomic appraisal. *Microbiology*, **152** (3), 831–853.

179. Jacques, P. (2011) Surfactin and other lipopeptides from *Bacillus* spp., vol. 20, Springer Berlin Heidelberg, Berlin, Heidelberg, pp. 57–91.

180. Ohno, A., Ano, T., and Shoda, M. (1995) Effect of temperature on production of lipopeptide antibiotics, iturin A and surfactin by a dual producer, *Bacillus subtilis* RB14, in solid-state fermentation. *J. Ferment. Bioeng.*, **80** (5), 517–519.

181. Jacques, P., Hbid, C., Destain, J., Razafindralambo, H., Paquot, M., De Pauw, E., and Thonart, P. (1999) Optimization of biosurfactant lipopeptide production from *Bacillus subtilis* S499 by Plackett-Burman Design. *Appl. Biochem. Biotechnol.*, **77**, 223–234.

182. Fickers, P., Leclère, V., Guez, J.S., Béchet, M., Coucheney, F., Joris, B., and Jacques, P. (2008) Temperature dependence of mycosubtilin homologue production in *Bacillus subtilis* ATCC6633. *Res. Microbiol.*, **159** (6), 449–457.

183. Hinsinger, P., Bengough, A.G., Vetterlein, D., and Young, I.M. (2009) Rhizosphere: Biophysics, biogeochemistry and ecological relevance. *Plant Soil*, **321** (1–2), 117–152.

184. Wang, R., Liang, X., Long, Z., Wang, X., Yang, L., Lu, B., and Gao, J. (2021) An LCI-like protein APC2 protects ginseng root from *Fusarium solani* infection. *J. Appl. Microbiol.*, **130** (1), 165–178.

185. Van Overbeek, L., and Van Elsas, J.D. (2008) Effects of plant genotype and growth stage on the structure of bacterial communities associated with potato (*Solanum tuberosum* L.). *FEMS Microbiol. Ecol.*, **64** (2), 283–296.

186. Zhang, N., Wang, D., Liu, Y., Li, S., Shen, Q., and Zhang, R. (2014) Effects of different plant root exudates and their organic acid components on chemotaxis, biofilm formation and colonization by beneficial rhizosphere-associated bacterial strains. *Plant Soil*, **374** (1–2), 689–700.

187. Sasse, J., Martinoia, E., and Northen, T. (2018) Feed your Friends: Do plant exudates shape the root microbiome? *Trends Plant Sci.*, **23** (1), 25–41.

188. Fan, B., Carvalhais, L.C., Becker, A., Fedoseyenko, D., von Wirén, N., and Borriss, R. (2012) Transcriptomic profiling of *Bacillus amyloliquefaciens* FZB42 in response to maize root exudates. *BMC Microbiol.*, **12** (1), 116.

189. Jin, Y., Zhu, H., Luo, S., Yang, W., Zhang, L., Li, S., Jin, Q., Cao, Q., Sun, S., and Xiao, M. (2019) Role of maize root exudates in promotion of colonization of *Bacillus velezensis* strain S3-1 in rhizosphere soil and root tissue. *Curr. Microbiol.*, **76** (7), 855–862.

190. Hoff, G., Argüelles Arias, A., Boubsi, F., Pršić, J., Meyer, T., Ibrahim, H.M.M., Steels, S., Luzuriaga, P., Legras, A., Franzil, L., Lequart-Pillon, M., Rayon, C., Osorio, V., de Pauw, E., Lara, Y., Deboever, E., de Coninck, B., Jacques, P., Deleu, M., Petit, E., Van Wuytswinkel, O., and Ongena, M. (2021) Surfactin stimulated by pectin molecular patterns and root exudates acts as a key driver of the *Bacillus*-plant mutualistic interaction. *MBio*, **12** (6), e01774-21.

191. Beauregard, P.B., Chai, Y., Vlamakis, H., Losick, R., and Kolter, R. (2013) *Bacillus subtilis* biofilm induction by plant polysaccharides. *Proc. Natl. Acad. Sci. U. S. A.*, **110** (17), E1621-30.

192. Wu, K., Fang, Z., Guo, R., Pan, B., Shi, W., Yuan, S., Guan, H., Gong, M., Shen, B., and Shen, Q. (2015) Pectin enhances bio-control efficacy by inducing colonization and secretion of secondary metabolites by *Bacillus amyloliquefaciens* SQY 162 in the rhizosphere of tobacco. *PLoS One*, **10** (5), e0127418.

193. Xie, S., Wu, H., Chen, L., Zang, H., Xie, Y., and Gao, X. (2015) Transcriptome profiling of *Bacillus subtilis* OKB105 in response to rice

seedlings. *BMC Microbiol.*, **15** (1), 1–14.

194. Zhang, N., Yang, D., Wang, D., Miao, Y., Shao, J., Zhou, X., Xu, Z., Li, Q., Feng, H., Li, S., Shen, Q., and Zhang, R. (2015) Whole transcriptomic analysis of the plant-beneficial rhizobacterium *Bacillus amyloliquefaciens* SQR9 during enhanced biofilm formation regulated by maize root exudates. *BMC Genomics*, **16** (1), 685.

195. Qiu, M., Xu, Z., Li, X., Li, Q., Zhang, N., Shen, Q., and Zhang, R. (2014) Comparative proteomics analysis of *Bacillus amyloliquefaciens* SQR9 revealed the key proteins involved in *in situ* root colonization. *J. Proteome Res.*, **13** (12), 5581–5591.

196. Liu, Y., Zhang, N., Qiu, M., Feng, H., Vivanco, J.M., Shen, Q., and Zhang, R. (2014) Enhanced rhizosphere colonization of beneficial *Bacillus amyloliquefaciens* SQR9 by pathogen infection. *FEMS Microbiol. Lett.*, **353** (1), 49–56.

197. Liu, Y., Feng, H., Fu, R., Zhang, N., Du, W., Shen, Q., and Zhang, R. (2020) Induced root-secreted D-galactose functions as a chemoattractant and enhances the biofilm formation of *Bacillus velezensis* SQR9 in an McpA-dependent manner. *Appl. Microbiol. Biotechnol.*, **104** (2), 785–797.

198. Abdallah, D. Ben, Krier, F., Jacques, P., Tounsi, S., and Frikha-Gargouri, O. (2020) *Agrobacterium tumefaciens* C58 presence affects *Bacillus velezensis* 32a ecological fitness in the tomato rhizosphere. *Environ. Sci. Pollut. Res.*, **27** (22), 28429–28437.

199. Rudrappa, T., Splaine, R.E., Biedrzycki, M.L., and Bais, H.P. (2008) Cyanogenic pseudomonads influence multitrophic interactions in the rhizosphere. *PLoS One*, **3** (4), e2073.

200. Tan, S., Yang, C., Mei, X., Shen, S., Raza, W., Shen, Q., and Xu, Y. (2013) The effect of organic acids from tomato root exudates on rhizosphere colonization of *Bacillus amyloliquefaciens* T-5. *Appl. Soil Ecol.*, **64**, 15–22.

201. Allard-Massicotte, R., Tessier, L., Lécuyer, F., Lakshmanan, V., Lucier, J.F., Garneau, D., Caudwell, L., Vlamakis, H., Bais, H.P., and Beauregard, P.B. (2016) *Bacillus subtilis* early colonization of *Arabidopsis thaliana* roots involves multiple chemotaxis receptors. *MBio*, **7** (6), e01664-16.

202. Feng, H., Zhang, N., Fu, R., Liu, Y., Krell, T., Du, W., Shao, J., Shen, Q., and Zhang, R. (2019) Recognition of dominant attractants by key chemoreceptors mediates recruitment of plant growth-promoting rhizobacteria. *Environ. Microbiol.*, **21** (1), 402–415.

203. Cawoy, H., Debois, D., Franzil, L., De Pauw, E., Thonart, P., and Ongena, M. (2015) Lipopeptides as main ingredients for inhibition of fungal phytopathogens by *Bacillus subtilis*/*amyloliquefaciens*. *Microb. Biotechnol.*,

8 (2), 281–295.

204. Kulimushi, Z., Argüelles Arias, A., Franzil, L., Steels, S., and Ongena, M. (2017) Stimulation of fengycin-type antifungal lipopeptides in *Bacillus amyloliquefaciens* in the presence of the maize fungal pathogen *Rhizomucor variabilis*. *Front. Microbiol.*, **8**, 850.

205. DeFilippi, S., Groulx, E., Megalla, M., Mohamed, R., and Avis, T.J. (2018) Fungal competitors affect production of antimicrobial lipopeptides in *Bacillus subtilis* strain B9–5. *J. Chem. Ecol.*, **44** (4), 374–383.

206. Pandin, C., Darsonval, M., Mayeur, C., Le Coq, D., Aymerich, S., and Briandet, R. (2019) Biofilm formation and synthesis of antimicrobial compounds by the biocontrol agent *Bacillus velezensis* QST713 in an *Agaricus bisporus* compost micromodel. *Appl. Environ. Microbiol.*, **85** (12), 1–13.

207. Raaijmakers, J.M., and Mazzola, M. (2012) Diversity and natural functions of antibiotics produced by beneficial and plant pathogenic bacteria. *Annu. Rev. Phytopathol.*, **50** (1), 403–424.

208. Rabbee, M., Ali, M., Choi, J., Hwang, B., Jeong, S., Baek, K., Rabbee, M.F., Ali, M.S., Choi, J., Hwang, B.S., Jeong, S.C., and Baek, K. (2019) *Bacillus velezensis*: A valuable member of bioactive molecules within plant microbiomes. *Molecules*, **24** (6), 1046.

209. Inaoka, T., Wang, G., and Ochi, K. (2009) ScoC regulates bacilysin production at the transcription level in *Bacillus subtilis*. *J. Bacteriol.*, **191** (23), 7367–7371.

210. López, D., Vlamakis, H., Losick, R., and Kolter, R. (2009) Cannibalism enhances biofilm development in *Bacillus subtilis*. *Mol. Microbiol.*, **74** (3), 609–618.

211. Vargas-Bautista, C., Rahlwes, K., and Straight, P. (2014) Bacterial competition reveals differential regulation of the *pks* genes by *Bacillus subtilis*. *J. Bacteriol.*, **196** (4), 717–728.

212. Bartolini, M., Cogliati, S., Vileta, D., Bauman, C., Ramirez, W., and Grau, R. (2019) Stress responsive alternative sigma factor SigB plays a positive role in the antifungal proficiency of *Bacillus subtilis*. *Appl. Environ. Microbiol.*, **85** (9), 1–15.

213. Kearns, D.B., Chu, F., Branda, S.S., Kolter, R., and Losick, R. (2005) A master regulator for biofilm formation by *Bacillus subtilis*. *Mol. Microbiol.*, **55** (3), 739–749.

214. Khezri, M., Jouzani, G.S., and Ahmadzadeh, M. (2016) *Fusarium culmorum* affects expression of biofilm formation key genes in *Bacillus subtilis*.

Brazilian J. Microbiol., **47** (1), 47–54.

215. Zhi, Y., Wu, Q., and Xu, Y. (2017) Genome and transcriptome analysis of surfactin biosynthesis in *Bacillus amyloliquefaciens* MT45. *Sci. Rep.*, **7** (1), 40976.

216. Ola, A.R.B., Thomy, D., Lai, D., Brötz-Oesterhelt, H., and Proksch, P. (2013) Inducing secondary metabolite production by the endophytic fungus *Fusarium tricinctum* through coculture with *Bacillus subtilis*. *J. Nat. Prod.*, **76** (11), 2094–2099.

217. Bacon, C.W., Hinton, D.M., Porter, J.K., Glenn, A.E., and Kuldau, G. (2004) Fusaric acid, a *Fusarium verticillioides* metabolite, antagonistic to the endophytic biocontrol bacterium *Bacillus mojavensis*. *Can. J. Bot.*, **82** (7), 878–885.

218. Bacon, C.W., Hinton, D.M., and Hinton, A. (2006) Growth-inhibiting effects of concentrations of fusaric acid on the growth of *Bacillus mojavensis* and other biocontrol *Bacillus* species. *J. Appl. Microbiol.*, **100** (1), 185–194.

219. Bani, M., Rispail, N., Evidente, A., Rubiales, D., and Cimmino, A. (2014) Identification of the main toxins isolated from *Fusarium oxysporum* f. sp. *pisi* race 2 and their relation with isolates' pathogenicity. *J. Agric. Food Chem.*, **62** (12), 2574–2580.

220. Bleich, R., Watrous, J.D., Dorrestein, P.C., Bowers, A.A., and Shank, E.A. (2015) Thiopeptide antibiotics stimulate biofilm formation in *Bacillus subtilis*. *Proc. Natl. Acad. Sci. U.S.A.*, **112** (10), 3086–3091.

221. Liu, Y., Kyle, S., and Straight, P.D. (2018) Antibiotic stimulation of a *Bacillus subtilis* migratory response. *mSphere*, **3** (1), e00586-17.

222. Izquierdo-García, L.F., González-Almario, A., Cotes, A.M., and Moreno-Velandia, C.A. (2020) *Trichoderma virens* Gl006 and *Bacillus velezensis* Bs006: A compatible interaction controlling *Fusarium* wilt of cape gooseberry. *Sci. Rep.*, **10** (1), 6857.

223. Karuppiah, V., Sun, J., Li, T., Vallikkannu, M., and Chen, J. (2019) Co-cultivation of *Trichoderma asperellum* GDFS1009 and *Bacillus amyloliquefaciens* 1841 causes differential gene expression and improvement in the wheat growth and biocontrol activity. *Front. Microbiol.*, **10**, 1–16.

224. Karuppiah, V., Vallikkannu, M., Li, T., and Chen, J. (2019) Simultaneous and sequential based co-fermentations of *Trichoderma asperellum* GDFS1009 and *Bacillus amyloliquefaciens* 1841: A strategy to enhance the gene expression and metabolites to improve the bio-control and plant growth promoting activi. *Microb. Cell Fact.*, **18** (1), 1–16.

225. Almoneafy, A.A., Kakar, K.U., Nawaz, Z., Li, B., Saand, M.A., Chun-Lan,

Y., and Xie, G.L. (2014) Tomato plant growth promotion and antibacterial related-mechanisms of four rhizobacterial *Bacillus* strains against *Ralstonia solanacearum*. *Symbiosis*, **63** (2), 59–70.

226. Kakar, K.U., Duan, Y.P., Nawaz, Z., Sun, G., Almoneafy, A.A., Hassan, M.A., Elshakh, A., Li, B., and Xie, G.L. (2014) A novel rhizobacterium Bk7 for biological control of brown sheath rot of rice caused by *Pseudomonas fuscovaginae* and its mode of action. *Eur. J. Plant Pathol.*, **138** (4), 819–834.

227. Straight, P.D., Fischbach, M.A., Walsh, C.T., Rudner, D.Z., and Kolter, R. (2007) A singular enzymatic megacomplex from *Bacillus subtilis*. *Proc. Natl. Acad. Sci. U.S.A.*, **104** (1), 305–310.

228. Molina-Santiago, C., Vela-Corcía, D., Petras, D., Díaz-Martínez, L., Pérez-Lorente, A.I., Sopeña-Torres, S., Pearson, J., Caraballo-Rodríguez, A.M., Dorrestein, P.C., de Vicente, A., and Romero, D. (2021) Chemical interplay and complementary adaptative strategies toggle bacterial antagonism and co-existence. *Cell Rep.*, **36** (4), 109449.

229. Ramses Gallegos-Monterrosa, Stefanie Kankel, S.G., Robert Barnett, P.S., and Ákos T. Kovácsa (2017) *Lysinibacillus fusiformis* M5 induces increased complexity in *Bacillus subtilis* 168 colony biofilms via hypoxanthine ramses. **199** (22), e00204-17.

230. Townsley, L., Yannarell, S.M., Huynh, T.N., Woodward, J.J., and Shank, E.A. (2018) Cyclic di-AMP acts as an extracellular signal that impacts *Bacillus subtilis* biofilm formation and plant attachment. *MBio*, **9** (2), e00341-18.

231. Molina-Santiago, C., Pearson, J.R., Navarro, Y., Berlanga-Clavero, M.V., Caraballo-Rodriguez, A.M., Petras, D., García-Martín, M.L., Lamon, G., Haberstein, B., Cazorla, F.M., de Vicente, A., Loquet, A., Dorrestein, P.C., and Romero, D. (2019) The extracellular matrix protects *Bacillus subtilis* colonies from *Pseudomonas* invasion and modulates plant co-colonization. *Nat. Commun.*, **10** (1), 1919.

232. Shank, E.A., Klepac-Ceraj, V., Collado-Torres, L., Powers, G.E., Losick, R., and Kolter, R. (2011) Interspecies interactions that result in *Bacillus subtilis* forming biofilms are mediated mainly by members of its own genus. *Proc. Natl. Acad. Sci. U.S.A.*, **108** (48), E1236.

233. Yannarell, S.M., Grandchamp, G.M., Chen, S.Y., Daniels, K.E., and Shank, E.A. (2019) A dual-species biofilm with emergent mechanical and protective properties. *J. Bacteriol.*, **201** (18), e00670-18.

234. Sun, X., Xu, Z., Xie, J., Hesselberg-Thomsen, V., Tan, T., Zheng, D., Strube, M.L., Dragoš, A., Shen, Q., Zhang, R., and Kovács, Á.T. (2021) *Bacillus velezensis* stimulates resident rhizosphere *Pseudomonas stutzeri* for plant

health through metabolic interactions. *ISME J.*

235. Eckshtain-Levi, N., Harris, S.L., Roscios, R.Q., and Shank, E.A. (2020) Bacterial community members increase *Bacillus subtilis* maintenance on the roots of *Arabidopsis thaliana*. *Phytobiomes J.*, **4** (4), 303–313.

236. Wadhams, G.H., and Armitage, J.P. (2004) Making sense of it all: Bacterial chemotaxis. *Nat. Rev. Mol. Cell Biol.*, **5** (12), 1024–1037.

237. Jones, S.E., Ho, L., Rees, C.A., Hill, J.E., Nodwell, J.R., and Elliot, M.A. (2017) *Streptomyces* exploration is triggered by fungal interactions and volatile signals. *Elife*, **6**, e21738.

238. McCully, L.M., Bitzer, A.S., Seaton, S.C., Smith, L.M., and Silby, M.W. (2019) Interspecies social spreading: Interaction between two sessile soil bacteria leads to emergence of surface motility. *mSphere*, **4** (1), e00696-18.

239. Stubbendieck, R.M., Vargas-Bautista, C., and Straight, P.D. (2016) Bacterial communities: Interactions to scale. *Front. Microbiol.*, **7**, 1–19.

240. Grau, R.R., De Oña, P., Kunert, M., Leñini, C., Gallegos-Monterrosa, R., Mhatre, E., Vileta, D., Donato, V., Hölscher, T., Boland, W., Kuipers, O.P., and Kovács, Á.T. (2015) A duo of potassium-responsive histidine kinases govern the multicellular destiny of *Bacillus subtilis*. *MBio*, **6** (4), e00581-15.

241. van Gestel, J., Vlamakis, H., and Kolter, R. (2015) From cell differentiation to cell collectives: *Bacillus subtilis* uses division of labor to migrate. *PLoS Biol.*, **13** (4), 1–29.

242. Grandchamp, G.M., Caro, L., and Shank, E.A. (2017) Pirated siderophores promote sporulation in *Bacillus subtilis*. *Appl. Environ. Microbiol.*, **83** (10), e03293-16.

243. Powers, M.J., Sanabria-Valentín, E., Bowers, A.A., and Shank, E.A. (2015) Inhibition of cell differentiation in *Bacillus subtilis* by *Pseudomonas protegens*. *J. Bacteriol.*, **197** (13), 2129–2138.

244. Fravel, D.R. (2005) Commercialization and implementation of biocontrol. *Annu. Rev. Phytopathol.*, **43** (1), 337–359.

245. Frey-Klett, P., Burlinson, P., Deveau, A., Barret, M., Tarkka, M., and Sarniguet, A. (2011) Bacterial-fungal interactions: Hyphens between agricultural, clinical, environmental, and food microbiologists. *Microbiol. Mol. Biol. Rev.*, **75** (4), 583–609.

246. Müller, D.B., Vogel, C., Bai, Y., and Vorholt, J.A. (2016) The plant microbiota: Systems-level insights and perspectives. *Annu. Rev. Genet.*, **50** (1), 211–234.

247. Penha, R.O., Vandenberghe, L.P.S., Faulds, C., Soccol, V.T., and Soccol,

C.R. (2020) *Bacillus* lipopeptides as powerful pest control agents for a more sustainable and healthy agriculture: Recent studies and innovations. *Planta*, **251** (3), 1–15.

248. Grubbs, K.J., Bleich, R.M., Santa Maria, K.C., Allen, S.E., Farag, S., Shank, E.A., and Bowers, A.A. (2017) Large-scale bioinformatics analysis of *Bacillus* genomes uncovers conserved roles of natural products in bacterial physiology. *mSystems*, **2** (6), e00040-17.

249. Ye, M., Tang, X., Yang, R., Zhang, H., Li, F., Tao, F., Li, F., and Wang, Z. (2018) Characteristics and application of a novel species of *Bacillus*: *Bacillus velezensis*. *ACS Chem. Biol.*, **13** (3), 500–505.

250. Li, Y., and Rebuffat, S. (2020) The manifold roles of microbial ribosomal peptide-based natural products in physiology and ecology. *J. Biol. Chem.*, **295** (1), 34–54.

251. Nayfach, S., Roux, S., Seshadri, R., Udwary, D., Varghese, N., Schulz, F., Wu, D., Paez-Espino, D., Chen, I.M., Huntemann, M., Palaniappan, K., Ladau, J., Mukherjee, S., Reddy, T.B.K., Nielsen, T., Kirton, E., Faria, J.P., Edirisinghe, J.N., Henry, C.S., Jungbluth, S.P., Chivian, D., Dehal, P., Wood-Charlson, E.M., Arkin, A.P., Tringe, S.G., Visel, A., Abreu, H., Acinas, S.G., Allen, E., Allen, M.A., Alteio, L. V., Andersen, G., Anesio, A.M., Attwood, G., Avila-Magaña, V., Badis, Y., Bailey, J., Baker, B., Baldrian, P., Barton, H.A., Beck, D.A.C., Becraft, E.D., Beller, H.R., Beman, J.M., Bernier-Latmani, R., Berry, T.D., Bertagnolli, A., Bertilsson, S., Bhatnagar, J.M., Bird, J.T., Blanchard, J.L., Blumer-Schuette, S.E., Bohannan, B., Borton, M.A., Brady, A., Brawley, S.H., Brodie, J., Brown, S., Brum, J.R., Brune, A., Bryant, D.A., Buchan, A., Buckley, D.H., Buongiorno, J., Cadillo-Quiroz, H., Caffrey, S.M., Campbell, A.N., Campbell, B., Carr, S., Carroll, J.L., Cary, S.C., Cates, A.M., Cattolico, R.A., Cavicchioli, R., Chistoserdova, L., Coleman, M.L., Constant, P., Conway, J.M., Mac Cormack, W.P., Crowe, S., Crump, B., Currie, C., Daly, R., DeAngelis, K.M., Denef, V., Denman, S.E., Desta, A., Dionisi, H., Dodsworth, J., Dombrowski, N., Donohue, T., Dopson, M., Driscoll, T., Dunfield, P., Dupont, C.L., Dynarski, K.A., Edgcomb, V., Edwards, E.A., Elshahed, M.S., Figueroa, I., Flood, B., Fortney, N., Fortunato, C.S., Francis, C., Gachon, C.M.M., Garcia, S.L., Gazitua, M.C., Gentry, T., Gerwick, L., Gharechahi, J., Girguis, P., Gladden, J., Gradoville, M., Grasby, S.E., Gravuer, K., Grettenberger, C.L., Gruninger, R.J., Guo, J., Habteselassie, M.Y., Hallam, S.J., Hatzenpichler, R., Hausmann, B., Hazen, T.C., Hedlund, B., Henny, C., Herfort, L., Hernandez, M., Hershey, O.S., Hess, M., Hollister, E.B., Hug, L.A., Hunt, D., Jansson, J., Jarett, J., Kadnikov, V. V., Kelly, C., Kelly, R., Kelly, W., Kerfeld, C.A., Kimbrel, J., Klassen, J.L., Konstantinidis, K.T., Lee, L.L., Li, W.J., Loder, A.J., Loy, A., Lozada, M., MacGregor, B., Magnabosco, C., Maria da Silva, A., McKay, R.M., McMahon, K., McSweeney, C.S., Medina, M., Meredith,

L., Mizzi, J., Mock, T., Momper, L., Moran, M.A., Morgan-Lang, C., Moser, D., Muyzer, G., Myrold, D., Nash, M., Nesbø, C.L., Neumann, A.P., Neumann, R.B., Noguera, D., Northen, T., Norton, J., Nowinski, B., Nüsslein, K., O'Malley, M.A., Oliveira, R.S., Maia de Oliveira, V., Onstott, T., Osvatic, J., Ouyang, Y., Pachiadaki, M., Parnell, J., Partida-Martinez, L.P., Peay, K.G., Pelletier, D., Peng, X., Pester, M., Pett-Ridge, J., Peura, S., Pjevac, P., Plominsky, A.M., Poehlein, A., Pope, P.B., Ravin, N., Redmond, M.C., Reiss, R., Rich, V., Rinke, C., Rodrigues, J.L.M., Rodriguez-Reillo, W., Rossmassler, K., Sackett, J., Salekdeh, G.H., Saleska, S., Scarborough, M., Schachtman, D., Schadt, C.W., Schrenk, M., Sczyrba, A., Sengupta, A., Setubal, J.C., Shade, A., Sharp, C., Sherman, D.H., Shubenkova, O.V., Sierra-Garcia, I.N., Simister, R., Simon, H., Sjöling, S., Slonczewski, J., Correa de Souza, R.S., Spear, J.R., Stegen, J.C., Stepanauskas, R., Stewart, F., Suen, G., Sullivan, M., Sumner, D., Swan, B.K., Swingley, W., Tarn, J., Taylor, G.T., Teeling, H., Tekere, M., Teske, A., Thomas, T., Thrash, C., Tiedje, J., Ting, C.S., Tully, B., Tyson, G., Ulloa, O., Valentine, D.L., Van Goethem, M.W., Vander Gheynst, J., Verbeke, T.J., Vollmers, J., Vuillemin, A., Waldo, N.B., Walsh, D.A., Weimer, B.C., Whitman, T., van der Wielen, P., Wilkins, M., Williams, T.J., Woodcroft, B., Woolet, J., Wrighton, K., Ye, J., Young, E.B., Youssef, N.H., Yu, F.B., Zemskaya, T.I., Ziels, R., Woyke, T., Mouncey, N.J., Ivanova, N.N., Kyrpides, N.C., and Eloe-Fadrosh, E.A. (2021) A genomic catalog of Earth's microbiomes. *Nat. Biotechnol.*, **39** (4), 499–509.

252. Hibbing, M.E., Fuqua, C., Parsek, M.R., and Peterson, S.B. (2010) Bacterial competition: Surviving and thriving in the microbial jungle. *Nat. Rev. Microbiol.*, **8** (1), 15–25.

253. Andrić, S., Meyer, T., and Ongena, M. (2020) *Bacillus* responses to plant-associated fungal and bacterial communities. *Front. Microbiol.*, **11**, 1350.

254. Townsley, L., and Shank, E.A. (2017) Natural-product antibiotics: Cues for modulating bacterial biofilm formation. *Trends Microbiol.*, **25** (12), 1016–1026.

255. Stubbendieck, R.M., and Straight, P.D. (2015) Escape from lethal bacterial competition through coupled activation of antibiotic resistance and a mobilized subpopulation. *PLoS Genet.*, **11** (12), e1005722.

256. Raaijmakers, J.M., de Bruijn, I., Nybroe, O., and Ongena, M. (2010) Natural functions of lipopeptides from *Bacillus* and *Pseudomonas*: More than surfactants and antibiotics. *FEMS Microbiol. Rev.*, **34** (6), 1037–1062.

257. Zboralski, A., and Filion, M. (2020) Genetic factors involved in rhizosphere colonization by phytobeneficial *Pseudomonas* spp. *Comput. Struct. Biotechnol. J.*, **18**, 3539–3554.

258. Rieusset, L., Rey, M., Muller, D., Vacheron, J., Gerin, F., Dubost, A., Comte, G., and Prigent-Combaret, C. (2020) Secondary metabolites from plant-associated *Pseudomonas* are overproduced in biofilm. *Microb. Biotechnol.*, **13** (5), 1562–1580.

259. Nguyen, D.D., Melnik, A.V, Koyama, N., Lu, X., Schorn, M., Fang, J., Aguinaldo, K., Lincecum, T.L., Ghequire, M.G.K., Carrion, V.J., Cheng, T.L., Duggan, B.M., Malone, J.G., Mauchline, T.H., Sanchez, L.M., Kilpatrick, A.M., Raaijmakers, J.M., De Mot, R., Moore, B.S., Medema, M.H., and Dorrestein, P.C. (2017) Indexing the *Pseudomonas* specialized metabolome enabled the discovery of poaeamide B and the bananamides. *Nat. Microbiol.*, **2** (1), 16197.

260. Götze, S., and Stallforth, P. (2020) Structure, properties, and biological functions of nonribosomal lipopeptides from pseudomonads. *Nat. Prod. Rep.*, **37** (1), 29–54.

261. Geudens, N., and Martins, J.C. (2018) Cyclic lipodepsipeptides from *Pseudomonas* spp. - Biological Swiss-Army knives. *Front. Microbiol.*, **9**, 1867.

262. Loper, J.E., Hassan, K.A., Mavrodi, D.V., Davis, E.W., Lim, C.K., Shaffer, B.T., Elbourne, L.D.H., Stockwell, V.O., Hartney, S.L., Breakwell, K., Henkels, M.D., Tetu, S.G., Rangel, L.I., Kidarsa, T.A., Wilson, N.L., van de Mortel, J.E., Song, C., Blumhagen, R., Radune, D., Hostetler, J.B., Brinkac, L.M., Durkin, A.S., Kluepfel, D.A., Wechter, W.P., Anderson, A.J., Kim, Y.C., Pierson, L.S., Pierson, E.A., Lindow, S.E., Kobayashi, D.Y., Raaijmakers, J.M., Weller, D.M., Thomashow, L.S., Allen, A.E., and Paulsen, I.T. (2012) Comparative genomics of plant-associated *Pseudomonas* spp.: Insights into diversity and inheritance of traits involved in multitrophic interactions. *PLoS Genet.*, **8** (7), e1002784.

263. Ansari, F.A., and Ahmad, I. (2019) Fluorescent *Pseudomonas* - FAP2 and *Bacillus licheniformis* interact positively in biofilm mode enhancing plant growth and photosynthetic attributes. *Sci. Rep.*, **9** (1), 4547.

264. Touré, Y., Ongena, M., Jacques, P., Guiro, A., and Thonart, P. (2004) Role of lipopeptides produced by *Bacillus subtilis* GA1 in the reduction of grey mould disease caused by *Botrytis cinerea* on apple. *J. Appl. Microbiol.*, **96** (5), 1151–1160.

265. Chen, X.H., Koumoutsi, A., Scholz, R., Eisenreich, A., Schneider, K., Heinemeyer, I., Morgenstern, B., Voss, B., Hess, W.R., Reva, O., Junge, H., Voigt, B., Jungblut, P.R., Vater, J., Süssmuth, R., Liesegang, H., Strittmatter, A., Gottschalk, G., and Borriss, R. (2007) Comparative analysis of the complete genome sequence of the plant growth-promoting bacterium *Bacillus amyloliquefaciens* FZB42. *Nat. Biotechnol.*, **25** (9), 1007–1014.

266. Perneel, M., Heyrman, J., Adiobo, A., De Maeyer, K., Raaijmakers, J.M., De Vos, P., and Höfte, M. (2007) Characterization of CMR5c and CMR12a, novel fluorescent *Pseudomonas* strains from the cocoyam rhizosphere with biocontrol activity. *J. Appl. Microbiol.*, **103** (4), 1007–1020.

267. Girard, L., Lood, C., Höfte, M., Vandamme, P., Rokni-Zadeh, H., van Noort, V., Lavigne, R., and De Mot, R. (2021) The ever-expanding *Pseudomonas* genus: Description of 43 new species and partition of the *Pseudomonas putida* group. *Microorganisms*, **9** (8), 1766.

268. D'aes, J., Hua, G.K.H., De Maeyer, K., Pannecoucque, J., Forrez, I., Ongena, M., Dietrich, L.E.P., Thomashow, L.S., Mavrodi, D.V., and Höfte, M. (2011) Biological control of rhizoctonia root rot on bean by phenazineand cyclic lipopeptide-producing *Pseudomonas* CMR12a. *Phytopathology*, **101** (8), 996–1004.

269. D'aes, J., Kieu, N.P., Léclère, V., Tokarski, C., Olorunleke, F.E., De Maeyer, K., Jacques, P., Höfte, M., and Ongena, M. (2014) To settle or to move? The interplay between two classes of cyclic lipopeptides in the biocontrol strain *Pseudomonas* CMR12a. *Environ. Microbiol.*, **16** (7), 2282–2300.

270. Paulsen, I.T., Press, C.M., Ravel, J., Kobayashi, D.Y., Myers, G.S.A., Mavrodi, D.V., DeBoy, R.T., Seshadri, R., Ren, Q., Madupu, R., Dodson, R.J., Durkin, A.S., Brinkac, L.M., Daugherty, S.C., Sullivan, S.A., Rosovitz, M.J., Gwinn, M.L., Zhou, L., Schneider, D.J., Cartinhour, S.W., Nelson, W.C., Weidman, J., Watkins, K., Tran, K., Khouri, H., Pierson, E.A., Pierson, L.S., Thomashow, L.S., and Loper, J.E. (2005) Complete genome sequence of the plant commensal *Pseudomonas fluorescens* Pf-5. *Nat. Biotechnol.*, **23** (7), 873–878.

271. Jousset, A., Schuldes, J., Keel, C., Maurhofer, M., Daniel, R., Scheu, S., and Thuermer, A. (2014) Full-genome sequence of the plant growth-promoting bacterium *Pseudomonas protegens* CHA0. *Genome Announc.*, **2** (2), 322–336.

272. Rokni-Zadeh, H., Li, W., Sanchez-Rodriguez, A., Sinnaeve, D., Rozenski, J., Martins, J.C., and De Mot, R. (2012) Genetic and functional characterization of cyclic lipopeptide white-line-inducing principle (WLIP) production by rice rhizosphere isolate *Pseudomonas putida* RW10S2. *Appl. Environ. Microbiol.*, **78** (14), 4826–4834.

273. Li, W., Rokni-Zadeh, H., De Vleeschouwer, M., Ghequire, M.G.K., Sinnaeve, D., Xie, G.L., Rozenski, J., Madder, A., Martins, J.C., and De Mot, R. (2013) The antimicrobial compound xantholysin defines a new group of *Pseudomonas* cyclic lipopeptides. *PLoS One*, **8** (5), e62946.

274. Oni, F.E., Geudens, N., Omoboye, O.O., Bertier, L., Hua, H.G.K., Adiobo, A., Sinnaeve, D., Martins, J.C., and Höfte, M. (2019) Fluorescent

Pseudomonas and cyclic lipopeptide diversity in the rhizosphere of cocoyam (*Xanthosoma sagittifolium*). *Environ. Microbiol.*, **21** (3), 1019–1034.

275. Miguel, R.N., Barret, M., Morrisey, J.P., Germaine, K., Francisco, M.G., Barahona, E., Navazo, A., María, S.C., Moynihan, J.A., Giddens, S.R., Coppoolse, E.R., Muriel, C., Stiekema, W.J., Rainey, P.B., Dowling, D., O'gara, F., Martín, M., and Rivilla, R. (2012) Genome sequence of the biocontrol strain *Pseudomonas fluorescens* F113. *J. Bacteriol.*, **194** (5), 1273–1274.

276. Hanahan, D. (1983) Studies on transformation of *Escherichia coli* with plasmids. *J. Mol. Biol.*, **166** (4), 557–580.

277. Bisicchia, P., Botella, E., and Devine, K.M. (2010) Suite of novel vectors for ectopic insertion of GFP, CFP and IYFP transcriptional fusions in single copy at the *amyE* and *bglS* loci in *Bacillus subtilis*. *Plasmid*, **64** (3), 143–149.

278. Meyer, T., Vigouroux, A., Aumont-Nicaise, M., Comte, G., Vial, L., Lavire, C., and Moréra, S. (2018) The plant defense signal galactinol is specifically used as a nutrient by the bacterial pathogen *Agrobacterium fabrum*. *J. Biol. Chem.*, **293** (21), 7930–7941.

279. Martínez-García, E., and de Lorenzo, V. (2011) Engineering multiple genomic deletions in Gram-negative bacteria: analysis of the multi-resistant antibiotic profile of *Pseudomonas putida* KT2440. *Environ. Microbiol.*, **13** (10), 2702–2716.

280. Jarmer, H., Berka, R., Knudsen, S., and Saxild, H.H. (2002) Transcriptome analysis documents induced competence of *Bacillus subtilis* during nitrogen limiting conditions. *FEMS Microbiol. Lett.*, **206** (2), 197–200.

281. Vacheron, J., Péchy-Tarr, M., Brochet, S., Heiman, C.M., Stojiljkovic, M., Maurhofer, M., and Keel, C. (2019) T6SS contributes to gut microbiome invasion and killing of an herbivorous pest insect by plant-beneficial *Pseudomonas protegens*. *ISME J.*, **13** (5), 1318–1329.

282. Pluskal, T., Castillo, S., Villar-Briones, A., and Orešič, M. (2010) MZmine 2: Modular framework for processing, visualizing, and analyzing mass spectrometry-based molecular profile data. *BMC Bioinformatics*, **11**, 395.

283. Kune, C., McCann, A., Raphaël, L.R., Argüelles Arias, A., Tiquet, M., Van Kruining, D., Martinez, P.M., Ongena, M., Eppe, G., Quinton, L., Far, J., and De Pauw, E. (2019) Rapid visualization of chemically related compounds using kendrick mass defect as a filter in mass spectrometry imaging. *Anal. Chem.*, **91** (20), 13112–13118.

284. (2020) R Core Team (2020). R: A language and environment for statistical computing. R Foundation for Statistical Computing, Vienna, Austria.

285. Blin, K., Shaw, S., Kloosterman, A.M., Charlop-Powers, Z., Van Wezel, G.P., Medema, M.H., and Weber, T. (2021) AntiSMASH 6.0: Improving cluster detection and comparison capabilities. *Nucleic Acids Res.*, **49** (W1), W29–W35.

286. Youard, Z.A., Wenner, N., and Reimmann, C. (2011) Iron acquisition with the natural siderophore enantiomers pyochelin and enantio-pyochelin in *Pseudomonas* species. *BioMetals*, **24** (3), 513–522.

287. Mavrodi, D.V., Parejko, J.A., Mavrodi, O.V., Kwak, Y.S., Weller, D.M., Blankenfeldt, W., and Thomashow, L.S. (2013) Recent insights into the diversity, frequency and ecological roles of phenazines in fluorescent *Pseudomonas* spp. *Environ. Microbiol.*, **15** (3), 675–686.

288. Sinnaeve, D., Michaux, C., Van hemel, J., Vandenkerckhove, J., Peys, E., Borremans, F.A.M., Sas, B., Wouters, J., and Martins, J.C. (2009) Structure and X-ray conformation of pseudodesmins A and B, two new cyclic lipodepsipeptides from *Pseudomonas* bacteria. *Tetrahedron*, **65** (21), 4173–4181.

289. Oni, F.E., Geudens, N., Onyeka, J.T., Olorunleke, O.F., Salami, A.E., Omoboye, O.O., Argüelles Arias, A., Adiobo, A., De Neve, S., Ongena, M., Martins, J.C., and Höfte, M. (2020) Cyclic lipopeptide-producing *Pseudomonas koreensis* group strains dominate the cocoyam rhizosphere of a *Pythium* root rot suppressive soil contrasting with *P. putida* prominence in conducive soils. *Environ. Microbiol.*, **22** (12), 5137–5155.

290. Kuiper, I., Lagendijk, E.L., Pickford, R., Derrick, J.P., Lamers, G.E.M., Thomas-Oates, J.E., Lugtenberg, B.J.J., and Bloemberg, G. V. (2004) Characterization of two *Pseudomonas putida* lipopeptide biosurfactants, putisolvin I and II, which inhibit biofilm formation and break down existing biofilms. *Mol. Microbiol.*, **51** (1), 97–113.

291. Bassarello, C., Lazzaroni, S., Bifulco, G., Lo Cantore, P., Iacobellis, N.S., Riccio, R., Gomez-Paloma, L., and Evidente, A. (2004) Tolaasins A−E, five new lipodepsipeptides produced by *Pseudomonas tolaasii*. *J. Nat. Prod.*, **67** (5), 811–816.

292. Ma, Z., Hoang Hua, G.K.H., Ongena, M., and Höfte, M. (2016) Role of phenazines and cyclic lipopeptides produced by *Pseudomonas* sp. CMR12a in induced systemic resistance on rice and bean. *Environ. Microbiol. Rep.*, **8** (5), 896–904.

293. Salari, F., Zare-Mirakabad, F., Alavi, M.H., Girard, L., Ghafari, M., De Mot, R., and Rokni-Zadeh, H. (2020) Draft genome sequence of *Pseudomonas aeruginosa* strain LMG 1272, an atypical white line reaction producer. *Microbiol. Resour. Announc.*, **9** (7), e01363-19.

294. Munsch, P., and Alatossava, T. (2002) The white-line-in-agar test is not specific for the two cultivated mushroom associated pseudomonads, *Pseudomonas tolaasii* and *Pseudomonas* "*reactans*." *Microbiol. Res.*, **157** (1), 7–11.

295. Biessy, A., Novinscak, A., Blom, J., Léger, G., Thomashow, L.S., Cazorla, F.M., Josic, D., and Filion, M. (2018) Diversity of phytobeneficial traits revealed by whole-genome analysis of worldwide-isolated phenazine-producing *Pseudomonas* spp. *Environ. Microbiol.*, **21** (1), 437–455.

296. Flury, P., Aellen, N., Ruffner, B., Péchy-Tarr, M., Fataar, S., Metla, Z., Dominguez-Ferreras, A., Bloemberg, G., Frey, J., Goesmann, A., Raaijmakers, J.M., Duffy, B., Höfte, M., Blom, J., Smits, T.H.M.M., Keel, C., and Maurhofer, M. (2016) Insect pathogenicity in plant-beneficial pseudomonads: Phylogenetic distribution and comparative genomics. *ISME J.*, **10** (10), 2527–2542.

297. Hesse, C., Schulz, F., Bull, C.T., Shaffer, B.T., Yan, Q., Shapiro, N., Hassan, K.A., Varghese, N., Elbourne, L.D.H., Paulsen, I.T., Kyrpides, N., Woyke, T., and Loper, J.E. (2018) Genome-based evolutionary history of *Pseudomonas* spp. *Environ. Microbiol.*, **20** (6), 2142–2159.

298. Lalucat, J., Mulet, M., Gomila, M., and García-Valdés, E. (2020) Genomics in bacterial taxonomy: Impact on the genus *Pseudomonas*. *Genes (Basel).*, **11** (2), 139.

299. Girard, L., Höfte, M., and Mot, R. De (2020) Lipopeptide families at the interface between pathogenic and beneficial *Pseudomonas*-plant interactions. *Crit. Rev. Microbiol.*, **46** (4), 397–419.

300. Michelsen, C.F., Watrous, J., Glaring, M.A., Kersten, R., Koyama, N., Dorrestein, P.C., and Stougaard, P. (2015) Nonribosomal peptides, key biocontrol components for *Pseudomonas fluorescens* in5, isolated from a Greenlandic suppressive soil. *MBio*, **6** (2), e00079-15.

301. Emanuele, M.C., Scaloni, A., Lavermicocca, P., Jacobellis, N.S., Camoni, L., Di Giorgio, D., Pucci, P., Paci, M., Segre, A., and Ballio, A. (1998) Corpeptins, new bioactive lipodepsipeptides from cultures of *Pseudomonas corrugata*. *FEBS Lett.*, **433** (3), 317–320.

302. Rosenberg, G., Steinberg, N., Oppenheimer-Shaanan, Y., Olender, T., Doron, S., Ben-Ari, J., Sirota-Madi, A., Bloom-Ackermann, Z., and Kolodkin-Gal, I. (2016) Not so simple, not so subtle: The interspecies competition between *Bacillus simplex* and *Bacillus subtilis* and its impact on the evolution of biofilms. *npj Biofilms Microbiomes*, **2** (1), 15027.

303. Hoefler, B.C., Gorzelnik, K.V, Yang, J.Y., Hendricks, N., Dorrestein, P.C., and Straight, P.D. (2012) Enzymatic resistance to the lipopeptide surfactin as

identified through imaging mass spectrometry of bacterial competition. *Proc. Natl. Acad. Sci U.S.A.*, **109**, 13082–13087.

304. Yang, Y.L., Xu, Y., Straight, P., and Dorrestein, P.C. (2009) Translating metabolic exchange with imaging mass spectrometry. *Nat. Chem. Biol.*, **5** (12), 885–887.

305. Straight, P.D., Willey, J.M., and Kolter, R. (2006) Interactions between *Streptomyces coelicolor* and *Bacillus subtilis*: Role of surfactants in raising aerial structures. *J. Bacteriol.*, **188** (13), 4918–4925.

306. Watrous, J., Hendricks, N., Meehan, M., and Dorrestein, P.C. (2010) Capturing bacterial metabolic exchange using thin film desorption electrospray ionization-imaging mass spectrometry. *Anal. Chem.*, **82** (5), 1598–1600.

307. Luzzatto-Knaan, T., Melnik, A.V., and Dorrestein, P.C. (2019) Mass spectrometry uncovers the role of surfactin as an interspecies recruitment factor. *ACS Chem. Biol.*, **14** (3), 459–467.

308. Combes-Meynet, E., Pothier, J.F., Moënne-Loccoz, Y., and Prigent-Combaret, C. (2011) The *Pseudomonas* secondary metabolite 2,4-diacetylphloroglucinol is a signal inducing rhizoplane expression of *Azospirillum* genes involved in plant-growth promotion. *Mol. Plant-Microbe Interact.*, **24** (2), 271–284.

309. Tyc, O., Song, C., Dickschat, J.S., Vos, M., and Garbeva, P. (2017) The ecological role of volatile and soluble secondary metabolites produced by soil bacteria. *Trends Microbiol.*, **25** (4), 280–292.

310. Bernal, P., Llamas, M.A., and Filloux, A. (2018) Type VI secretion systems in plant-associated bacteria. *Environ. Microbiol.*, **20** (1), 1–15.

311. Netzker, T., Shepherdson, E.M.F., Zambri, M.P., and Elliot, M.A. (2020) Annual review of microbiology bacterial volatile compounds: Functions in communication, cooperation, and competition. *Annu. Rev. Microbiol. 2020*, **74**, 409–430.

312. Anckaert, A., Argüelles Arias, A., Hoff, G., Calonne-Salmon, M., Declerck, S., and Ongena, M. (2021) The use of *Bacillus* spp. as bacterial biocontrol agents to control plant diseases, pp. 247–300.

313. Abreu, N.A., and Taga, M.E. (2016) Decoding molecular interactions in microbial communitiesa. *FEMS Microbiol. Rev.*, **40** (5), 648–663.

314. Shank, E.A. (2018) Considering the lives of microbes in microbial communities. *mSystems*, **3** (2), e00155-17.

315. Stover, C.K., Pham, X.Q., Erwin, A.L., Mizoguchi, S.D., Warrener, P., Hickey, M.J., Brinkman, F.S.L., Hufnagle, W.O., Kowalik, D.J., Lagrou, M.,

Garber, R.L., Goltry, L., Tolentino, E., Westbrock-Wadman, S., Yuan, Y., Brody, L.L., Coulter, S.N., Folger, K.R., Kas, A., Larbig, K., Lim, R., Smith, K., Spencer, D., Wong, G.K.S., Wu, Z., Paulsen, I.T., Reizer, J., Saier, M.H., Hancock, R.E.W., Lory, S., and Olson, M.V. (2000) Complete genome sequence of *Pseudomonas aeruginosa* PA01, an opportunistic pathogen. *Nature*, **406** (6799), 959–964.

316. Hoegy, F., Mislin, G.L.A., and Schalk, I.J. (2014) Pyoverdine and pyochelin measurements. *Methods Mol. Biol.*, **1149**, 293–301.

317. Hartney, S.L., Mazurier, S., Girard, M.K., Mehnaz, S., Davis, E.W., Gross, H., Lemanceau, P., and Loper, J.E. (2013) Ferric-pyoverdine recognition by Fpv outer membrane proteins of *Pseudomonas protegens* PF-5. *J. Bacteriol.*, **195** (4), 765–776.

318. Argüelles Arias, A., Ongena, M., Halimi, B., Lara, Y., Brans, A., Joris, B., and Fickers, P. (2009) *Bacillus amyloliquefaciens* GA1 as a source of potent antibiotics and other secondary metabolites for biocontrol of plant pathogens. *Microb. Cell Fact.*, **8** (1), 63.

319. Hua, G.K.H., and Höfte, M. (2015) The involvement of phenazines and cyclic lipopeptide sessilin in biocontrol of *Rhizoctonia* root rot on bean (*Phaseolus vulgaris*) by *Pseudomonas* sp. CMR12a is influenced by substrate composition. *Plant Soil*, **388** (1–2), 243–253.

320. Olorunleke, F.E., Kieu, N.P., De Waele, E., Timmerman, M., Ongena, M., and Höfte, M. (2017) Coregulation of the cyclic lipopeptides orfamide and sessilin in the biocontrol strain *Pseudomonas* sp. CMR12a. *Microbiologyopen*, **6** (5), e00499.

321. Olorunleke, F.E., Hua, G.K.H., Kieu, N.P., Ma, Z., and Höfte, M. (2015) Interplay between orfamides, sessilins and phenazines in the control of *Rhizoctonia* diseases by *Pseudomonas* sp. CMR12a. *Environ. Microbiol. Rep.*, **7** (5), 774–781.

322. Wu, L., Wu, H.J., Qiao, J., Gao, X., and Borriss, R. (2015) Novel routes for improving biocontrol activity of *Bacillus* based bioinoculants. *Front. Microbiol.*, **6** (DEC), 1395.

323. Hossain, M.J., Ran, C., Liu, K., Ryu, C.M., Rasmussen-Ivey, C.R., Williams, M.A., Hassan, M.K., Choi, S.K., Jeong, H., Newman, M., Kloepper, J.W., and Liles, M.R. (2015) Deciphering the conserved genetic loci implicated in plant disease control through comparative genomics of *Bacillus amyloliquefaciens* subsp. *plantarum*. *Front. Plant Sci.*, **6**, 631.

324. Miethke, M., Klotz, O., Linne, U., May, J.J., Beckering, C.L., and Marahiel, M.A. (2006) Ferri-bacillibactin uptake and hydrolysis in *Bacillus subtilis*. *Mol. Microbiol.*, **61** (6), 1413–1427.

325. Pi, H., and Helmann, J.D. (2018) Genome-wide characterization of the fur regulatory network reveals a link between catechol degradation and bacillibactin metabolism in bacillus subtilis. *MBio*, **9** (5), 1–15.

326. Cornelis, P. (2020) Putting an end to the *Pseudomonas aeruginosa* IQS controversy. *Microbiologyopen*, **9** (2).

327. Adler, C., Corbalán, N.S., Seyedsayamdost, M.R., Pomares, M.F., de Cristóbal, R.E., Clardy, J., Kolter, R., and Vincent, P.A. (2012) Catecholate Siderophores protect bacteria from pyochelin toxicity. *PLoS One*, **7** (10), e46754.

328. Trottmann, F., Franke, J., Ishida, K., García-Altares, M., and Hertweck, C. (2019) A pair of bacterial siderophores releases and traps an intercellular signal molecule: An unusual case of natural nitrone bioconjugation. *Angew. Chemie*, **131** (1), 206–210.

329. Mongkolsuk, S., and Helmann, J.D. (2002) Regulation of inducible peroxide stress responses. *Mol. Microbiol.*, **45** (1), 9–15.

330. Cox, C.D., Rinehart, K.L., Moore, M.L., and Cook, J.C. (1981) Pyochelin: Novel structure of an iron-chelating growth promoter for *Pseudomonas aeruginosa*. *Proc. Natl. Acad. Sci. U. S. A.*, **78** (7), 4256–4260.

331. Youard, Z.A., Mislin, G.L.A., Majcherczyk, P.A., Schalk, I.J., and Reimmann, C. (2007) *Pseudomonas fluorescens* CHA0 produces enantio-pyochelin, the optical antipode of the *Pseudomonas aeruginosa* siderophore pyochelin. *J. Biol. Chem.*, **282** (49), 35546–35553.

332. Granato, E.T., Meiller-Legrand, T.A., and Foster, K.R. (2019) The evolution and ecology of bacterial warfare. *Curr. Biol.*, **29** (11), R521–R537.

333. Cordero, O.X., and Datta, M.S. (2016) Microbial interactions and community assembly at microscales. *Curr. Opin. Microbiol.*, **31**, 227–234.

334. Ghoul, M., and Mitri, S. (2016) The ecology and evolution of microbial competition. *Trends Microbiol.*, **24** (10), 833–845.

335. Davies, J., Spiegelman, G.B., and Yim, G. (2006) The world of subinhibitory antibiotic concentrations. *Curr. Opin. Microbiol.*, **9** (5), 445–453.

336. Romero, D., Traxler, M.F., López, D., and Kolter, R. (2011) Antibiotics as signal molecules. *Chem. Rev.*, **111** (9), 5492–5505.

337. Dumas, Z., Ross-Gillespie, A., and Kümmerli, R. (2013) Switching between apparently redundant iron-uptake mechanisms benefits bacteria in changeable environments. *Proc. R. Soc. B Biol. Sci.*, **280** (1764), 20131055.

338. Lee, N., Kim, W., Chung, J., Lee, Y., Cho, S., Jang, K.S., Kim, S.C., Palsson, B., and Cho, B.K. (2020) Iron competition triggers antibiotic biosynthesis in

Streptomyces coelicolor during coculture with *Myxococcus xanthus*. *ISME J.*, **14** (5), 1111–1124.

339. Kramer, J., Özkaya, Ö., and Kümmerli, R. (2020) Bacterial siderophores in community and host interactions. *Nat. Rev. Microbiol.*, **18** (3), 152–163.

340. Niehus, R., Picot, A., Oliveira, N.M., Mitri, S., and Foster, K.R. (2017) The evolution of siderophore production as a competitive trait. *Evolution (N.Y).*, **71** (6), 1443–1455.

341. Ogran, A., Yardeni, E.H., Keren-Paz, A., Bucher, T., Jain, R., Gilhar, O., and Kolodkin-Gal, I. (2019) The plant host induces antibiotic production to select the most-beneficial colonizers. *Appl. Environ. Microbiol.*, **85** (13), 1–15.

342. Qi, G., Zhu, F., Du, P., Yang, X., Qiu, D., Yu, Z., Chen, J., and Zhao, X. (2010) Lipopeptide induces apoptosis in fungal cells by a mitochondria-dependent pathway. *Peptides*, **31** (11), 1978–1986.

343. Kozlova, O.V., Egorov, S.Y., Kupriyanova-Ashina, F.G., Rid, N., and El-Registan, G.I. (2004) Analysis of the Ca^{2+} response of mycelial fungi to external effects by the recombinant aequorin method. *Microbiology*, **73** (6), 629–634.

344. Aiyar, P., Schaeme, D., García-Altares, M., Carrasco Flores, D., Dathe, H., Hertweck, C., Sasso, S., and Mittag, M. (2017) Antagonistic bacteria disrupt calcium homeostasis and immobilize algal cells. *Nat. Commun.*, **8** (1756).

345. Coraiola, M., Lo Cantore, P., Lazzaroni, S., Evidente, A., Iacobellis, N.S., and Dalla Serra, M. (2006) WLIP and tolaasin I, lipodepsipeptides from *Pseudomonas reactans* and *Pseudomonas tolaasii*, permeabilise model membranes. *Biochim. Biophys. Acta - Biomembr.*, **1758** (11), 1713–1722.

346. Cho, K.H., and Kim, Y.K. (2003) Two types of ion channel formation of tolaasin, a *Pseudomonas* peptide toxin. *FEMS Microbiol. Lett.*, **221** (2), 221–226.

347. Oni, F.E., Olorunleke, O.F., and Höfte, M. (2019) Phenazines and cyclic lipopeptides produced by *Pseudomonas* sp. CMR12a are involved in the biological control of *Pythium myriotylum* on cocoyam (*Xanthosoma sagittifolium*). *Biol. Control*, **129**, 109–114.

348. Steigenberger, J., Verleysen, Y., Geudens, N., Martins, J.C., and Heerklotz, H. (2021) The optimal lipid chain length of a membrane-permeabilizing lipopeptide results from the balance of membrane partitioning and local damage. *Front. Microbiol.*, **12**, 669709.

349. Mantil, E., Crippin, T., and Avis, T.J. (2019) Domain redistribution within ergosterol-containing model membranes in the presence of the antimicrobial compound fengycin. *Biochim. Biophys. Acta - Biomembr.*, **1861** (4), 738–

747.

350. Heerklotz, H., and Seelig, J. (2007) Leakage and lysis of lipid membranes induced by the lipopeptide surfactin. *Eur. Biophys. J.*, **36** (4–5), 305–314.

351. Geudens, N., Nasir, M.N., Crowet, J.M., Raaijmakers, J.M., Fehér, K., Coenye, T., Martins, J.C., Lins, L., Sinnaeve, D., and Deleu, M. (2017) Membrane interactions of natural cyclic lipodepsipeptides of the viscosin group. *Biochim. Biophys. Acta - Biomembr.*, **1859** (3), 331–339.

352. Fiedler, S., and Heerklotz, H. (2015) Vesicle leakage reflects the target selectivity of antimicrobial lipopeptides from *Bacillus subtilis*. *Biophys. J.*, **109** (10), 2079–2089.

353. Lo Cantore, P., Lazzaroni, S., Coraiola, M., Dalla Serra, M., Cafarchia, C., Evidente, A., and Iacobellis, N.S. (2006) Biological characterization of white line-inducing principle (WLIP) produced by *Pseudomonas reactans* NCPPB1311. *Mol. Plant-Microbe Interact.*, **19** (10), 1113–1120.

354. Raaijmakers, J.M., De Bruijn, I., and De Kock, M.J.D. (2006) Cyclic lipopeptide production by plant-associated *Pseudomonas* spp.: Diversity, activity, biosynthesis, and regulation. *Mol. Plant-Microbe Interact.*, **19** (7), 699–710.

355. Sun, P., Hui, C., Wang, S., Wan, L., Zhang, X., and Zhao, Y. (2016) *Bacillus amyloliquefaciens* biofilm as a novel biosorbent for the removal of crystal violet from solution. *Colloids Surfaces B Biointerfaces*, **139**, 164–170.

356. Cornelis, P. (2010) Iron uptake and metabolism in pseudomonads. *Appl. Microbiol. Biotechnol.*, **86** (6), 1637–1645.

357. Ronnebaum, T.A., and Lamb, A.L. (2018) Nonribosomal peptides for iron acquisition: Pyochelin biosynthesis as a case study. *Curr. Opin. Struct. Biol.*, **53**, 1–11.

358. Esmaeel, Q., Pupin, M., Kieu, N.P., Chataigné, G., Béchet, M., Deravel, J., Krier, F., Höfte, M., Jacques, P., and Leclère, V. (2016) *Burkholderia* genome mining for nonribosomal peptide synthetases reveals a great potential for novel siderophores and lipopeptides synthesis. *Microbiologyopen*, **5** (3), 512–526.

359. Seipke, R.F., Song, L., Bicz, J., Laskaris, P., Yaxley, A.M., Challis, G.L., and Loria, R. (2011) The plant pathogen *Streptomyces scabies* 87-22 has a functional pyochelin biosynthetic pathway that is regulated by TetR- and AfsR-family proteins. *Microbiology*, **157** (9), 2681–2693.

360. Inahashi, Y., Zhou, S., Bibb, M.J., Song, L., Al-Bassam, M.M., Bibb, M.J., and Challis, G.L. (2017) Watasemycin biosynthesis in *Streptomyces venezuelae*: Thiazoline C-methylation by a type B radical-SAM methylase

homologue. *Chem. Sci.*, **8** (4), 2823–2831.

361. Ho, Y.N., Lee, H.J., Hsieh, C.T., Peng, C.C., and Yang, Y.L. (2018) Chemistry and biology of salicyl-capped siderophores, in *Studies in Natural Products Chemistry*, vol. 59, Elsevier BV., pp. 431–490.

362. Schalk, I.J., Rigouin, C., and Godet, J. (2020) An overview of siderophore biosynthesis among fluorescent pseudomonads and new insights into their complex cellular organization. *Environ. Microbiol.*, **22** (4), 1447–1466.

363. Mishra, S., and Arora, N.K. (2012) Evaluation of rhizospheric *Pseudomonas* and *Bacillus* as biocontrol tool for *Xanthomonas campestris* pv *campestris*. *World J. Microbiol. Biotechnol.*, **28** (2), 693–702.